THE BEHAVIOUR OF OVERCONSOLIDATED CLAYEY SOIL

Thesis by

ISA KUL

B.S. in C.E., Bogazici University, 1982

Submitted to the Institute for Graduate Studies in
Science and Engineering in partial fulfillment of
the requirements for the degree of
Master of Science
in
Civil Engineering

Bogazici University
Bebek - Istanbul
January - 1985

THE BEHAVIOUR OF OVERCONSOLIDATED CLAYEY SOIL

This Thesis has been approved by

Doç. Dr. Erol Güler (Thesis Supervisor) ....

Prof. Dr. Ergün Togrol ....

Doç. Dr. Turan H. Durgunoğlu ....

Prof. Dr. Vahit Kumbasar ....

Doç. Dr. Vural Altın ....

Boğaziçi University

Bebek - Istanbul

January - 1985

ACKNOWLEDGEMENT

I would like to express my sincere gratitude to Doc. Dr. Erol Guler, for his invaluable suggestions, guidence, encouragements throughout the course of my study and in evaluation of results.

I also would like to thank Mr. Mustafa Tuncan and Mr. Ahmet Tuncan for helping me preparing the test apparatus and test specimens.

Isa Kul

ABSTRACT

THE BEHAVIOUR OF OVERCONSOLIDATED CLAYEY SOIL

Upto this time, the scientific approach to the study and analisys of soil mechanics was to understand and reasonably predict the behavior of clay using different types of tests. In this investigation, the behavior of normally consolidated and overconsolidated clays are evaluated with critical state theories. In this research, a series of undrained compression tests have been carried out on clayey soil, using triaxial testing apparatus. The specimen are first compacted by using proctor mold and then normally consolidated or overconsolidated before testing. The overconsolidation ratios were chosen to be 5, 10, and 15. The relationship q' vs. p', q' vs. ε, u vs. ε, and water content distribution in the specimen are tabulated and drown.

The main result is that the water content of the shear surface increases in comparison to its surrounding and that therefore, the specimen fails, before it reaches the theoritical expected value.

ÖZET

AŞIRI KONSOLİDE KİLLİ ZEMİNLERİN DAVRANIŞI

Bugüne kadar zemin mekanigi üzerindeki bilimsel yaklaşımlar, çalışmalar ve incelemelerle çeşitli deney sonuçlarını kullanarak killerin davranışlarını önceden kesin olarak tahmin etmek ve anlamak mümkün hale gelmiştir.Bu tez çalışmasın kritik durum teorisi ışığı altında normal ve aşırı konsolide olmuş killerin davranışları incelenmiştir. Bu araştırmalar için killi zeminler üzerinde üç eksenli deney aleti ile bir seri deney drenaja musade edilmeden yapılmıştır. Deneylerde kullanılan numuneler önce kompacsıyon aletinde hazırlanıp normal konsolide ve aşırı konsolide deneyler için üç eksenli deney aleti ile çeşitli yükler altında konsolide edilmiştir. Aşırı konsolide numunelerin aşırı konsolide oranı 5, 10, ve 15 olarak seçilmiş olup bütün deney sonuçları ile deney sonunda numune içerisindeki su muhtevası dağılımı tablolar halinde verilmiş, ayrıca q' : p', q' : ε, u : ε ve numune boyunca su muhtevası dağılımı çizilmiştir.

Bu çalışmalarla elde edilin sonucu kısaca şöyle özetleyebiliriz Deney sonunda ulaşılan kesme yüzeyindeki su muhtevası çevresine göre bir artış göterir. Bu artış numunenin teorik olarak kırılması gereken yükten önce kırılmasına neden olur.

TABLE OF CONTENTS

Acknowledgement iii

Abstract iv

Ozet v

List of Figures viii

List of Tables xiv

List of Symbols xv

Chapter 1 INTRODUCTION 1

Chapter 2 PREVIOUS RESEARCH 3

2.1 Clay Minerology 3

2.1.1 Structure of Clay 3

2.2 Properties and Structure of Compacted Clay 8

2.3 Effect of Structure on Shear Strength 12

2.4 Shear Strength Properties 18

2.5 The Roscoe Surface 21

2.6 The Hvorslev Surface 23

2.7 Critical State Concept and Critical State Line 27

2.8 Complate State Boundary Surface 46

Chapter 3 EXPERIMENTAL STUDY 50

3.1 Equipment 50

3.2	Testing Procedure	54
3.2.1	Material and Sample Preparation ...	54
3.2.2	Preparing the Triaxial Cell	61
3.2.3	Placing the Specimen	61
3.2.4	Placing the Triaxial Cell to the Loading Apparatus	66
3.2.5	Coupling the Pore Pressure System .	67
3.2.6	Loading the Sample and Reamoving the Sample	67
3.3	Evaluation of Test Results	75
Chapter 4	TEST RESULTS	79
Chapter 5	CONCLUSION	167
Appendix A	Normalized Test Results	171
	REFERENCES	172

LIST OF FIGURES

FIGURES

2.1 Distribution of Ion with distance from the clay particles.

2.2 Qualitative effect of compaction on soil fabric and structure.

2.3 (a) and (b) Microstructure of Kaolin compacted dry and wet of optimum.

2.4 (a) and (b) Dispersed and flocculate structure of Illite.

2.5 Dispersed and flocculate structure.

2.6 Behaviour of clays in shear,(a) dispersed, (b) flocculate clay.

2.7 Cone index and dry dencity vs. molding water content for Boston Blue Clay.

2.8 Structure of failure zone.

2.9 Stress paths in q': p': v space.

2.10 Methods of optaining the equivalent pressure, p'_{ei}.

2.11 Stress paths for Kaolin Clay.

2.12 Failure state of drained and undrained tests on overconsolidated samples of Wealt Clay.

2.13 The complate state boundary surface in q'/p'_{ei}: p'/p'_{ei} space.

2.14 Stress paths (a) in q' vs. p', (b) in v vs. p' spaces for drained triaxial test on NC specimens.

2.15 Stress paths (a) in q' vs. p', (b) v vs. p' spaces for Undrained test on NC samples.

2.16 Failure points, CSL and NCL for drained and undrained test on NC specimen of Weald Clay.

2.17 Stress-strain curve for an overconsolidated clay.

2.18 Rate of pore water change in undrained test.

2.19 Failure state of undrained specimen in v vs. lnp' space.

2.20 The condition of NCL, CSL, and Swelling Line on v vs. lnp' space.

2.21 The condition of NCL, CSL, and Swellin Line on v vs. p' space.

2.22 An elastic wall and undrained plane on q' : p' : v space.

2.23 Rigidity, Stability, and Instability.

2.8.1 The complate state boundary surface in q'/p'_{ei} vs. p'/p'_{ei} space.

2.8.2 Constant v planes in q' vs. p' vs. v space.

2.8.3 Expected undrained test path for samples at different OCR's.

2.8.4 Normilized stress paths for undrained test on over-consolidated samples of Kaolin Clay.

3.1 Triaxial cell.

3.2 Constant pressure cell.

3.3 Details of side drains for 38 mm. diameter samples.

3.4 Sample preparation process and apparatus.

3.5 Sample preparation process.

3.6 Compaction curve for " Topser Sari Clay ".

3.7 Grain size distribution diagram for " Topser Sari Clay".

3.8 Trimming process and apparatus.

3.9 Trimming apparatus.

3.10 Placing the specimen in the Triaxial Cell.

3.11 Consolidation and swelling process.

3.12 Pore pressure instrument.

3.13 Testing process.

3.14 Self compensating gear drive unit.

3.15 Gear tables.

3.16 Removing the specimen after testing process.

3.17 The triaxial apparatus

3.18 Shematic view of triaxial apparatus.

3.19 Membrane and filter drain correction.

4.1 Normal Consolidation and Critical State Line for "Topser Sari Clay"

4.2
4.6
4.10
4.14
4.18
4.22
4.26
4.30
4.34
4.38
4.42 Deviator Stress versus Axial Strain for various tests
4.46
4.50
4.54
4.58
4.62
4.66
4.70
4.74
4.78

4.82
4.86
4.90
4.94

Deviator Stress versus Axial Strain for various tests

4.3
4.7
4.11
4.15
4.19
4.23
4.27
4.32
4.35
4.39
4.43
4.47
4.51
4.55
4.59
4.63
4.67
4.71
4.75
4.79
4.83
4.87
4.91
4.95

Pore Water Pressure versus Axial Strain for various tsts

4.4 Deviator Stress versus Effective Mean Normal Stress

4.8, 4.12, 4.16, 4.20, 4.24, 4.28, 4.32, 4.36, 4.40, 4.44, 4.48, 4.52, 4.56, 4.60, 4.64, 4.68, 4.72, 4.76, 4.80, 4.84, 4.88, 4.92, 4.96 — Deviator Stress versus Effective Mean Normal Stress for various tests

4.5, 4.9, 4.13, 4.17, 4.21, 4.25 — Height (Unit) versus Water Content for various tests

4.29
4.33
4.37
4.41
4.45
4.49
4.53
4.57
4.61
4.65
4.69
4.73
4.77
4.81
4.85
4.89
4.93
4.97

Height (Unit) versus Water Content for various tests

5.1 Failure Mechanism (a) in q':p': v space, (b) in q':p' space for an overconsolidated clay in undrained condition.

5.2 Deviator Stress (lnq') versus Specific Volume for " Topser Sari Clay".

LIST OF TABLES

TABLES

Table 4.1 Undrained test results of overconsolidated specimens, OCR's 5

Table 4.2 Undrained test results for overconsolidated specimens, OCR's 10.

Table 4.3 Undrained test results of overconsolidated specimens, OCR's 15.

Table 4.4 Undrained test results of normally consolidated specimens.

Table 4.5 The values of v, p'_{ei}, and p'_u for normally consolidated and overconsolidated specimens.

Table 4.6 The value of specific volume and effective mean normal stress for normally consolidated specimens.

Table 4.7 The data values for NCL and CSL, optained from normally consolidated specimens test results.

Table 4.8 Soil constants for " Topser Sari Clay ".

LIST OF SYMBOLS

SYMBOLS

A (cm^2)	=	cross-section area.
A_o (cm^2)	=	initial cross-section area.
B	=	Skompton's pore pressure parameters.
CSL	=	critical state line.
E	=	loading power.
G_s	=	specific gravity of soil grains.
K_o	=	coefficient of earth pressure at rest.
K	=	slope of swelling line when projected onto v vs. lnp' space.
LL	=	liquid limit.
M	=	slope of critical state line when it is projected onto a constant volume plane.
N	=	specific volume of isotropically normally consolidated soil at p'= 1.0 $kgcm^{-2}$.
NC	=	normally consolidated.
NCL	=	normal consolidation line.
OMC (%)	=	optimum moisture content.
OCR	=	over consolidation ratio.
PL	=	plastic limit.
PI	=	plasticity index.
P_2 (kg/cm^2)	=	radial cell pressure.
P_3 (kg/cm^2)	=	
P_1 (kg/cm^2)	=	axial load.
S (%)	=	degree of saturation.
U	=	recoverable power.

W	= dissipated power.
a	= (v_o / l_o) initial specific volume/ initial length.
e (%)	= void ratio.
e_f(%)	= the value of e at failure.
g = h =	soil constants defining the Hvorslev surface.
l (cm)	= axial length of the specimen.
l_o(cm)	= initial axial length.
n	= number of data points.
p'(kg/cm^2)	= 1/3 (P_1 + P_2 + P_3) effective mean normal stress.
p'_o(kg/cm^2)	= initial effective mean normal stress.
p'_f(kg/cm^2)	= value of p' at failure.
p'_{ei}(kg/cm^2)	= equivalent pressure; value of p' at the point on the normal consolidation line at the same specific volume.
p'_u(kg/cm^2)	= value of p' at the point on the critical state line at the same specific volume.
q (kg/cm^2)	= deviator stress, $(P_1 - P_3) = (P'_1 - P'_3)$.
q_f(kg/cm^2)	= value of q at failure.
u (kg/cm^2)	= pore water pressure.
v	= specific volume.
v_o	= initial specific volume.
v_f	= value of v at failure.
v_K	= specific volume of isotropically overconsolidated soil swelled to p = 1.0 kg/cm^2.
v	= $v + \lambda \ln p'$, specific volume on reference sectio
v^p	= irrecoverable volumetric strain.

v^r = recoverable volumetric strain.

w (%) = water content

w_f(%) = value of w at shear surface.

Γ = specific voleme of soil at critical state with $p = 1.0\ kg/cm^2$.

λ = slope of normal consolidation line and critical state line.

ε (%) = shear strain.

ε_v (%) = vertical shear strain (Chapter 2.3).

ε_h (%) = horizantal shear strain.

ε^r (%) = recoverable shear strain.

ε^p (%) = irrecoverable shear strain.

ε_1 (%) = axial shear strain (length reduction) .

ε_r (%) = radial shear strain (radius reduction).

ε_s (%) = $2/3\ (\varepsilon_1 - \varepsilon_3)$, shear strain for $\varepsilon_2 = \varepsilon_3$.

ε_v (%) = volumetric strain.

γ_d(gr/cm^3) = dry unit weight.

γ_s(gr/cm^3) = unit weight of soil particles.

γ_w(gr/cm^3) = unit weight of water.

$\delta s / \delta t$ = shear deformation velocity.

CHAPTER 1 INTRODUCTION

The theories developed for soil mechanics in the early years different aspects of soil behaviour with different test formulas and theories. In the year 1958 Roscoe, Schofield and Wroth brought a new understanding to the relations of water content, shear stress and effective mean normal stress and explained many aspect of existing theories with just one theory.

In the second half of the 20th century, new great buildings, retaining walls, road embankment, airfield pavements are needed. The civil engineers are concerned with the design and construction of civil engineering works and are obliged to perform calculations which demonstrate the safety and servicebility of any new structure. But, before these calculations can be performed, the mechanical behaviour of soil must be understood. The building area, in Turkey, is mostly covered by overconsolidated clayey deposits. Therefore, purpose of this thesis was chosen to determine the behaviour of "overconsolidated clays" in common triaxial compression tests to give some valuable information to the civil engineer for planning new engineering works.

The tests were performed on normally consolidated and overconsolidated specimens. The specimen were prepared in proctor mold at optimum moisture content. And they were consolidated at different constant triaxial cell pressures for normally consolidated or overconsolidated samples. The OCR's were chosen as 5, 10, and 15. All the samples were tested in undrained condition. Critical State Line and Normal Consolidation Line on v vs. lnp' space, Hvorslev surface and Roscoe surface on q' vs. p' space were drown from normally consolidated and overconsolidated test results. Then the soil constants M, N, Γ, λ, and h were found for " Topser Sari Clay ". All test results were plotted in q' vs. ε, u vs. ε, and q' vs. p' spaces. The water content distribution trough the specimen were also determined and plotted.

The main conclusion was that the water content at the shear surface increases relative to its surrounding, and that therefore, the specimen fails,before it reaches the deviator stress, at which the corresponding Hvorslev Surface meets the Critical State Line. As a result,the strength of the overconsolidated clay is less than the theoretically expected value.

CHAPTER 2 PREVIOUS RESEARCH

2.1 CLAY MINEROLOGY

2.1.1 STRUCTURE OF CLAY

According to Lambe (1958) "structure" means the arrangement of soil particle, which is controlled by the electrical forces acting between adjacent particles. Previously "structure" was limited to the arrangement of soil particles only. The concept of electrical forces and environmental factors entered into the discussions of structure with the principals of colloid chemistry. The importance of particle arrangements however,was recognized many years ego by Terzaghy (1925), Casagrande (1932), and Hvorslev (1938).

The concepts of soil structure are concerned primarily with very small particles about two micron in size or smaller. In cohesive soil the structure is explained largely by the clay minerals and the forces acting between them. There are many forms of clay minerals, with some similarities and wide differences in composition, structure and behaviour.The most important minerals are (i) kaolinite, (ii) montmorillonite, (iii) halloysite, and (iv) illite. All have crystal structures that include large numbers of atoms arranged in complex three dimensional patterns. Most clay crystals consist of Silica and Alumuna and/or Iron and Magnesium. Most of clay minerals have sheet or layered structures. Soil masses generally contain a mixture of several clay minerals named for the predominating clay mineral with varying amounts of other nonclay minerals.

Clay particles are usually of small size lessthan two microns and most clay minerals are thin flat plates. All are extremely fine grained, with large surface ares per unit mass. For this reason, clay particles usually stay in colloidal range; and,electrical forces acting between adjacent particles and environmental conditions become important.

In coloidal range electrical forces between particles may be divided into three groups. Primary valence bonds, which are the strongest, hold atoms together in the basic mineral units, and can be grouped as ionic bonds (an exchange of electrons by the linked atoms), covalent bonds (sharing of electrons by the linked atoms), and heterpolar bonds (part ionic and part covalent, since it results from an uniqual sharing of electrons by the linked atoms). The hydrogen bonds happens when an atoms of hydrogen is rather strongly atracted by two other atoms (e.g oxygen, nitrogen atoms).The primary valance and hydrogen bonds can not be broken by the stresses applied normally to a soil system. The secondary valance forces (also known as Van der Weals foces) arise from electrical moments existing within the units. They are like forces acting between two short bar magnents, in certain positions the magnets repel each other and in others they atract.Because attractive position are more frequent. Hence the net effect of secondary valance forces between clay plates are attraction. Secondary valance forces are much weeker than the other two and decrease with increasing distances between particles. Van der Weals forces are important for soil engineer because they contribute to clay strength most and cause soil to hold water.

Clay particles in the presence of water exhibit greatly different behaviorthan do other minerals because of the interaction of the electro static fields and the diffuse dauble layers.

Clay mineral faces are generally negative, due to isomorphous substitution, and the edges positive or negative depending on the nature of minerals and the environment with which it is in contact. At lower water contents, the cation cluster on negatively charged clay faces to neutralize the particles. When the water content is increased the cations held at the face of dry clay tend to spread out into the diffuce double layer. Water molecules behave as dipoles although natural. Therefore water closest to the surface is held and the molecules are oriented in the electrostatic field. The water closest to the clay surface appears dencer than ordinary water. The thickness of the innermost layer of water is probably 10 A^o (10^{-6} mm) and the total thickness of water that is attracted to the clay may approach 400 A^o. This orientated water zone is called diffuse double layer and is shown in Fig. 2.1. The distribution of Ion with distance from the clay particles in seen in Fig. 2.1(b). The concentration of cations in the double layer decreases with the distance from clay faces.

A particular phenomenon of clay is that a clay mass which has dried some initial water content forms a mass which has considerable strength. If these lumps are broken down to elemental particles, the material behaves as cohesionless particulate medium. When water is again added, the material becomes plastic with some strength in termediate to the dry strength. If the wet of clay is again dried, it forms hard, strong lumps.

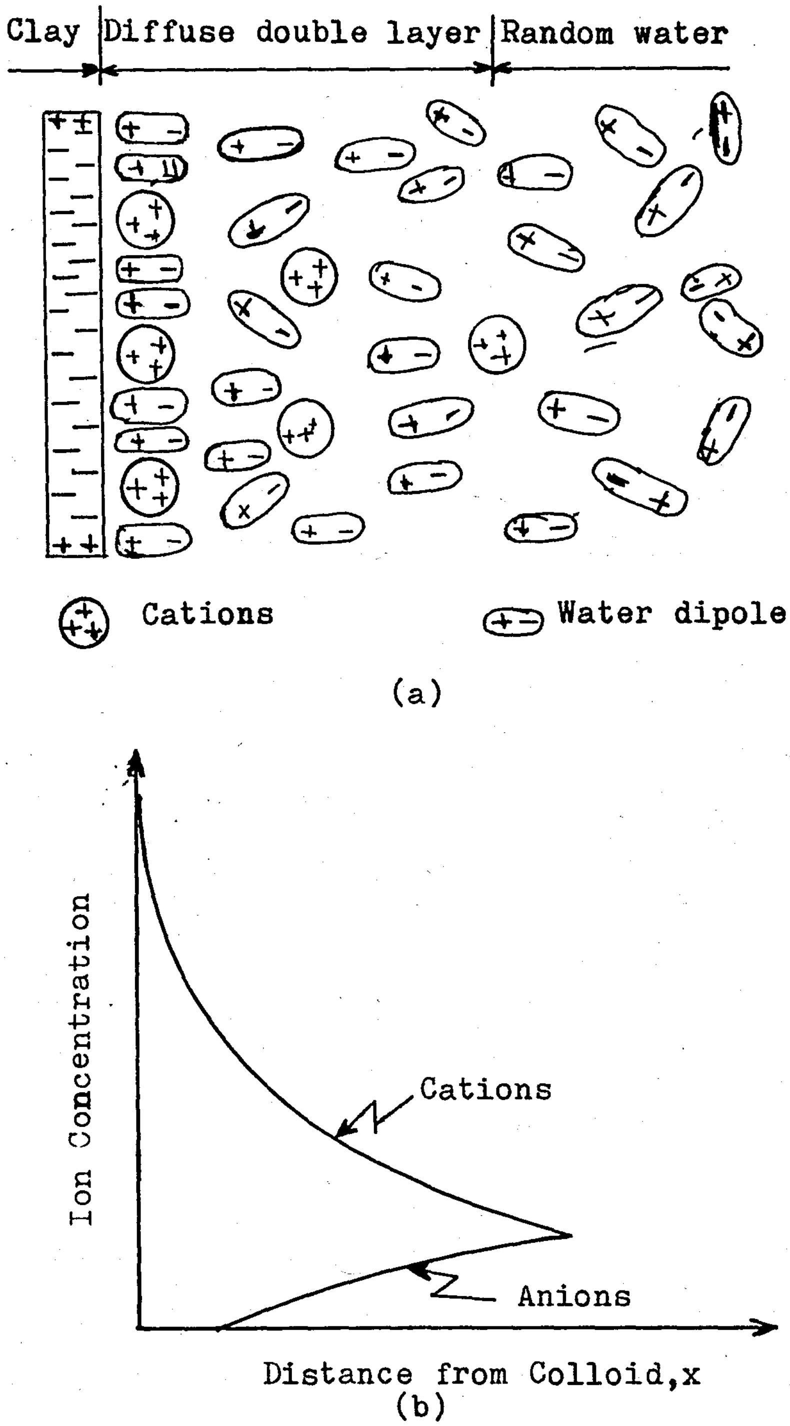

Fig. 2.1 Diffuse Double Layer (After Lambe, 1958)

The role of water in this phenomeno is not fully understood, although in drying, surface tension certainly pulls the particles into maximum contact with the very minimum of interparticle spacing so that the inter particle forces are a maximum. It appears that the higher dencity resulting from packing and the close spacing resulting in the maximum effect of interparticle force attruction give this very high strength. We can readily observe that the strength of the clay varies from a very low value at $S \rightarrow 100$ percent to a very high values at $S \rightarrow 0$. It is of interest to note that theuse of water, which is dipolar agent such as carbon tetrachloride (CCl_4) does not. Adipolar agent is one which tend to devoloped a (+) and (-) charge on opposite sides of the molecule. The (+) charge on one side of a dipole tends to attract the (-) charge of any material present including both clay particle and the negative side of other water molecules.

Since the cation are clustered on particle surfaces when the clay is dry, the attructions between the negatively charged edges and the surface holding cations result in edge to surface contacts and flocculation of particles. When the clay is wetted, the added water helps to the development of dauble layer. With the development and inter action of these layers the repulsive forces are created between cations contained in two interacting dauble layers. If these electrostatic repulsive forces become larger than the attractive forces at edge to surface contacts,the particles reorient themselves into a more dispersed and parallel situations. In the way,the particle orientation of a clay may be of any arrangement between two different cases. (i) A complately random orientation which is a flocculated structure. (ii) A complately parallel orientation whicw is a dispersed structure.

2.2 PROPERTIES AND STRUCTURE OF COMPACTED CLAY

The structure and, thus, the engineering properties of compacted clay will depend greadly on the method or type of compaction, the compactive effort, the soil type, and the water content. Usually, the water content of compacted soil is refer ence to the optimum moisture content (OMC in short) for the given type of compactiondepending on the relative position , this may be "dry of optimum", "near or at optimum", or "wet of optimum". Researh on compacted clays has shown that when they are compacted dry of optimum, the structure of the soil is essentially independent of the type of compaction (Lambe, 1958; Seed and Chan, 1959). Wet of optimum, however, the type of compaction has a significant effected on the soil fabric and thus on the strength and compressibility of the soil.

The structure of compacted clay is about as complex as the structure of natural clays. At the same time compactive effort with increasing water content the soil fabric becomes increasingly oriented (or dispersed). Dry of optimum, the soil tend to produce a flocculated (or card house) fabric. This is qualitatively illustrated in Fig 2.2. In the Fig.,at point A,there is not enough water for the diffuse double layers of the soil particles to develop fully, or clay is water deficient. Hence , the electricrepulsive forces between particles

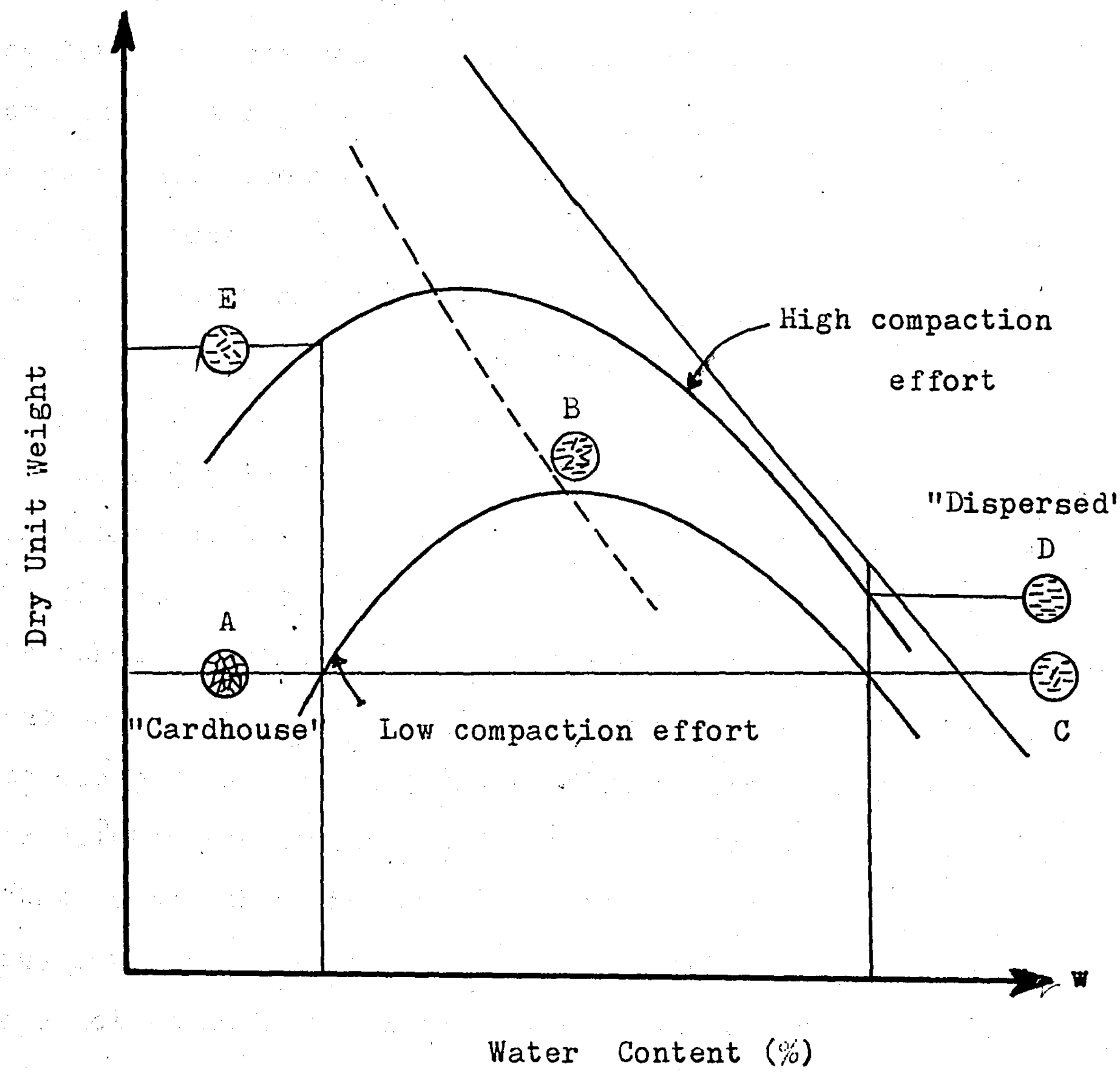

Fig 2.2 Qualitative effect of compaction on soil fabric and structure (after Lambe, 1958)

are smaller than the attractive forcec,resulting in a net attruction between particles, and the particles therefore tend to flocculate in a disorderly array. When the water content is increased toward B, electrolyte concentration decreases, the repulsion between clay particles increases, and dauble layer around particles become larger. Therefore,flocculation decreases. Decreasing degree of flocculation permits a more orderly arrangementof particles. Increasing the order of particles increases the density until the water content of point B is reached

Beyond point B particle parallelism increases. A further expension of the dauble layer causes the repulsion between particles to increase and the attructive force to decrease. Eventhough a more orderly arrangement exist,beyond point B the compacted dencity begins to degreas because water starts to occupy space which could be filled with soil particles, or dilutes the concentration of soil particles,per volume; that means, there is not a market decrease in air content any more. The changes in structure which are described above can not be seen in all compacted clays, especially in the clays with particles having great tendencies to flocculate.

Also, if the compactive effortis increased, the soil tend to become more dispersed eventhough the water content remains constant, as a point E in Fig 2.2. The sample structure is considerably more oriented at C than at A for the same energy since it is wet of optimum. Also the fabric at D will be more oriented than at (C) for the same water due to the increased compactin effort.

There are similarities between dry-side and wet-side compacted clays and between undisturbed and remoulded clays The dry-side compacted clay and undisterbed clay both tend to have a flocculated type of structure,while a wet-side compacted clay and a remoudedclay both tend to have dispersed types of structure. Sample compacted dry and wet of optimum are shown in Fig 2.3 (a) and (b). Dispersed and flocculate structure are seen in Fig 2.4 (a) and (b).

Fig 2.3(a)
Microstructure of Kaolin
compacted dry of optimum

Fig 2.3 (b)
Microstructure of Kaolin
compacted wet of optimum

Fig 2.4 (a)

Vertical section of dispersed Illite

Fig 2.4 (b)

Vertical section of flocculated Illite

2.3 EFFECT OF STRUCTURE ON SHEAR STRENGTH

According to Arpad Kezdi (1974) the structure effect the behavior of clays subjected to streesses. As shown in Fig 2.5, clay structure can be classified in to two kinds; dispersed and flocculate structure. In a dispersed clay, the particles repell each other and are arranged randomly without actually being in contact. When shearing stresses are applied to the soil, the particle will be oriented, to some degree until with increasing stress they become, at least in the zone of shear, full oriented.i.e. parallel to eahh other. Therefore, to maintain a constant rate of shear strains requires gradually increasing stresses until a maximumis reached.

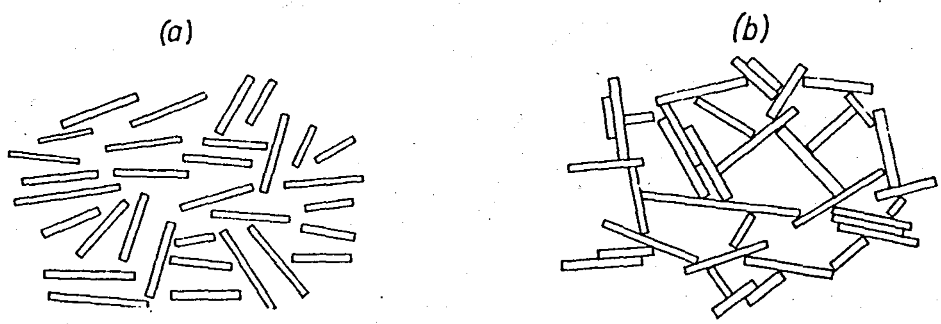

Fig 2.5 Structure of clay consisting of flat particles (a) in dispersed state, (b) in flocculated state

On the stress-strain curve there is no charatteristics point that would indicate an essential change in soil behavior, Fig 2.6. No frictional resistance is developed during the processes,,no internal friction. If, on the other hand, the total stress due to external load is increased, the distance between the particles are decreased with the results that a greater shearing stress will be requred to maintain the same constant shear deformation velocity (ds/dt).

If clay with a flocculated structure is subjected to shear, some of the interparticle bonds break down in the course of shear deformations, while new ones are formed continuously. If the break down of the bonds becomes predominant, the clay suffers an essential change in its structuralstrength, so that constant shear strain can be maintained even by greatly reduces stresses. Interparticle forces of adhesion cease to exist, since the bond themselves are destroyed.

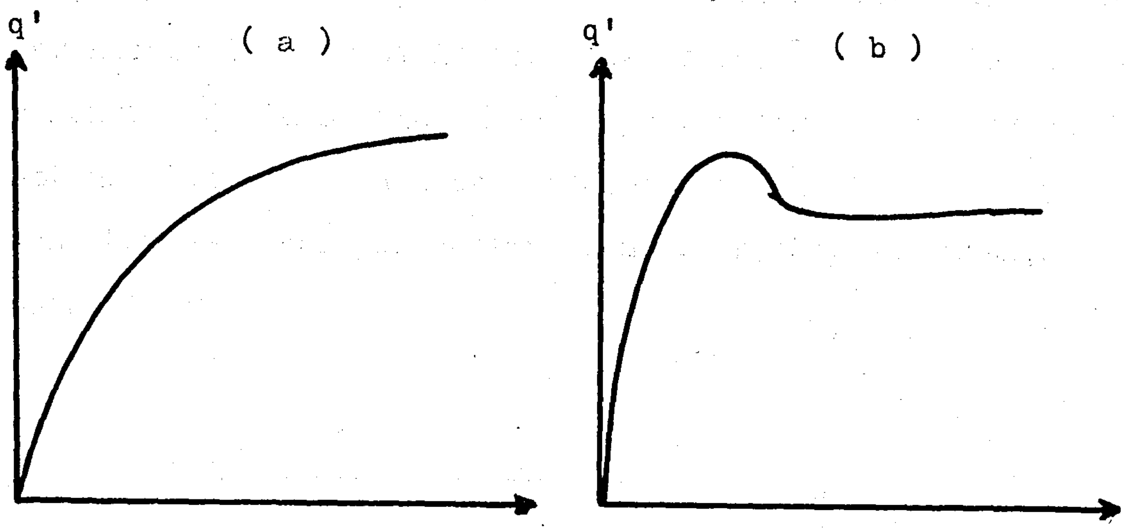

Fig 2.6 Behaviour of clays in shear (a) dispersed clay, (b) flocculated clay.

thus, the part of the shearing stress due to cohesion decreases whereas the frictional resistance increases.

According to Lambe (1958), the entire force system between clay particles should be considered for studying the shear strength of the compacted clays, He explained that four main horizantal forces act between adjacent particles, these are; the externallyapplied inter granunal stress, the electrical attraction forces, the electrical repulsion forces, and the geometric interaction, i.e, contact pressure.

Main factors which are effecting the strength are spacing orientation of particles of clay and the type of compaction used. When a clay specimen is compacted on the dry side of optimum, a flocculated structure is formed and the edge-to-face contact between soil particles provides high resistance to load. On the other hand, when compacted on wet of optimum, the specimen has a dispersed structure with relatively few strong interparticle contacts, resulting in a low shear strength. Besides, increased compactive energy at dry of optimum causes in an increase of strength, at wet of optimum, however there is no important change in strength,as shown in Fig 2.7

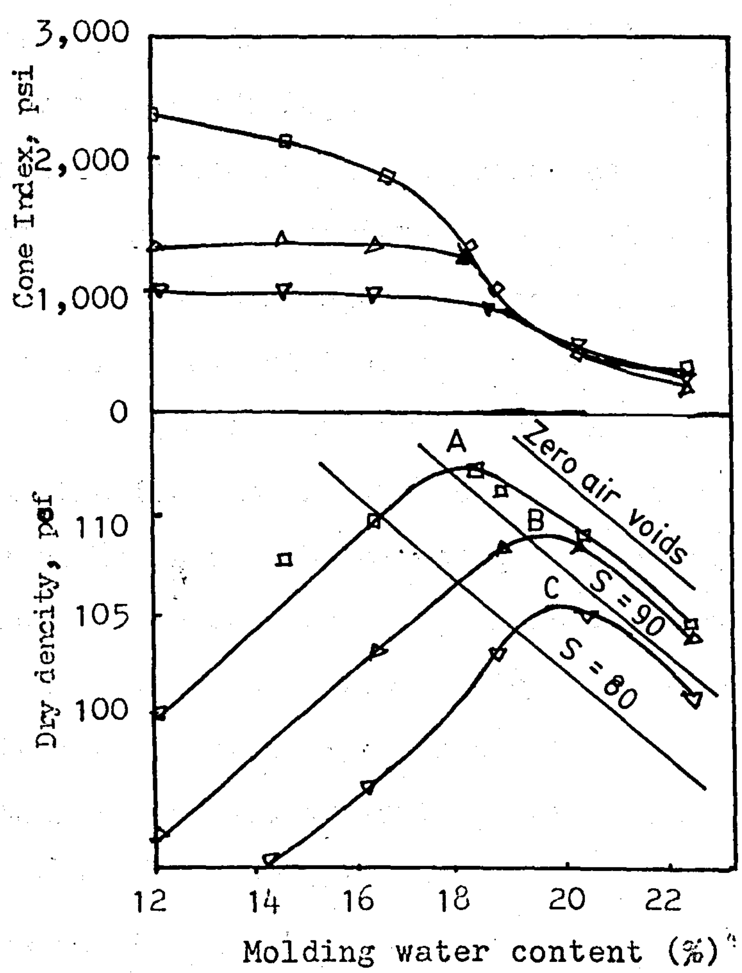

$W_{A(opt)}$ = 17.19

$W_{B(opt)}$ = 19.3

$W_{C(opt)}$ = 19.7

Fig 2.7 Cone index and dry dencity vs. molding water content for Boston Blue Clay (After Pacey,1956)

A study of the influence of particle orientation on the stress-strain properties of laboratory consolidated Kaolin has been condácted by Mr. I.A. Rennie at the University of Strathclyde under the direction of Dr. W.M.Kirkpatrick. A random structure was produced by consolidating a slurry of Kaolinite under an isotropic stress system in a 250mm diameter triaxial cell; and highly oriented structure was produce by one dimensionally consolidating a slurry of Kaolinite in a 250 mm Rowe cell. these two very different microstructures were verified in the scanning electron microscope.Small samples of these clays were then tested in triaxial compression,,triaxil extension and plane strain. The tests involved a variety of stress path under undrained, consolidated undrained and fully drained conditions.

From the tests result, in construst to the values the axil strain at peak strength were greatly influenced by the structure of the clay and the drection of sampling. The isotropic samples gave similar strains in vertical and horizantal samples $\varepsilon_v = \varepsilon_h$. However for the highly oriented clay the failure strains for the triaxial compression test showed $\varepsilon_v \hat{=} 0.5\,\varepsilon_h$ and in plain strain the effect was extremely marked with $\varepsilon_v \hat{=} 0.1\,\varepsilon_h$

Thus it can be seen that, while the strain behaviour of Kaolin is highly sensitive to microstructure and orientation the strenth is suprisingly insensitive. It might be assumed that this is because at failure the clay is complately reoriented in a narrow failure zone.

The above study by Rennie and and a separate study at Manchester by Karunaratne have investigated the reorientation of Kaolin particles caused by shearing action,with the main emphasis on plane strain deformation.Karunaratne subjected

100 mm high x 100 mm wide x 150 mm long cuboidal sample of K_o consolidated Kaolin to undrained shear in a plane strain apparatus. One test was stopped at the point where the effective stress ratio reached its peak at a strain $\varepsilon_1 = 4.4\%$. A second test wasstopped at the peak deviator stress at a strain of $\varepsilon_1 = 6.5\%$. Both samples were removed and cut in to sections 100mm x 100 mm x 10 mm thick parallel to the plane. Some of these sections were air dried and athers impregnated with carbowax. Carbowax sections were ground down to form thin sections for viewing between crossed nicols in the polarizing microscope, to detect the presence of oriented shear zones The sample taken at $\varepsilon_1=4.4\%$ showed a genaral horizantal orientation caused by the K_o consolidation, but no trace of a shear zone of oriented particles. However the sample taken at $\varepsilon_1=6.5\%$ showed a single dominant shear zone inclined at ap roximately 50^o to the horizantal,although this was not apparent to a visual examination of the specimen.

Detailed examination reveal that this zone had the structure XYZYX illustrated in Fig 2.8 X is the original K_o consolidated sample. Y and Y are two thin slip surface containing particles with a tendency to be oriented parallel to the slip surface. Z is a zone of the original material undergoing simple shear between the two slip surface Y.

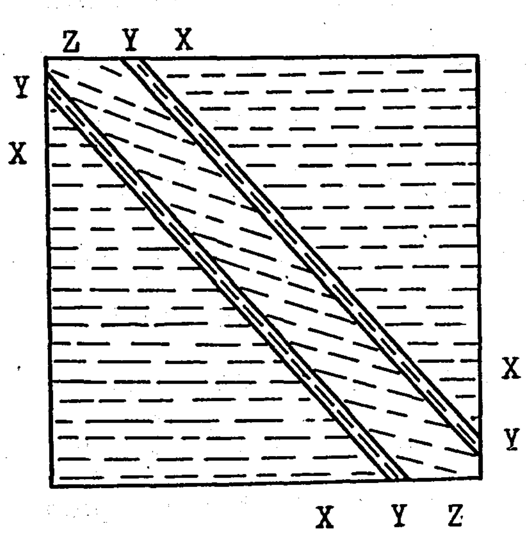

Fig 2.8 Structure of failure zone

2.4 SHEAR STRENGTH PROPERTIES

The clasic work of Hvorslev (1937) on the shear resistance of remoulded saturated cohesive soil at failure contains a clear statement of the fundamentals upon which the present knowledge of subject is based. He showed that the peak shear stress at failure of such a soil is a function of the effective normal stress p'_f on, and of the void ratio of e_f in, the plain of the failure at the moment of the failure and this function is independent of the stress history of the sample. Hvorslev's equation for the shear strength of clay is shown to define a surface in a space of three variable p', e (v), and q, see Fig 2.9 . The progresive yielding of a sample define as a loading path in this spaces, and the paths taken by samples in differing test can be correlated if a boundary energy correction is applied. The final portions of all paths then lie in a unique surface, and the paths end at a unique critical void ratio line. At the critical void ratio state unlimited deformations can be take place while p', e (v), and q remain constant. The two concepts of the existance of such a surface and such a critical voids ratio line are verified by an analysis of results of triaxial tests on a clay by K. H. Roscoe A. N. Schofield and C. P. Wroth (1958)

D. J. Henkel (1960) has shown that there are found unique relationships between water content and the effective stress on remoulded saturated normally consolidated clay specimens, irrespective of wether drained or undrained tests are performed. For overconsolidated samples having the same maximum consolidation pressure, unique relationships between the water content and the effective stresses are also found.

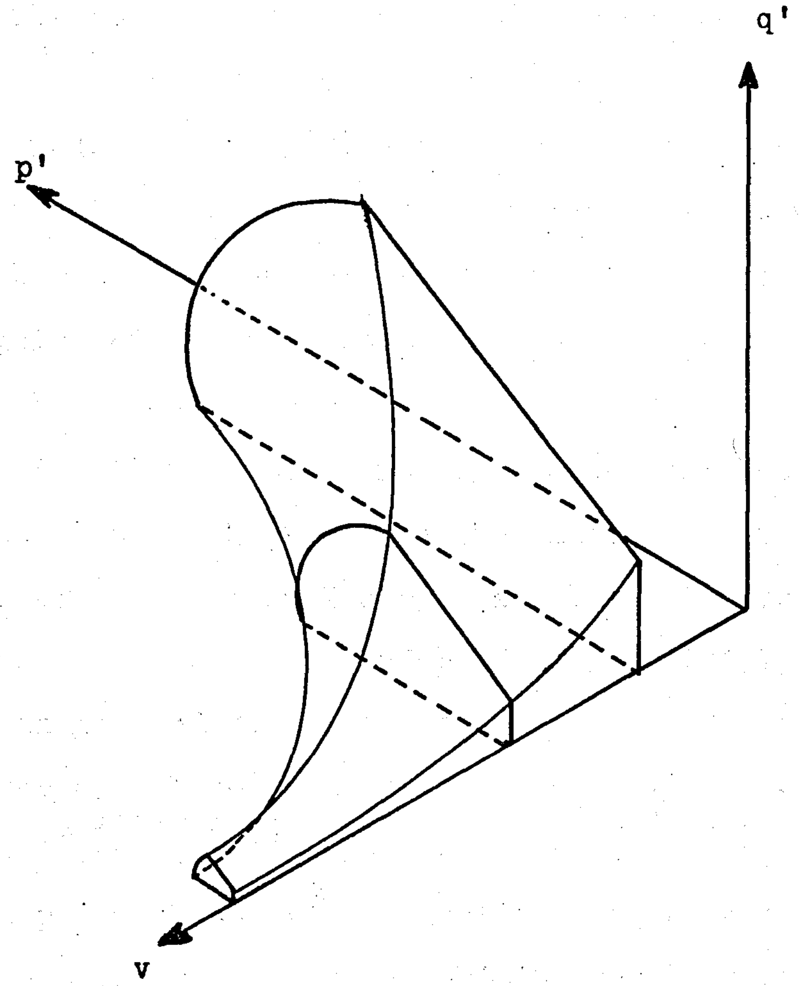

Fig 2.9 Stress paths in q' : p' : v spaces

K. H. Roscoe and H. B. Poorooshasp (1963)have developed a stress-strain theory for normally consolidated clay when subjected to triaxial comppression test. The theory can only be applied for the prediction of the strain where the moisture content is a unique function of the imposed stress. The incremental strain assosiated with a given stress increment can be considered as the sum of two component that occure in (i) constant volume process and (ii) a process in which the stress ratio remain constant. Therefore, a series of drained and undrainedtest are performed. The tests with geometrically similar stress paths show that the change in moisture content and the axial strain are identical.

Togrol, E. (1962) has reported the relationship between shear strength, effective normal stress and water content. He has studied on remoulded saturated cohesive soil which has highly uniform characteristics (Bentler Kaolini). His study can be summarized as

(i) It is experimentally proven that there exists a unique relationship between the maximum shear stress at failure and effective normal stress and the water content, and that this relationship is independent of initial consolidation and drainage conditions. For triaxial test, this relationship gives a well defined curve in the deviator stress (q'),the mean principal effective stress (p), and the water content (w) space. This curve has logaritmic projection on the q : w and p : w planes and projection oan the q : p plane is a strigth line passing through the origin. The projection on p : w plane is found to be parallel to the triaxial consolidation curve

(ii) The experimental evidence optained reveals the water content at the complation of consolidation as being independent of the initial water content.

(iii) The test paths consistent with the test conditions, i.e. consolidation and drainage condition.

(iv) By using undrained test paths, a fundamental relationship, applicable also to ather cohessive soil, is optained. This relationship give excess pore pressure when maximum deviator stress at failure is reached.

2.5 THE ROSCOE SURFACE

When normal consolidated specimens are tested in drained or undrained condition,the tests seem to define a curved three dimentional surface linking the normal consolidation line to the critical state line. For eachtest path traces out a section of the surface at constant v.

It is tempting to ask if the family of undrained and drained tests on normally consolidatedsamples define the same threedimentional surface in q':p':v space. Clearly it is reasonable that they should for both drained and undrained tests start from the normal consolidation line and finish at the critical state line. One way of checking whether the surface is unique is to investigate whether samples in the course of drained or undrained tests have the same specific volumes when they are subjected to the same effective stress

A more systematic procedure would be to perform a series of drained tests on normally consolidated samples and, from the specific volume measured at different stage of the test, construct a series of contours of constant v in q':p' space. The undrained test paths in q': p' space are themselves contours of constant v, see Fig 2.10 It is clear that the contours optained from drained and undrained tests are entairely consistent with each other, and are of the same shape. These shape of the constant v contours, which are optained from drained or undrained tests are called as ROSCOE surface.

All stress paths are the same shape in q'; p' space but different size, because the initial isotropic stress P'_{ei} and, hence, initial volume, is different for each test. Thus, if the stresses were scalled by division by P'_{ei}, all tests paths would reduce to the single curve. Where the parameter P'_{ei}, the equivalent pressure, at any specific volume is optained from the equation for the normal consolidation line using current value of v for the specimen

$$P'_{ei} = \exp\left((N - v) \lambda \right) \qquad \text{Eq. 2.1}$$

The procedure is illustrated in Fig 2.10

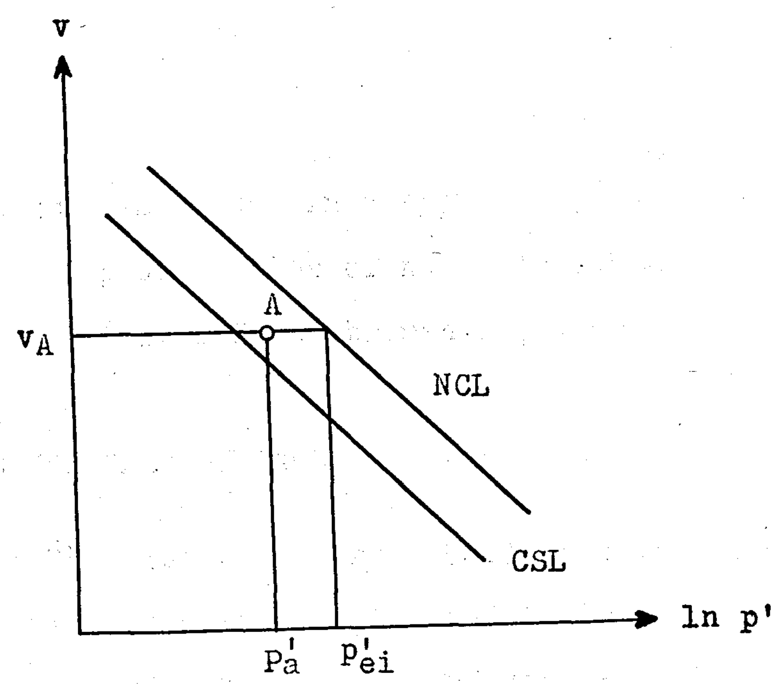

Fig 2.10 Methods of optaining the equivalent pressure, P'_{ei}

Blasubramaniam (1969) optainedsome data from tests on remoulded Kaolin. the agreement between the drained and undrained test is sufficiently good for all compressiontests, irrespective of the applied loading paths. His data are seen in Fig 2.11

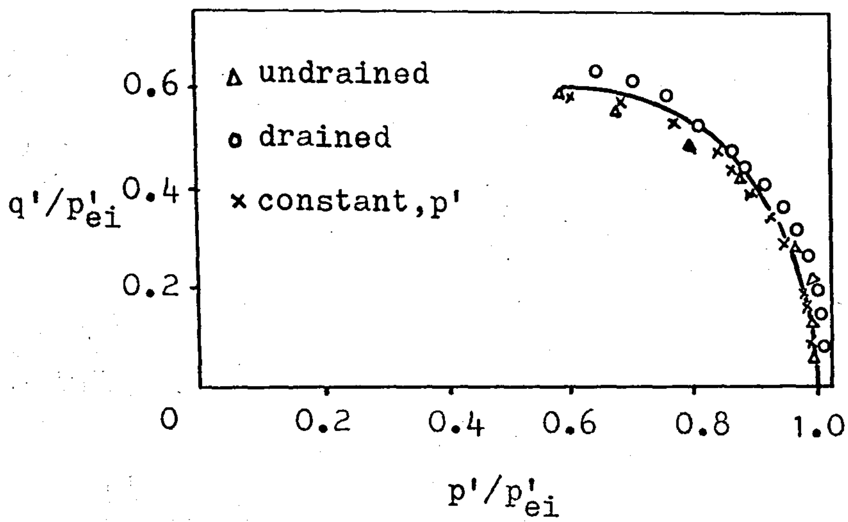

Fig 2.11 Test paths in q'/p'_{ei} : p'/p'_{ei} space for constant p on samples of normally consolidated Kaolin clay (after Balasubramaniam, 1969)

2.6 THE HVORSLEV SURFACE

After Hvorslev and Parry (1960) were made a seriesof compression test on over consolidated Weald Clay. It is clear that the data of both drained and undrainedtest lie on a single line in q'/p'_{ei} : p'/p'_{ei} space. The line is limited on its right-hand end by the point representing the critical state line at the top edge of the Roscoe state boundary surface.
By the folowing argument, the line of failure points is also limited on its left- hand end as seen in Fig 2.12 The maximum value of q'/p' would be when p'_1 was large and p'_3 was small If the soilcould not withstant tensile effective stresses, the

highest value of q'/p' that could be observed would correspond to $p_3' = 0$. Then, for a triaxial compression test

$$q' = p_1' \qquad \text{Eq. 2.2}$$

$$p' = 1/3\ p_1' \qquad \text{Eq. 2.3}$$

$$q'/p' = 3 \qquad \text{Eq. 2.4}$$

The locus of failure point can then be idealized as line AB inFig 2.13 The locus is limited on its left-hand side by

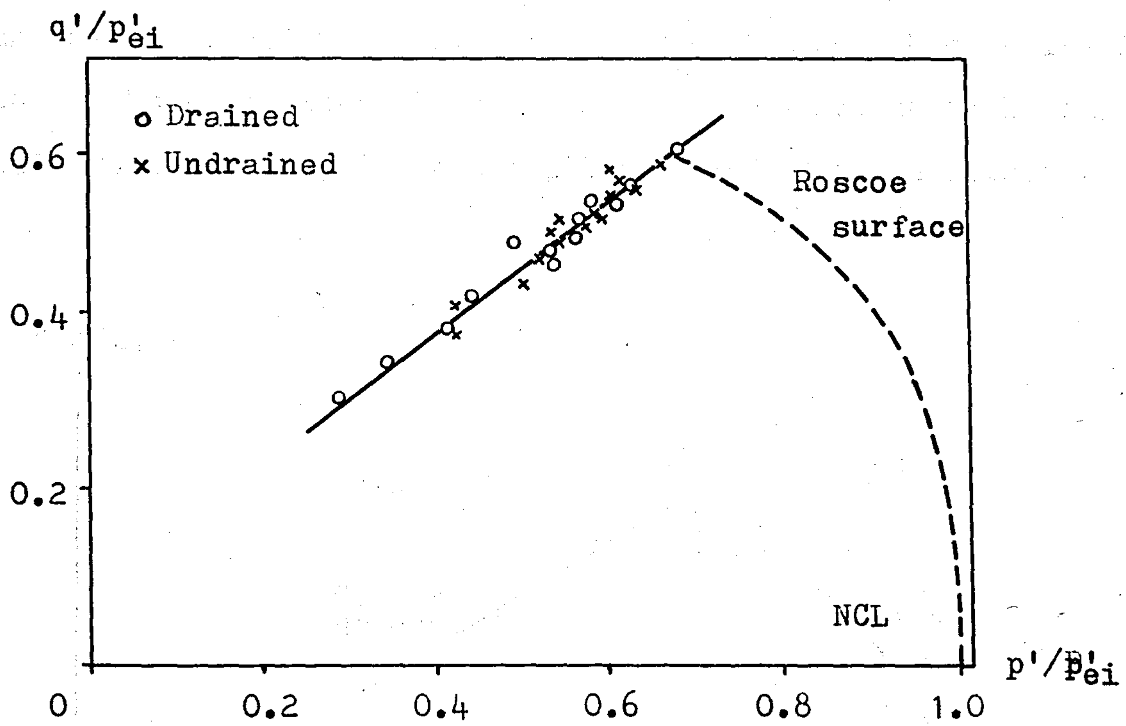

Fig 2.12 Failure state of drained and undrained tests on overconsolidated samples of Weald Clay (data from Parry, 1960)

the line OA which has slope 3, corresponding to tensile failure ure, and on its right-hand side by the critical state line (point B),and the Roscoe surface (BC). Ofcourse, if the soil could sustain tensile effective stresses, the line corresponding to tensile failure would lie to the left of OA, and might be curved. This latter possibility is relevant for many cohesive powders whose handling is important in the chemical engineering industry.

The locus AB of failure points in Fig 2.13 are called as HVORSLEVsurface. The significant feature of the surface with which Hvorslev was particularly concerned is that the shear strenghh of a specimen at failure is a funtion both of the mean normal stress p', and of the specific volume appears in Fig 2.13 through its influenceon the equivalent stress p'_{ei}, which depends directly on specific volume. The point can beillustrated if we idealized the

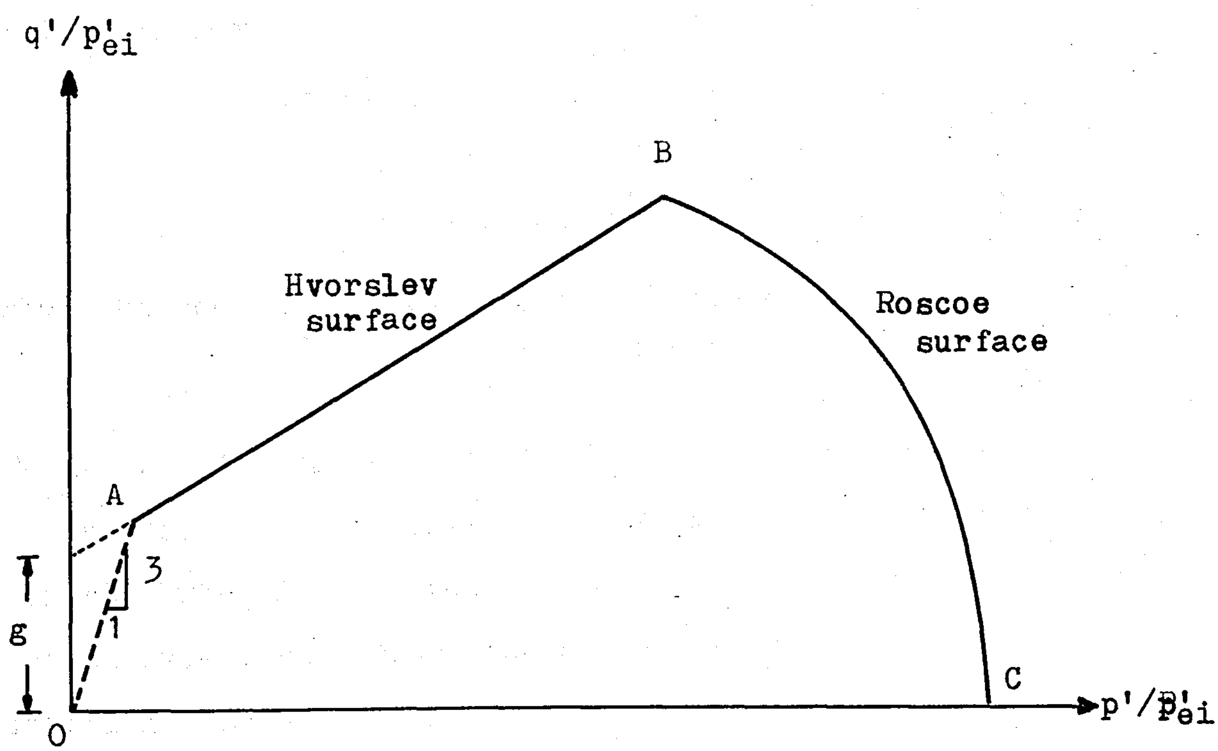

Fig 2. 13 The coplate state boundary surface in q'/P'_{ei}: p'/P'_{ei} space

Hvorslev surface as a stright line whose equation is

$$q'/p'_{ei} = g + h \; (\; p'/p'_{ei} \;) \qquad \text{Eq. 2.5}$$

where g and h are soil constant as shown Fig 2.13 , also equation 2.5 can be rewritten as

$$q' \; = \; g \; p'_{ei} + h \; p' \qquad \text{Eq. 2.6}$$

using eq. 2.1

$$p'_{ei} = \exp \; ((\; N - v \;) \; \lambda \;) \qquad \text{Eq. 2.7}$$

so that eq. 2.6 can be rewritten as

$$q' = \; g \exp \; ((\; N - v \;) \lambda \;) + h \; p' \qquad \text{Eq. 2.8}$$

The Hvorslev surface intersect the critical state line by eq. 2.13 and 2.14 and v_f

$$q'_f = M \; p'_f \quad \text{and} \quad v_f = \Gamma - \lambda \ln \; p'_f \qquad \text{Eq. 2.9}$$

and hence from eq. 2.8

$$(M - h) \; p'_f = g \; \exp \; ((\frac{N - \Gamma}{\lambda}) + \ln p'_f) \qquad \text{Eq. 2.10}$$

$$g \; = \; (\; M - h \;) \; \exp \; (\frac{\Gamma - N}{\lambda}) \qquad \text{Eq. 2.11}$$

Thus the equation of the Hvorslev surface is

$$q' = (\; M - h \;) \; \exp \; (\frac{\Gamma - v}{\lambda}) + h \; p' \qquad \text{Eq. 2.12}$$

Equation 2.12 states explicitly that the deviator stress at failure of an overconsolidated specimen is made up of two components. The first component (h p') is proportional to mean normal effective stress, and so may be though of a being frictional by nature. Second component

$$(\; M - h \;) \; \exp \; (\frac{\Gamma - v}{\lambda})$$

depent only on the current specific volume, and the value of certain soil constant.

2.7 CRITICAL STATE CONCEPT AND CRITICAL STATE LINE

Recently, various research workers have been devoloping new conceptual models. The critical state concept has been worked into a variety of models which are now well developed and acceptable in the contexst of isotropic hardening elastic/plastic media. The basic idea is the concept that soil and other granular materials,if continiously distorted until they flow like a frictional fluid,willcome into critical state,where they fail.

In Fig 2.14and Fig 2.15 are illustrated seperately the failure of clay samples which were initially isotropicly compressed and then, loaded in drained and undrained triaxial compression tests and it is instructive to compare these directly.

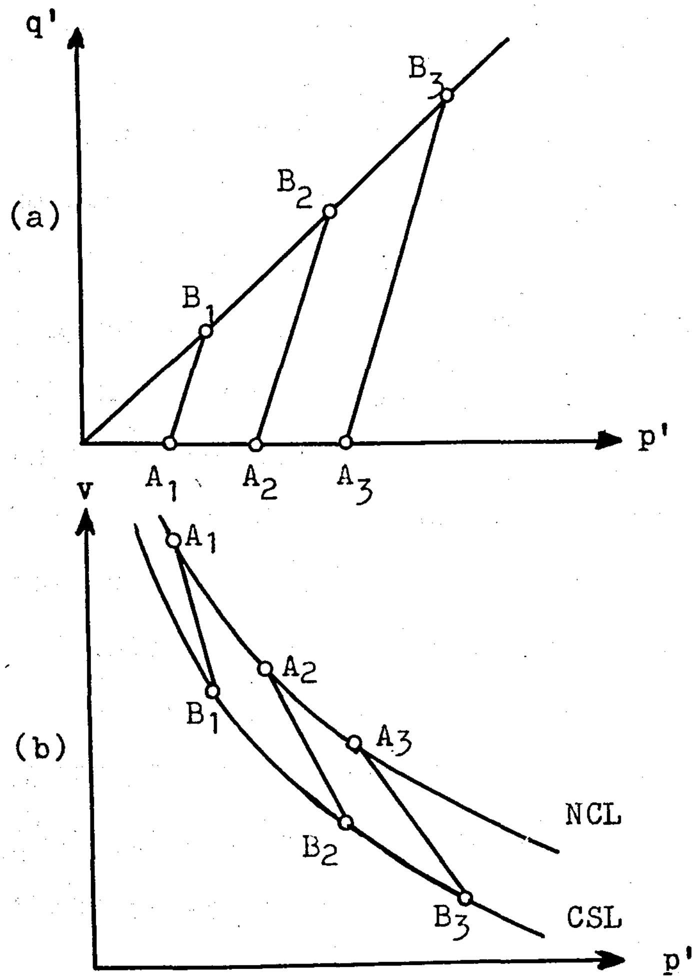

Fig. 2.14

Stress paths in (a) q':p', (b) v:p' space for drained triaxial test on NC specimen

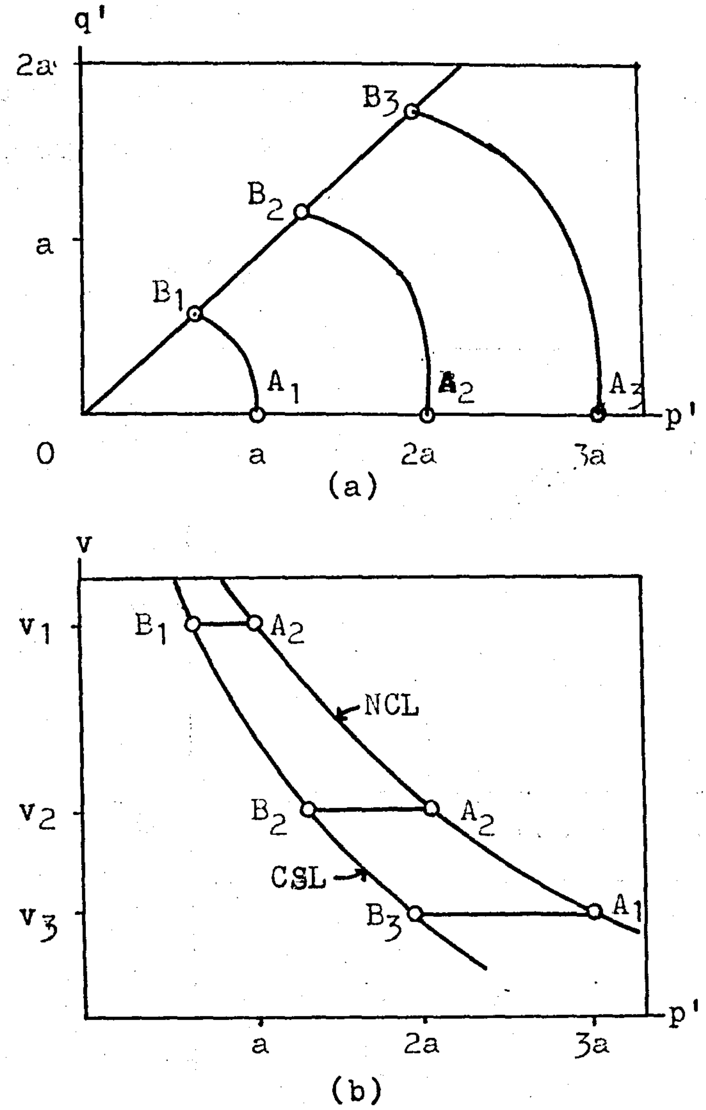

Fig 2.15

Stress paths (a) in q':p' and (b) v:p' spaces for undrained test on NC samples

Two set of tests are made on initially isotropicly consolidated sample of Wealt Clay, as reported by Parry (1960) These samples are tested in drained and undrained triaxial compression tests. Then these data are plotted together in Fig 2.16. The data points define a single straight line through the origin in q':p' space and a single straight line in v:lnp' space whose shape is parrallel to normal consolidation line.

This single and unique line of failure points of both drained and undrained tests are defined as the CRITICAL STATE LINE. Its crucial property is that failure of initial isotropically normal consolidated samples will occur once that stress states of the samples reach the line, irrespective of the test path followed by the samples on their way to the critical state line.

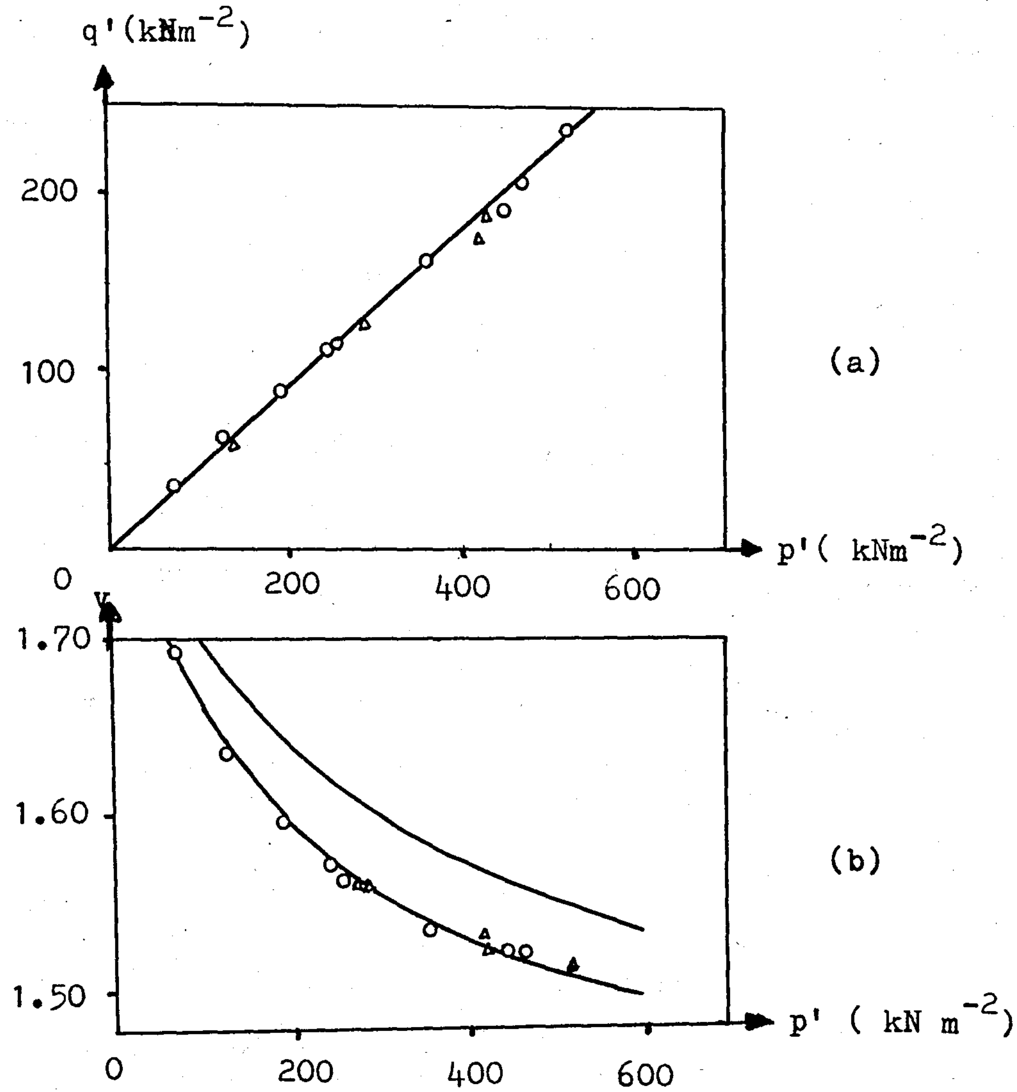

Fig 2.16 Failure points for drained and undrained tests on NC specimen of Wealt Clay (Data from Parry,1960)

Failure will be manifested as a state at which large shear distortion occur whith no change in stress, or inspecific volume.

The projection of the critical state line onto the q':p' plane in Fig 2.16 (a) may be described by

$$q' = Mp' \qquad \text{Eq 2.13}$$

and the projection of CSL onto the v:lnp' plane in Fig 2.16 (c) may be described by

$$v = \Gamma - \lambda \ln p' \qquad \text{Eq. 2.14}$$

also we may be described normal consolidation line in the same plain in Fig 2.16 (c)

$$v = N - \lambda \ln p' \qquad \text{Eq. 2.15}$$

where

M = gradiant of the CSL onto q':p' space

λ = gradiant of the CSL onto v:lnp' space

Γ = the value of v corresponding to p = 1.0 $kgcm^{-2}$ on the CSL in v:lnp'spaces

N = the value of v corresponding to p = 1.0 $kgcm^{-2}$ on the NCL in v : lnp'spaces

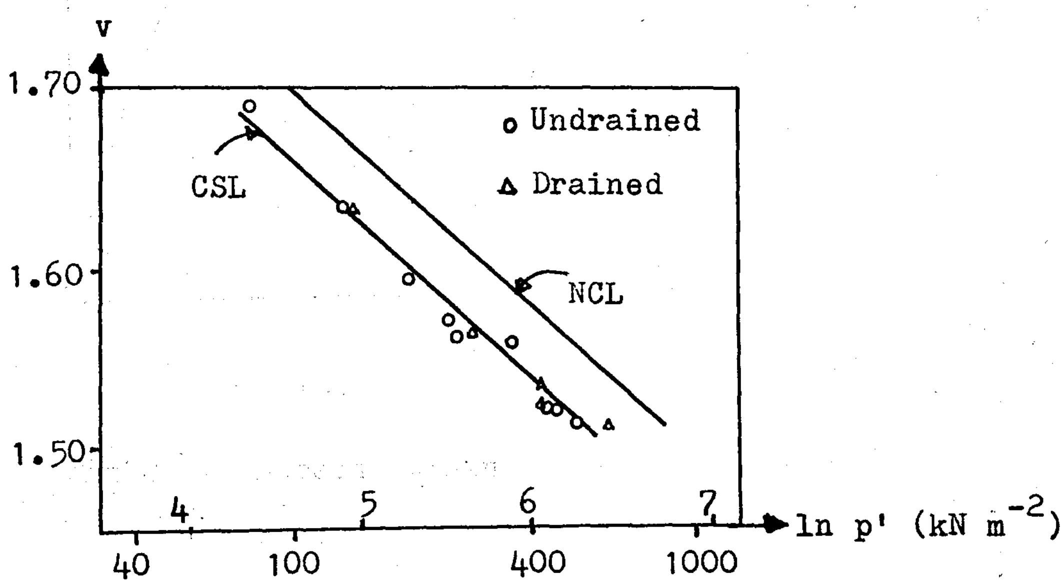

Fig 2.16 (c) The critical state line in v : lnp' space
(Data from Parry, 1960)

reliable at large strain. For the initial part of the curve upto point F (in Fig 2.17),the sample get stronger as it deforms. Thus, any small inhomogeneities of strain will be reduced as the sample is loaded, for the more strained elements of soil will be stronger than those wich have strained less. After point F, the sample becomes weaker as it strain furter . Thus, any inhomogeneities of strain will become intensified, becouse further strain will be concentrated in the weaker regions of thespecimen. We espect, therefore,to observe the formation of thin zones of concentrated deformation within the specimen after failure.

One way of proceeding is to ask in which direction the sample were moving in q': p': v spaces at failure. This was the approach adopted by Parry (1958). For undrained test, Parry examined the ratio of pore pressure change at failure He plotted $((\delta u / p'_f) / \delta \varepsilon_s)$ against p'_u / p'_f (Fig 2.18) Then the change of pore pressure is expressed as u / p'_f so that samples which fail at different mean normal effective stresses may be compared directly. The rate of pore pressure change at failure is largest for sampless which fail furthest away from the criticalstate line, and the sign of the pore water pressure change is such as to move the specimen towards the critical state line (Fig 2.19). Sample A has $p'_f < p'_u$, and so from Fig 2.18 $\delta u/\delta \varepsilon$ is negative; the sample therefore, moving to the right from A. The sample which fails at point B has $\delta u / \delta \varepsilon$ positive and so it is moving to the left in Fig 2.19 .

We say conclude that at failure both drained and undrained samples are moving tovards the critical state line at rates which are related to the distance of samples from the critical state line

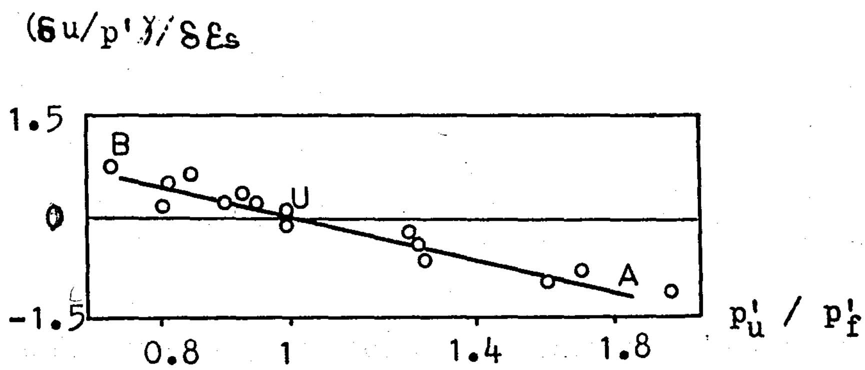

Fig 2.18 Rate of pore pressure change in undrained test (After Parry, 1958)

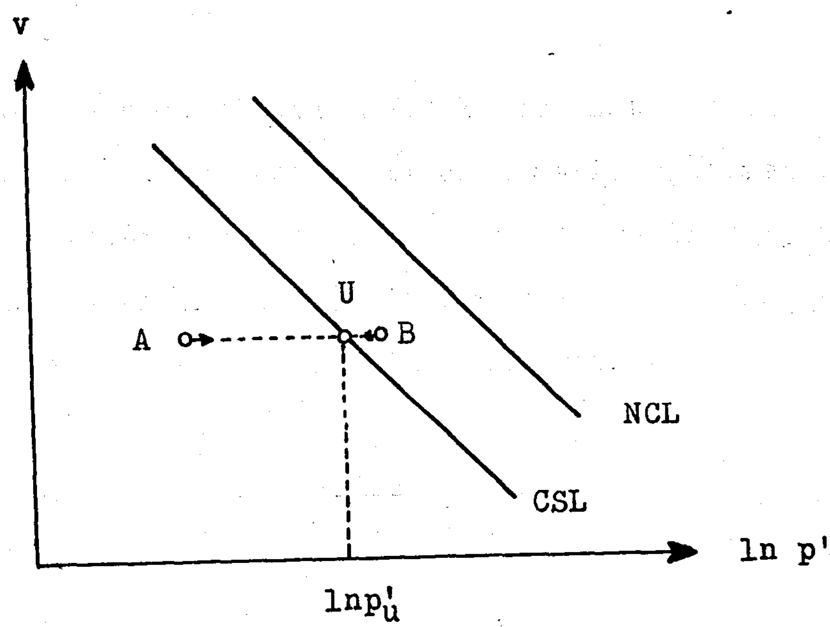

Fig 2.19 Failure state of undrained specimen in v : ln p' space

It should be noted that this conclution applies for both overconsolidated and normally consolidated samples, even-

$$\dot{p} = \frac{\dot{p}_1 + 2\,\dot{p}_3}{3} - u_w \qquad \text{Eq. 2.19}$$

and

$$\dot{q} = (\dot{p}_1 - \dot{p}_3) - u_w \qquad \text{Eq. 2.20}$$

If the cell pressure is constant, then we can rewrite equation 2.19 and 2.20 as

$$\dot{p} = \frac{\dot{p}_1}{3} \qquad \text{and} \qquad \dot{q} = \dot{p}_1$$

so

$$\dot{p} / \dot{q} = 1 / 3 \qquad \text{Eq. 2.21}$$

The load piston displacement $\dot{l}$ does not correspond simply to vertical deviator stress; if an elastic specimen is subjected to effective spherical cell pressure increment without any vertical deviator stress, there will be a longituditional strain of one third of the volumetric strain.

$$\dot{\varepsilon} = \frac{\dot{l}}{l} - \frac{1}{3}\,\frac{\dot{v}}{v} \qquad \text{Eq. 2.22}$$

Since stress is defined to be positive in compression, it is necessary to define length reduction and radius reduction as positive strain increments $\dot{\varepsilon}_l$ and $\dot{\varepsilon}_r$ respectively. then defining longitudinal strain increament as

$$\dot{\varepsilon}_l = \frac{\dot{l}}{l} = \frac{\delta l}{l}$$

and radial strain increament as

$$\dot{\varepsilon}_r = -\frac{\dot{r}}{r} = -\frac{\delta r}{r}$$

Eq. 2.23

voluementric strain increament,

$$\frac{\dot{V}}{V} = -\frac{\delta V}{V} = \dot{\varepsilon}_l + 2\dot{\varepsilon}_r \qquad \text{Eq. 2.24}$$

Equation 2.22 can be rewritten as

$$\varepsilon = \frac{2}{3}(\dot{\varepsilon}_l - \dot{\varepsilon}_r) \qquad \text{Eq. 2.25}$$

It can be appropriate to distinguish between deformation called

length reduction when $\dot{\varepsilon} > 0$

redius reduction when $\dot{\varepsilon} < 0$

The rate of vertical load increament within the system on the speciman due to strain which is called the loading power.

$$\dot{E} = -u_w\dot{v} + p_3\dot{v} + (p_1 - p_3)a\dot{l} \qquad \text{Eq. 2.26}$$

The upward displacement of the pore-pressure piston is equal and opposite to the downward displacement of the cell-pressure piston, and so the loading power depends only on the effective stresses

$$p_3' = p_3 - u_w \quad \text{and} \quad p_1' = p_1 - u_w \qquad \text{Eq 2.27}$$

and equation 2.26 can be rewritten

$$\dot{E} = p_3' \dot{v} + (p_1' - p_3') a \dot{l} \qquad \text{Eq 2.28}$$

where

$$a = \frac{v}{l}$$

Then the loading power per unit volume of specimen becomes

$$\frac{\dot{E}}{v} = p_3' \frac{\dot{v}}{v} + (p_1' - p_3') \frac{\dot{l}}{l}$$

$$= p_3' (\dot{\varepsilon}_1 + 2 \dot{\varepsilon}_r) + (p_1' - p_3') \dot{\varepsilon}_1$$

$$= p_3' \dot{\varepsilon}_1 + 2 p_3' \dot{\varepsilon}_r + p_1' \dot{\varepsilon}_1 - p_3' \dot{\varepsilon}_1$$

$$= p_1' \dot{\varepsilon}_1 + 2 p_3' \dot{\varepsilon}_r \qquad \text{Eq 2.29}$$

In which form the rate of increment of effective stress moving at their respective strain rates is directly evident. But from equation 2.17 , 2.18 , 2.24 and 2.25 we obtain

$$p \frac{\dot{v}}{v} = \left(\frac{p_1' + 2 p_3'}{3} \right) (\dot{\varepsilon}_1 + 2 \dot{\varepsilon}_r)$$

$$= \frac{p_1' \dot{\varepsilon}_1}{3} + \frac{4\, p_3' \dot{\varepsilon}_r}{3} + \frac{2\, p_1' \dot{\varepsilon}_r}{3} + \frac{2\, p_3' \dot{\varepsilon}_1}{3} \quad (a)$$

and

$$q\,\dot{\varepsilon} = \frac{2}{3} (p_1' - p_3') (\dot{\varepsilon}_1 - \dot{\varepsilon}_r)$$

$$= \frac{2\, p_1' \dot{\varepsilon}_1}{3} - \frac{2\, p_1' \dot{\varepsilon}_r}{3} - \frac{2\, p_3' \dot{\varepsilon}_1}{3} - \frac{2\, p_3' \dot{\varepsilon}_r}{3} \quad (b)$$

which when added (a) and (b) gives

$$P \frac{\dot{v}}{v} + q\,\dot{\varepsilon} = p_1' \dot{\varepsilon}_1 + 2\, p_3' \dot{\varepsilon}_r \qquad \text{Eq. 2.30}$$

This confirms the correctness of the choice of strain increment parameters

$$\frac{\dot{E}}{v} = \frac{P\,\dot{v}}{v} + q\,\dot{\varepsilon} \qquad \text{Eq. 2.31}$$

During the small displacements that are prevoked by the external load increment moving within the system generate power $\dot{E}$ which the specimen must either store or dissipate. The application of load increment, the loading power per unit volume transfered from increasing loads to the specimen is

$$\frac{\dot{E}}{v} = \frac{P\,v}{v} + q\,\dot{\varepsilon} \qquad \text{Eq. 2.31}$$

During subsequent unloading the recoverable power per unit volume returned by the specimen to the increasing loads within the system is

$$\frac{\dot{u}}{v} = -\left(\frac{p\,\dot{v}^r}{v} + q\,\dot{\varepsilon}^r\right) \qquad \text{Eq. 2.32}$$

The remainder of the loading power which is not transfered back and has been dissipated within the spacimen is

$$\frac{\dot{W}}{v} = \frac{\dot{E}}{v} - \frac{\dot{U}}{v} = \left(\frac{p\,\dot{v}^p}{v} + q\,\dot{\varepsilon}^p\right) \qquad \text{Eq. 2.33}$$

so the criterion of stability is required

$$\dot{p}\,\frac{\dot{v}}{v} + \dot{q}\,\dot{\varepsilon}^p \geqslant 0$$

In overconsolidated specimen, during loading, it reachs a peak value and the deviator stress reduces from its peak value on q/ε diagram. This does not verify

If the shear strength is increased by the mean normal stress, we may say that the volume change must follow the irrecoverable deformation. And the change in recoverable work depends only effective mean normal stress

$$\dot{\varepsilon}^r \equiv 0$$
$$\dot{\varepsilon} = \dot{\varepsilon}^p \qquad \text{Eq. 2.34}$$

And we assume that the isotropic swelling line and recompression line of a clay specimen lie on the same line which is given by

$$v = v_o - K \ln \left(p / p_o \right) \qquad \text{Eq. 2.35}$$

and virgin consolidation line

$$v = v_o - \lambda \ln (p / p_o) \qquad \text{Eq. 2.36}$$

$$q = M p \qquad \text{Eq. 2.37}$$

where

K = gradiant of swelling line

λ = gradiant of normal consolidation line and critical state line onto v : lnp' space

M = gradiant of critical state line onto q' : p' space

as seen in Fig 2.20 and Fig 2.21

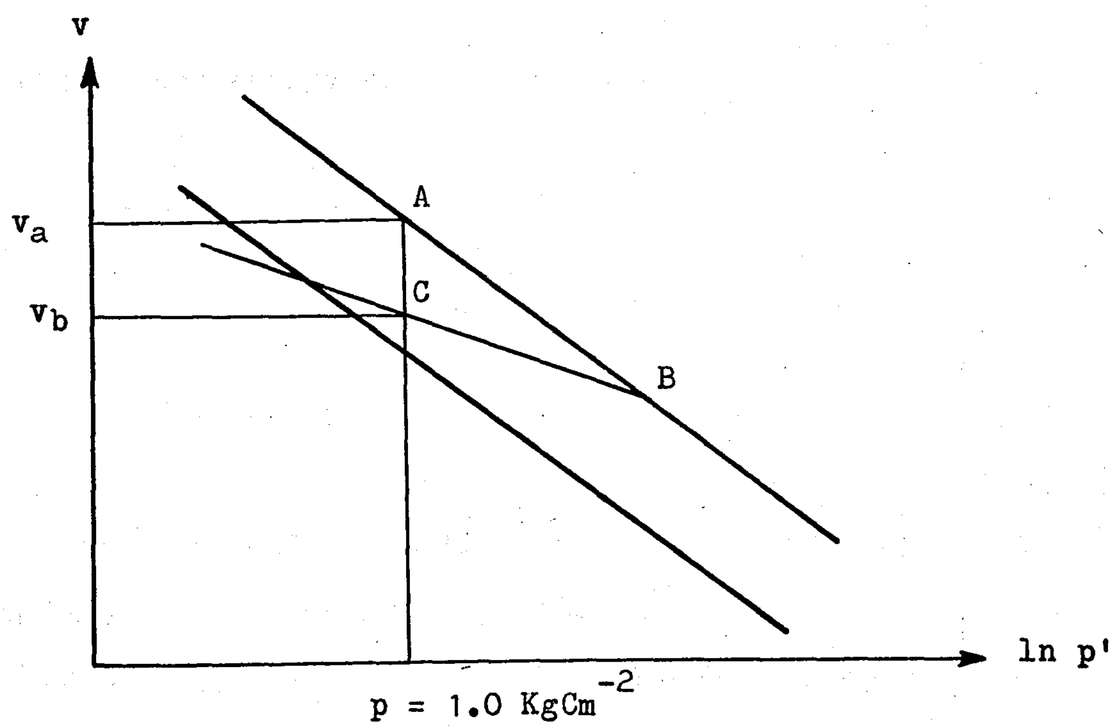

Fig 2.20 The condition of NCL and CSL and svelling line on v : ln p' space

When the specimen reaches the critical state line, it will deform continiously without any volume change.

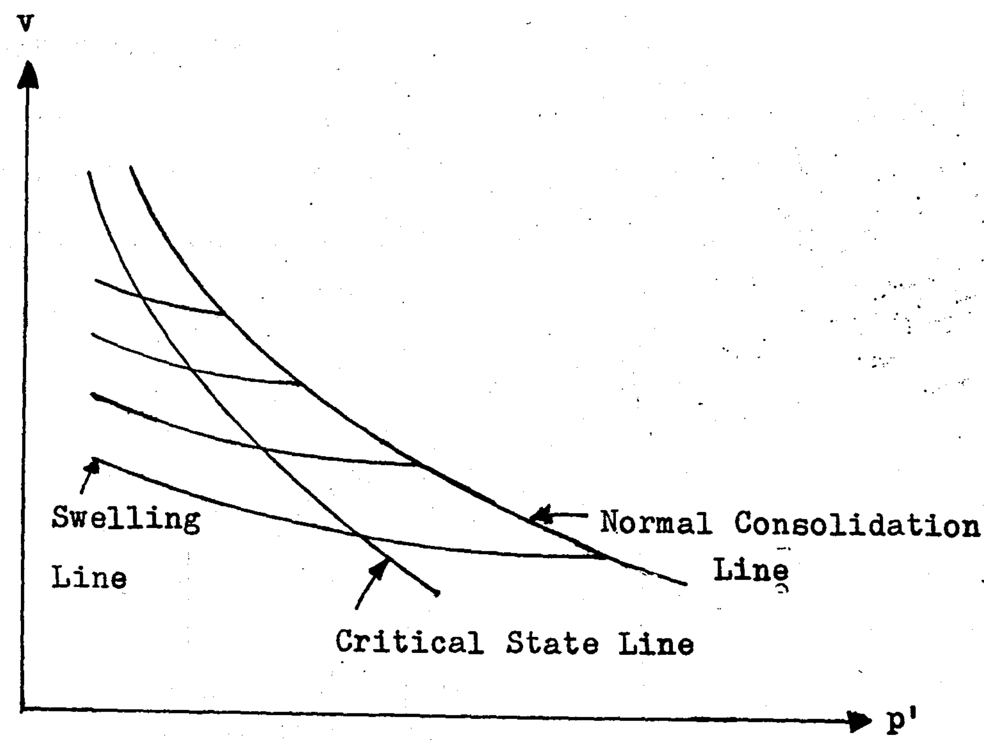

Fig 2.21 The condition of NCL, CSL and swelling line on v : p' space.

The dissipated energy becames

$$\frac{\dot{W}}{v} = q\dot{\varepsilon} \qquad \text{Eq. 2.38}$$

$$\frac{\dot{W}}{v} = M\,P\,|\dot{\varepsilon}| \qquad \text{Eq. 2.39}$$

At the critical state line, the dissipated energy is independent from v as seen in equation 2.38 and equation 2.39 .

The assumption on the theory of plasticity is that the failure surface represent irrecoverable potantial power. From definition, the normality of the irrecoverable potantial power gives us the increament of deformation vector. So that the amount of irrecoverable deformation of the specimen which is loaded to its elastic limits can be found from its condition on the failure surface.

Calladine (1963), explained that the loading and unloading path of a specimen in the q': p': v space are found on an elastic wall on the swelling line as seen in Fig 2.22

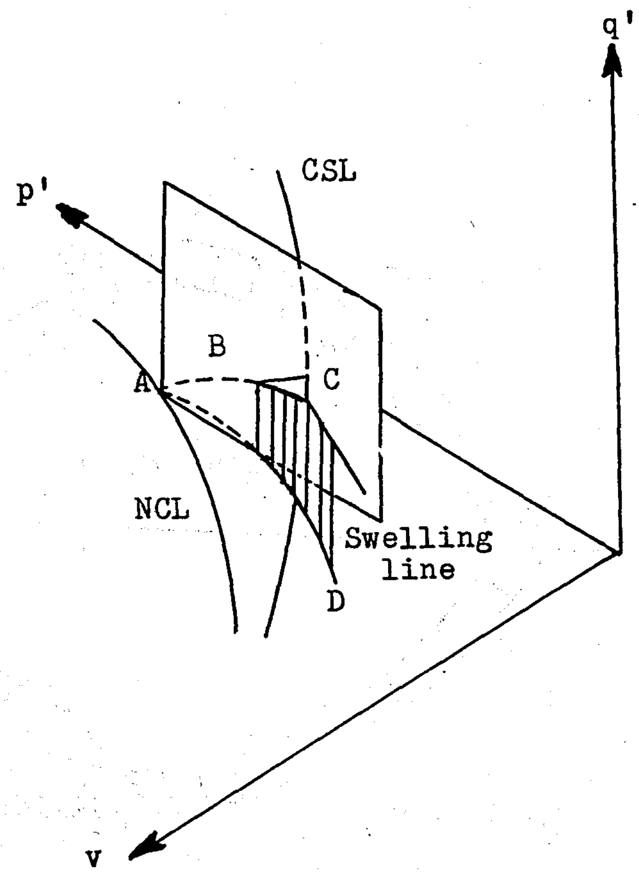

Fig 2.22 An elastic wall and undrained plane on q' : p':v space

If the load is increased after B in Fig 2.22 irrecoverable deformation occures on the specimen. Therefore, the specimen may be moved towards a point on another elastic wall. During this phenomeno the condition of the specimen is represented as a stress path on the yielding surface.

The q':p' space is divided to two regions by the critical state line area of stability and area of instability. If the specimen are found in stability region it hardens during testing procedure, but if it is found in the instable region, it softens during testing proces. Fig 2.23 shows stability, and instability regions.

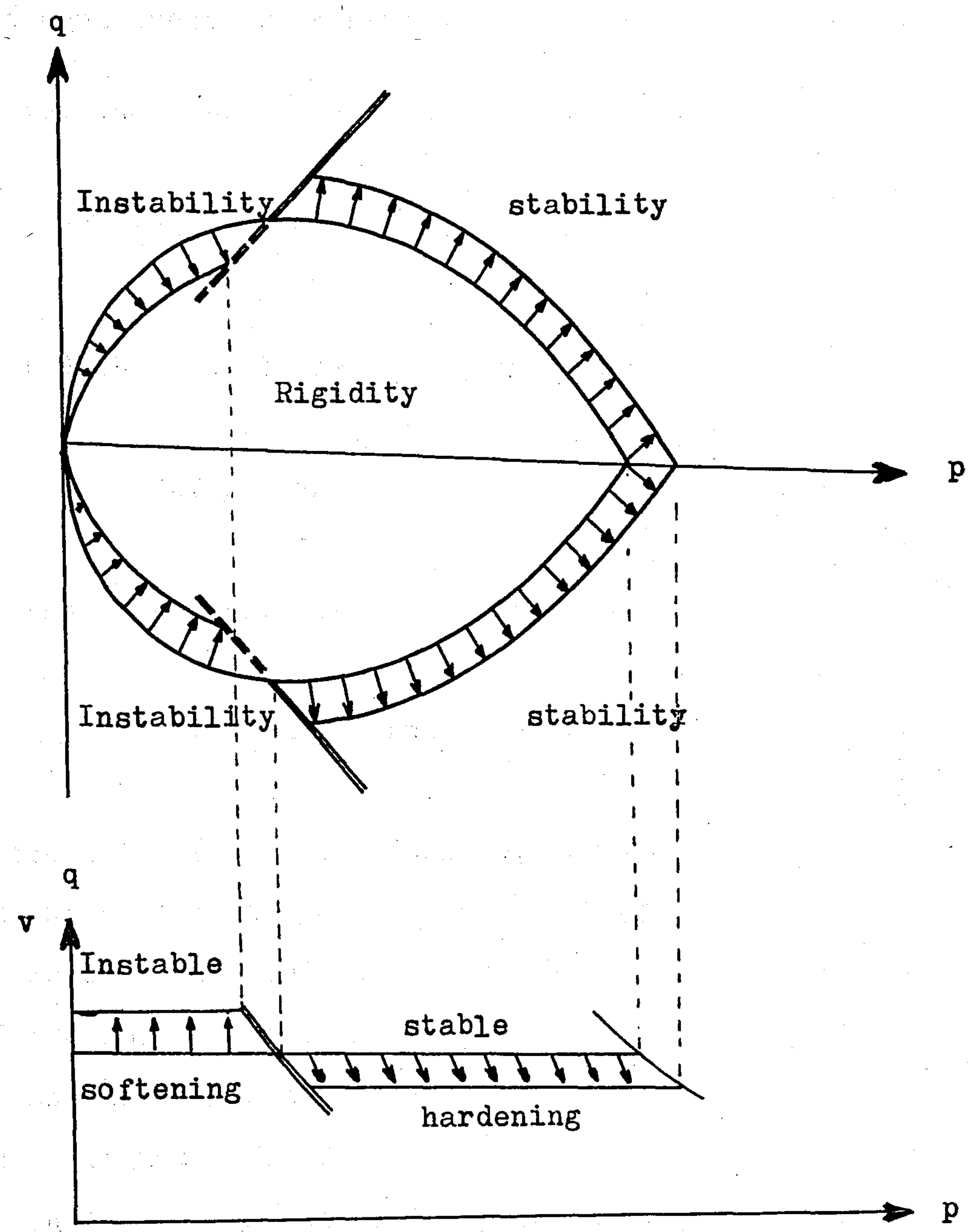

Fig 2.23 Rigidity, stability, and instability

It is important to appreciate that yield of the specimen has permanently moved its state from one swelling line with associated yield curve to another swelling line having a different yield curve. It is the shift of K-line, measured as $\dot{v}_K$, that allways represents the plastic volume change $\dot{v}^p$ and governs the amount of distortion that occurs.

As a consequence we distinguish between specimens

(a) Those that are weak at yield when

$$(|q| / p) < M \quad \text{and} \quad \dot{v}_K = - \delta v_K > 0$$

(b) Those that are strong at yield when

$$(|q| / p) > M \quad \text{and} \quad \dot{v}_K = - \delta \dot{v}_K < 0$$

(c) Those that are at the critical states given by

$$|q| = M p \quad \text{and} \quad v = \Gamma - \lambda \ln p$$

In condition (a) at the failure, the sample is compressed and the soil particles approach each other.

In condition (b) at the failure the volume is extented and the specimen softens.

And in (c) during the failure volume does not change and is not defined.

During the consolidation process, important different may occure in the soil particle, and they are reoriented in the sample,but any shape change is not appear. An overconsolidated sample behave a non-linear elastic media.

2.8 COMPLETE STATE BOUNDARY SURFACE

We can now define the complate state boundary surface and the position of the critical state line on it.We now that the curved Roscoe surface joins the normal consolidation line to the critical state line and that the Hvorslev surfave extends up to the critical state line from the other side. The most precise representation of the complate state boundary surface is to plot the surface in $q' / p'_{ei} : p' / p'_{ei}$ space, as shown in Fig 2.8.1. The shape of the complate boundary surface can be represented more graphically in $q' : p' : v$ space as shown in Fig 2.8.2; allowing for the change of view, the shape of any constant specific volume (v) section of the surface can be seen to be the same as that shown in Fig 2.8.1.

The critical state line forms a ridge separating the Roscoe and Hvorslev surfaces, and its height and gradient increase as the mean normal effective pressure increases.

We can now find the intersection of different test planes with the state bondary surface. An undrained plane is identical with a constant v section of the surface and has the shape illustrated in Fig 2.8.2. We note that the critical state is the state at which the maximum value of q' can be sustained by a sample if it is tested undrained.We would expect if con-

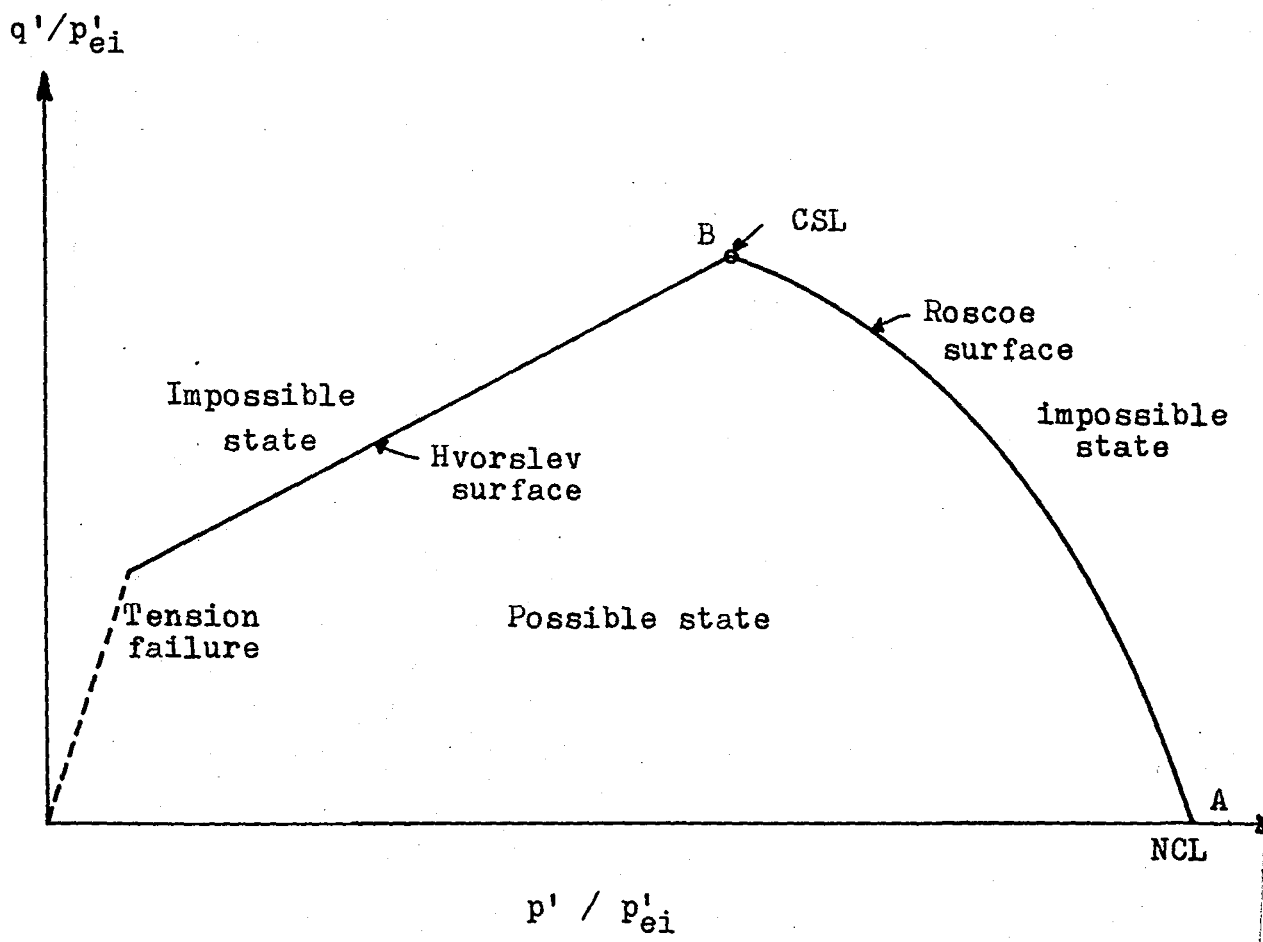

Fig 2.8.1 The complate state boundary surface in $q' / p'_{ei} : p' / p'_{ei}$ space.

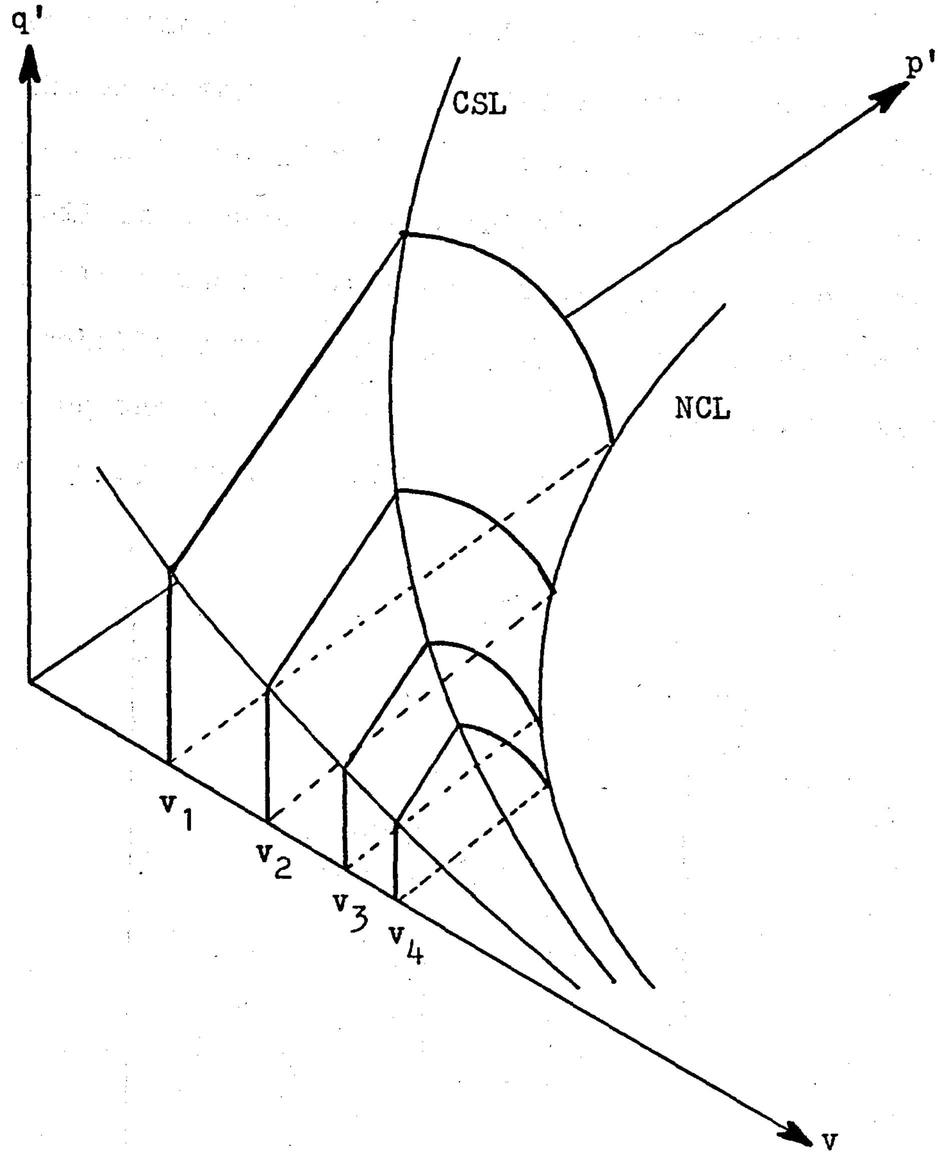

Fig 2.8.2 Constant specific volume planes in $q' : p' : v$ spaces

ditions within a sample were uniform, that undrained tests on heavily overconsolidated samples would follow paths which rose almost vertically upto the state baundary surface, in the same way as observed for lightly overconsolidated sample. The paths would then be expected to traverse the surface until failure occured at the critical state line. There is the possibility that failure of a triaxial sample occure prematurely probably soon after the sample reaches the Hvorslev surface even though the undrained paths folowed by uniform element of clay would be those shown in Fig 2.8.3

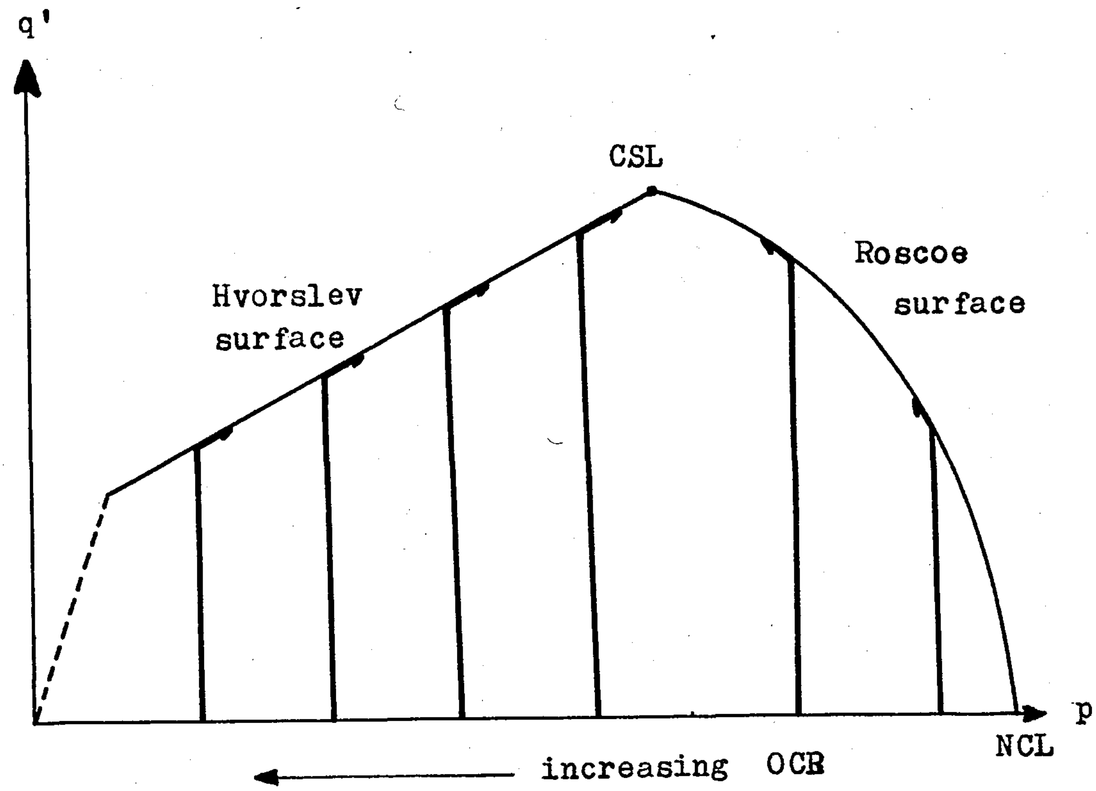

Fig 2.8.3 Expected undrained test paths for samples at different OCR's

Data from a family of undrained tests on kaolin conducted by Loudon (1967) are illustrated in Fig 2.8.4 the general pattern of the behaviour is what we expect, except that the sharp corners of the in Fig 2.8.3 have been rounded off.

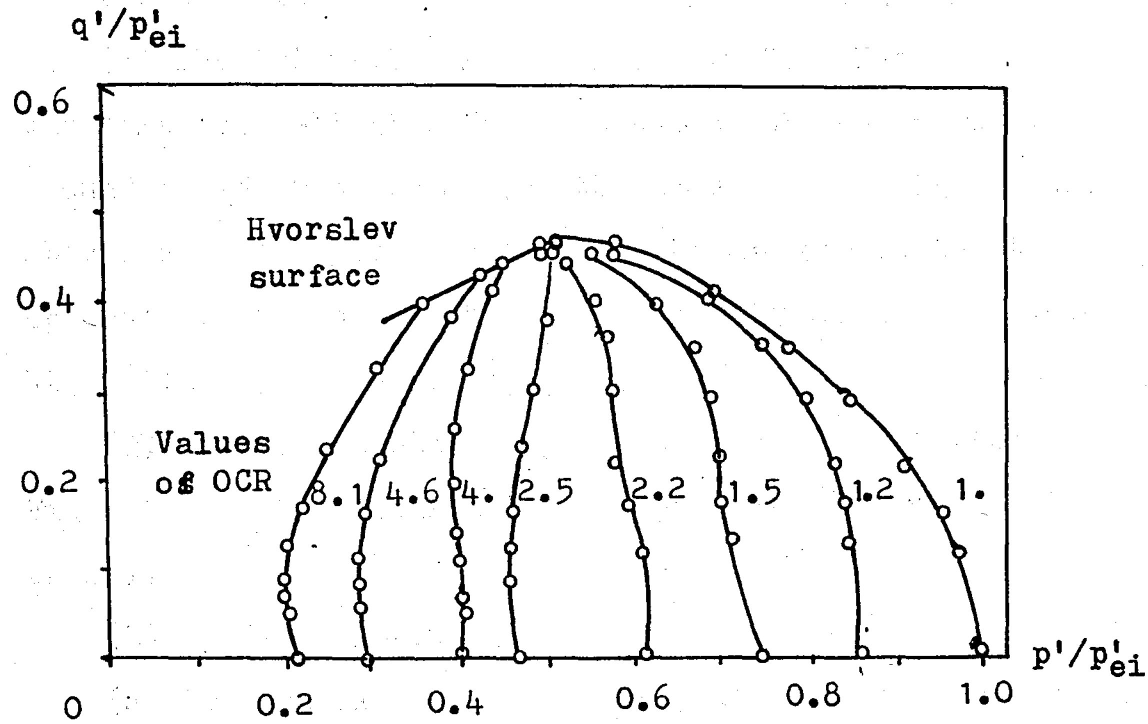

Fig 2.8.4 Normalized stress paths for undrained tests on overconsolidated samplesof Kaolin Clay (after LOUDON, 1967)

CHAPTER 3 EXPERIMENTAL STUDY

3.1 EQUIPMENT

The triaxial equipment consist of the following items

(1) The triaxial cell shown in Fig 3.1. The purpose of the triaxial cell is to confine the sample under an all around fluid pressure and at the same time provide a suitable means of applying axial load to the end of the test specimen.it is constructed for a cylindrical sample 8.0cm high with a 3.57 cm diameter.

(2) Constant pressure application system are shown in Fig 3.2 (Cell pressure and back pressure are provided by them).

(3) Loading system

(4) Proving ring and two dial-gauge (Proving ring provides a continious measurement of the force acting at the piston. The high tensile steel proving ring is equipped with a mechanical dial-gauge for measuring the deformation of the ring. This dial-gauge is graduated in divisionof 0.002 mm. Another dial-gauge mounted on the proving ring measures the vertical deformation of the test specimen,this dial-gauge is graduated in division of 0,01 mm.

(5) Pores filter stone: The pores filter stones prevent the fine soil particles from being washed out of the sample. The filter stone should be boiled in water before each test to remove any soil particles and air bubbles imbeddedin the porous.

(6) Rubber membrane, O-ring and two cm wide rubber band. the rubber membrane surrounds the sample and the water in the

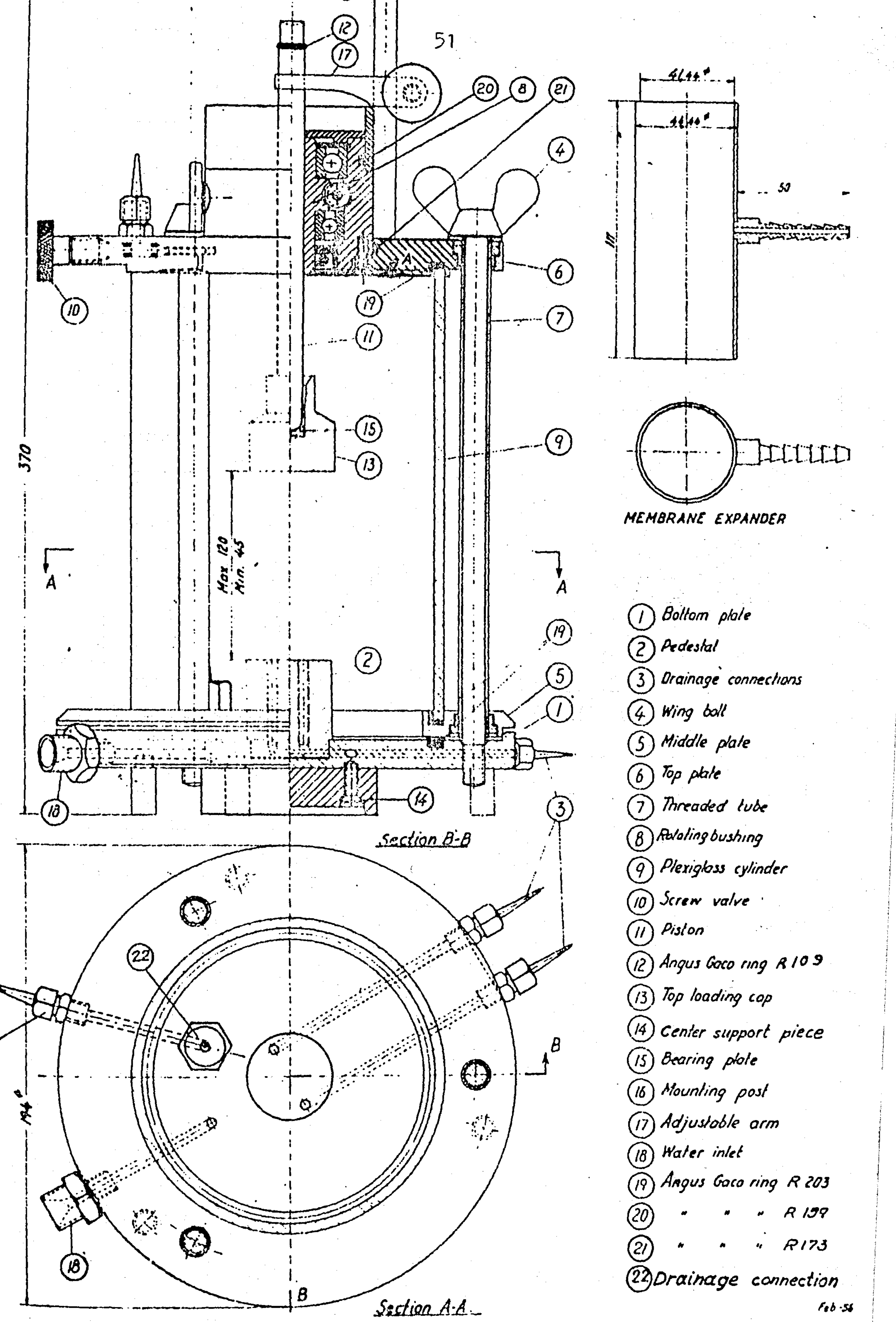

Fig 3.1 Triaxial Cell

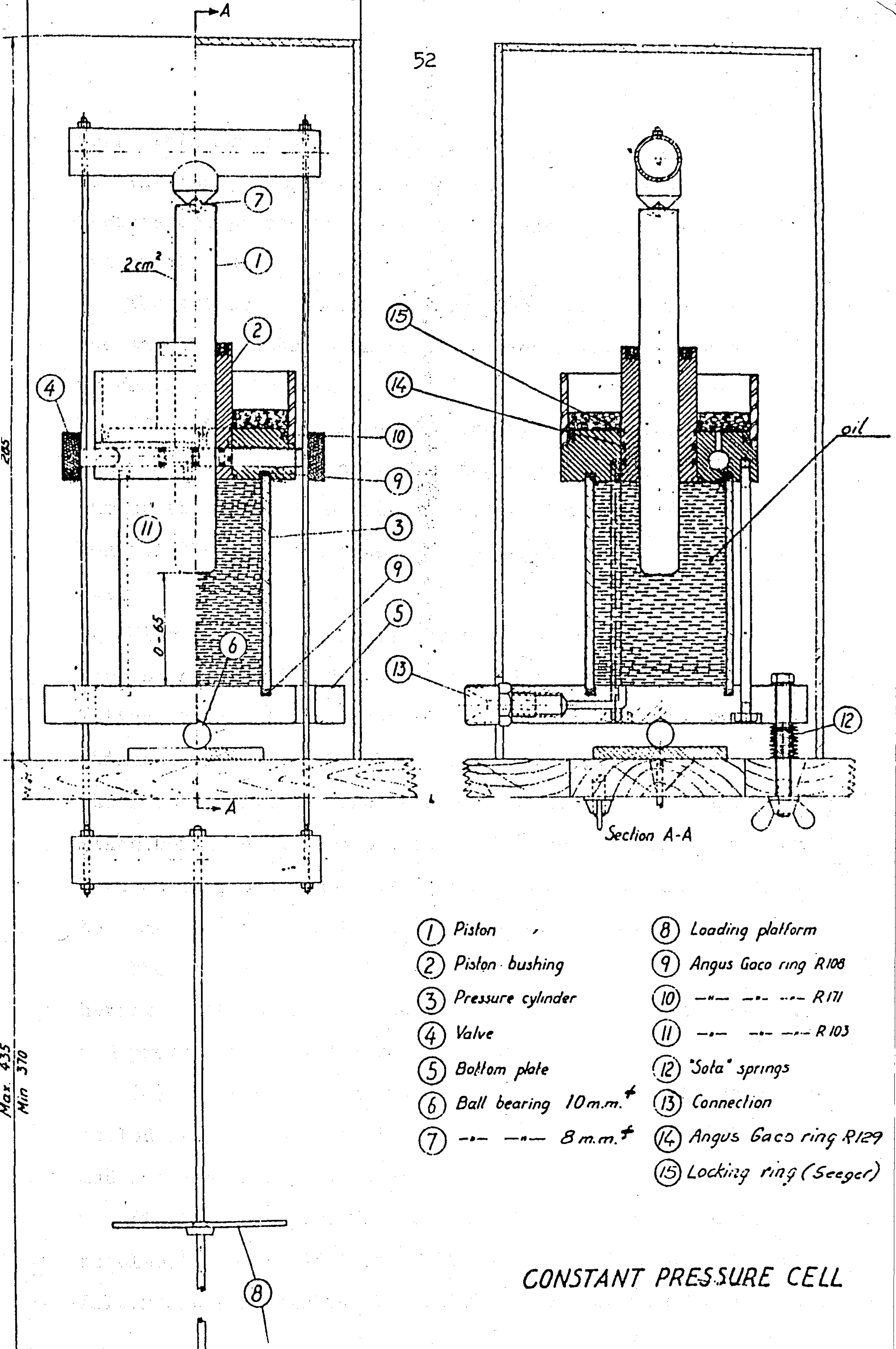

Fig 3.2 Constant Pressure Cell

cell. This membrane should be as thin as possible in order to minimize pressure exerted on the sample as its expands. O-Rings are placed to seal the membrane on the lower pedestal and the cap.

The two cm. rubber bands are placed on the ends caps of the sample to asure a tight connection between the rubber membrane and the caps.

(7) trimming apparatus, including wire saw, cradle, calliper and aluminium foil. Trimming apparatus holds the sample during the trimming operation and has trimming edges that control the final diameter of the sample. It is shown in Fig-3.9

Wire saw is constructed by tensioning a wire between the tips of a metal " U " frame. And adjusting screw for regulating the tension in the wire is provided at the tips. The thinnest wire possible should be used. Cradle is used to hold the sample while the ends are being trimmed. Its length detrmines height of the sample end its trimming edges assure than both ends of the smaple are parallel. And the calliper is used to measure the diameter of the sample.

The aluminium foil is used to prevent the sample from adhering to the metal surface of the cradle, trimming apparatus and protect the sample from drying.

(8) burette: the burette is used to measure the water expelled from the sample. It is graduated in o.1 ml division and has a capacity of 25 ml.

(9) Filter paper: The purpose of the filter paper is to accelerate coonsolidation of the sample during the test. The filter paper is slotted to minimize restriction of the sample

deformations. It is shown in Fig 3.3

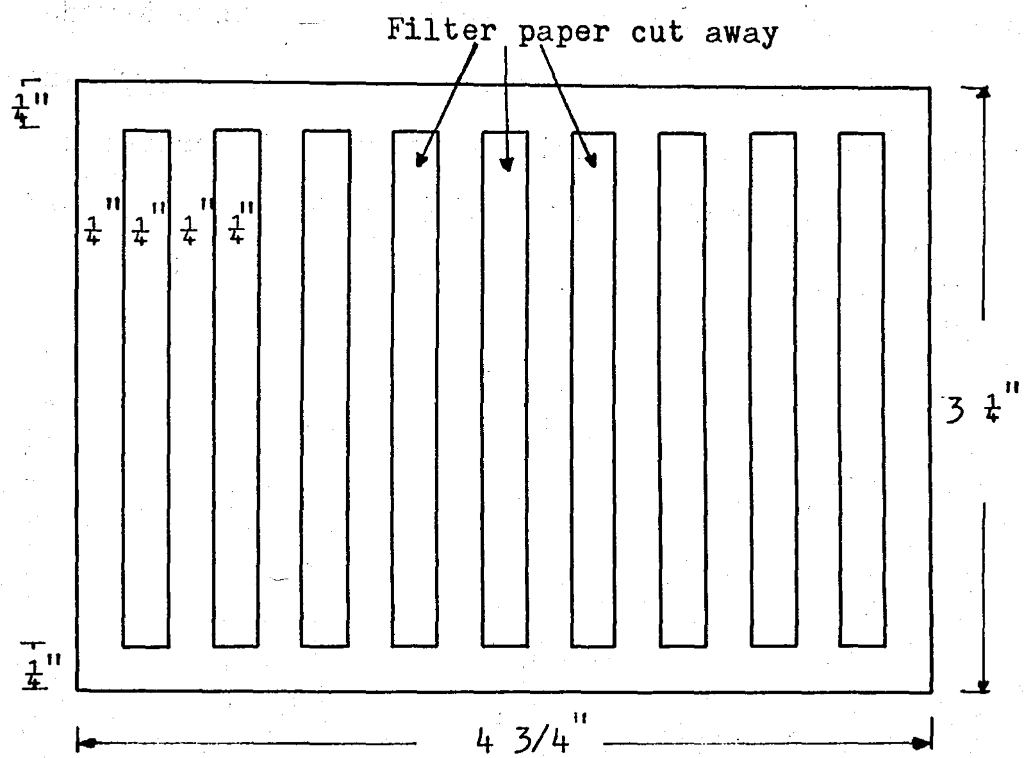

Fig 3.3 Details of side drains for 38 mm.diameter sample

3.2 TESTING PROCEDURE

3.2.1 Material and Sample Preparation

The material used in the tests are first dried in the oven and then sieved from a No=40 sieved. To prepare triaxial specimens, the material is first trougly mixed with sufficient water. The water content for test specimens are choosen to be the optimum water content optained from standart compaction test. Then the water-clay mixture is left for curing for 12 haurs, so that water could disperse trough the clay particles.troughly. After this, samples are optained by compacting it in a standart proctor mold. The samples are compacted in five layers with 16 drops each layer.When we prepared the specimen in three layers with 25 drops to each layer it showed nonuniform behaviour during the consolidation process. Sample prepation apparatus is seen on Fig 3.4 and Fig 3.5

A series of standart proctor tests are performed and the water content vs dencity curve is plotted as seen on Fig 3.6

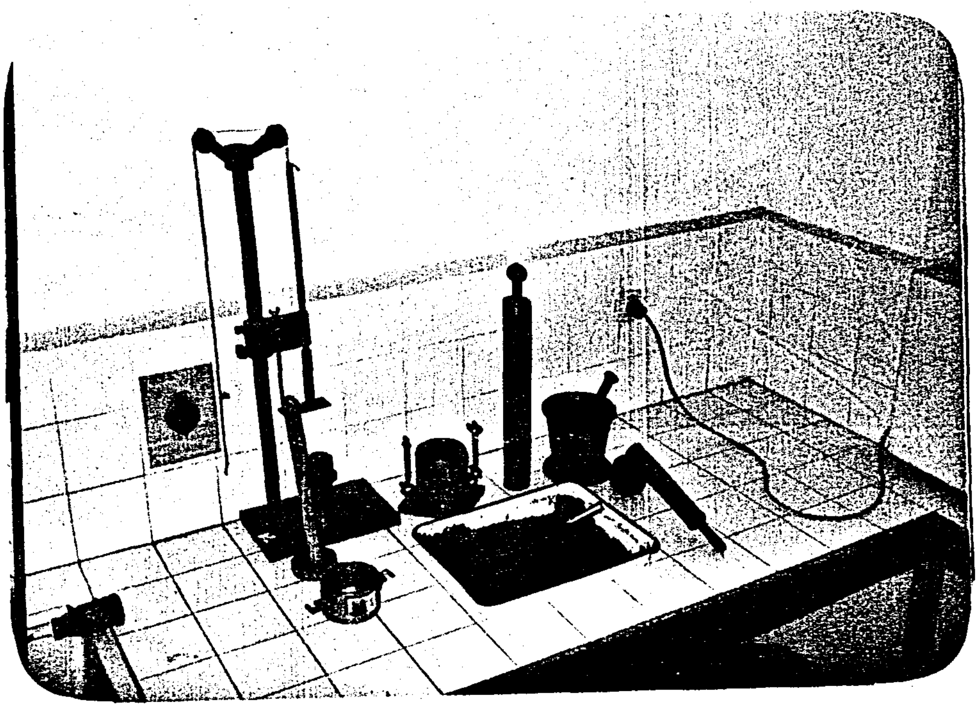

Fig 3.4 Sample preparation process and apparatus

Index properties optained from labaratory tests are given below.

$$LL = 50.0\ \%$$
$$PL = 24.8\ \%$$
$$PI = 25.2\ \%$$
$$G_s = 2.70$$

The particle size distribution is given in Fig 3.7

Fig 3.5 Sample Preparation Process

From the standart proctor mould, the sample is optained having a diameter of 4 in. and heighh of 4.6 in. This specimen is divided into four equal pieces. The samples are wrapped with alüminium foil and protected in the moist room.Then the tri-axial specimens are prepared following the procedure below.

(i) The sample are taken from moist room just before trimming. A pice of aluminium foil are placed at each endsof the sample before positioning it in tha trimming apparatus. Then the top plate is lowered carefully until it comes in contact with the sample. Then the arm is set to prevent upwart move-

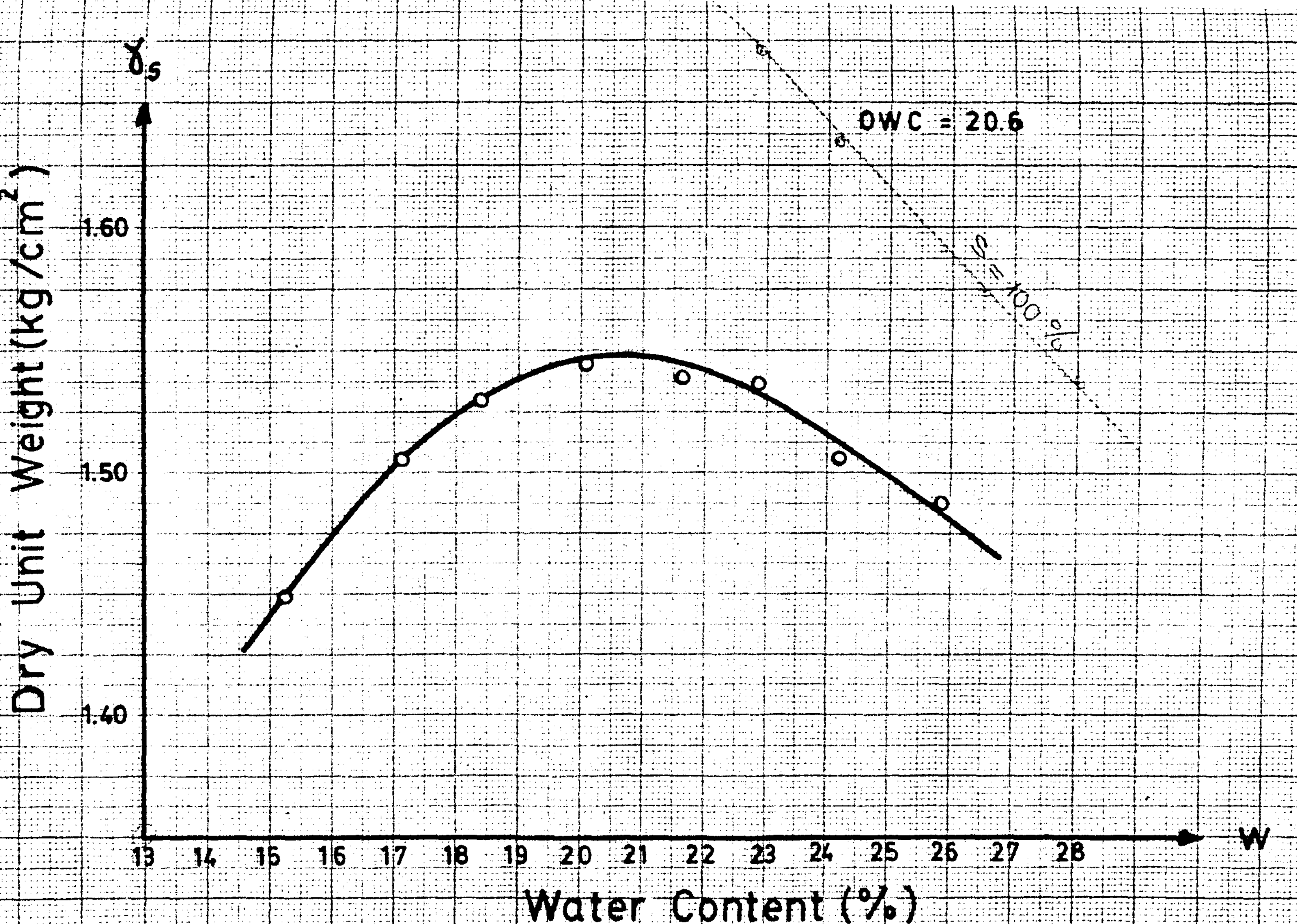

Fig 3.6 Compation Curve for Topser Sari Clay

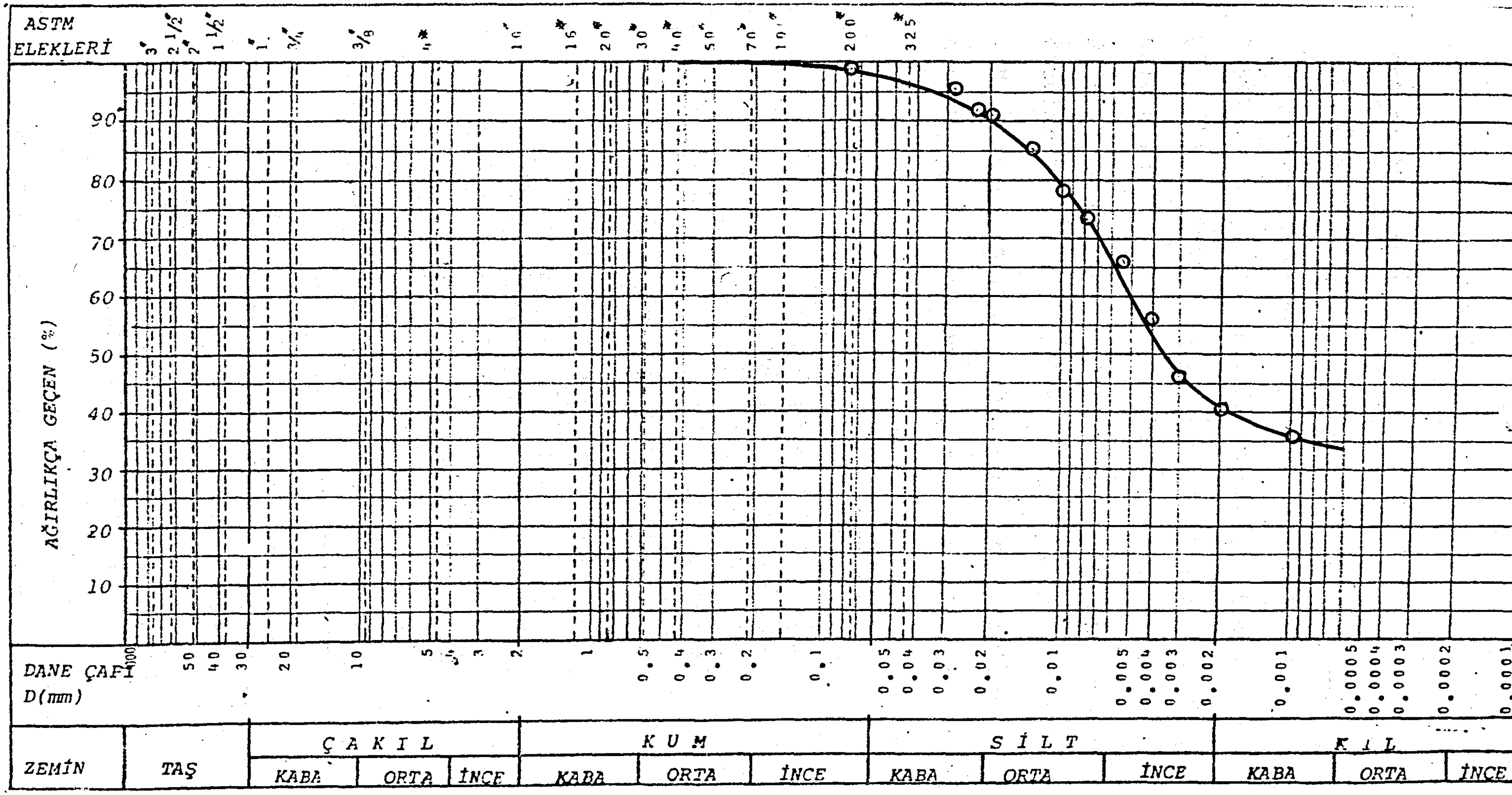

Fig 3.7 Grain Size Distribution for TOPSER SARI CLAY

ment of the shaft.

Trimming process are performed by pressing wire saw along the trimming edge of the frame, and cutting from top to bottom. During the trimming process, pieces of slices will give the surface of the sample a "wooly" texture, large slices may tear out chunks of the sample. When the trimming process is finished, the ends of the sample are cut perpendicular to its vertical axial on the cradle. Then the diameter, length and its weightare measured. Trimming process is seen on Fig 3.8 and trimming apparatus is seen in Fig 3.9

Fig 3.8 trimming Process and Apparatus

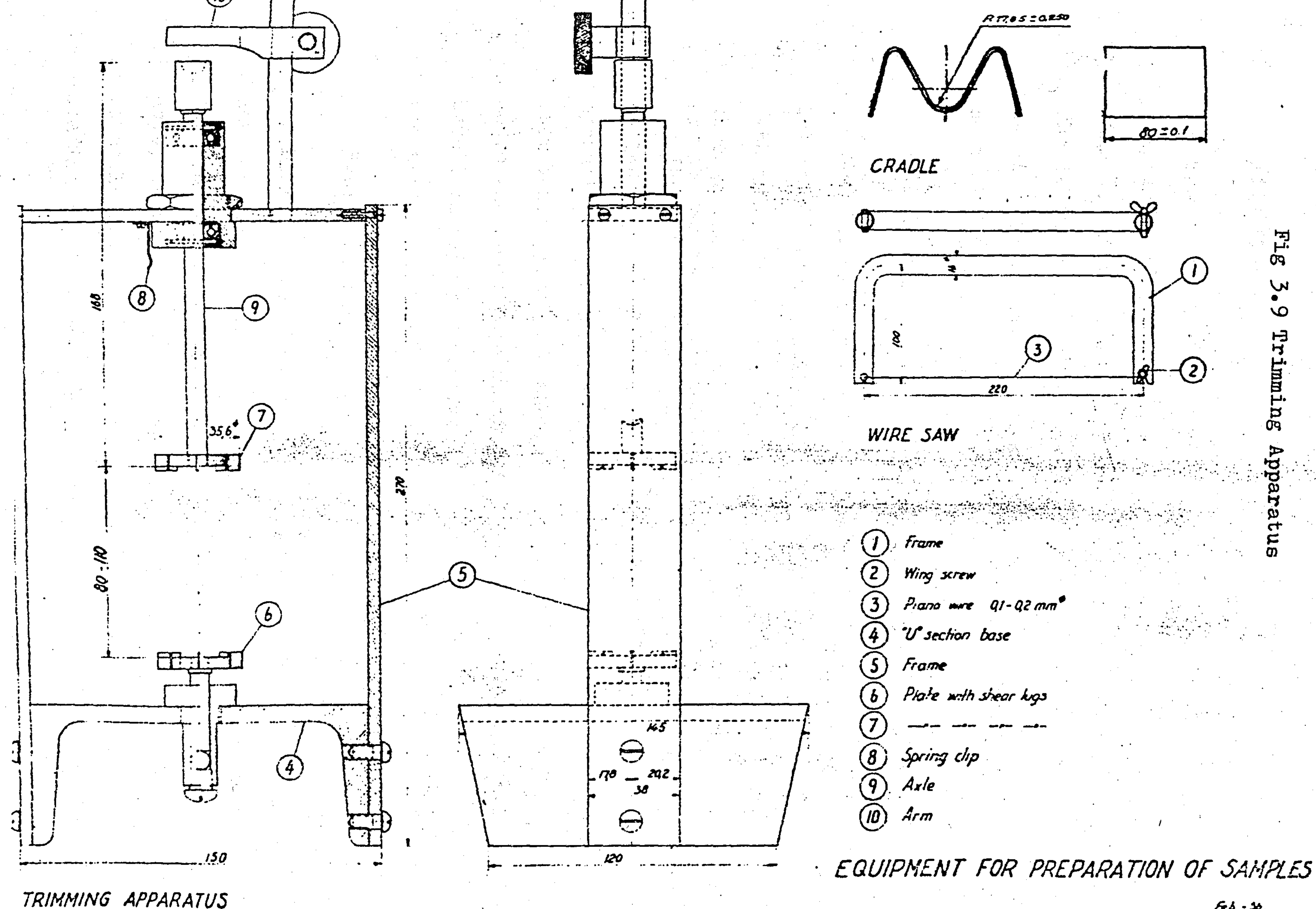

Fig 3.9 Trimming Apparatus

(ii) Placing The Filter Paper

The filter paper is saturated to prevent absorption of moisture from the sample. It is satureted by placing in a film of water. (There should be no free water on the paper). The filter paper is wrapped neatlyaround the sample, as seen in Fig 3.10 in white colour and weighed together to the nearest 0.01 gr.

3.2.2 Preparing The Triaxial Cell

Two cm. wide rubber bands are placed on the bottom pedestal and loading cap.The edge of the rubber should be flush with the surface of the cap. Then the water was allowed to flow through the entire pore-water pressure mechanizm until the system was complately deared.

The filter stone is placed, which has previously been boiled in water, directly on the pedestal. It is pressed against the pedestal. In order to protect the rubber membrane from being punctured, the rubber band is extended slightly above the upper edge of the filter stone. The valve to the buretteis closed when some water has circulated throughout the system.

3.2.3 Placing The Specimen

Besides handling the sample carefully, it is also important to prevent the formation of air bubbles on the end surfaces of the specimen. After checking the water level is exactly at the top of the filter stone,the sample is placed directly from the cradle on to the filter stone. And the loading cap is placed on top of the sample. The rubber mem-

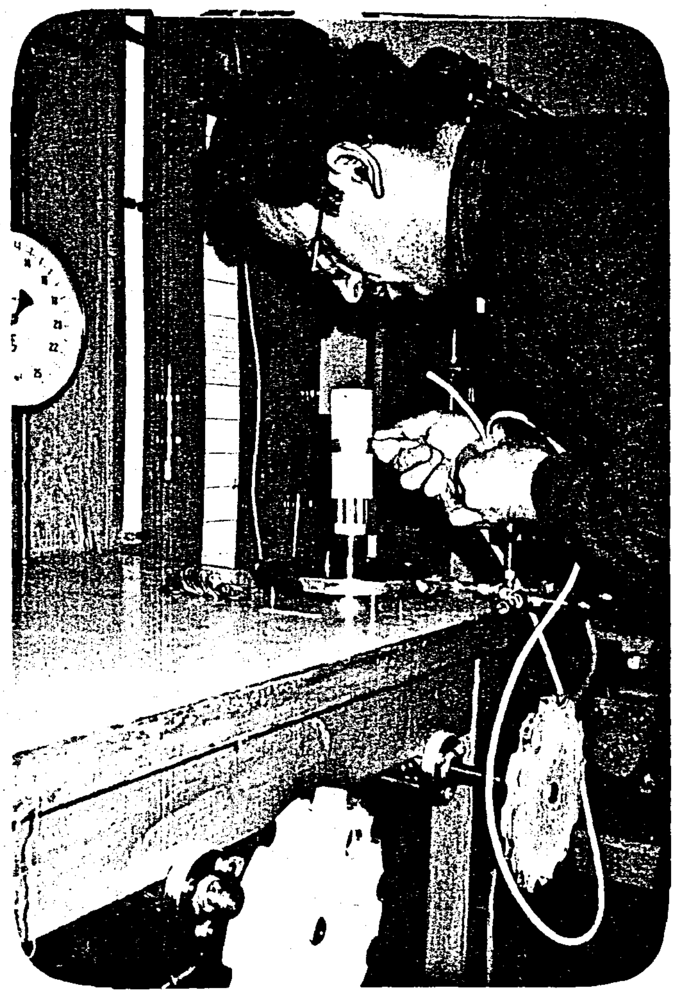

Fig 3.10 Placing The Specimen In The Triaxial Cell

brane is placed on the mounting cylinder as seen in Fig 3.10 A suction is applied to hold the membrane tight against the walls of the cylinder. The mounting cylinder is directly placed over the sample and lovered. By blowing the rubber tubing which will force the upper end of the membrane to slide over the loading cap. The fingers are used to push the bottom end of the membrane down over the pedestal. The mounting cylindeis removed and smooth out the membrane.
Two O-Ring are stretchover each ends of the mounting cylinder The cylinder is placed over the sample and rolled the lower O-ring of the end on the pedestal. Then the cylinder is removed and turned it around. Then roled the remaining O-ring on the loading cap.

The diameter at both ends and middle of the sample are measured. Two measurements are taken at each location. Position the top section of the triaxial. When lowering this upper unit over the sample, the piston must be held up so that it does not hit the sample.Three wing bolts are tigtened in a such manner that the top and bottom plates are parallel. Then the piston is allowed to fall into the socet of the loading cap.

The cell is filled with water after opening the valve top of the cell to escape the entrapped air. The water inlet is closed when the cell is full. The adjustable arm is positioned to keep the piston from being forced out by the cell presure.

After the saturation of the test spacimen, consolidation process can be started.

(a) Saturation under back pressure.

Before carrying out tests on any partly saturated ,or on stiff clays, which mould soften in contact with free water it is necessary to satureted the soil material by applying a back pressure. Increasing pore water pressure in this way dissolves the air contained in the void spaces and correct por water pressure reading to be taken. Usually a pressure of abot 2.5 kg/cm^2 is sufficient to dissolve all the air.

The standart method of ensuring full saturation is to measure the response of pore pressure to an increment of confining pressure, from which the value of pore waterpressure paremeter is calculated by definition

$$B = \frac{\Delta U}{\Delta P_3} \quad \text{when soil is 100\% saturated } B = 1$$

As mentioned before, our samples are prepared in standart compactionapparatus, therefore the saturation degree of them is less than 100%. Saturation process is as follow.

After setting up the spacemen, the cell pressure built up 3.0 kg/cm^2, and it remains constant with constant cell pressure. Another constant cellpressure adjusted to 2.5 kg/cm^2 and connected with the drainage system of sample is poned. After 24 hours the B value is checket. If a B value is close to one,the specimen is used as a test specimen.

After achiving saturation process, the cell pressure decreased to 0.1 kg/cm^2 step by step. At the same time also back pressure decreased to zero with decreasing cell pressure.Then water is circulated through the drain system and connected with the burette. After all air bubbles disappear in the drainage system, the connection of back pressure line is closed. And the water level in the burette is recorded. Then the consolidation process is started. The triaxial cell pressure is increased to consolidation pressure. And regularly the dissipated water from sample is recorded from the burette. The consolidation process is terminated when the water level in the burette is approximately constant.

After consolidation process is terminated. For overconsolidated specimens, the cell pressure is reduced from normal consolidation pressure to swelling pressure step by step. Before this, the water level in the burette is recorded and then the burette valve is left open. So swelling process is started. The water level in the burette is observed after 24 hours. If its level remain constant, the swelling process is terminated, if not, it is continued until its decreasing remain constant. After this process the overconsolidated specimen is ready for testing. Consolidation (on right) and swelling (on left) processes are seen in Fig 3.11

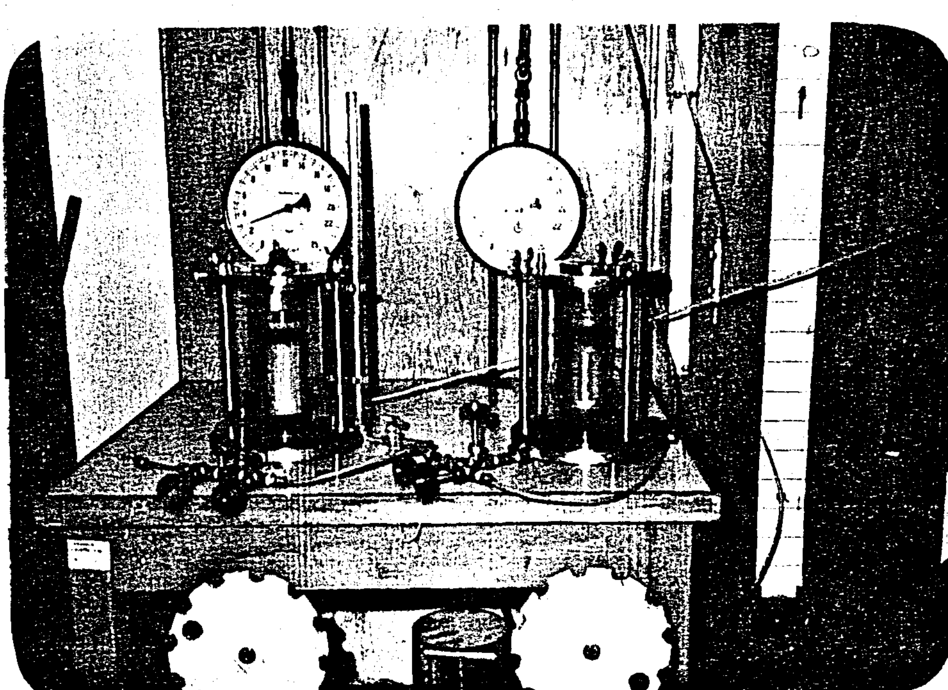

Fig 3.11 Consolidation and Swelling Processes

The upper unit of consolidation cell is taken out when consolidation procedure terminates. Then we measure the diameter of the specimen at top, bottom and middle, then also measured its length. After this, the upper unit of the loading triaxial cell is set up as mentioned before.

3.2.4 Placing The Traxial Cell To The Loading Apparatus

The loading table is lowered by hand and the cell placed on the table of the press. The proving ring is connected to the yoke with rubber rings. The yoke is lovered until the lower end of the ring is almost in contact with the arm holding the piston, then the arm removed and allowed the piston to slide upwards until it comes in contact with the proving ring.The loading table is rised by using small hand-wheel until the dial- gauge of the prowing ring indicates that the piston has come in contact with the sample. The gauge is adjusted to zero. Also onother dial-gauge on proving ring is adjusted to measure the vertical displacement. Before test is started, the center lines of the piston and proving ring must line up. If the center lines do not line up, the following items shoult be inspected.

(i) chek that the cell is on the center of the table.

(ii) check the wing bolts have been tightened properly.

(iii) examine the bearing points pieces on the proving ring to determine if they are loose or have moved. The proving ring must be recalibrated if one of these parts are moved or adjusted.

(iv) check that the loading table is level and that its center falls directly under the pressure point of the yoke.

3.2.5 Coupling The Pore Pressure System

When the consolidation triaxial cell is changed with the loading triaxial cell, the cell pressure is increased up to the consolidation pressure. And clean water is circulated through the drainage system. Before this process the pore pressure system must be complately saturated. After circulating clean water, is connected drain line. During the connecting process water must be flowing through the drainage, otherwise same air bubble may remain in the system. Then walfes the burette and the short circle line of the " V " manometer are closed, as seen in Fig 3. 12. And the manometer walf is opened. And then the triaxial cell pressure is remained constant at required pressure.

3.2.6 Loading The Sample and Removing The Sample

An axial compressive force is aplied to the ends of the test specimen by a constant rate of strain type loading press (Fig 3.13). the loding table is moved up by gear drive unit (in Fig 3.14) with a constant rate. The rate of strain can be adjusted by changing gear table which is explained in Fig 3.15. The rate of strain is 0.0303mm/min. When the sample reache failure condition, the pore pressure walve is closed. The pressure in the loading triaxial cell is decreased to zero. Water in the cellis emptied by opening cell pressure line. Upper unit of loading triaxial cell is remowed (in Fig 3.16) Then the O-Ring at each end of membrane is taken out. And membrane is taken out with extreme care. The sample is removed from the loading pedestal and weighted. After that it

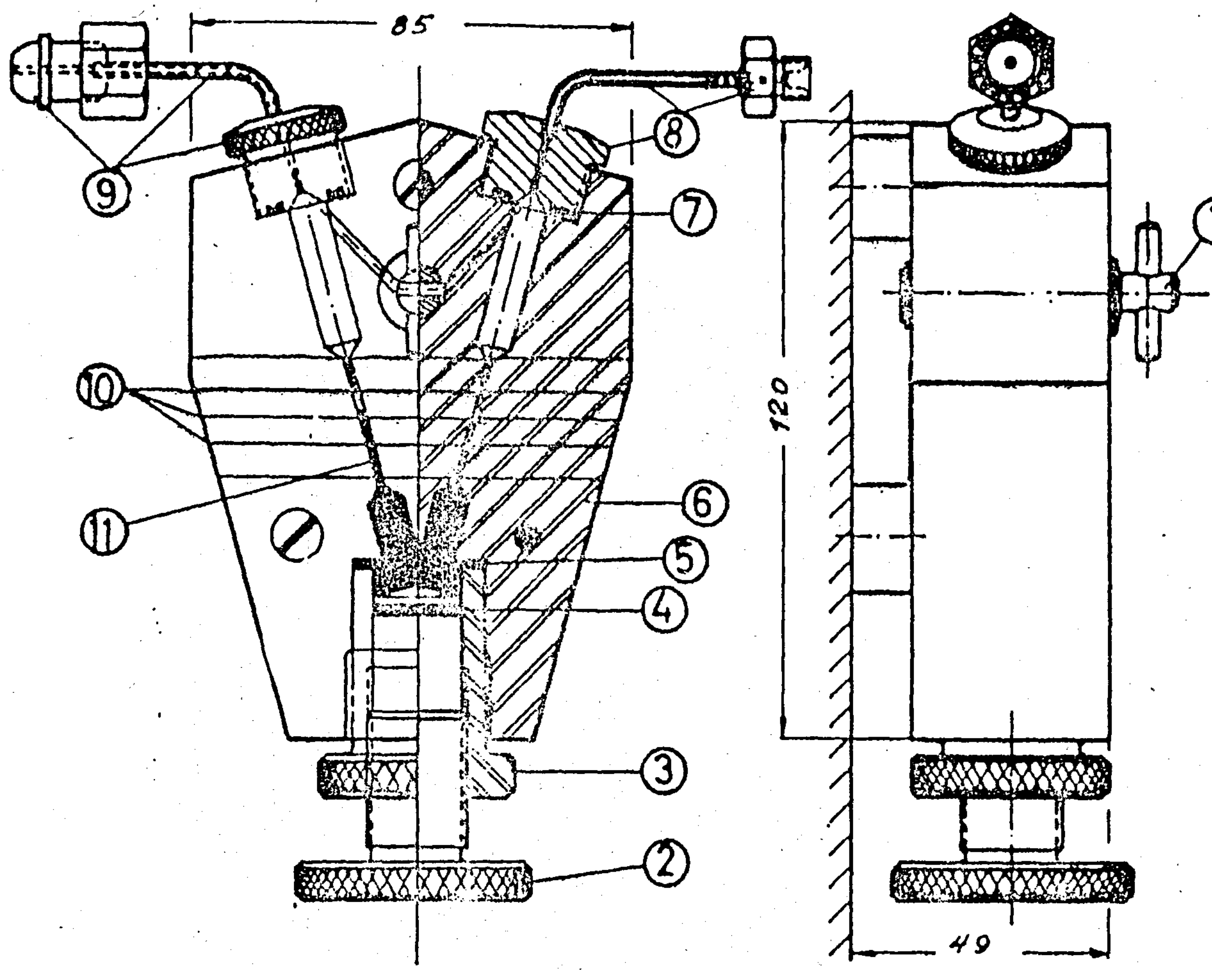

1 Cock
2 Adjusting knob.
3 Mercury container.
4 Angus Gaco ring R 115
5 Angus Gaco ring SOR 132
6 Housing.
7 Angus Gaco ring R115.
8 Coupling for copper tubing.
9 Connection
10 Pressure reference lines
11 Mercury

Lengths in millimetres

Fig 3.12 Pore Pressure instrument

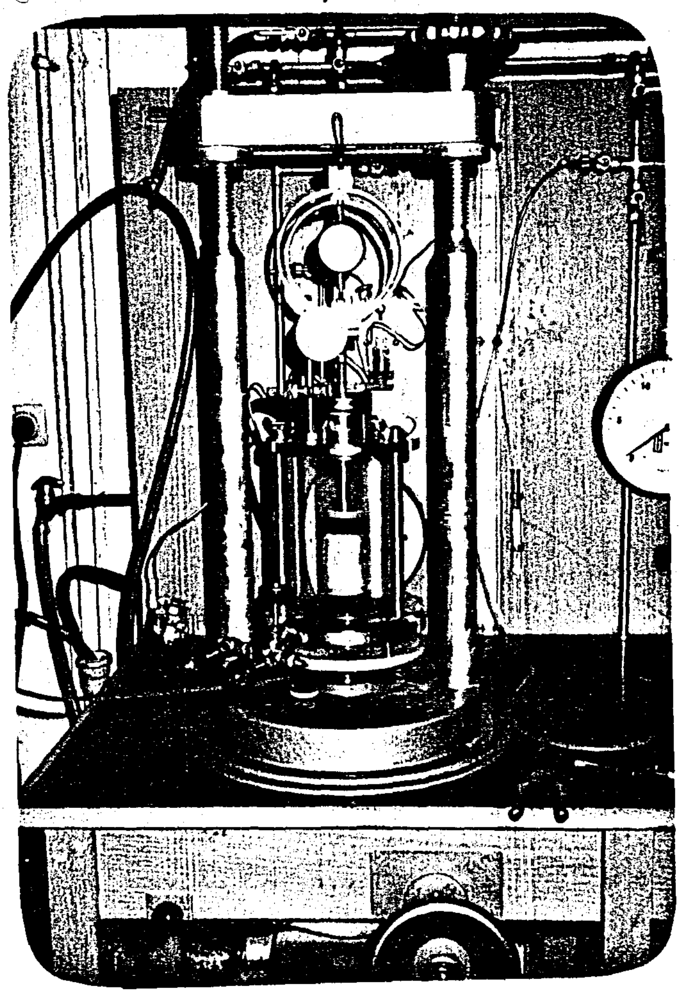

Fig 3.13 Testing Process

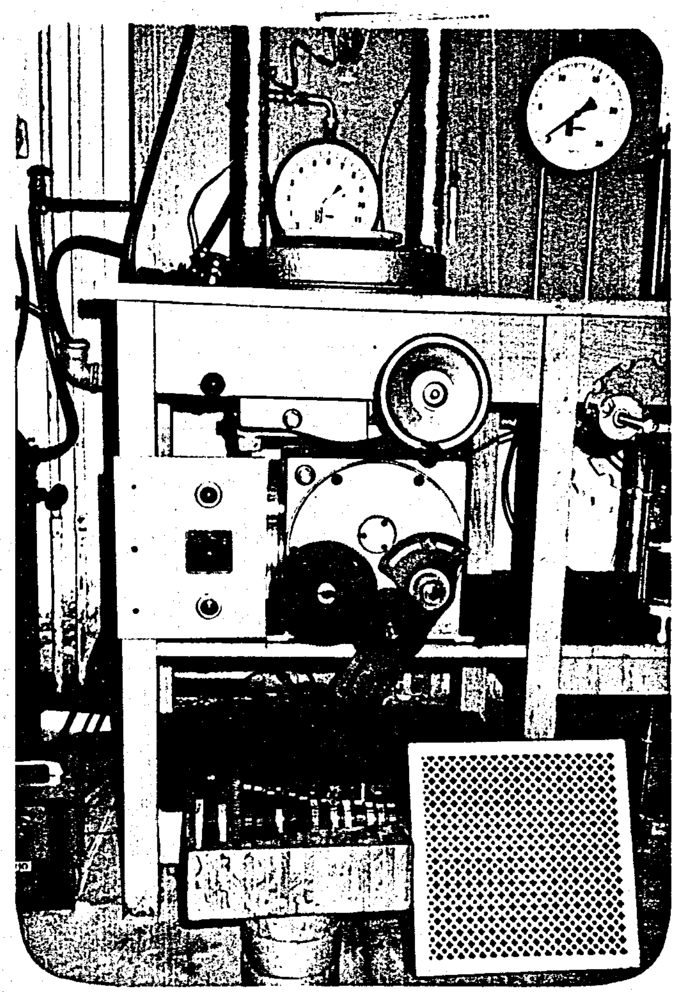

Fig 3.14 Self Compensating Gear Drive Unit

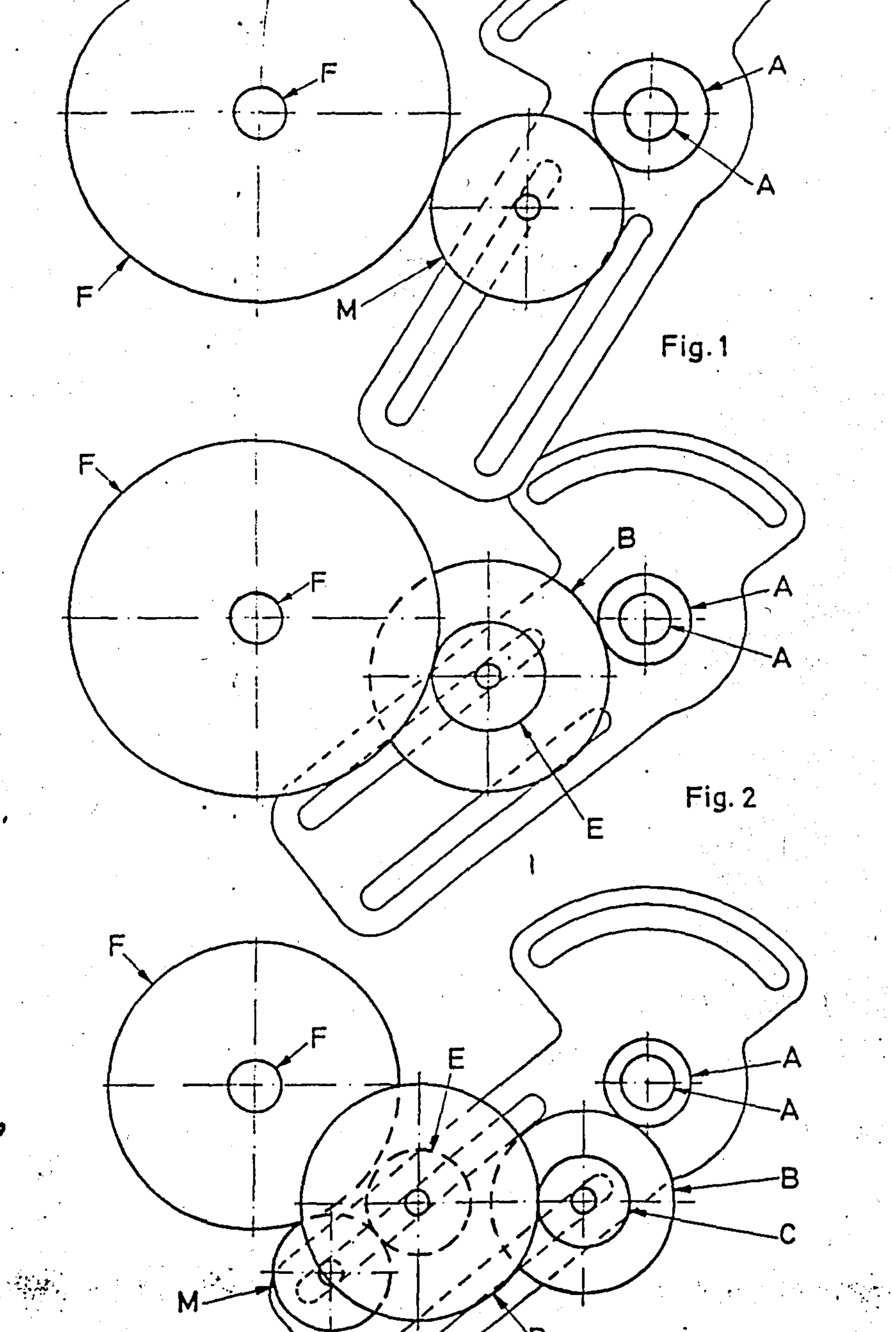

V = TIME / 10 mm

Day	Hour	Min.	Sec.	Fig.	M	A	B	C	D	E	F	U= $\frac{A \times C \times E}{B \times D \times F}$
		7	25	2		96	40			60	30	4,8
		11	50	2		96	50			63	40	3,024
		14	59	1	72	96					40	2,4
		22	42	1	40	96					60	1,6
		30	35	1	71	72					60	1,2
		44	50	1	71	60					72	0,8333
		55	26	2		82	50			40	96	0,6833
	1	16	28	1	82	24					47	0,511
	1	28	44	1	82	28					63	0,4449
	2	18	35	1	50	29					96	0,302
	4	39	15	2		24	72			50	96	0,1736
	5	36	22	2		28	63			33	96	0,15277
	9	16	23	2		24	63			28	96	0,1111
	23	43	5	3	32	24	46	24	60	25	72	0,07246
1	3	24	26	3	32	24	46	24	63	25	72	0,0690131
2	19	23	43	3	32	24	50	24	71	25	72	0,056338
3	16	5	43	3	32	24	46	24	60	25	96	0,054348
4	13	8	40	3	32	24	46	24	72	25	82	0,053022
4	16	7	16	3	32	24	60	24	72	25	63	0,05291
10	6	40	00	3	32	24	50	24	60	25	96	0,0500
11	22	49	18	3	32	24	47	24	72	28	96	0,0496454
14	16	22	52	3	32	25	50	24	71	28	96	0,04929577
21	1	27	52	3	32	24	50	24	72	25	82	0,04878049
513	21	20	00	3	32	24	63	24	72	72	72	0,047619

NB.

This table is based on the motor's speed without load. The speed will decrease with increasing load to a maximum of 7% at full load.

I/s Morsco Oslo, pat.nr. 78431

FIG. 3.15 GEAR TABLE

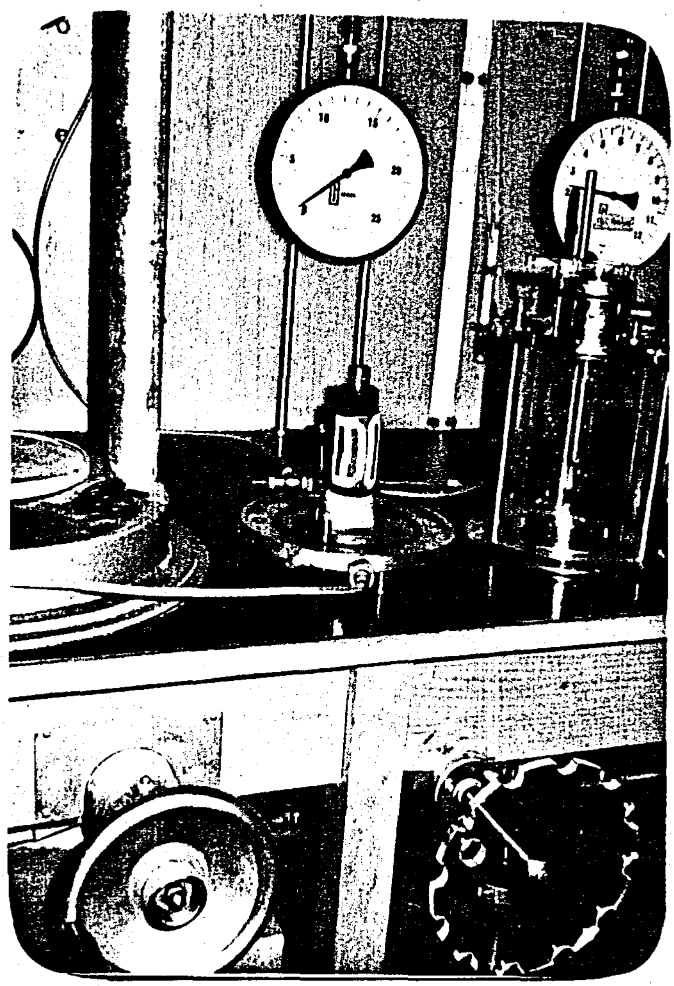

Fig 3.16 Removing The Specimen After Testing Process

is divided into several silices and weighted seperately.The water content of these silices are determined seperately. In Fig 3.17 and Fig 3.18 represent general view of the tri-axial apparatus.

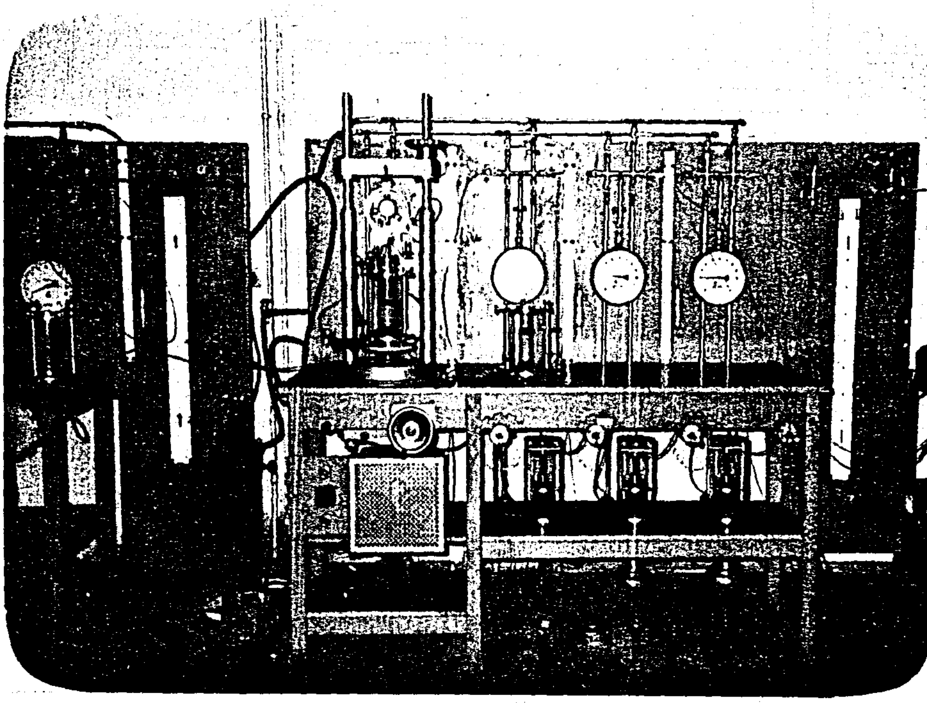

Fig 3.17 The Triaxial Apparatus

Fig 3.18 Shematic View of Triaxial Apparatus

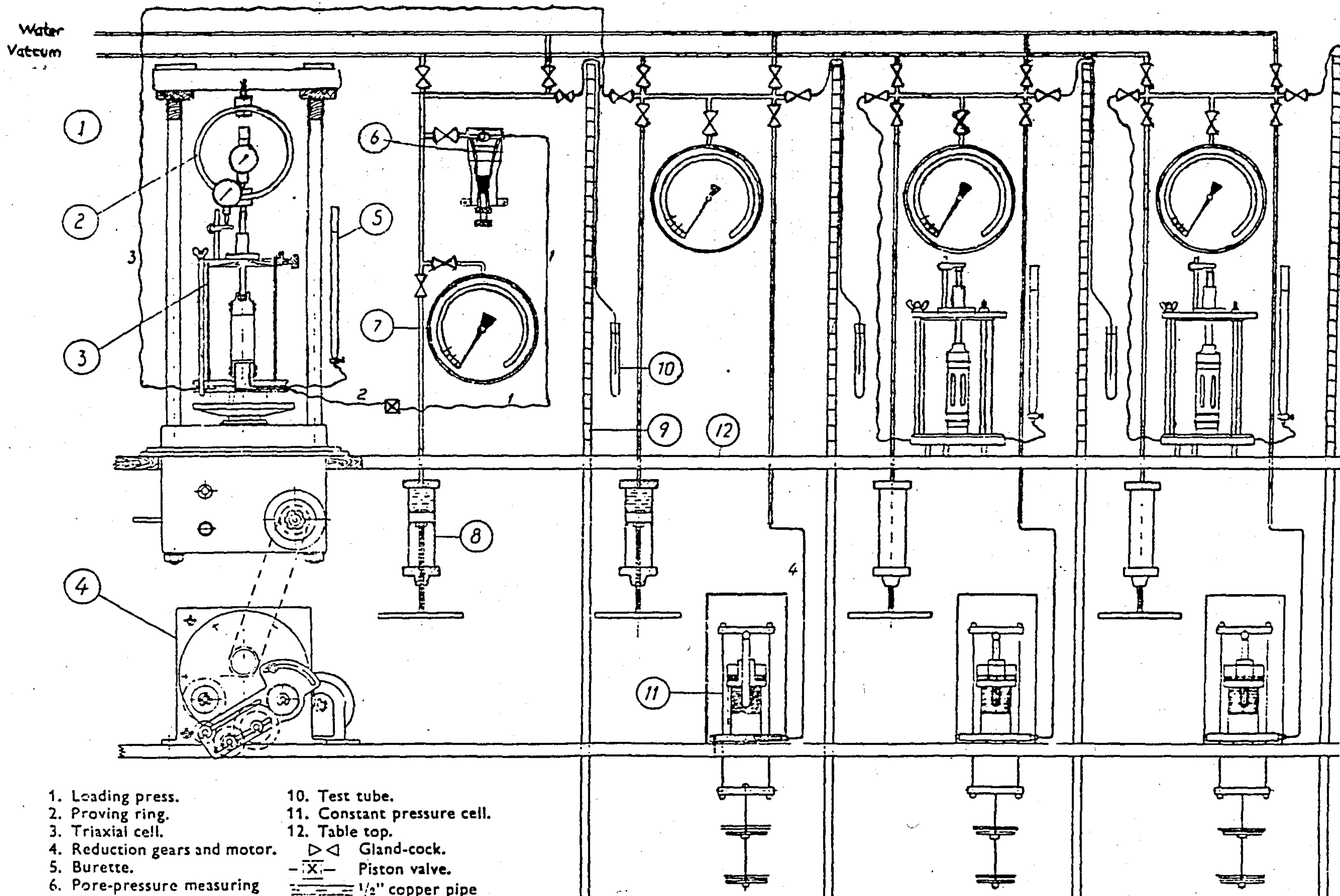

1. Loading press.
2. Proving ring.
3. Triaxial cell.
4. Reduction gears and motor.
5. Burette.
6. Pore-pressure measuring devise.
7. Bourdon gage 0-12 kg/cm².
8. Screw control.
9. Mercury-water manometer.
10. Test tube.
11. Constant pressure cell.
12. Table top.

▷◁ Gland-cock.
–X– Piston valve.
═ 1/2" copper pipe
1 — 1/8" O.D.-copper tubing.
2 — 1/8" » plastic tubing
3 — 1/4" » » »
4 — 1/4" I.D. » »

Fig. 1. Triaxial unit consisting of one loading press, one pore pressure instrument, and three cell chambers, each with a constant pressure cell.

3.3 EVALUATION OF TEST RESULTS

The avaliable data optained from the tests is processed as follows.

Deviatoric stress is calculated from axial load increment wich is divided by the average cross-sectional area of the specimen. the simple equation is

$$A = A_o \times \frac{1 - \Delta V / V_o}{1 - \varepsilon} \qquad 3.1$$

where

A = average cross-sectional area

A_o= initial cross-sectional area after consolidation process which is V_o / l_o

ΔV= change in volume

ε = axial strain which is $\Delta l / l_o$

Δl= change in axial length

l_o= initial length after consolidation

In undrained test on saturated soil ΔV is zero and hence the actual area is a function of axial strain only. then equation 3.1 becomes

$$A = A_o \times \frac{1}{1 - \varepsilon} \qquad 3.2$$

Deviatoric load is optained from the ring dial-gauge of the proving ring during the test regularly. Axial strain is measured with a dial-gauge

Pore water pressure (u) is optained directly from bourdan- gauge or mercury manometer during the test.

Mean normal stress is calculated as

$$P = \frac{P_1 + P_2 + P_3}{3} \qquad 3.3$$

where

$$P_2 = P_3 = \text{cell pressure}$$

$$P = \frac{P_1 + 2P_3}{3} \qquad 3.4$$

And the effective mean normal stress is calculated as

$$P' = P - U \qquad 3.5$$

The effective deviator stress is equal to the total deviator stress

$$q' = q \qquad 3.6$$

Membrane and drain paper correction, the correction to be applied to calculated deviator stress is similar for all test. The presence of a rubber membrane, and filter drains imposes additional restraint on the specimen. It is particularly important to make allowance for this in tests on soft clay and other weak material.

For particular purposes the correction curve given in Fig 3.19 may be used for standart membranes of 0.2 mm thickness. Fig 3.19 gives the correction to apply for a bar-

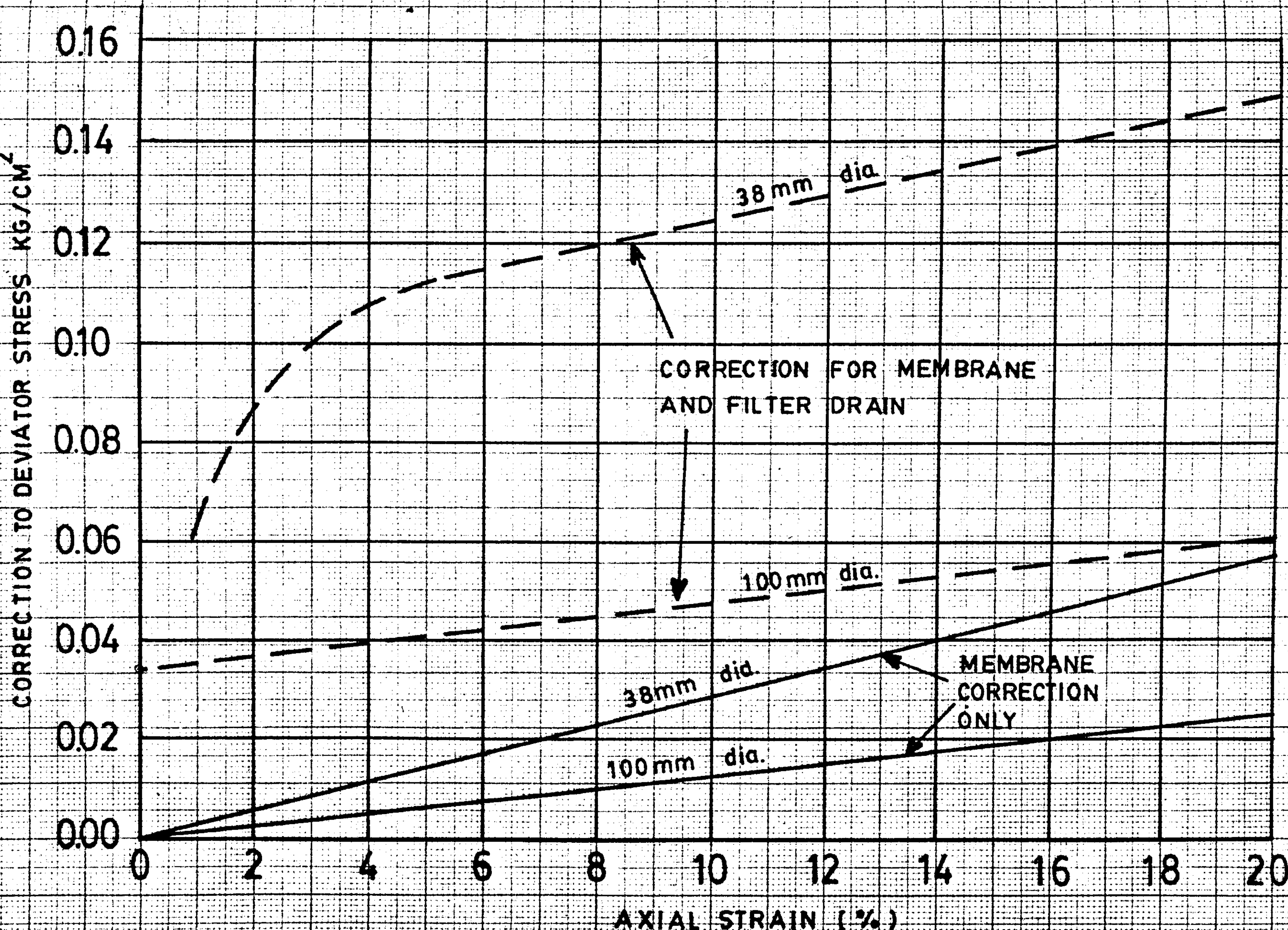

FIG 3.19 Membrane and Filter Drain Corrections

relling type of deformation. The full two line curves give the stress (KG / CM^2) to be deducted from measured deviator stress due to membranes only, for 38 mm and 100 mm diameter specimens. If filter drains are used, the broken line curves apply.

After this calculation and membrane and drain correction the $q' : \varepsilon$, $q' : p'$ and $u : \varepsilon$ curves are plotted.

Soil parameters M , λ , N , and Γ are optained from critical state line and normally consolidation lines. These line were passed through the data points applying the least square method.

$$m = \frac{\dfrac{\Sigma x_i \ \Sigma y_i}{n} - \Sigma x_i \ y_i}{\dfrac{(\Sigma x_i)^2}{n} - \Sigma x_i^2} \qquad 3.7$$

where

n = number of nodes

m = gradiant of the line

b = value of y at intersection point

$b = \bar{y} - m \bar{x}$

$\bar{y} = \Sigma y_i / n$

$\bar{x} = \Sigma x_i / n$

CHAPTER 4 TEST RESULTS

Fifteen overconsolidated specimens and nine normally consolidated specimens were tested in undrained condition, by the triaxial apparatus. The overconsolidation ratios(OCR) were chosen as 5, 10, and 15. Five specimen, having O.C.R. of five were consolidated at different consolidation pressures. One sample was consolidated under 2.5 kg/cm^2 constant cell pressure and it was allowed to swell to o.50 kg/cm^2. Two samples were consolidated under a cell pressure of 4.0 kg/cm^2 and was allowed to swell to 0.80 kg/cm^2.And two other samples were consolidated under a cell pressure of 7.5 kg/cm^2 and was allowed to swell to 1.50 kg/cm^2. Then the specimen are tested as described in chapter three. The data optained from the tests were calculated using equations 3.2 and 3.4 Data sheets are prepared for each test. These sheets alang with the drawings are given for each test. The results of tests having an O.C.R. of five are given in table 4.1

As seen in Table 4.1 the walue af water content increased at failure surface. On q' : p' spaces the stress curve reaches a peak value and the deviator stresses reduces from its peak value to a lower value. In u : ε space pore pressure increases initially after vertical reaches 6 - 8 % pore pressure reduces continiously until the failure point.

The results of tests having an O.C.R. of ten are given in TABLE 4.2. One sample was consolidated under a cell pressure of 2.50 Kg/cm^2 and was allowed to swell to o.25 kg / cm^2. One sample was consolidated under 4.50 kg / cm^2

TABLE 4.1

Test Number	OCR	Consolidation Pressure (Kg/Cm^2)	Sweelling Pressure (Kg/Cm^2)	Max.Deviator Stress (Kg/Cm^2)	Av. Water Content %	Water Con. at Failure surface %
1	5	2.50	0.50	2.033	23.937	24.570
4	5	4.00	0.80	2.008	24.941	25.946
5	5	4.00	0.80	1.921	25.441	25.823
10	5	7.50	1.50	3.865	21.555	21.968
11	5	7.50	1.50	3.508	21.715	21.805

constant cell pressure and was allowed to swell to 0.45 kg / cm^2.One sample was consolidated under a cell pressure of 5.00 kg / cm^2 and was allowed to swell to 0.50 kg / cm^2. And two other samples were consolidated under a cell pressure of 7.50 kg / cm^2 and were allowed to swell to 0.75 kg / cm^2. The pore pressure of the tests 6 and 7 have reached the maximum value at 2 % strain then reduce continiously to the end of thetesting process. These specimens were tested under 5.00 kg / cm^2 constant cell pressure, therefore, they reached the maximum value at less strain than the others.Other specimens were showed to failure under a cell pressure of 3.0 kg / cm^2. The other tests, pore water pressures reached the maximum value at 6 - 8 % of strain. Also the value of water content increases at failure (shear) surface.

The results of five other tests having an O.C.R. of fifteen are given in Table 4.3. One of them was consolidated under a cell pressure of 2.50 kg / cm^2 and was allowed to swell to 0.17 kg / cm^2. Two samples were consolidated under cell pressure of 6.00 kg / cm^2 and were allowed to swell to 0.40 kg / cm^2. And two other samples were consolidated under a cell pressure of 7.50 kg / cm^2 and was allowed to sweel to 0.50 kg / cm^2. All this specimens were tested in undrained condition. The pore water pressure of these specimens have increased only to a maximum value 1.0 kg / cm^2. The deviator stress increased with increasing consolidation pressure. Also the water content has increased at the failure surface in the specimen for specimens having O.C.R. of fifteen.

TABLE 4.2

Test Number	OCR	Consolidation Pressure (Kg/Cm^2)	Swelling Pressure (Kg/Cm^2)	Max. Deviator Stress (Kg/Cm^2)	Av. Water Content %	Water Con. At Failure Surface %
2	10	2.50	0.25	1.964	25.577	26.148
6	10	4.50	0.45	2.074	24.080	25.381
7	10	5.00	0.50	1.856	25.151	26.183
12	10	7.50	0.75	2.749	23.783	24.897
13	10	7.50	0.75	3.166	22.114	22.678

TABLE 4.3

Test Number	OCR	Consolidation Pressure (Kg/Cm^2)	Swelling Pressure (Kg/Cm^2)	Max.Deviator Stress (Kg/Cm^2)	Av.Water Content %	Water Con. at Failure Surface %
3	15	2.50	0.17	2.845	23.309	21.406
8	15	6.00	0.40	1.780	25.519	26.647
9	15	6.00	0.40	2.231	24.183	25.180
14	15	7.50	0.50	3.374	21.984	22.655
15	15	7.50	0.50	2.726	23.542	24.334

Then nine normally consolidated specimens are tested in undrained triaxial test apparatus to draw the Critical State Line and the Normal Consolidation Line to find the soil parameters M, N, Γ, λ. Three of the tests were consolidated under 2.50 kg / cm^2 constant cell pressure. Three samples were consolidated under a cell pressure of 5.00 kg / cm^2. And three others were consolidated under a cell pressure 7.50 kg / cm^2.The specimen 16 is prepared in the proctor mold, when we tested it under 2.50 kg/cm^2 constant cell pressure, it behave like an overconsolidated specimen therefore, the specimen for normal consolidated testing process were prepared at a water content close to the plastic limit. Otherwise they behave like overconsolidated specimen. Critical State Line and Normal Consolidated Line are drown using all tests results except test 16.

The variation and results are seen in Table 4.4. All the specimen have failed at the Critical State Line except the specimens 21, 22, 23, and 24. They have failed before tey reached the Critical State Line. We can say that when the consolidation pressure increases the permeability of the specimen decreases, so relative increase of water content at the surrounding of the shear surface, become in a thinner surface than specimen consolidated at low pressures and pore pressure and water content at shear surface can not be measured as accurately. So that the stress paths do not reach the critical state line.

The stress paths of these tests in q' : ε space and pore pressure in u : ε space, do not have peaks. They increases continiously and then remained constant. The pore pressure increament in NC specimen which is consolidated to 7.50 kg / cm^2 cell pressure, increase slowly to the 10 % strain then the pore water pressure has increases rapitly as seen in Figures 4.87, 4.91 and 4.95

TABLE 4.4

Test Number	OCR	Consolidation Pressure (kg/cm^2)	Max.Deviator Stress (kg/cm^2)	Av.Water Content %	Water Con. at Failure surface %
16	1	2.50	2.308	25.056	25.083
17	1	2.50	1.880	26.273	26.675
18	1	2.50	1.706	26.235	26.647
19	1	5.00	3.543	23.166	23.545
20	1	5.00	3.502	22.429	22.847
21	1	5.00	3.205	23.604	24.197
22	1	7.50	4.036	21.469	22.180
23	1	7.50	4.718	20.671	20.847
24	1	7.50	4.791	22.329	22.786

All the tests were performed in undrained condition, therefore, there are no change in specific volume.

TABLE 4.5

Test Number	Specific Volume(v)	Equi. Mean Normal Stress at NCL (P_{ei}) (Kg/Cm^2)	Ef. Mean Normal Stress at CSL (P_u) (Kg/Cm^2)
1	1.646	4.202	3.173
2	1.691	2.887	2.180
3	1.629	4.852	3.663
4	1.673	3.339	2.521
5	1.686	2.999	2.264
6	1.650	4.067	3.071
7	1.679	3.182	2.403
8	1.689	2.925	2.209
9	1.653	3.972	3.007
10	1.582	7.249	5.473
11	1.586	6.989	5.277
12	1.642	4.351	3.285
13	1.597	6.379	4.816
14	1.594	6.571	4.962
15	1.636	4.600	3.473
16	1.676	3.253	2.556
17	1.709	2.462	1.859
18	1.708	2.483	1.875
19	1.626	5.013	3.786
20	1.606	5.935	4.481
21	1.637	4.535	3.424
22	1.579	7.393	5.582
23	1.558	8.875	6.701
24	1.603	6.072	4.585

From equatin

$$v == 1 + w\,\gamma_s \qquad \text{Eq. 4.1}$$

The specific volume is faund both normally consolidated and overconsolidated that are tabulated in Table 4.5. These values for normally consolidated specimen are tabulated in Table 4.6 and Table 4.7 .The data poins which is optained from normally consolidated specimen are marked in v : lnP' space and using the least-square method, the suitable lines were passed through these data points.

TABLE 4.6

Consolidation Pressure (Kg/Cm^2)	Specific Volume (v)	Ef. Mean Normal Stress (Kg/Cm^2)
2.50	1.676	2.370
2.50	1.709	1.862
2.50	1.708	1.874
5.00	1.626	3.747
5.00	1.606	3.717
5.00	1.637	4.108
7.50	1.579	5.638
7.50	1.558	6.162
7.50	1.603	4.948

TABLE 4.7

Node Number	$\ln p_{ei}$ (Kg/Cm^2)	$\ln p_u$ (Kg/Cm^2)	v_i	$\ln p_{ei} \times v_i$ (Kg/Cm^2)	$\ln p_u \times v_i$ (Kg/Cm^2)	$\ln p_{ei}^2$	$\ln p_u^2$
1	0.916	0.622	1.709	1.565	1.063	0.839	0.387
2	0.916	0.628	1.708	1.564	1.073	0.839	0.394
3	1.609	1.321	1.626	2.616	2.148	2.589	1.745
4	1.609	1.313	1.606	2.584	2.109	2.589	1.724
5	1.609	1.413	1.637	2.634	2.313	2.589	1.996
6	2.015	1.729	1.579	3.182	2.730	4.060	2.989
7	2.015	1.818	1.558	3.139	2.832	4.060	3.305
8	2.015	1.599	1.603	3.230	2.563	4.060	2.557

$$\lambda = \frac{\dfrac{\sum \ln P_{oi} \sum v_i}{n} - \sum \ln P_{oi}\, v_i}{\dfrac{(\quad \ln P_{oi})^2}{n} - \sum \ln P_{oi}^2} \qquad \text{Eq. 4.2}$$

$$\lambda = \frac{\dfrac{12.704 \times 13.026}{8} - 20.514}{\dfrac{(12.704)^2}{8} - 21.625}$$

$\lambda = -\ 0.118$ for NCL

$$\lambda = \frac{\dfrac{10.443 \times 13.026}{8} - 16.831}{\dfrac{(\ 10.443\ )^2}{8} - 15.097}$$

$\lambda = -\ 0.1179$ for Critical State Lime

The results are equal each ather that give the gradient of CSL and NCL in $v : \ln P'$ space. Let we take it

$$\overline{\ln P_{oi}} = \frac{\sum \ln P_{oi}}{n} = \frac{12.704}{8} = -\ 1.588$$

Eq. 4.3

$$\overline{v} = \frac{v_i}{n} = \frac{13.026}{8} = 1.628 \qquad \text{Eq. 4.4}$$

$$N = \overline{v} - \lambda \ln \overline{P_0} \qquad \text{Eq. 4.5}$$

$$N = 1.628 - (- 0.118 \times 1.588)$$

$$N = 1.8156$$

$$\Gamma = \overline{v} - \lambda \ln \overline{P_f} \qquad \text{Eq. 4.6}$$

$$\Gamma = 1.62825 - (- 0.118 \times 10.443 / 4)$$

$$\Gamma = 1.7823$$

Normally consolidated line and critical state line are seen in Fig 4.1

Then all the test results are plotted in q'/p'_{ei} : p'/p'_{ei} space (in Appendix 1). The Hvorslev surface are drawn,(see appendix one),as tangent to the failure points of overconsolidated specimen. Then the slope of Hvorslev surface is found as $h = 34^\circ\!.5$ and $M = 43^\circ\!.8$. The soil parameters are tabulated in Table 4.8

TABLE 4.8

N	$= 1.8156$
Γ	$= 1.7823$
M	$= 43^\circ\!.8$
h	$= 34^\circ\!.5$
λ	$= -0.118$

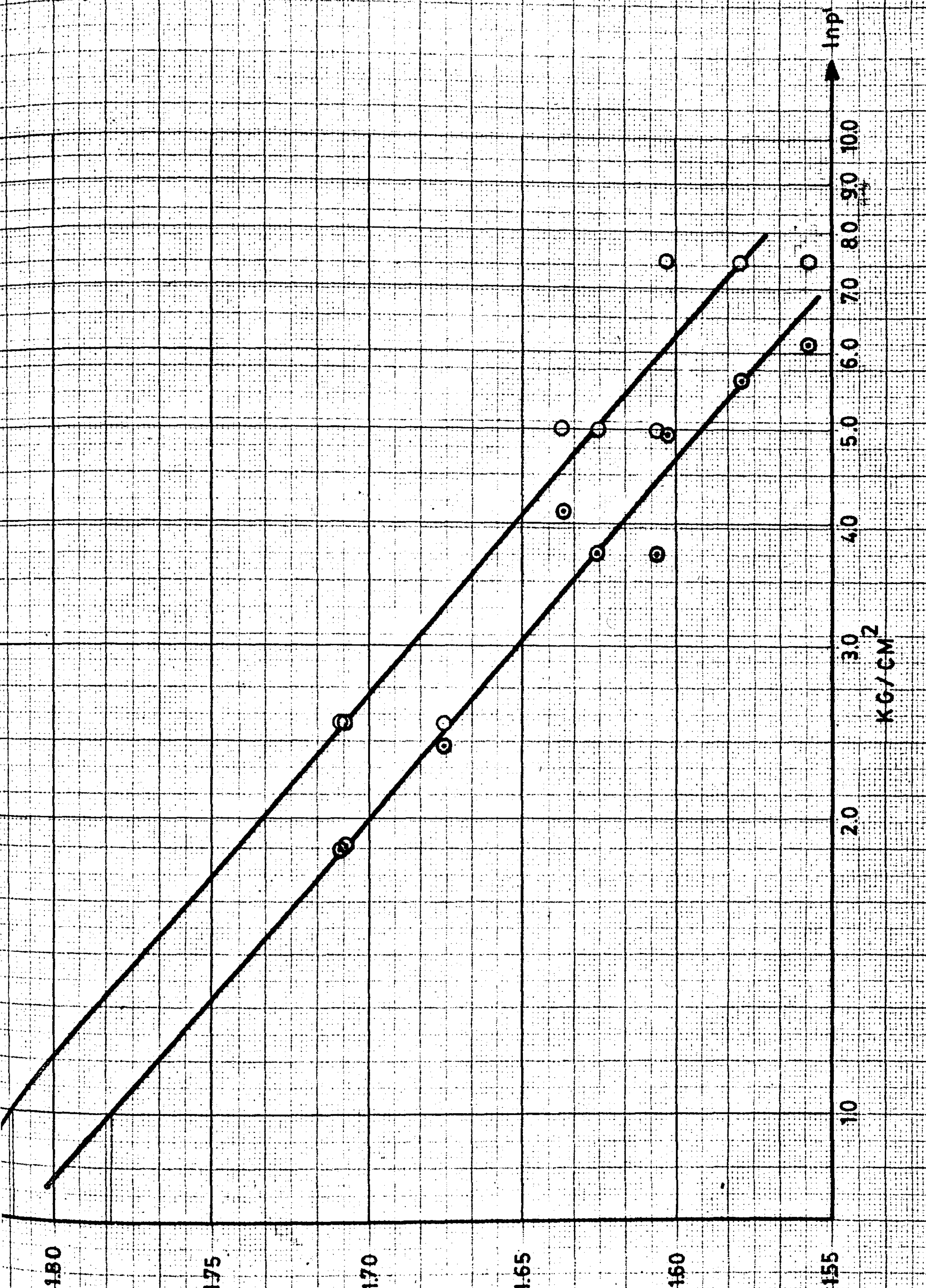

Fig 4.1 Normal Consolidation and Critical State Line for TOPSER SARI CLAY

so the equation of normal consolidation line in the v : ln p' space is

$$v = 1.8156 - 0.118 \ln p'_o$$

and the critical state line is

$$v = 1.7823 - 0.118 \ln p'$$

All the testing results are represent in q' : ε , u : ε and q' : p' space. The water content distribution through the specimen after the test also are represented the following pages.

Consolidation Pressure : 2.5 $Kgcm^{-2}$

Equivalent Mean Normal Stress : 4.202 $Kgcm^{-2}$

Proving Ring Number and Constant : 12365 / 0.09639 O. C. R. : 5

Specimen Diameter Top : 3.57 cm. Bottom : 3.58 cm. Average : 3.575 cm.

Specimen Weight : 166.97 gr. Specimen Height : 8.01 cm.

Av. Specimen Area : 10.037 cm^{-2} Av.Loading Rate : 0.0303 mm/ min.

Loading dial In.$\times 10^{-4}$	Axial strain %	Pore pressure Kg. / cm2	Deviator stress Kg. / cm2	Ef. Mean normal stress Kg. / cm2	Water Content %	
0.0	0.00	1.72	0.000	1.280	Slice No.	Water Content
54.0	0.31	1.84	0.504	1.302		
86.0	0.56	1.96	0.775	1.283	1	23.447
102.5	1.00	2.00	0.911	1.310	2	23.542
132.0	1.69	2.06	1.168	1.298	3	23.662
160.0	2.68	2.05	1.399	1.400	4	24.059
196.5	4.56	1.98	1.691	1.570	5	24.456
213.0	5.87	1.90	1.811	1.703	6	24.570
227.0	7.24	1.87	1.904	1.808	7	24.153
239.5	9.18	1.67	1.966	1.933	8	23.606
250.0	11.05	1.62	2.006	2.060		
261.2	13.55	1.50	2.033	2.178	Average w : 23.937	
265.3	14.94	1.48	2.028	2.216	Sketch of Failure	
270.8	18.10	1.39	1.982	2.280		
274.0	20.04	1.33	1.950	2.320		
277.5	21.78	1.31	1.926	2.330		
277.8	23.53	1.28	1.877	2.345		
267.5	26.53	1.24	1.714	2.320		
265.5	27.40	1.23	1.677	2.322		

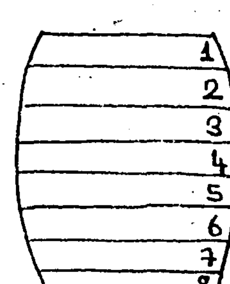

Max. Axial Stress: 2.033 $kgcm^{-2}$ Water Con. at Failure Surface: 24.570 %

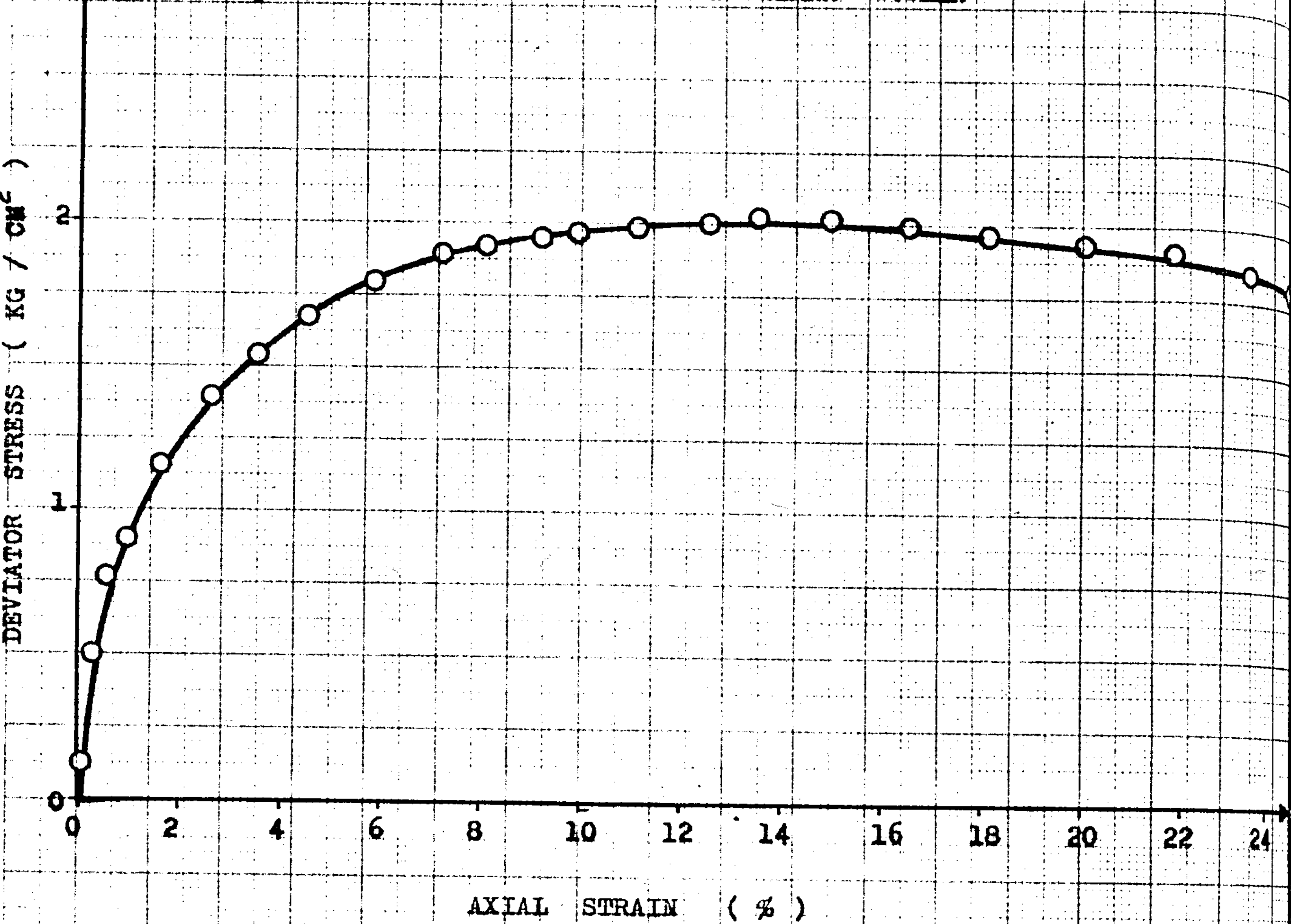

Fig 4.2 Deviator Stress versus Axial Strain

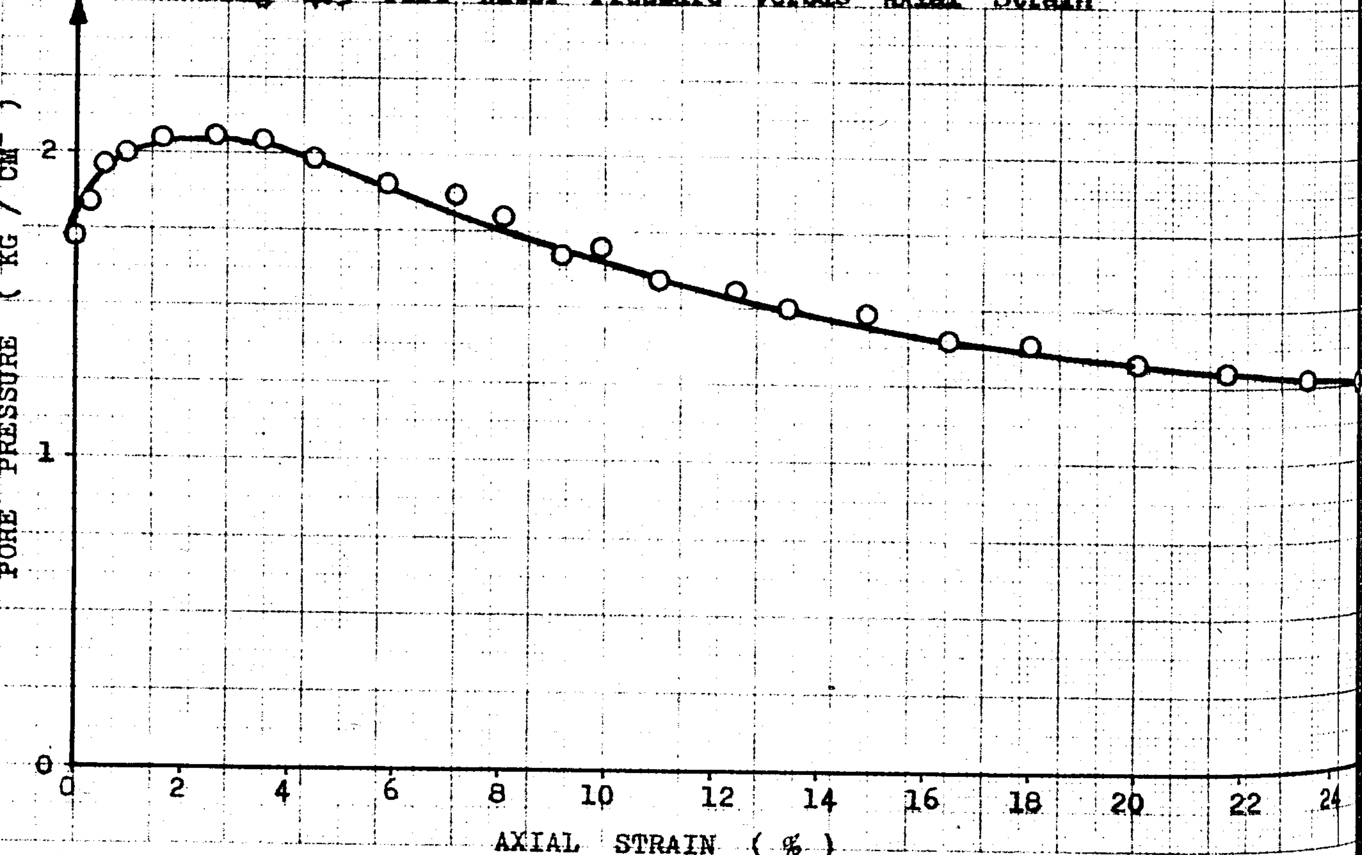

Fig 4.3 Pore Water Pressure versus Axial Strain

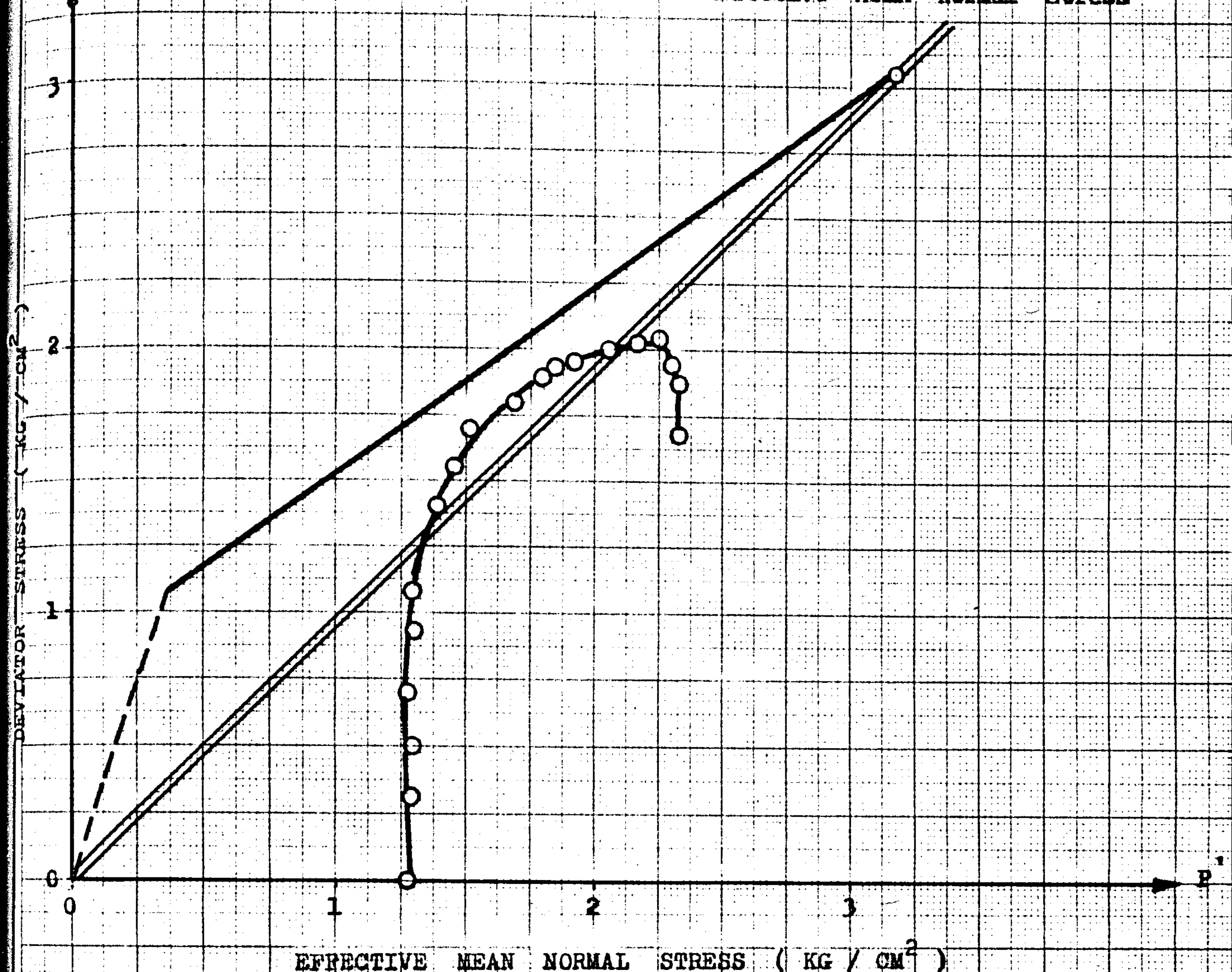

Fig 4.4 Deviator Stress versus Effective Mean Normal Stress

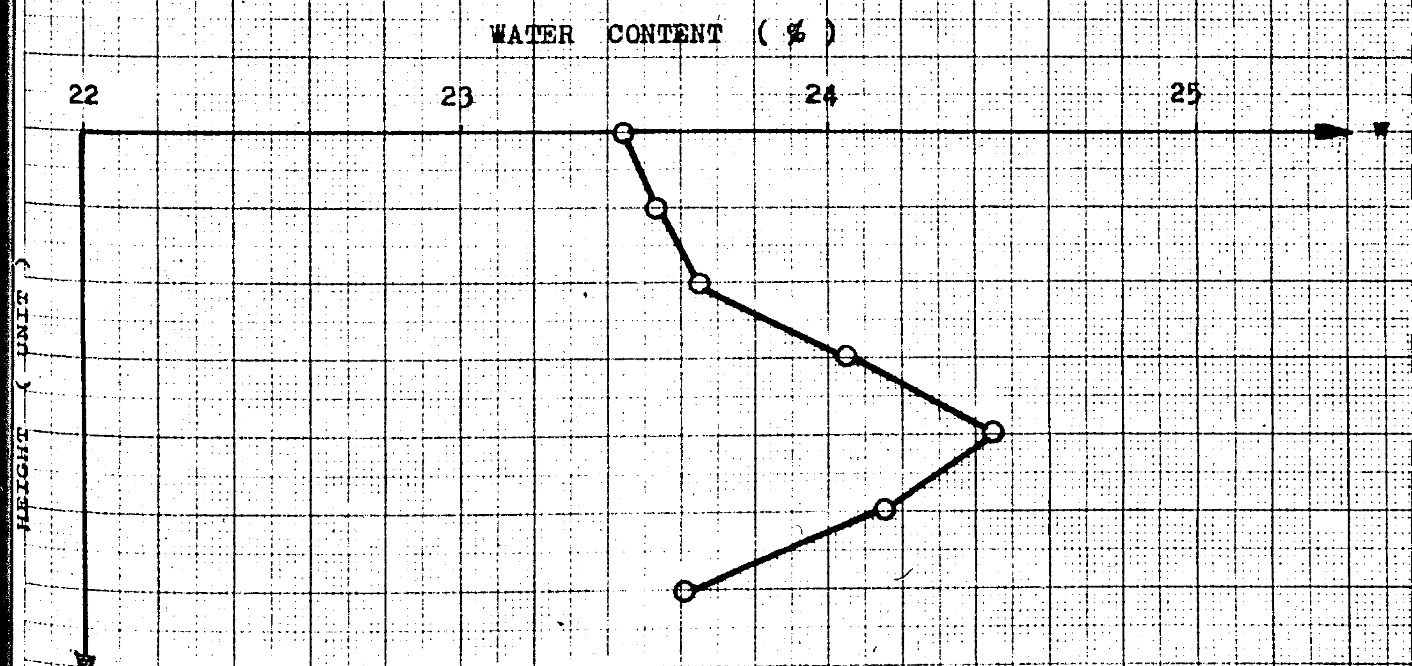

Fig 4.5 Height (Unit) versus Water Content

Consolidation Pressure : 2.5 $Kgcm^{-2}$

Equivalent Mean Normal Stress : 2.887 $Kgcm^{-2}$

Proving Ring Number and Constant : 12365/0.09639 O. C. R. : 10

Specimen Diameter Top : 3.57cm. Bottom : 3.57 cm. Average : 3.57 cm.

Specimen Weight : 170.02gr. Specimen Height : 8.02 cm.

Av. Specimen Area : 10.01 cm^{-2} Av.Loading Rate : 0.0303 mm/min.

Loading dial In.x10^{-4}	Axial strain %	Pore pressure Kg. / cm^2	Deviator stress Kg. / cm^2	Ef. Mean normal stress Kg. / cm^2	Water Content %	
0.0	0.00	0.90	0.000	2.100	Slice No.	Water Content
35.6	0.30	1.00	0.329	2.093		
69.0	0.80	1.15	0.609	2.053	1	25.085
91.6	1.45	1.30	0.800	1.967	2	25.159
112.0	2.17	1.46	0.967	1.862	3	25.687
139.5	3.54	1.70	1.191	1.697	4	25.877
164.5	5.29	1.90	1.382	1.561	5	25.994
183.5	7.28	2.03	1.520	1.486	6	26.148
203.5	9.84	2.09	1.642	1.457	7	25.464
214.5	12.14	2.05	1.682	1.511	8	25.203
223.0	14.76	2.00	1.691	1.564		
226.1	17.13	1.99	1.662	1.574	Average w : 25.577	
227.3	18.63	1.98	1.632	1.574	Sketch of Failure	
228.2	20.25	1.96	1.598	1.583		
228.5	21.56	1.95	1.568	1.577		
229.0	23.24	1.92	1.531	1.575		
229.0	24.36	1.92	1.502	1.571		
228.5	26.86	1.91	1.440	1.570		
224.0	28.23	1.90	1.372	1.557		

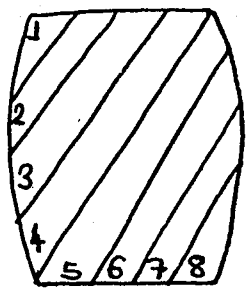

Max. Axial Stress: 1.694 $kgcm^{-2}$ Water Con. at Failure Surface: 26.148 %

Fig 4.6 Deviator Stress versus Axial Strain

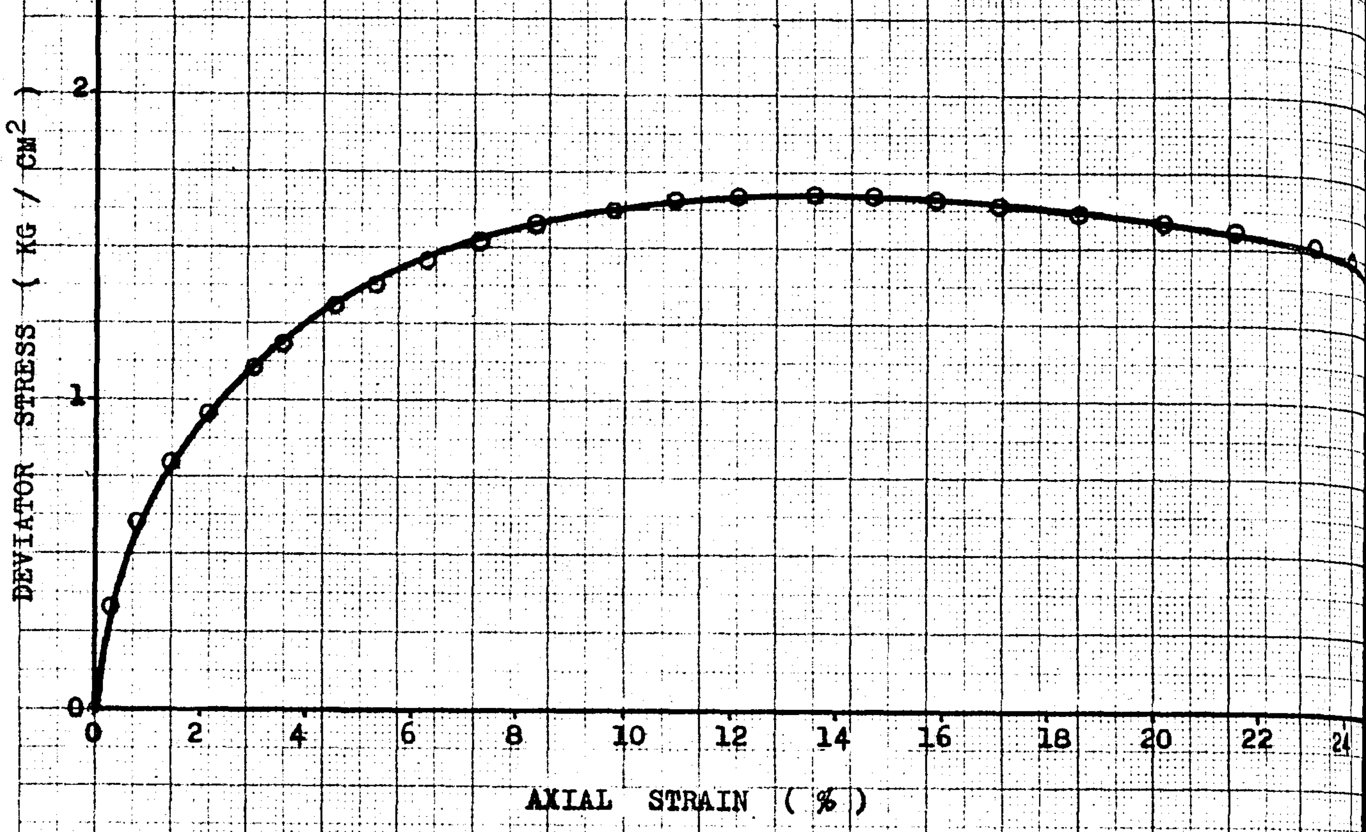

Fig 4.7 Pore Water Pressure versus Axial Strain

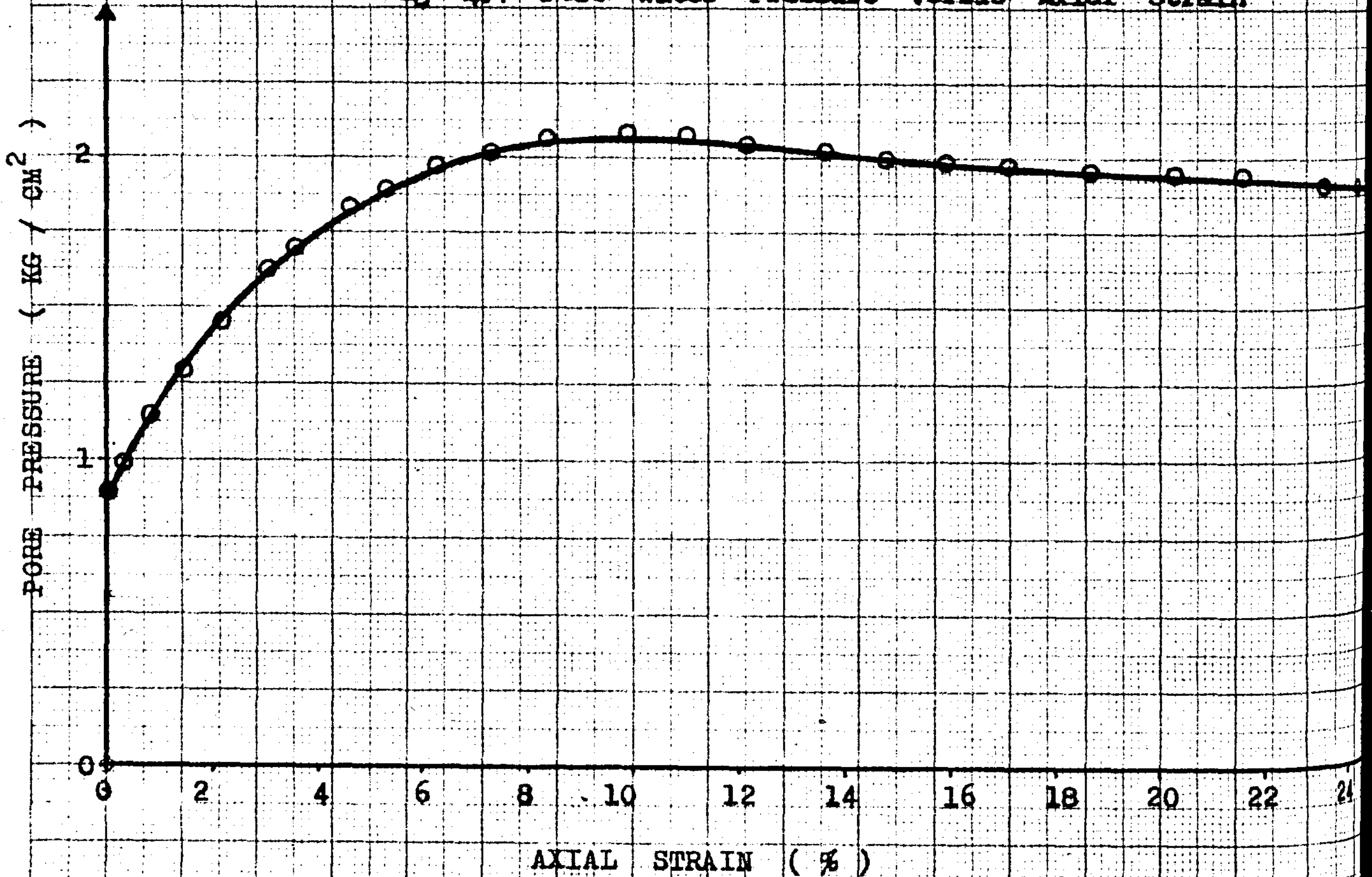

Fig 4.8 Deviator Stress versus Effective Mean Normal Stress

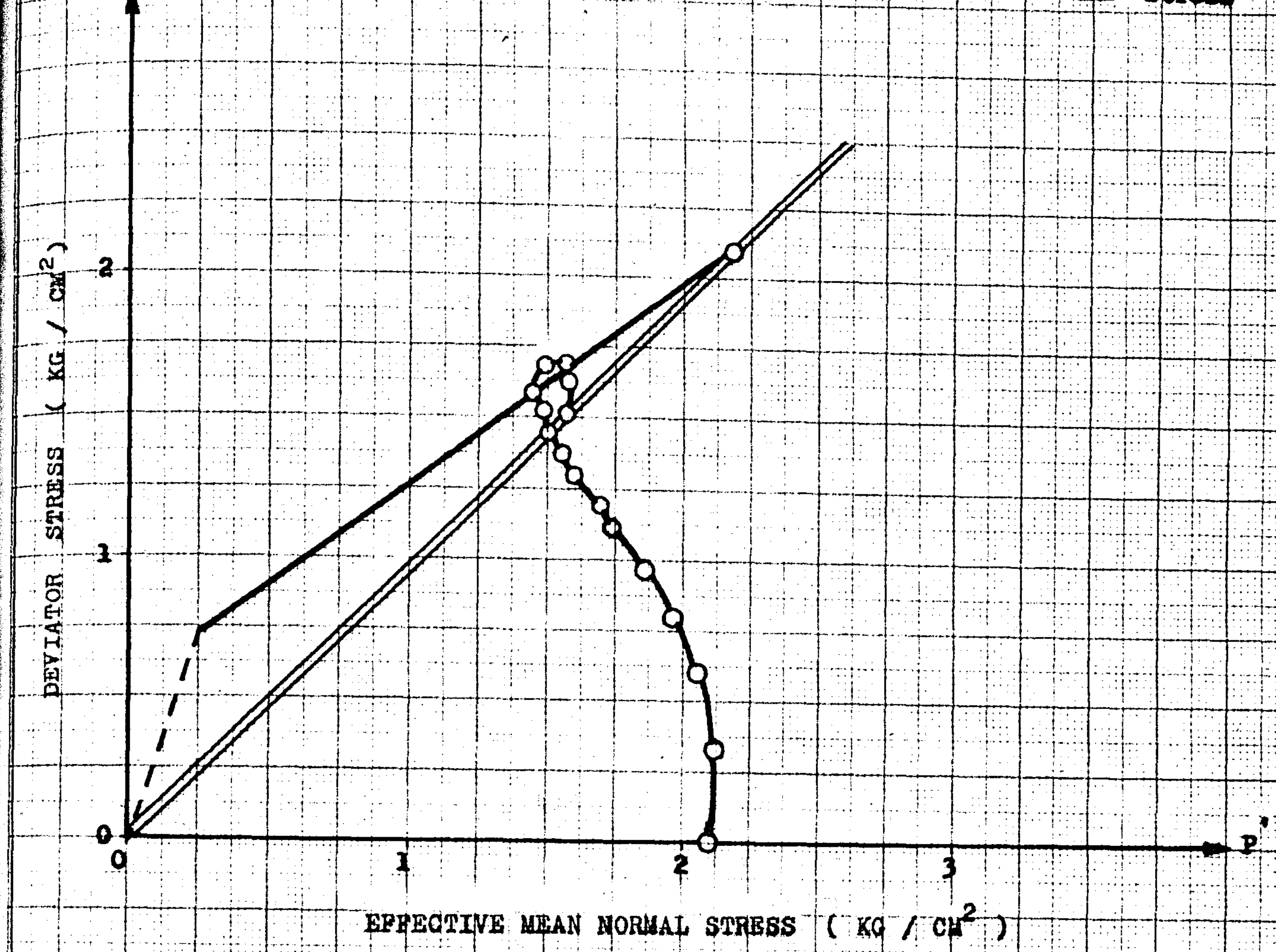

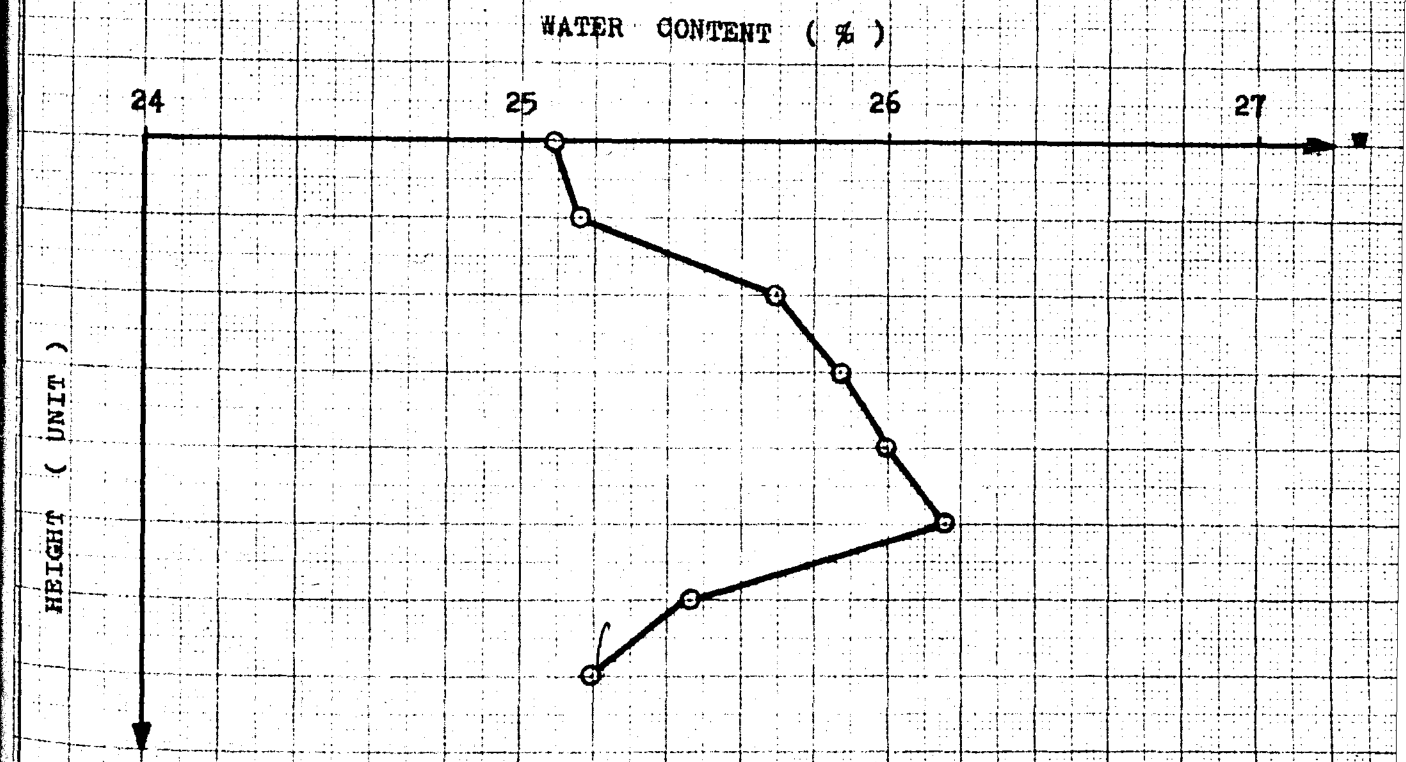

Fig 4. 9 Height (Unit) versus Water Content

Consolidation Pressure : 2.5 $Kgcm^{-2}$

Equivalent Mean Normal Stress : 4.852 $Kgcm^{-2}$

Proving Ring Number and Constant : 12365/0.09639 O. C. R. : 15

Specimen Diameter Top : 3.58 cm. Bottom : 3.59 cm. Average : 3.585 cm.

Specimen Weight : 166.24 gr. Specimen Height : 8.0 cm.

Av. Specimen Area : 10.094 cm^{-2} Av.Loading Rate : 0.0303 mm/min.

Loading dial $In. x 10^{-4}$	Axial strain %	Pore pressure Kg. / cm^2	Deviator stress Kg. / cm^2	Ef. Mean normal stress Kg. / cm^2	Water Content %	
0.0	0.00	0.90	0.000	2.100	Slice No.	Water Content
18.5	0.10	0.92	0.173	2.137		
62.5	0.40	0.98	0.576	2.212	1	22.330
101.9	0.91	1.11	0.912	2.194	2	22.776
120.5	1.22	1.17	1.071	2.187	3	24.406
152.5	1.97	1.34	1.346	2.110	4	23.628
185.5	3.04	1.52	1.617	2.060	5	23.446
214.2	4.10	1.54	1.854	2.073	6	23.766
244.5	5.85	1.55	2.084	2.141	7	23.269
275.3	8.35	1.45	2.288	2.300	8	22.855
290.0	9.98	1.40	2.367	2.404		
309.5	12.85	1.27	2.443	2.544	Average w : 23.309	
324.0	15.85	1.17	2.462	2.650	Sketch of Failure	
343.0	19.6	1.07	2.481	2.757		
349.0	20.85	1.03	2.482	2.800		
355.1	23.35	1.00	2.436	2.812		
360.1	24.60	0.98	2.427	2.824		
363.0	26.04	0.95	2.394	2.828		
370.8	27.10	0.90	2.403	2.845		

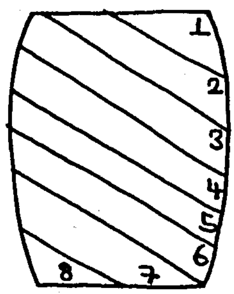

Max. Axial Stress: 2.845 $kgcm^{-2}$ Water Con. at Failure Surface: 24.406 %

Fig 4.10 Deviator Stress versus Axial Strain

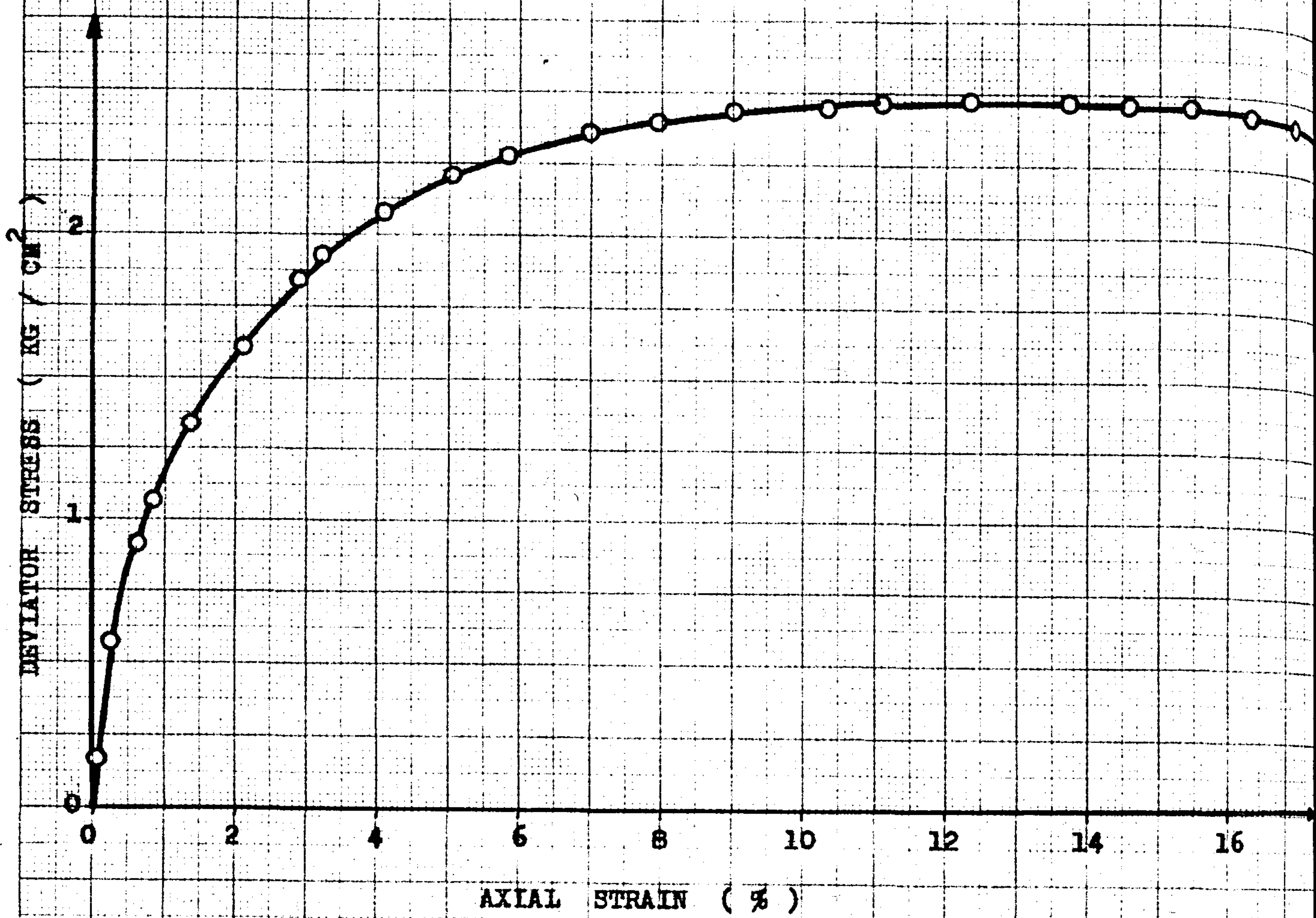

Fig 4.11 Pore Water Pressure versus Axial Strain

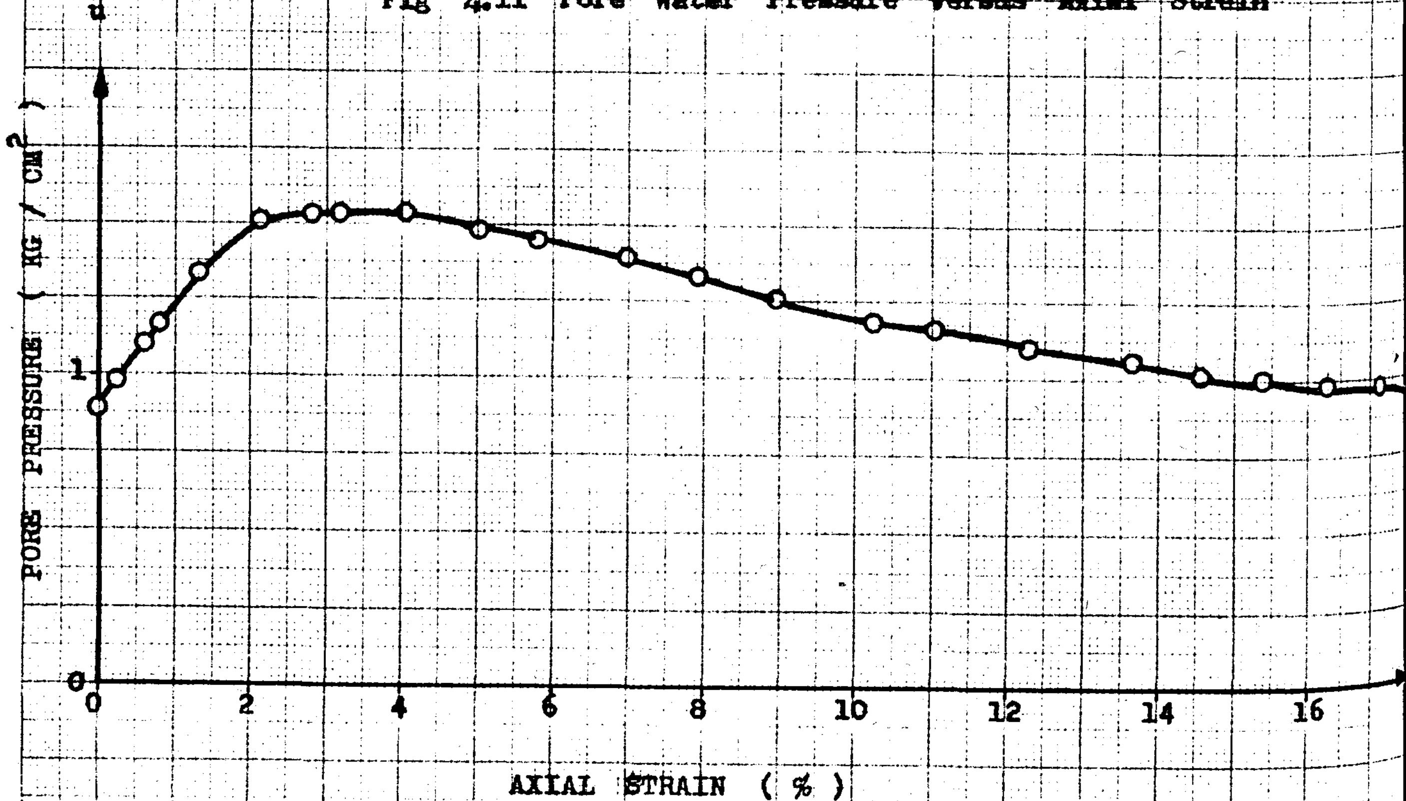

Fig 4.12 Deviator Stress versus Effective Mean Normal Stress

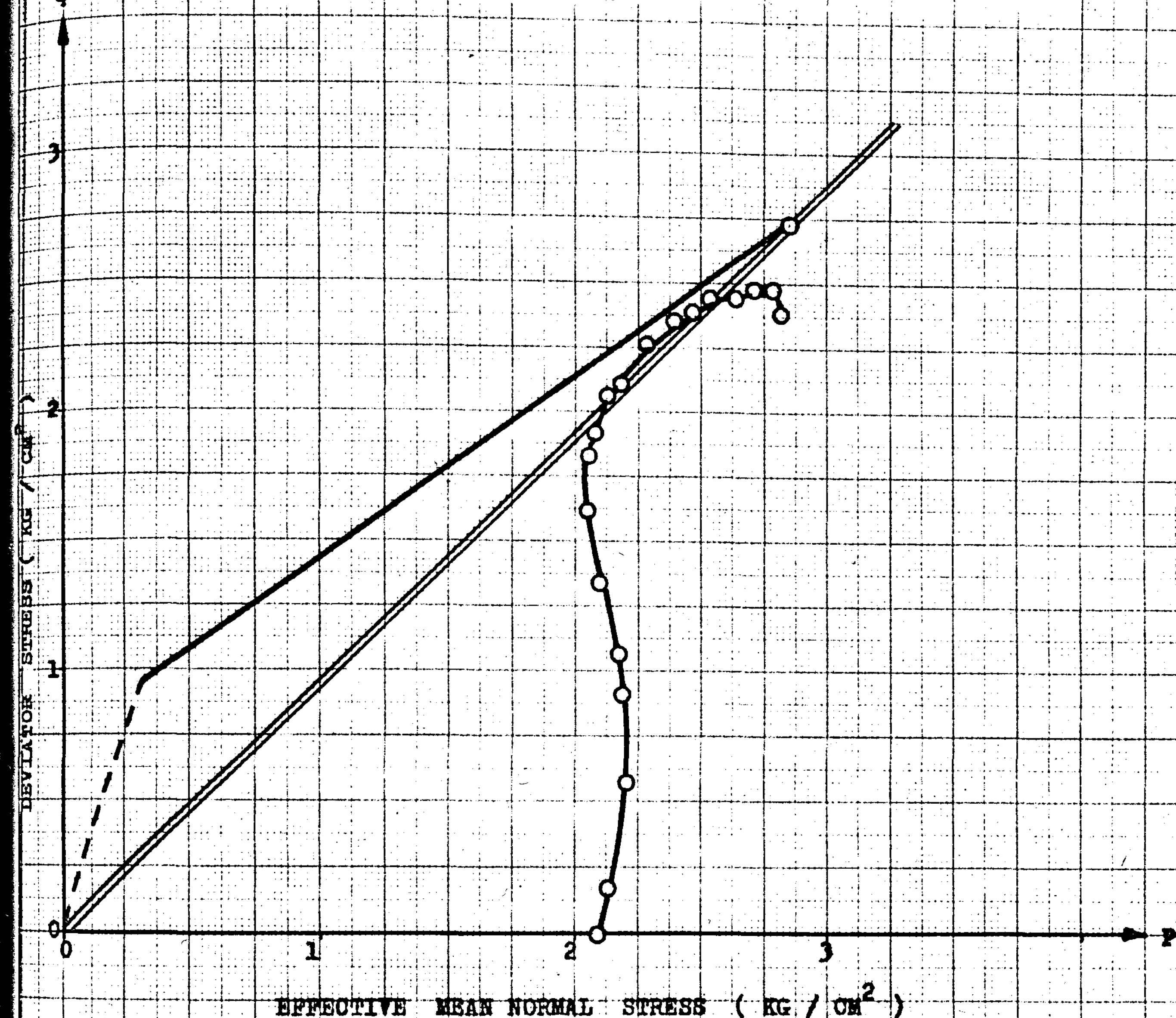

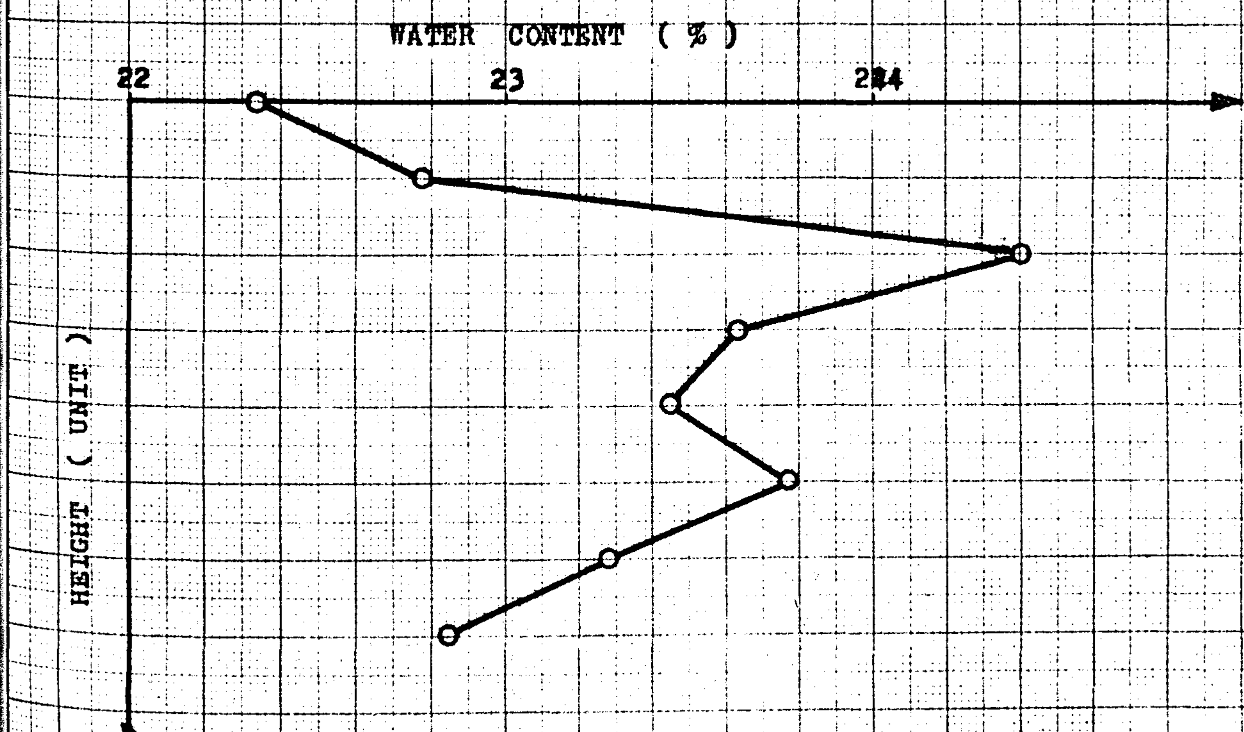

Fig 4.13 Height (Unit) versus Water Content

Consolidation Pressure : 4.0 $Kgcm^{-2}$

Equivalent Mean Normal Stress : 3.339 $Kgcm^{-2}$

Proving Ring Number and Constant : 12365/0.09639 O. C. R. : 5

Specimen Diameter Top : 3.57cm. Bottom : 3.57cm. Average : 3.57cm.

Specimen Weight : 164.25 gr. Specimen Height : 8.0 cm.

Av. Specimen Area : 10.01 cm^{-2} Av.Loading Rate : 0.0303 mm/min.

Loading dial $In. \times 10^{-4}$	Axial strain %	Pore pressure $Kg. / cm^2$	Deviator stress $Kg. / cm^2$	Ef. Mean normal stress $Kg. / cm^2$	Water Content %	
0.0	0.00	3.70	0.000	1.300	Slice	Water
41.2	0.31	3.89	0.382	1.237	No.	Content
78.9	0.81	4.03	0.703	1.203	1	24.188
100.7	1.31	4.25	0.890	1.171	2	24.167
130.2	2.31	4.12	1.136	1.168	3	25.063
160.0	3.81	4.10	1.377	1.310	4	25.946
190.0	5.81	4.00	1.609	1.552	5	25.106
212.0	7.81	3.91	1.763	1.702	6	25.290
230.0	10.06	3.79	1.866	1.832	7	25.571
239.4	11.31	3.75	1.915	1.887	8	24.198
246.0	12.31	3.70	1.945	1.948		
253.0	13.56	3.66	1.971	1.997	Average w :24.941	
264.5	16.06	3.58	1.996	2.105	Sketch of Failure	
270.5	17.31	3.50	2.008	2.149		
274.2	18.56	3.50	2.001	2.177		
276.3	19.81	3.45	1.981	2.193		
272.5	21.06	3.45	1.915	2.188		
266.8	22.06	3.41	1.845	2.184		
251.5	23.19	3.40	1.698	2.151		

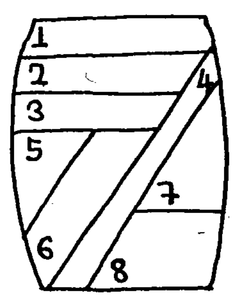

Max. Axial Stress: 2.008 $kgcm^{-2}$ Water Con. at Failure Surface: 25.946 %

Fig 4.14 Deviator Stress versus Axial Strain

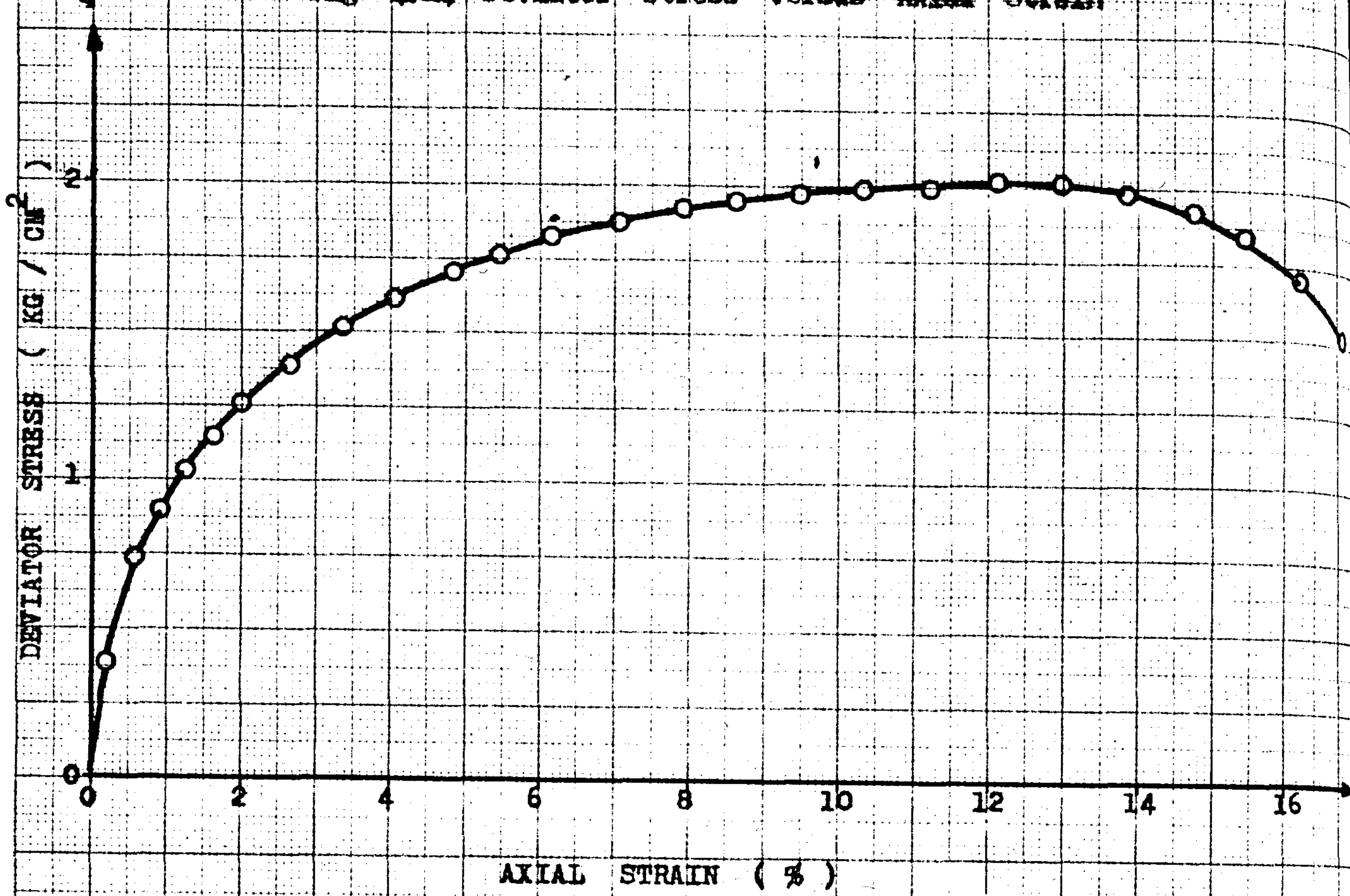

Fig 4.15 Pore Water Content versus Axial Strain

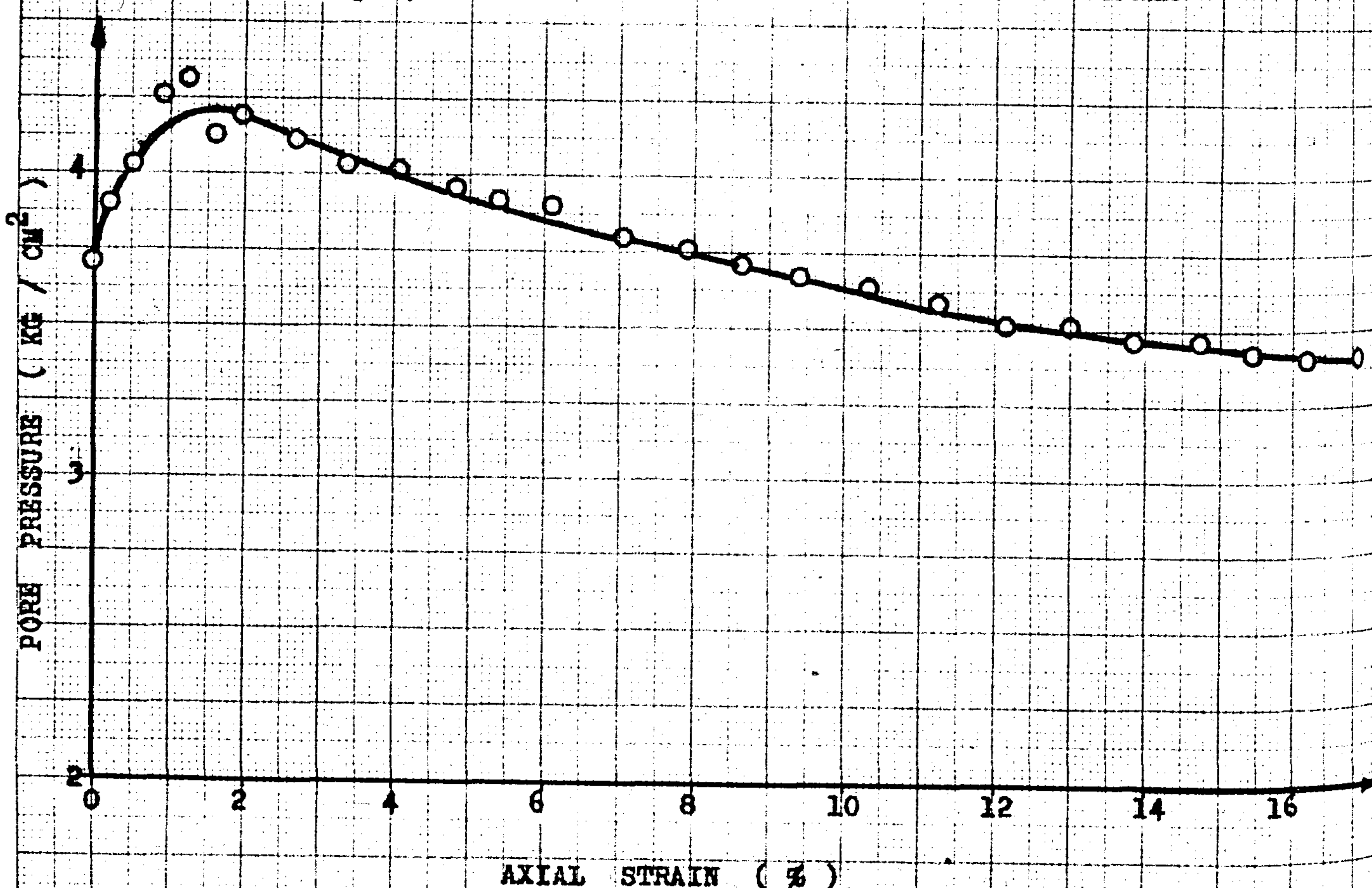

Fig 4.16 Deviator Stress versus Effective Mean Normal Stress

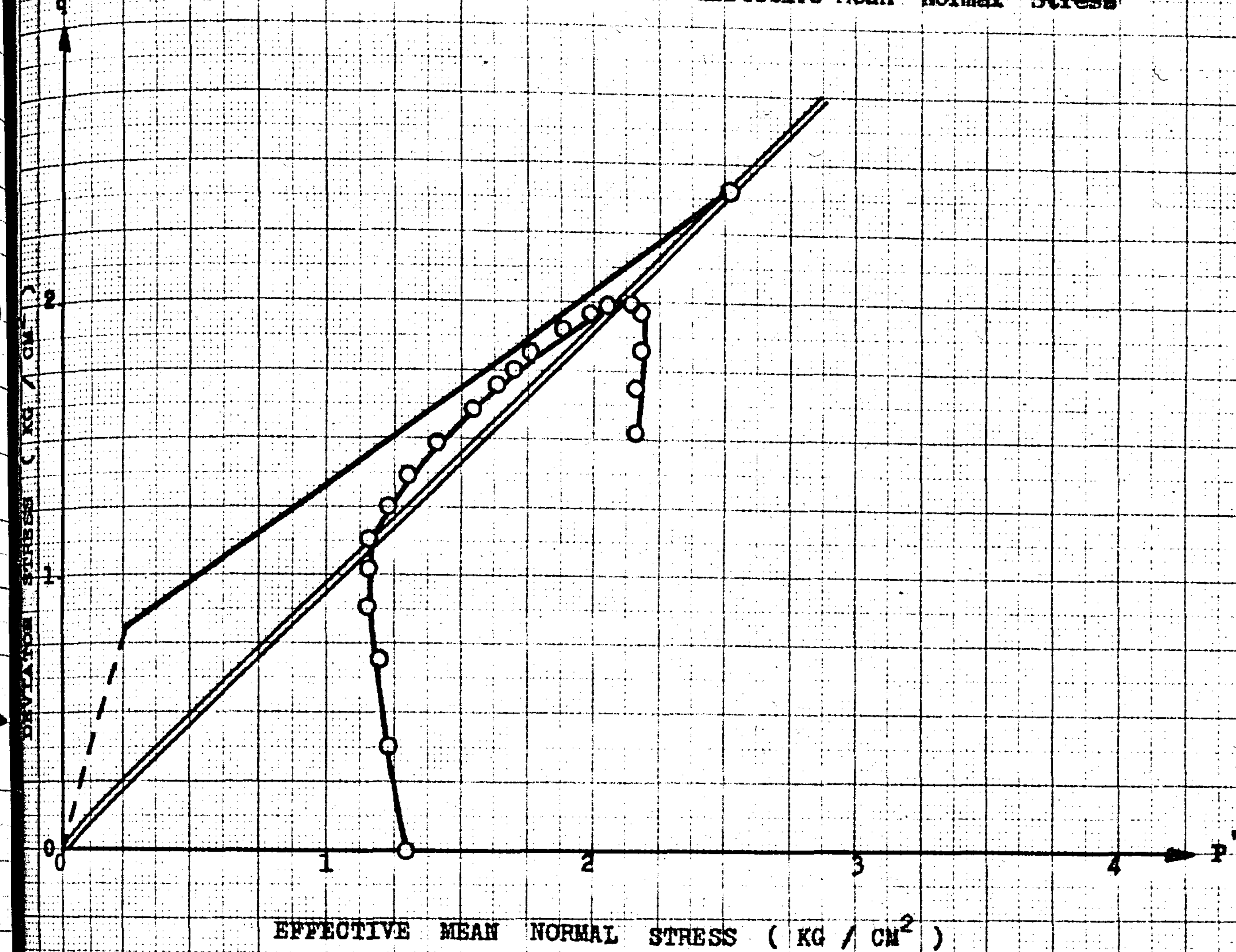

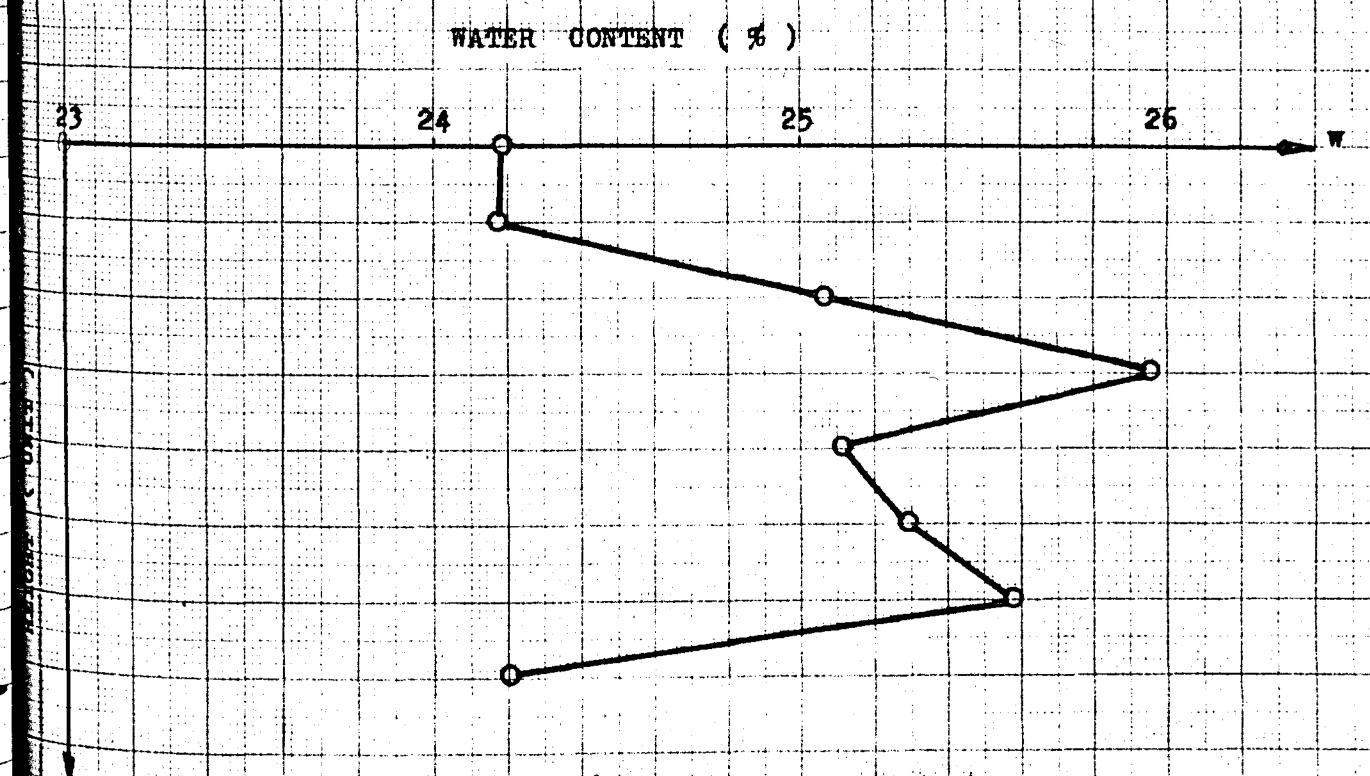

Fig 4.17 Height (Unit) versus Water Content

Fig 4.18 Deviator Stress versus Axial Strain

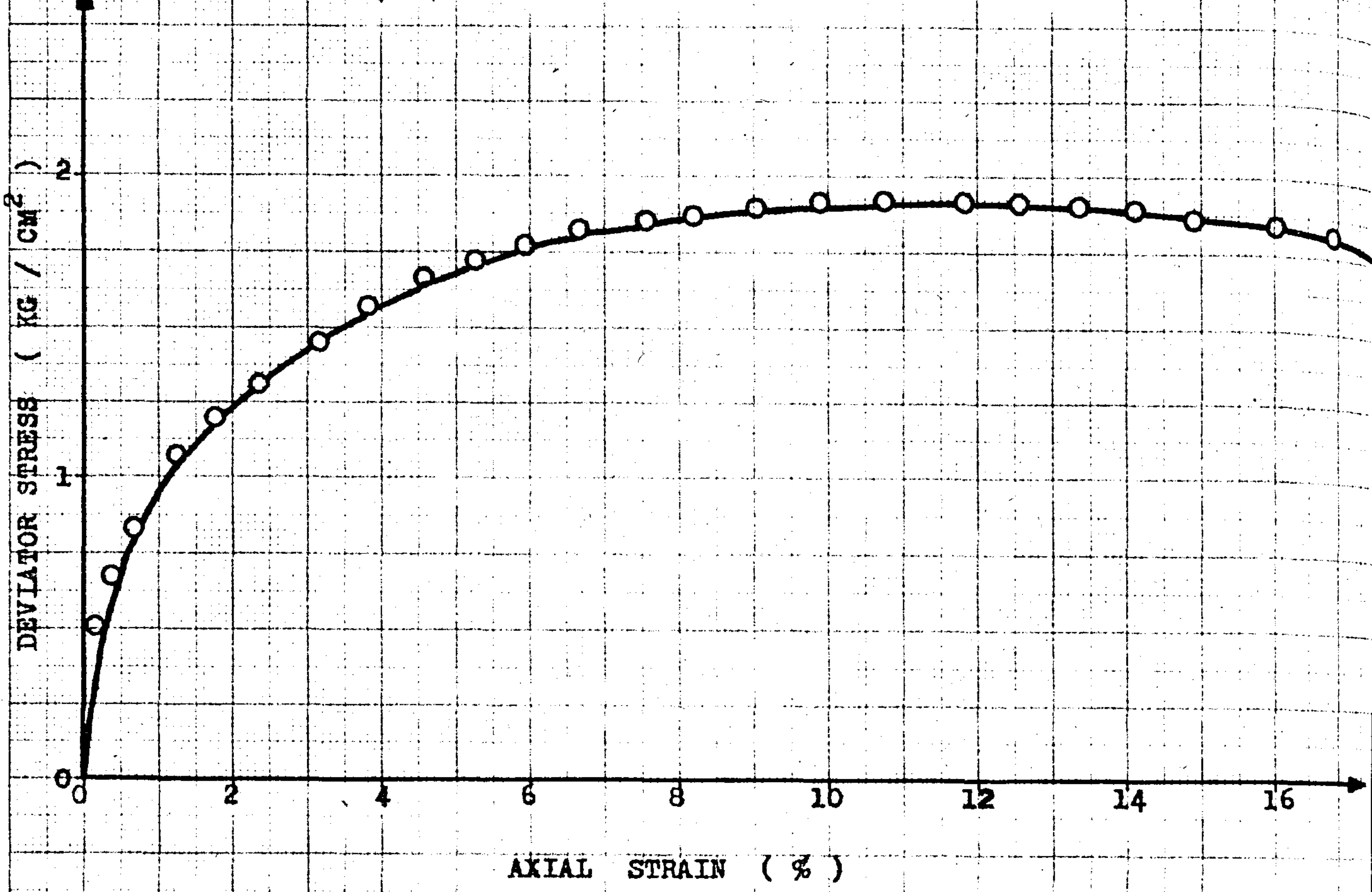

Fig 4.19 Pore Water Pressure versus Axial Strain

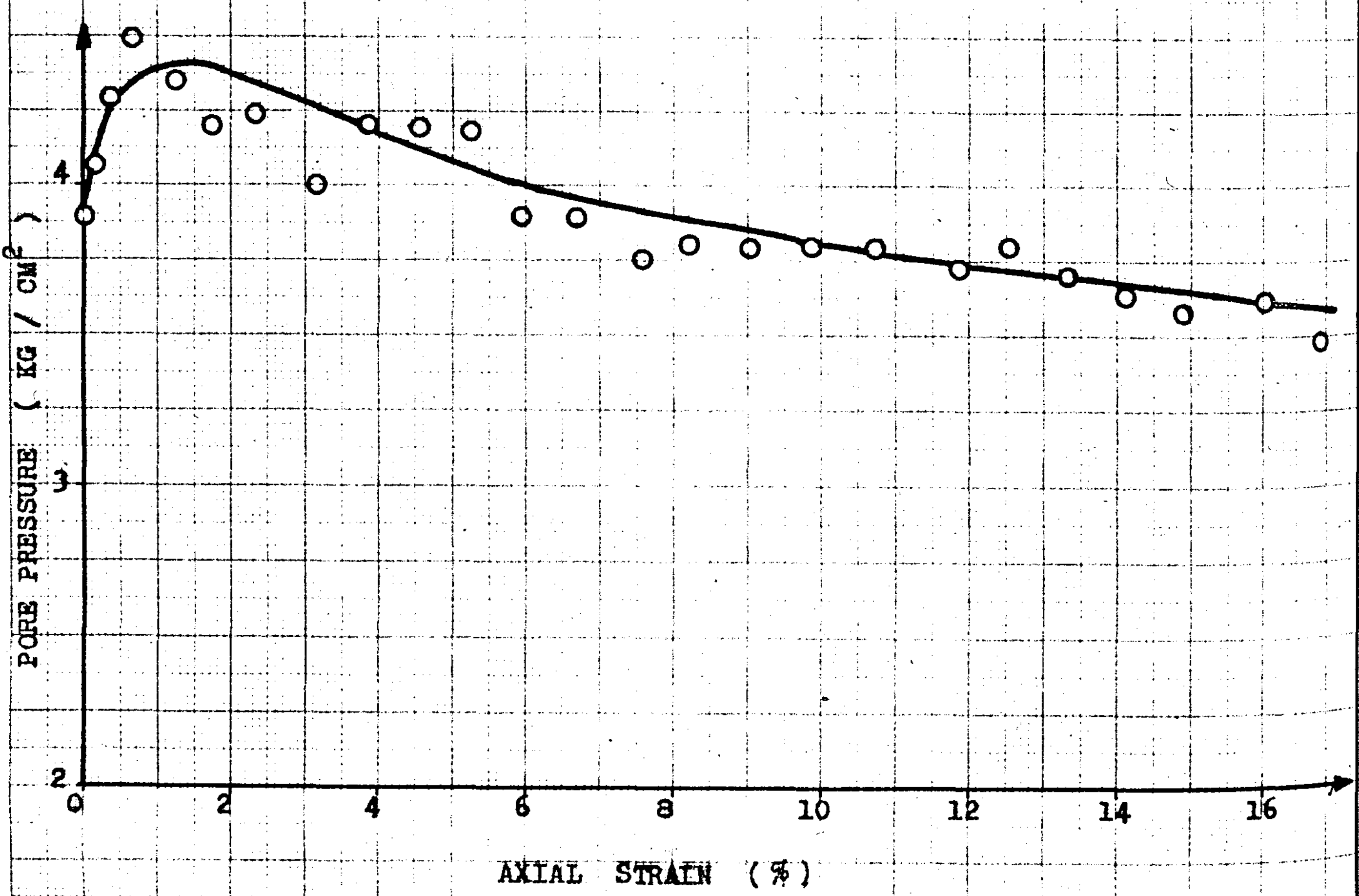

Fig 4.20 Deviator Stress versus Effective Mean Normal Stress

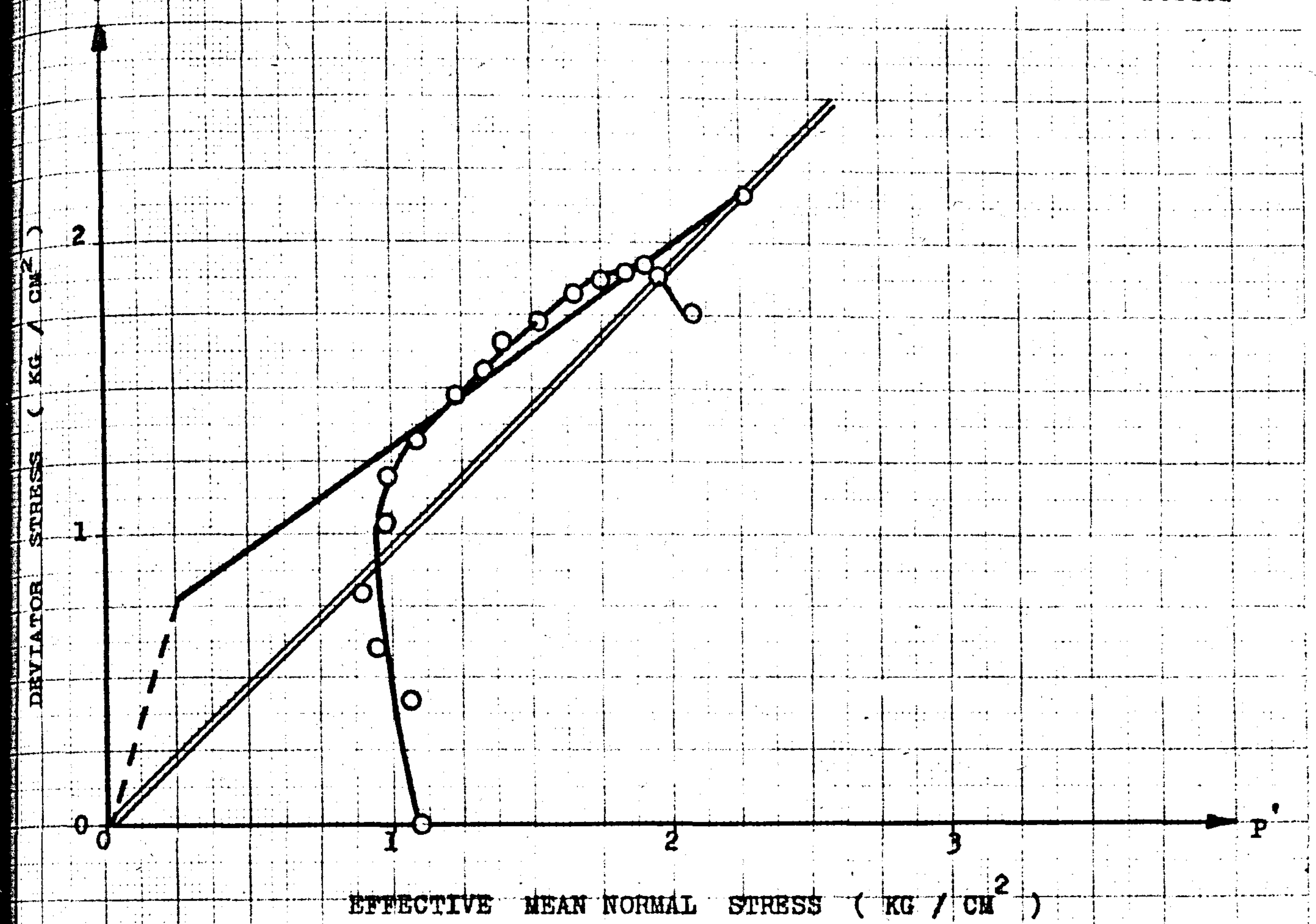

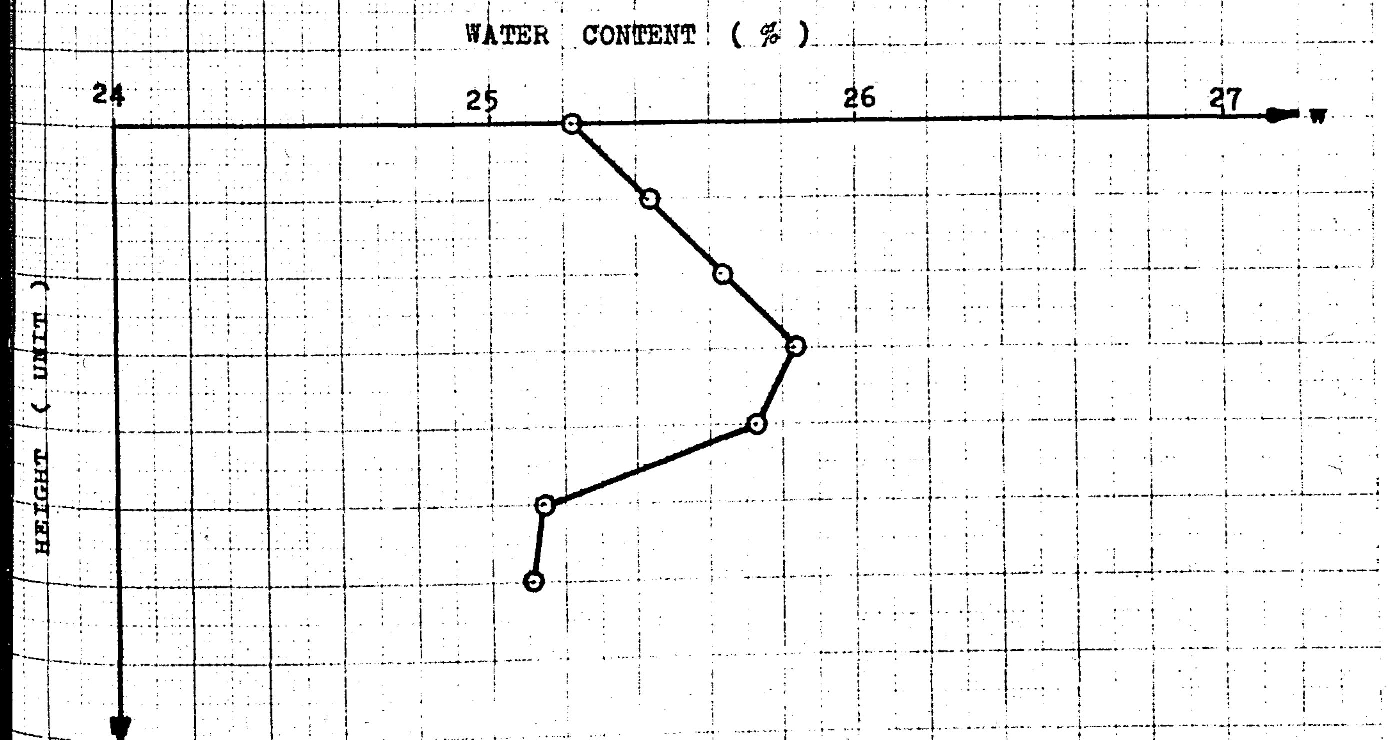

Fig 4.21 Height (Unit) vesus Water Content

Consolidation Pressure : 4.5 Kgcm^{-2}

Equivalent Mean Normal Stress $(Pe)_i$: 4.067 Kgcm^{-2}

Proving Ring Number and Constant : 12365 / 0.09639 O. C. R. : 10

Specimen Diameter Top : 3.59 cm. Bottom : 3.61 cm. Average : 3.60 cm.

Specimen Weight : 168.10 gr. Specimen Height : 8.04 cm.

Av. Specimen Area : 10.179 cm^{-2} Av. Loading Rate : 0.0303 mm/min.

Loading dial In. x10^{-4}	Axial strain %	Pore pressure Kg. / cm^2	Deviator stress Kg. / cm^2	Ef. Mean normal stress Kg. / cm^2	Water Content %	
0.0	0.00	4.61	0.000	1.390	Slice No.	Water Content
22.2	0.25	4.70	0.199	1.367		
91.3	0.50	5.08	0.815	1.283	1	22.751
119.0	1.49	5.18	1.040	1.162	2	23.827
142.7	2.36	5.19	1.230	1.235	3	24.471
161.2	2.86	5.11	1.386	1.287	4	23.560
181.0	3.67	5.08	1.546	1.370	5	25.381
197.2	4.60	5.00	1.671	1.457	6	24.825
218.9	6.22	5.08	1.829	1.580	7	23.743
228.5	7.09	4.90	1.893	1.646		
235.5	7.84	4.95	1.936	1.695		
250.0	9.76	4.87	2.011	1.800	Average w : 24.080	
261.5	11.81	4.75	2.053	1.894	Sketch of Failure	
269.5	13.81	4.70	2.064	1.948		
277.9	15.98	4.65	2.069	1.995		
281.5	16.79	4.65	2.074	2.011		
288.9	18.91	4.60	2.060	2.051		
291.5	20.27	4.60	2.047	2.071		
294.5	21.14	4.60	2.043	2.018		

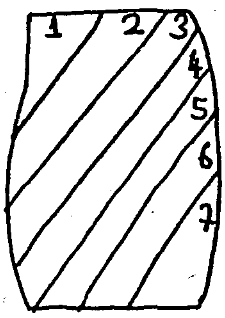

Max. Axial Stress: 2.074 kgcm^{-2} Water Con. at Failure Surface: 25.381 %

Fig 4.22 Deviator Stress versus Axial Strain

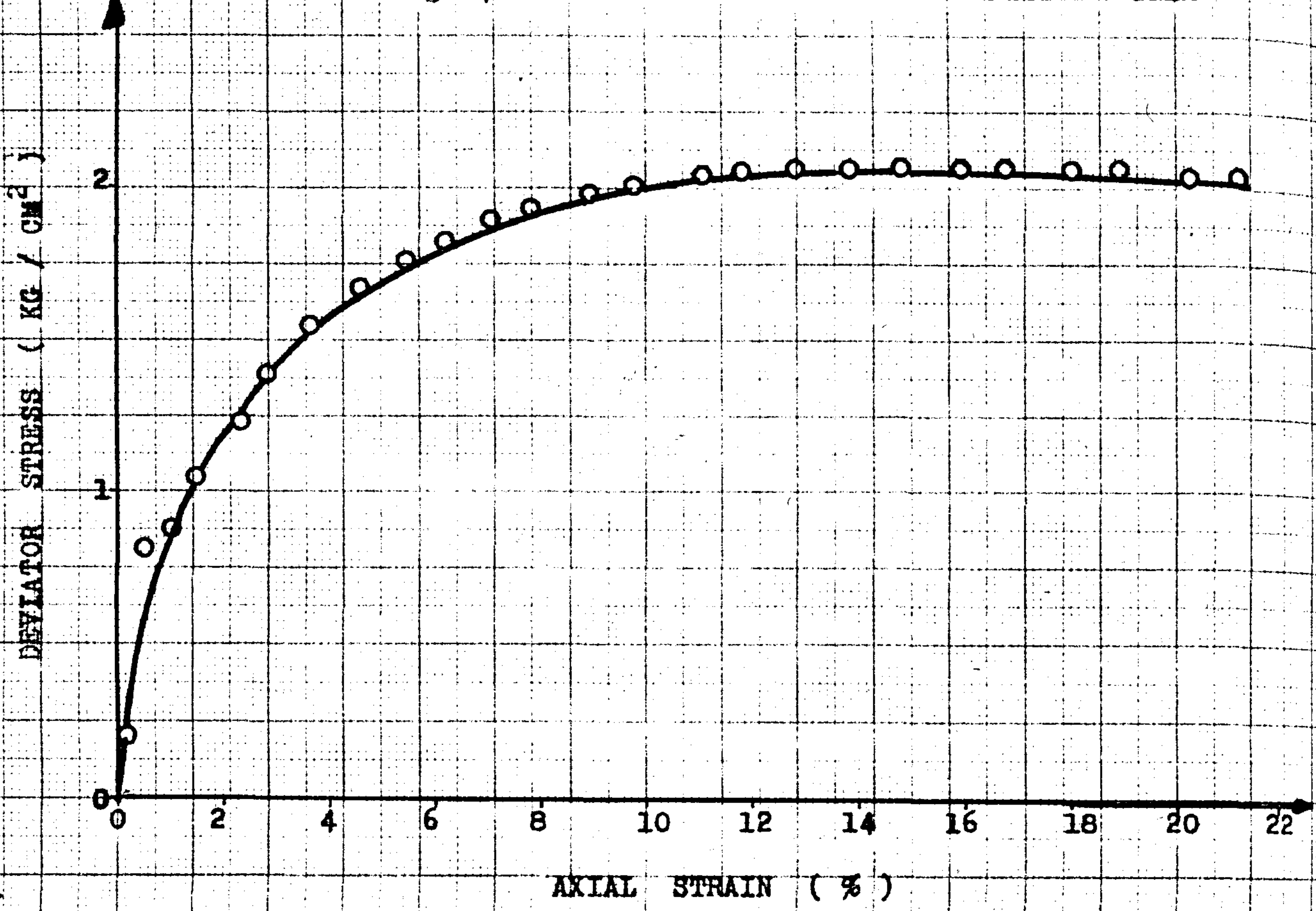

Fig 4.23 Pore Water Pressure versus Axial Strain

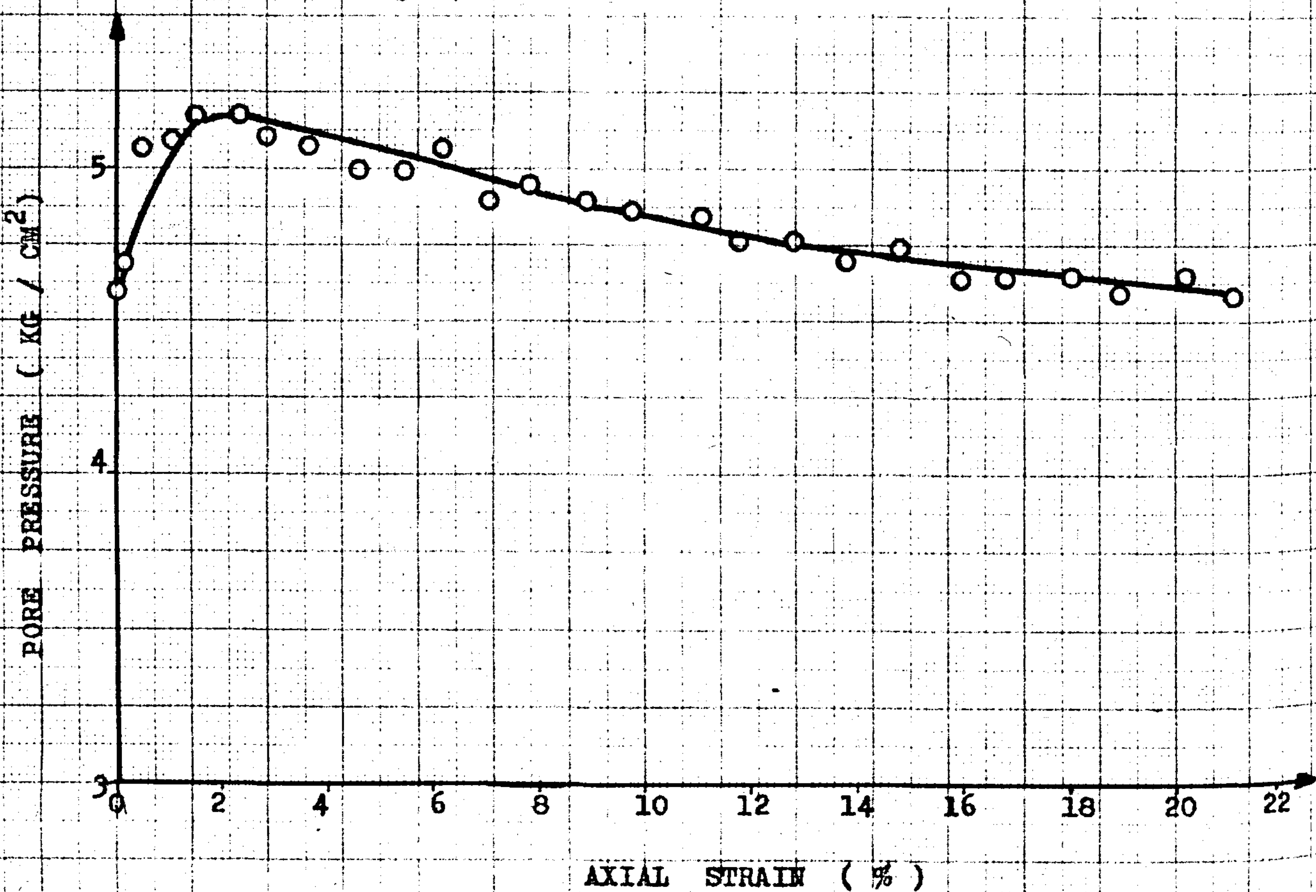

Fig 4.24 Deviator Stress versus Effective Mean Normal Stress

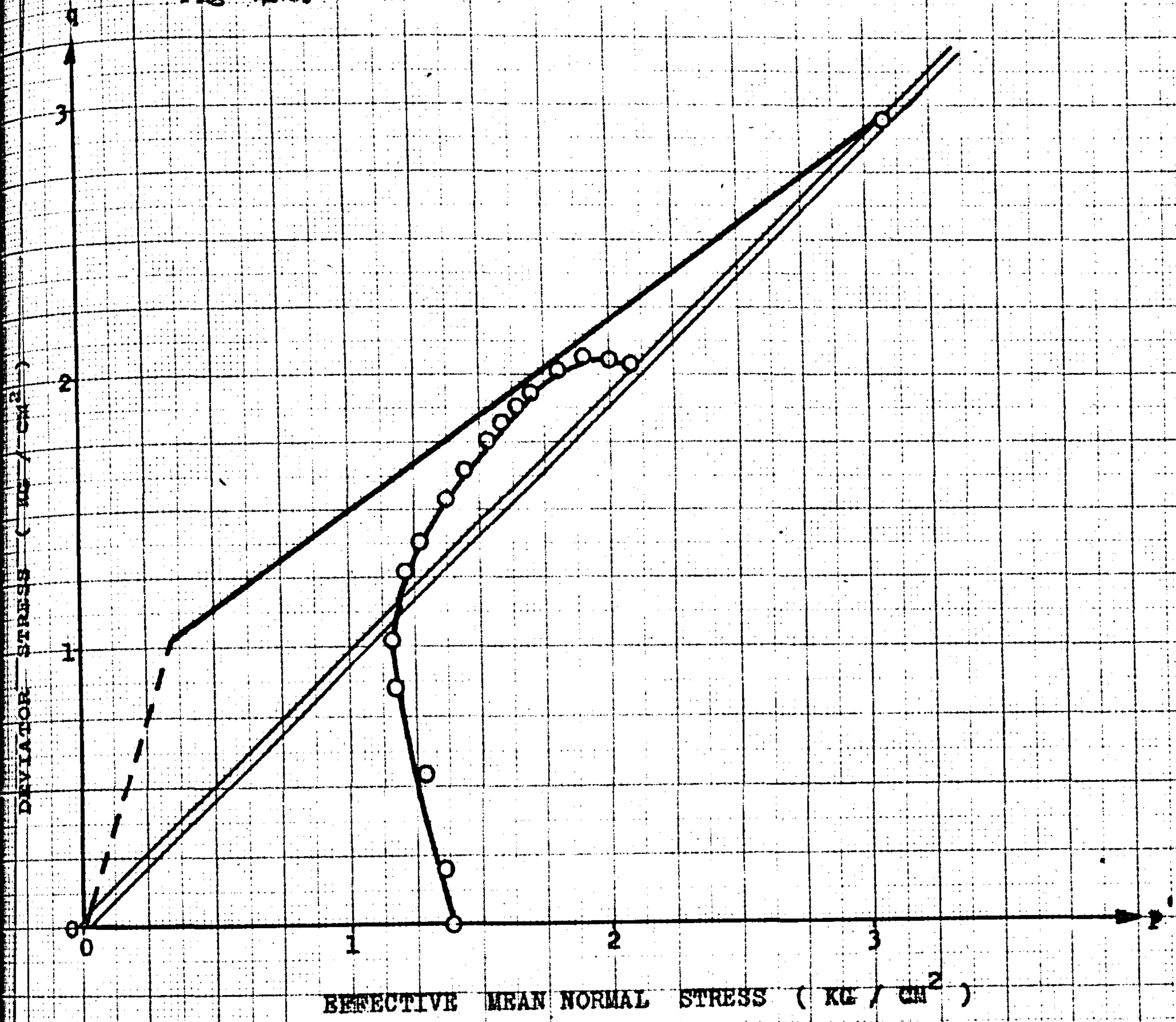

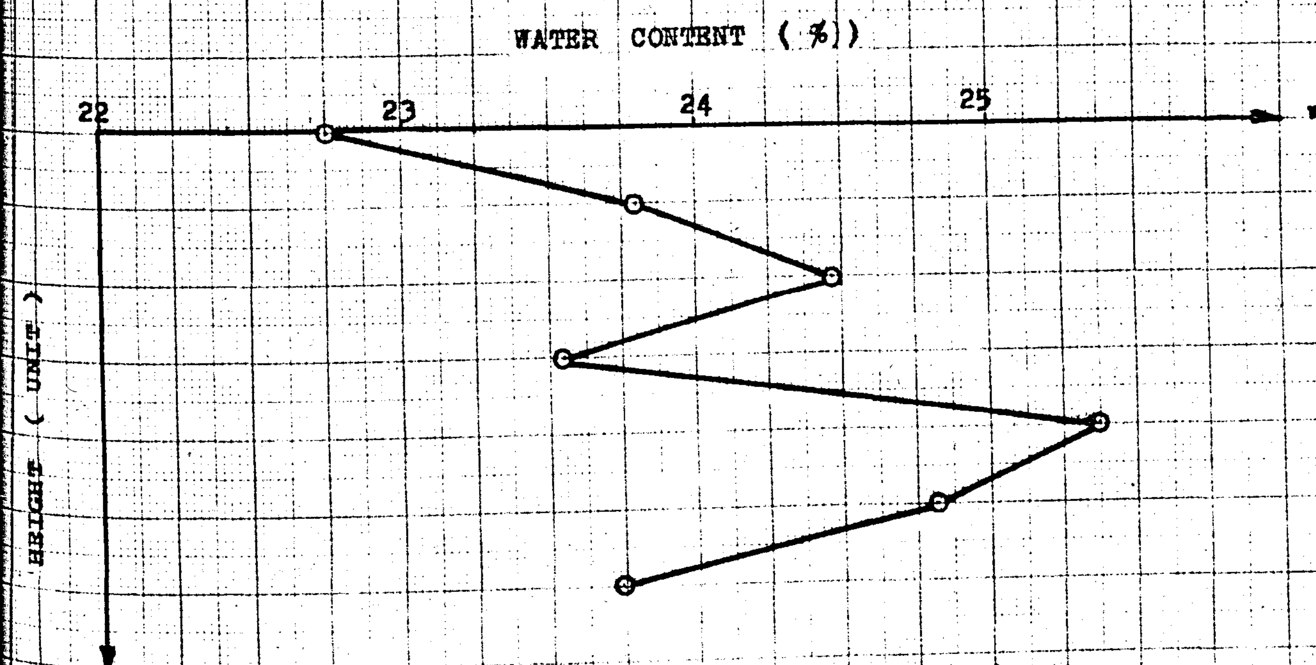

Fig 4.25 Height (Unit) versus Water Content

Consolidation Pressure : 5.0 $Kgcm^{-2}$

Equivalent Mean Normal Stress $(Pe)_i$: 3.182 $Kgcm^{-2}$

Proving Ring Number and Constant : 12365 / 0.09639 O. C. R. : 10

Specimen Diameter Top : 3.58 cm Bottom : 3.60 cm Average : 3.59 cm

Specimen Weight : 170.56 gr. Specimen Height : 8.03 cm.

Av. Specimen Area : 10.122 cm^{-2} Av. Loading Rate : 0.0303 mm/min.

Loading dial In. $\times 10^{-4}$	Axial strain %	Pore pressure Kg. / cm^2	Deviator stress Kg. / cm^2	Ef. Mean normal stress Kg. / cm^2	Water Content %	
0.0	0.00	4.20	0.000	1.800	Slice No.	Water Content
29.0	0.25	4.35	0.264	1.688		
63.0	0.50	4.70	0.552	1.384	1	23.540
106.8	1.06	5.30	0.942	1.295	2	24.430
122.3	1.43	5.25	1.079	1.257	3	25.530
148.2	1.99	5.20	1.297	1.220	4	26.183
160.5	2.86	5.20	1.388	1.237	5	26.030
175.0	3.62	5.13	1.501	1.300	6	25.290
196.0	5.06	5.40	1.660	1.418	7	25.065
214.5	7.10	5.10	1.781	1.533		
225.3	9.03	5.00	1.829	1.605		
231.3	10.96	5.00	1.833	1.647	Average w	25.151
235.0	12.08	4.90	1.836	1.672	Sketch of Failure	
238.5	14.20	4.95	1.812	1.699		
239.1	15.32	4.85	1.780	1.701		
239.9	16.50	4.85	1.763	1.713		
238.4	17.87	4.81	1.717	1.707		
236.0	19.43	4.81	1.658	1.700		
229.5	21.05	4.80	1.569	1.682		

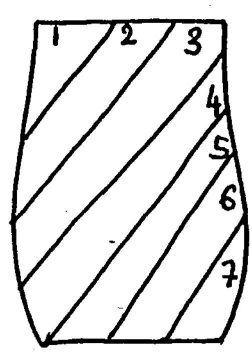

Max. Axial Stress: 1.836 $kgcm^{-2}$ Water Con. at Failure Surface: 26.183 %

Fig 4.26 Deviator Stress versus Axial Strain

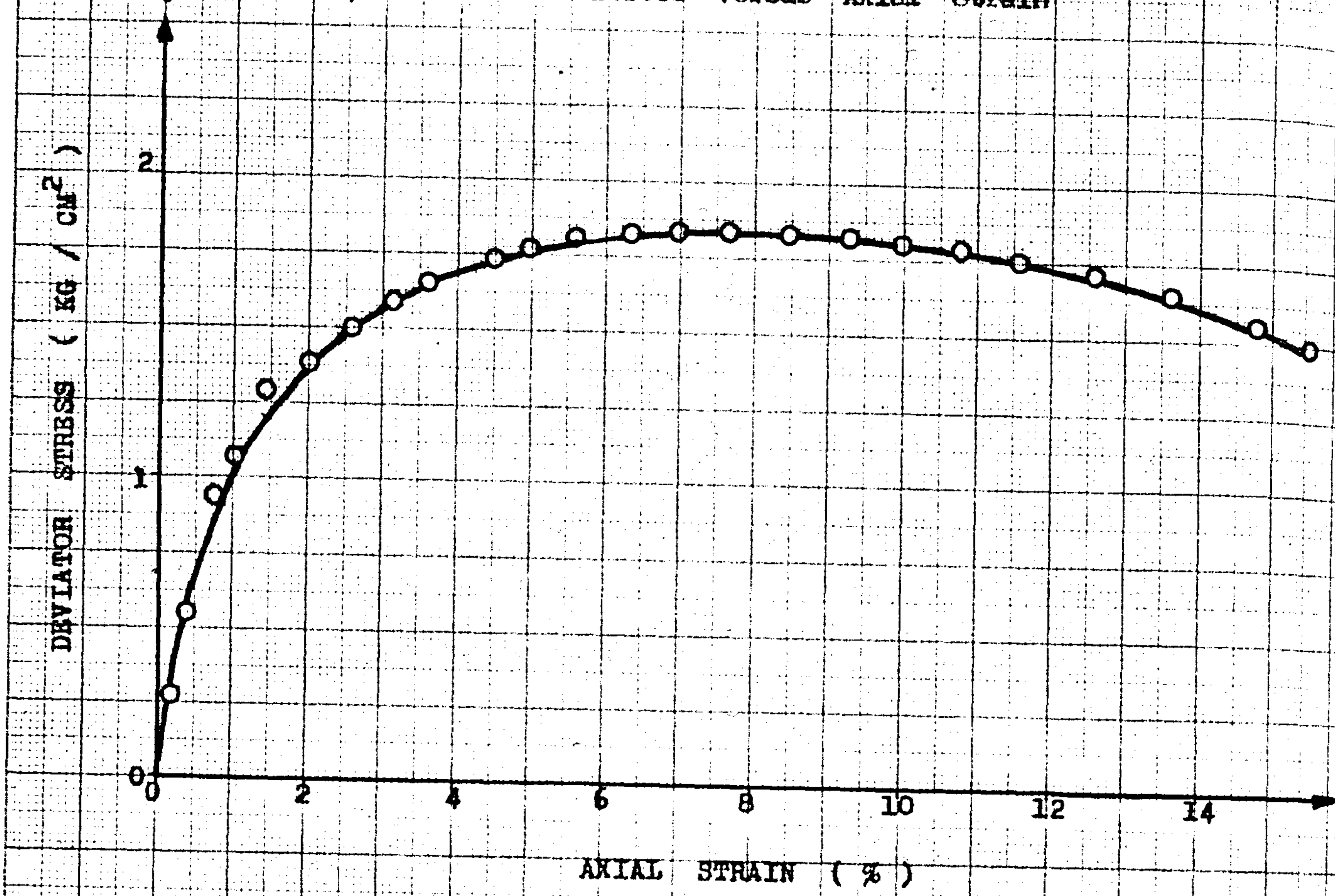

Fig 4.27 Pore Water Pressure versus Axial Strain

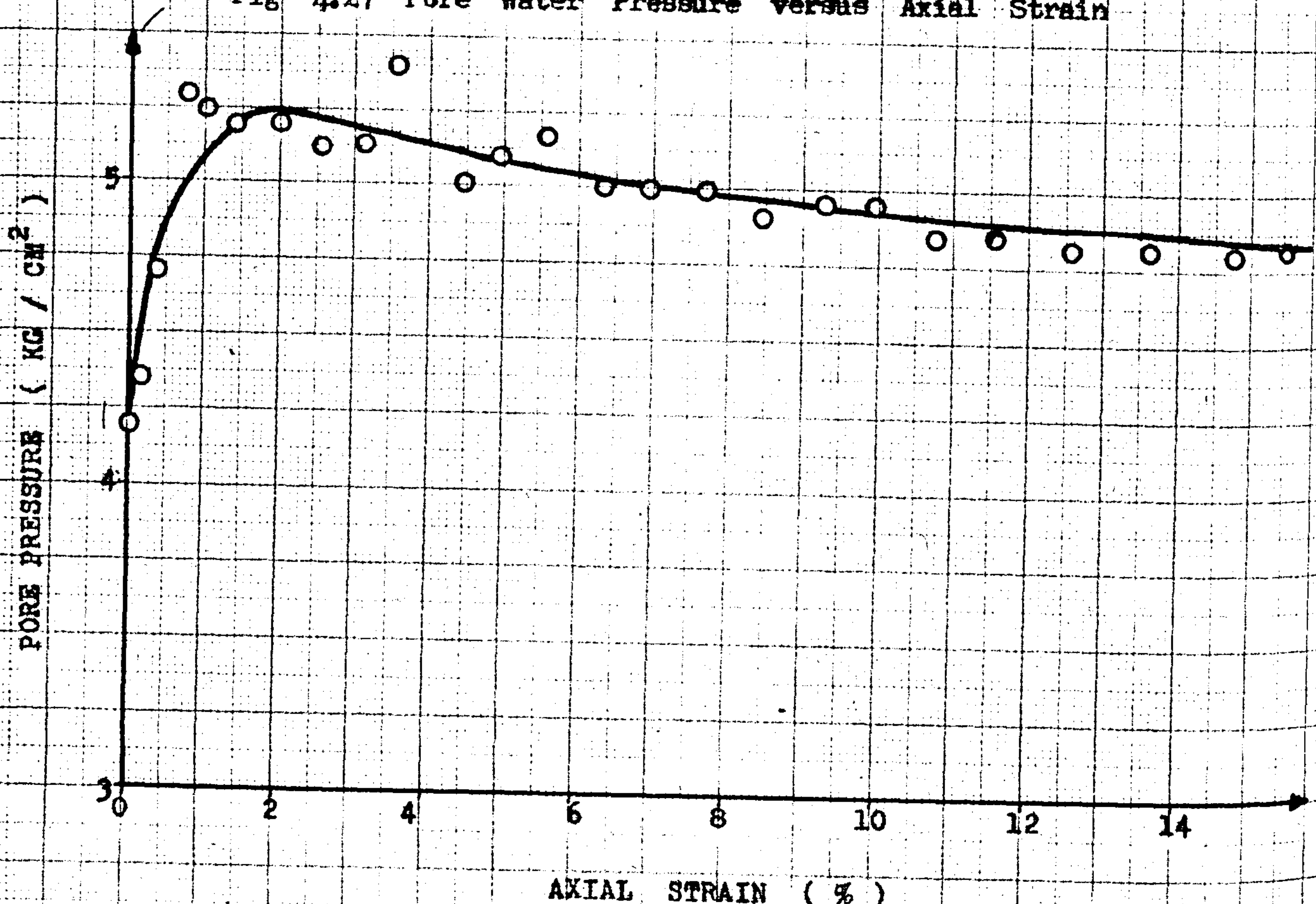

Fig 4.28 Deviator Stress versus Effective Mean Normal Stress

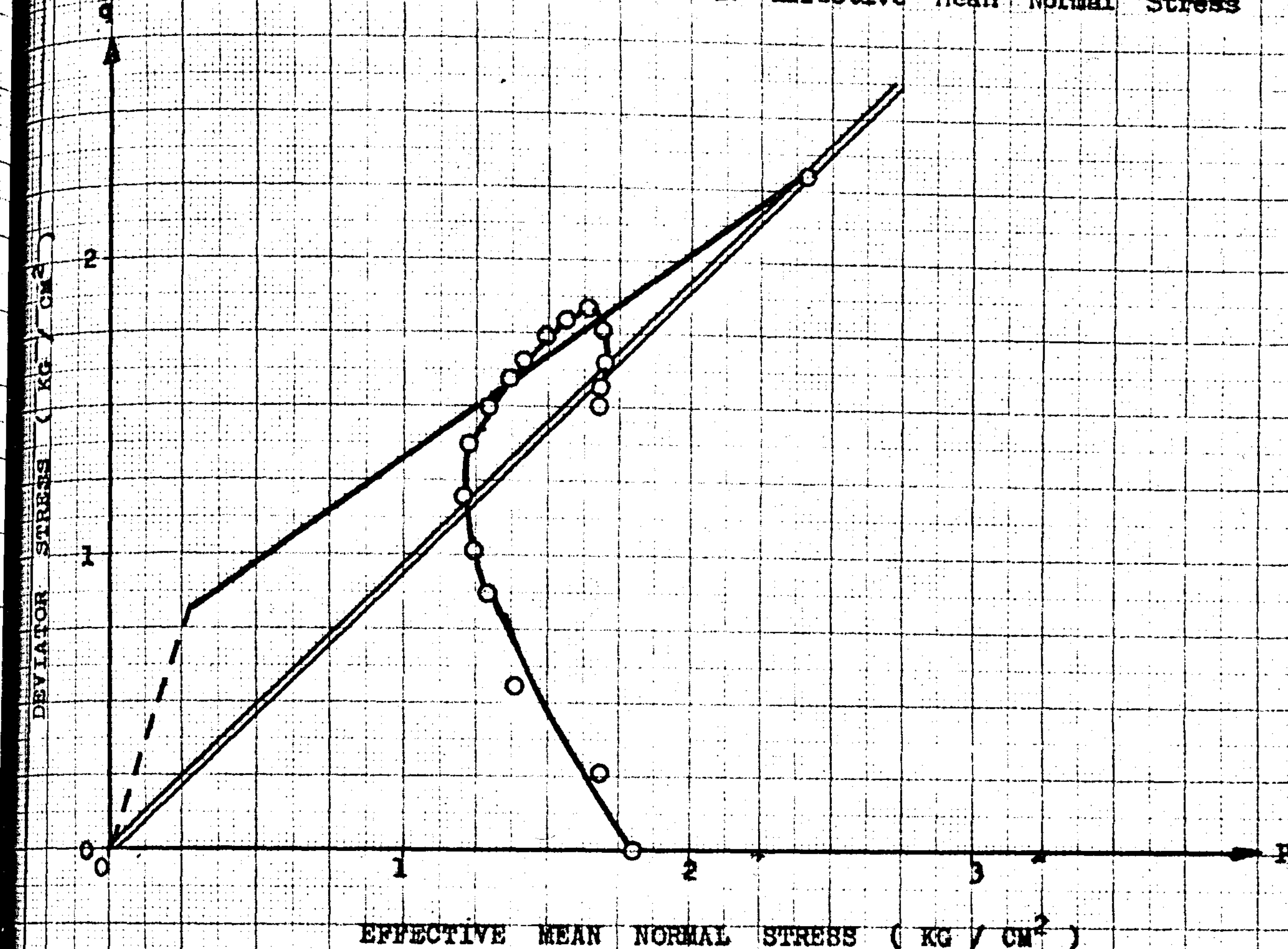

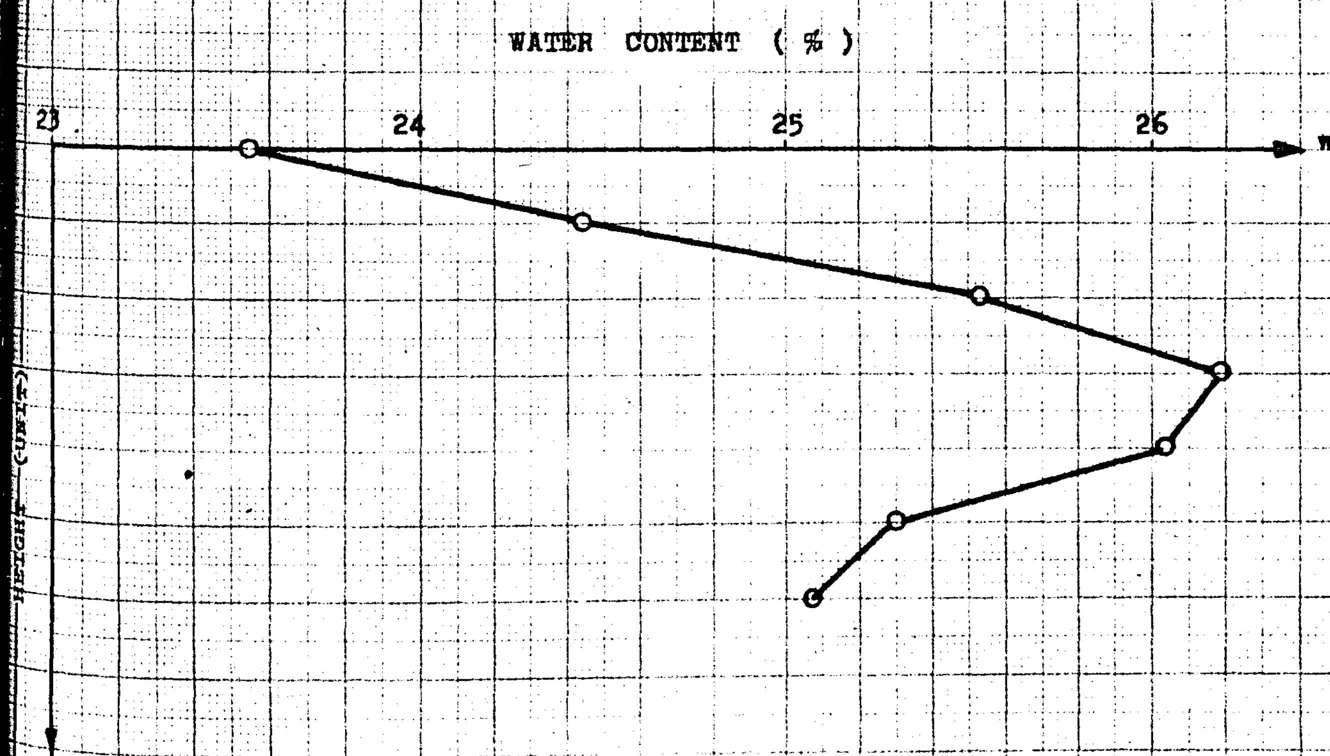

Fig 4.29 Height (Unit) versus Water Content

Consolidation Pressure : 6.0 $Kgcm^{-2}$

Equivalent Mean Normal Stress $(Pe)_i$: 2.925 $Kgcm^{-2}$

Proving Ring Number and Constant :12365/0.09639 O. C. R. : 15

Specimen Diameter Top : 3.60 cm. Bottom : 3.60 cm. Average : 3.60 cm.

Specimen Weight : 168.80 gr. Specimen Height :8.04 cm.

Av. Specimen Area : 10.178 cm^{-2} Av.Loading Rate : 0.0303 mm/min.

Loading dial $In. \times 10^{-4}$	Axial strain %	Pore pressure Kg. / cm^2	Deviator stress Kg. / cm^2	Ef. Mean normal stress Kg. / cm^2	Water Content %	
					Slice No.	Water Content
0.0	0.00	0.95	0.000	2.050		
31.0	0.25	1.22	0.250	1.863		
58.7	1.00	1.45	0.468	1.671	1	24.669
70.0	1.24	1.53	0.588	1.597	2	24.636
100.8	1.99	1.85	0.850	1.433	3	25.674
116.0	2.55	2.09	0.975	1.340	4	25.476
128.2	2.98	2.19	1.078	1.319	5	25.829
142.5	3.54	2.05	1.198	1.244	6	26.647
150.3	4.04	2.00	1.253	1.272	7	25.640
162.5	4.97	2.05	1.351	1.309		
168.0	5.76	1.98	1.386	1.364		
179.9	6.22	2.07	1.483	1.393	Average w :25.519	
187.3	6.77	2.10	1.538	1.438	Sketch of Failure	
203.5	8.21	2.00	1.648	1.544		
210.0	8.96	2.00	1.687	1.592		
221.5	10.70	1.95	1.746	1.682		
226.0	11.69	1.89	1.760	1.725		
232.8	13.18	1.75	1.780	1.788		
234.7	14.30	1.74	1.767	1.829		

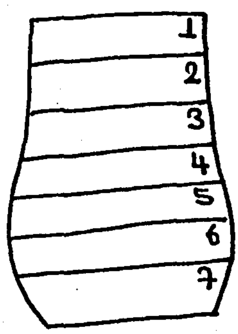

Max. Axial Stress: 1.780 $kgcm^{-2}$ Water Con. at Failure Surface: 26.647 %

Fig 4.30 Deviator Stress versus Axial Strain

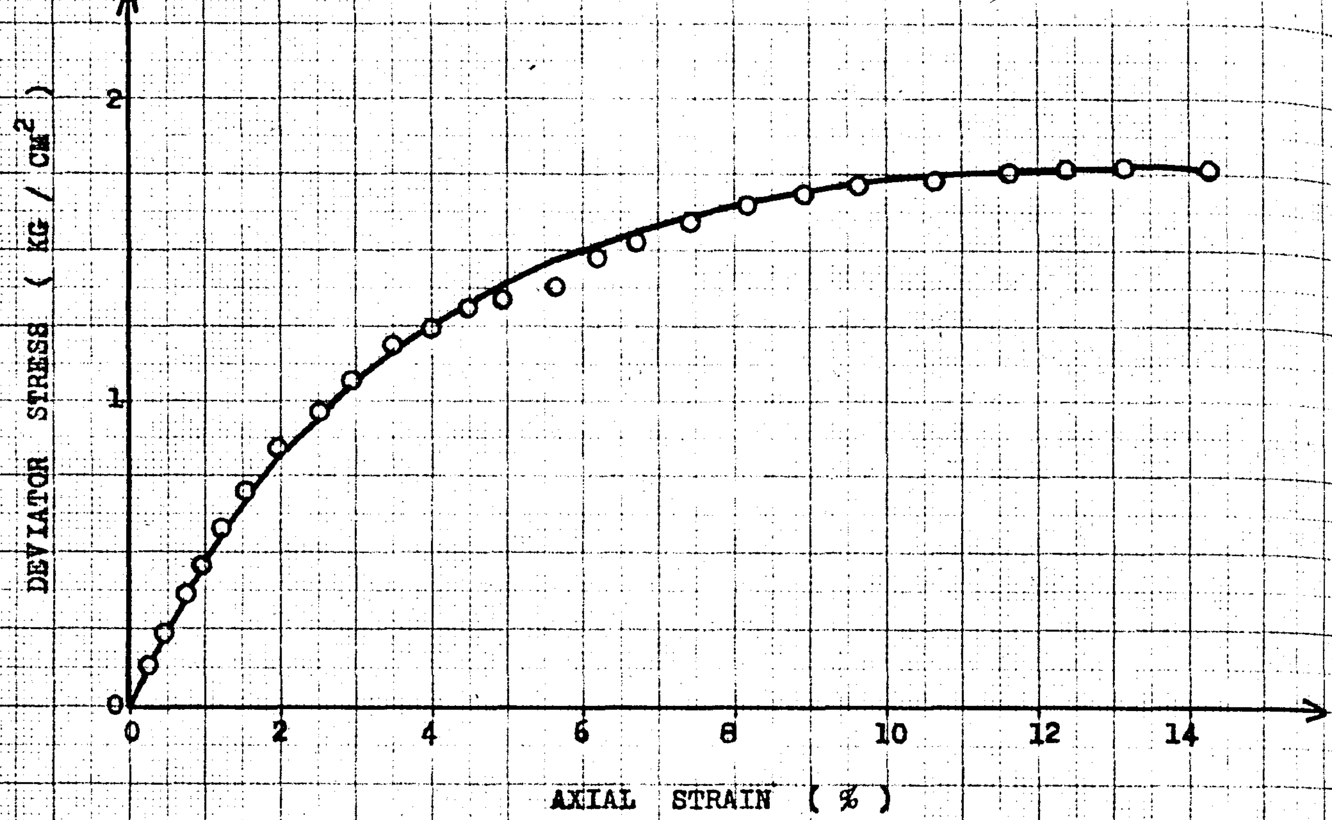

Fig 4.31 Pore Water Pressure versus Axial Strain

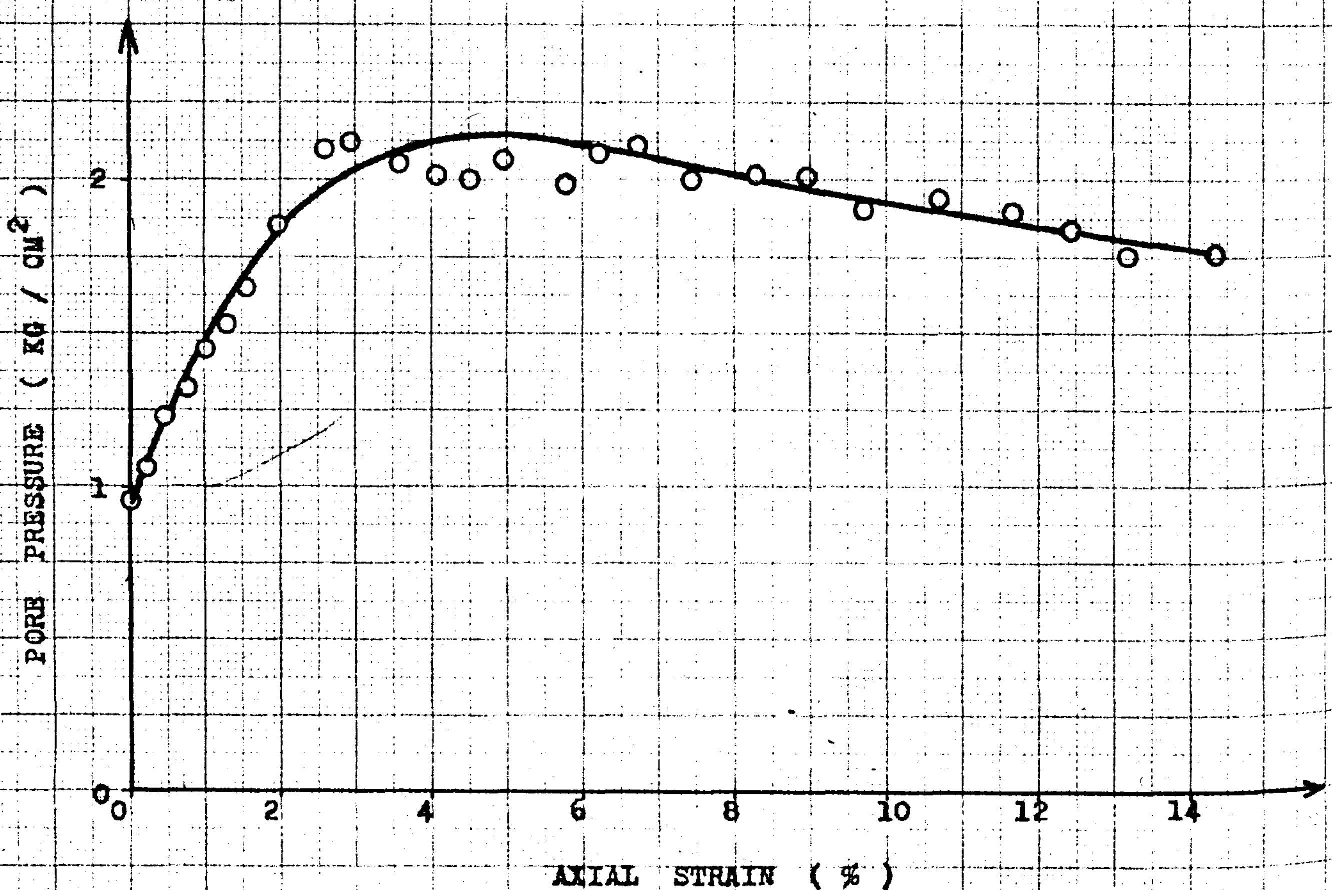

Fig 4.32 Deviator Stress versus Effective Mean Normal Strain

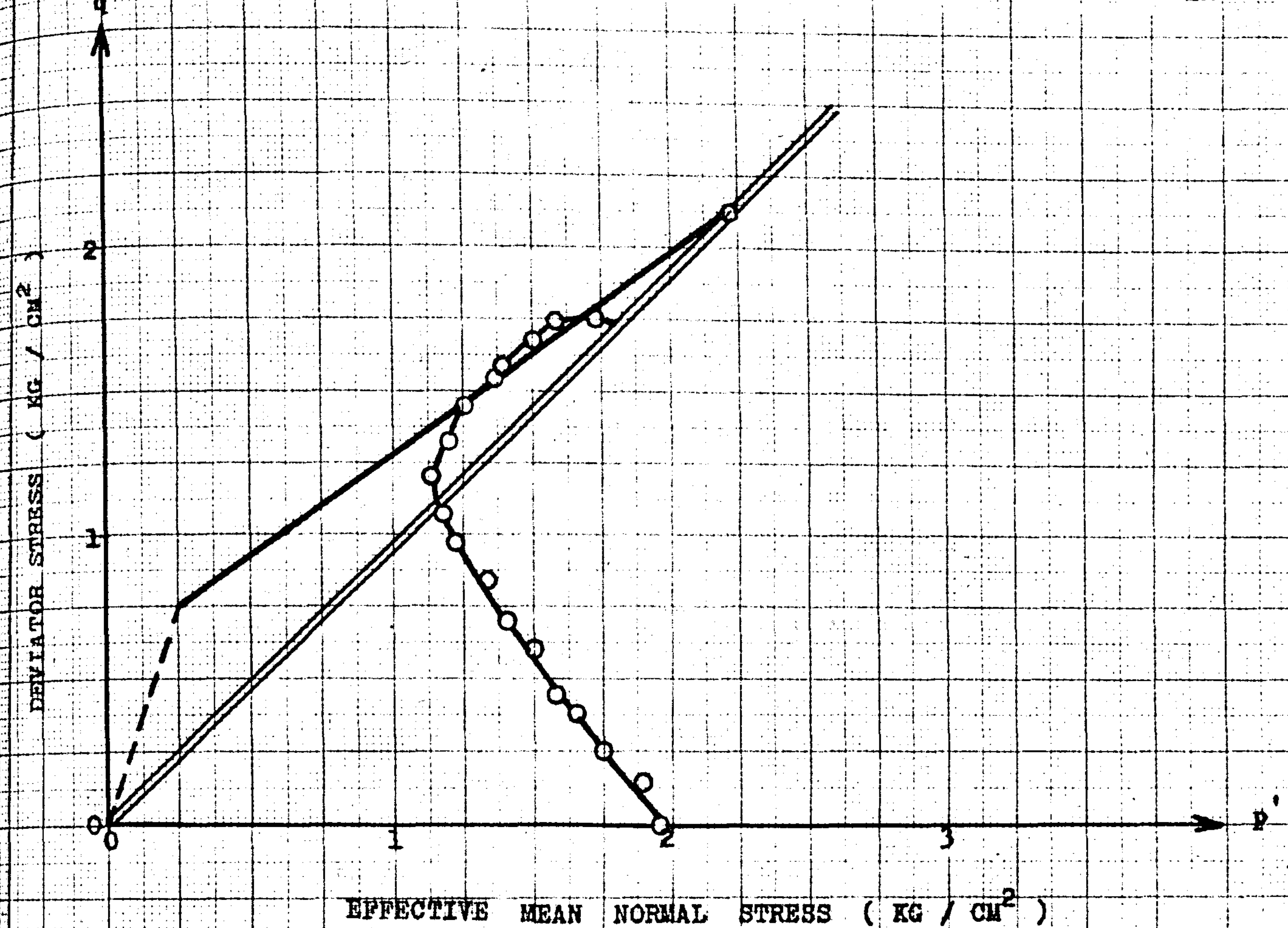

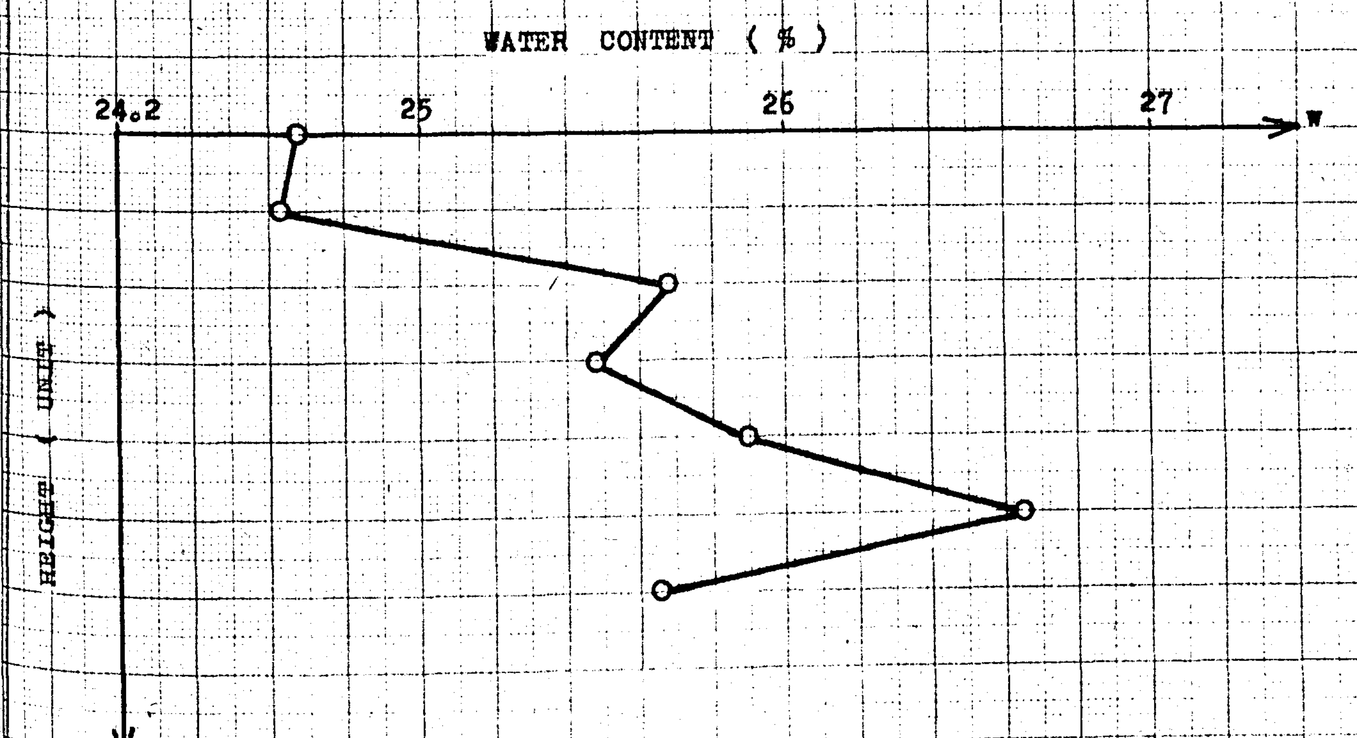

Fig 4.33 Height (Unit) versus Water Content

Consolidation Pressure : 6.0 $kgcm^{-2}$

Equivalent Mean Normal Stress $(Pe)_i$: 3.972 $Kgcm^{-2}$

Proving Ring Number and Constant :12365/0.09639 O. C. R. : 15

Specimen Diameter Top : 3.6 cm. Bottom : 3.6 cm. Average :3.6 cm.

Specimen Weight :167.38 gr. Specimen Height : 8.04

Av. Specimen Area : 10.178 cm^{-2} Av.Loading Rate : 0.0303 mm/min.

Loading dial $In.\times10^{-4}$	Axial strain %	Pore pressure $Kg./cm^2$	Deviator stress $Kg./cm^2$	Ef. Mean normal stress $Kg./cm^2$	Water Content %	
0.0	0.00	1.60	0.000	1.400	Slice No.	Water Content
16.5	0.25	1.80	0.145	1.275		
56.1	0.50	1.92	0.484	1.235	1	22.679
78.0	0.75	2.00	0.684	1.267	2	23.470
106.0	1.24	2.05	0.925	1.223	3	24.360
128.8	1.75	2.10	1.119	1.263	4	24.627
143.7	2.24	2.07	1.242	1.339	5	25.180
160.0	2.86	2.04	1.375	1.408	6	25.050
180.0	3.73	2.00	1.536	1.512	7	24.580
202.3	5.10	1.92	1.706	1.675	8	23.516
214.0	5.91	1.90	1.793	1.743		
229.6	6.96	1.82	1.906	1.835	Average w :24.183	
251.2	8.98	1.68	2.042	1.977	Sketch of Failure	
262.5	10.26	1.69	2.105	2.057		
277.5	12.33	1.52	2.172	2.162		
287.1	14.43	1.47	2.188	2.262		
298.5	16.29	1.40	2.223	2.341		
302.0	17.16	1.35	2.224	2.381		
306.0	17.91	1.32	2.231	2.401		

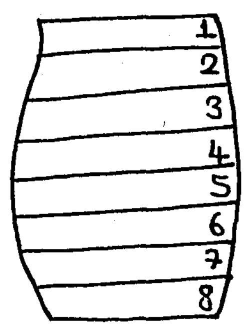

Max. Axial Stress: 2.231 $kgcm^{-2}$ Water Con. at Failure Surface: 25.180 %

Fig 4.34 Deviator Stress versus Axial Strain

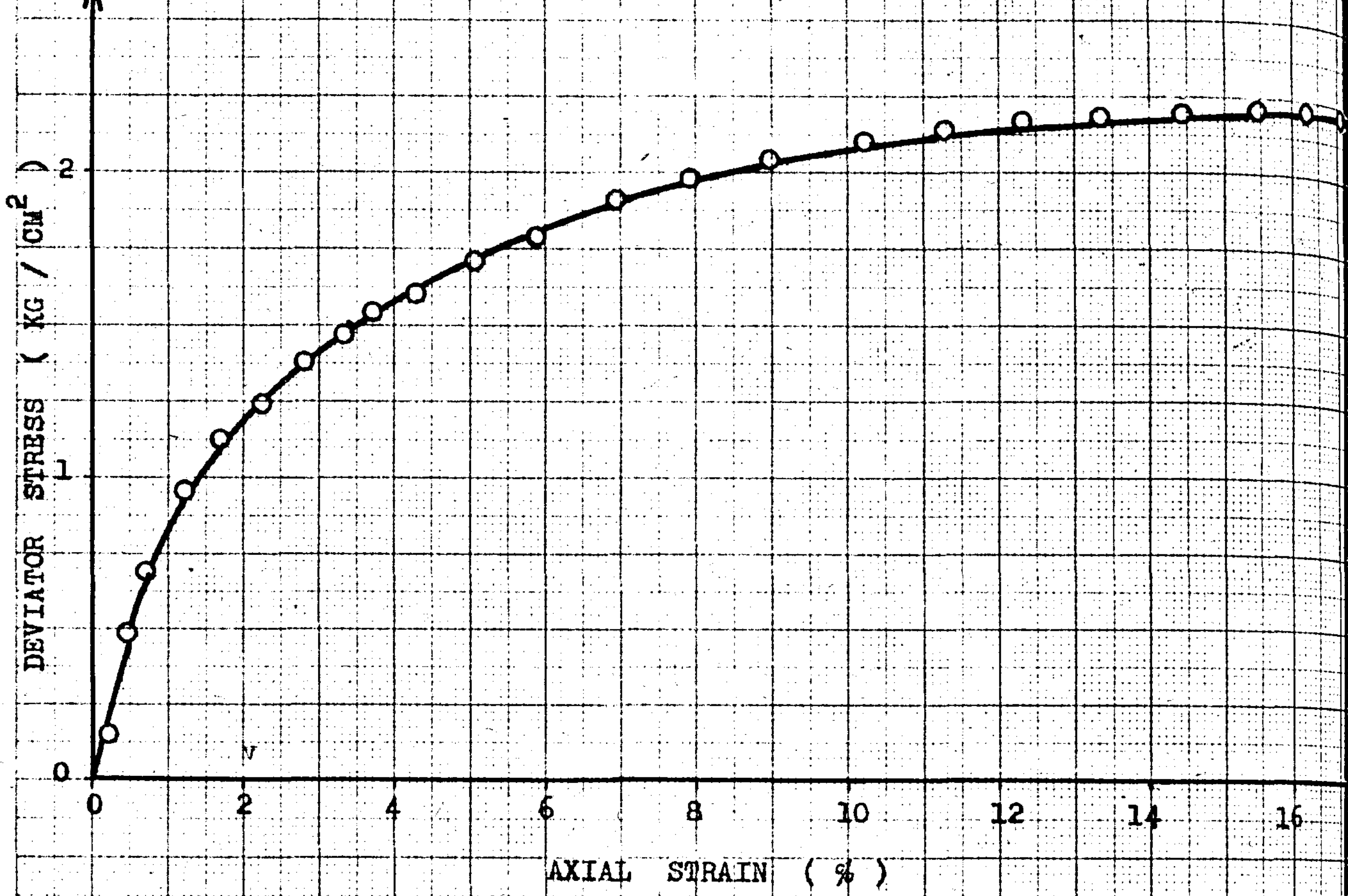

Fig 4.35 Pore Water Pressure versus Axial Strain

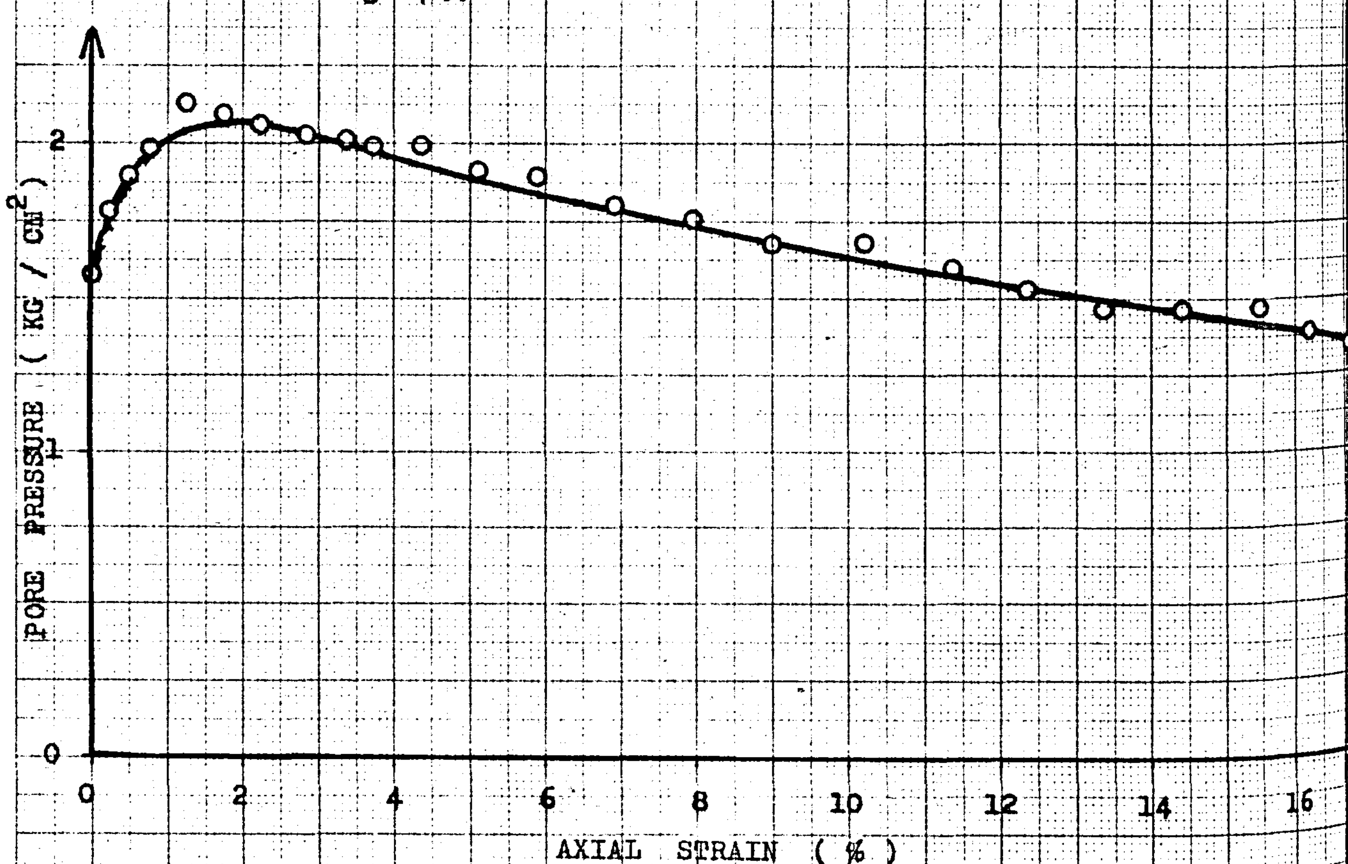

Fig 4.36 Deviator Stress versus Effective Mean Normal Stress

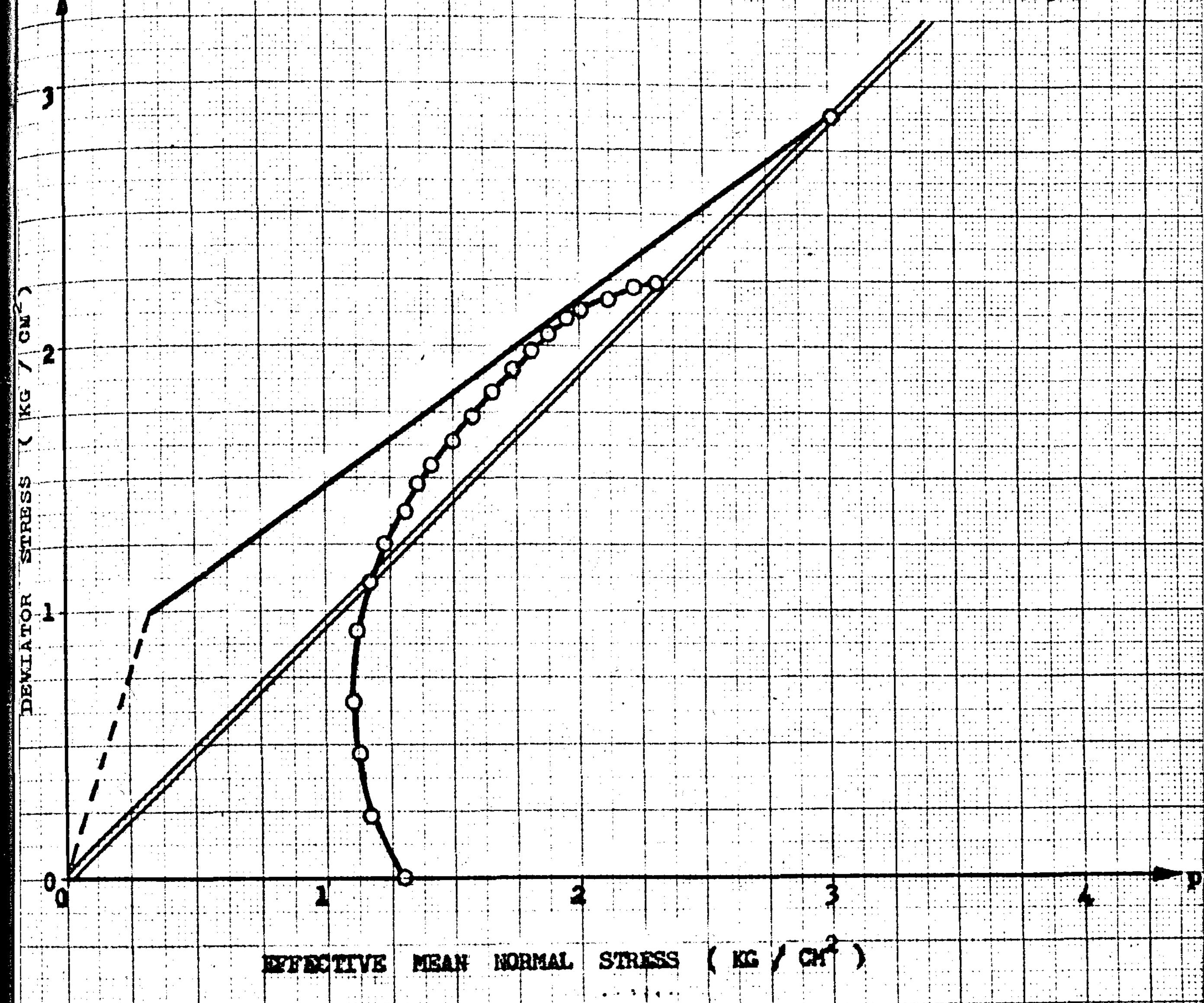

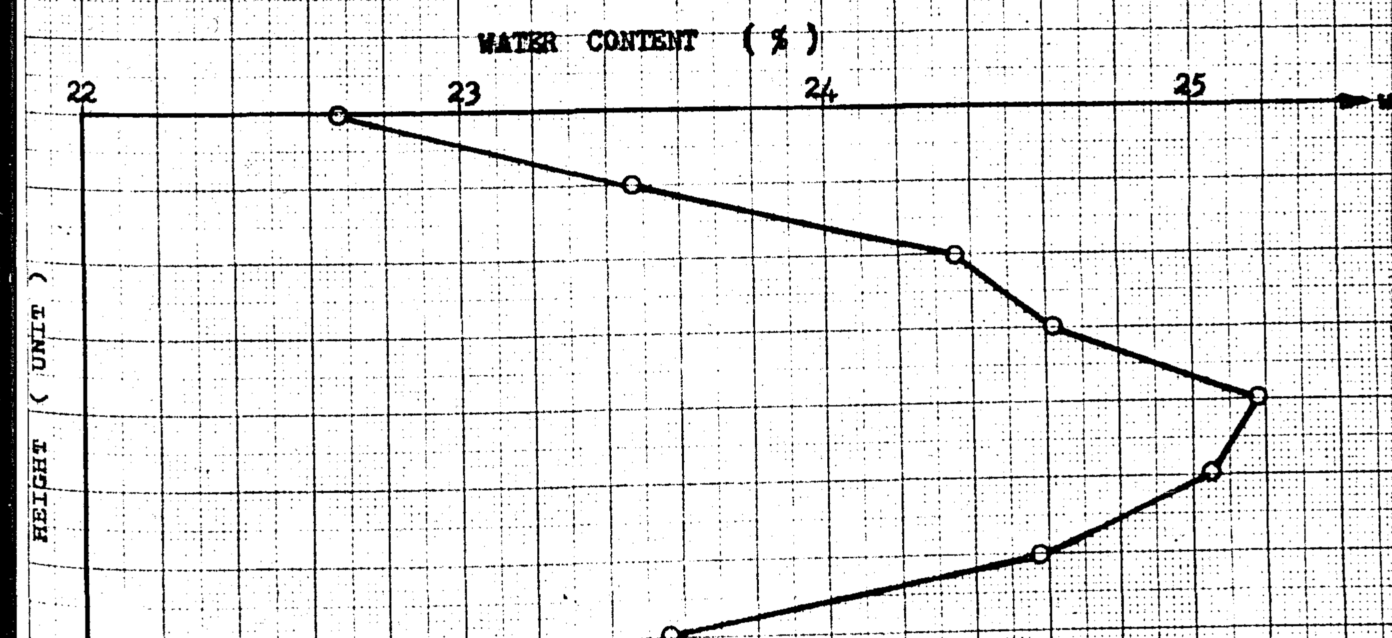

Fig 4.37 Height (Unit) versus Water Content

Consolidation Pressure : 7.5 $Kgcm^{-2}$

Equivalent Mean Normal Stress $(Pe)_i$: 7.249 $Kgcm^{-2}$

Proving Ring Number and Constant :12365/0.09639   O. C. R. : 5

Specimen Diameter   Top : 3.57 cm. Bottom : 3.58cm. Average : 3.575 cm.

Specimen Weight : 168.55 gr.   Specimen Height : 8.00 cm.

Av. Specimen Area : 10.039 cm^{-2} Av.Loading Rate : 0.0303 mm/min.

Loading dial In.x10^{-4}	Axial strain %	Pore pressure Kg. / cm^2	Deviator stress Kg. / cm^2	Ef. Mean normal stress Kg. / cm^2	Water Content % Slice No.	Water Content
0.0	0.00	0.41	0.000	2.590		
24.0	0.13	0.44	0.224	2.968		
137.0	1.62	0.49	1.257	2.927	1	21.096
175.0	1.00	0.52	1.601	3.014	2	21.346
215.0	1.44	0.54	1.966	3.112	3	21.518
247.0	1.94	0.58	2.245	3.168	4	21.573
281.8	2.62	0.65	2.539	3.216	5	21.968
311.0	3.37	0.66	2.784	3.263	6	21.600
343.5	4.50	0.70	3.042	3.324	7	21.572
367.5	5.37	0.72	3.226	3.354	8	21.484
390.0	6.75	0.72	3.376	3.410	9	21.839
417.5	9.38	0.72	3.752	3.426	Average w	:21.555
431.5	12.88	0.72	3.849	3.470	Sketch of Failure	
437.5	14.75	0.81	3.865	3.479		
441.0	17.62	0.79	3.782	3.475		
442.0	19.09	0.77	3.725	3.475		
436.0	22.94	0.72	3.433	3.425		
433.2	23.65	0.72	3.354	3.417		
433.0	24.87	0.69	3.291	3.395		

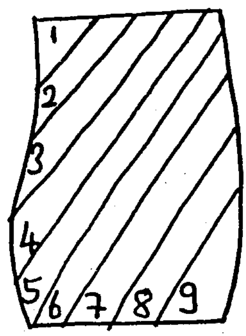

Max. Axial Stress: 3.865 $kgcm^{-2}$ Water Con. at Failure Surface: 21.968 %

Fig 4.38 Deviator Stress versus Axial Strain

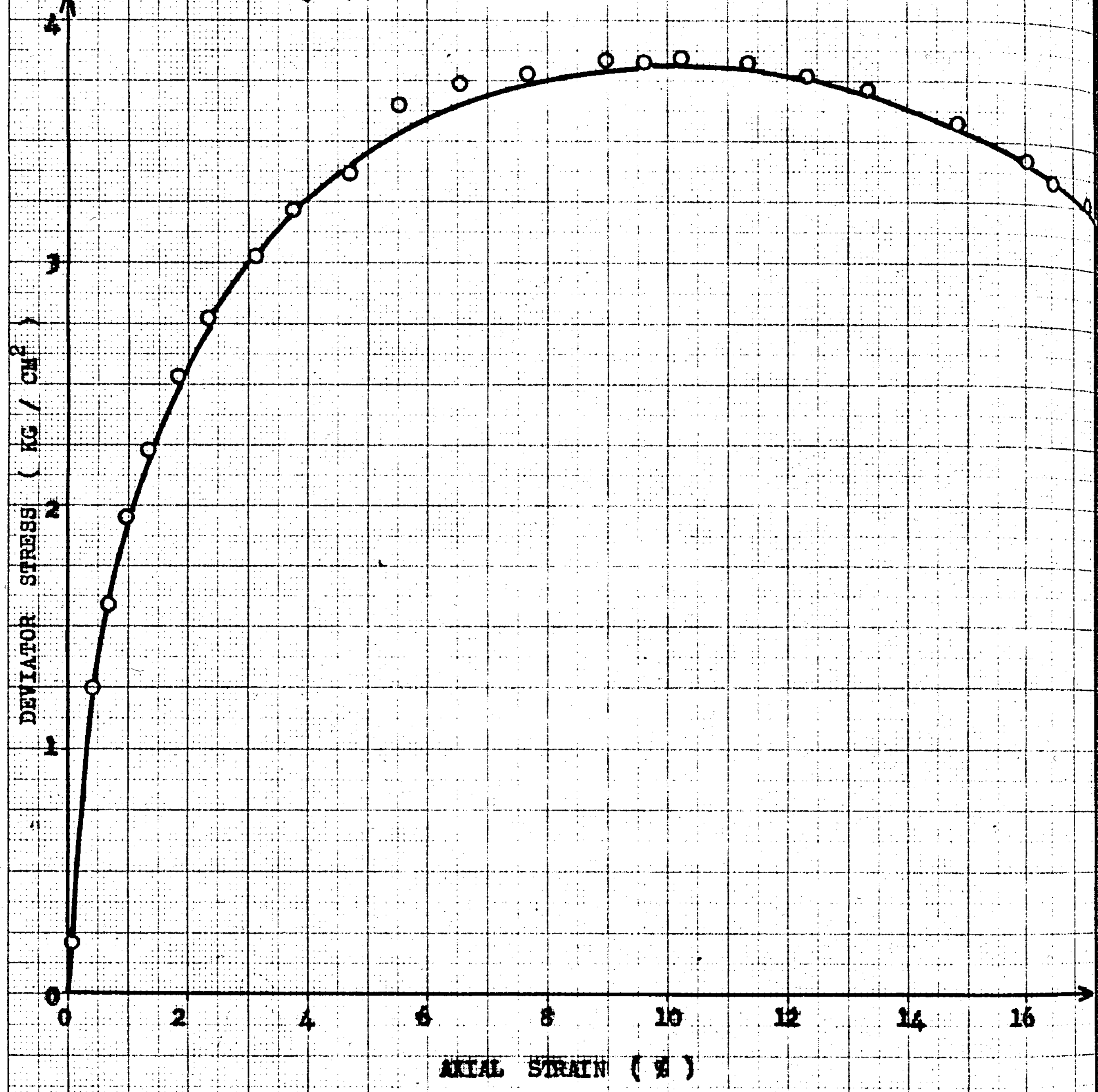

Fig 4.39 Pore Water Pressure versus Axial Strain

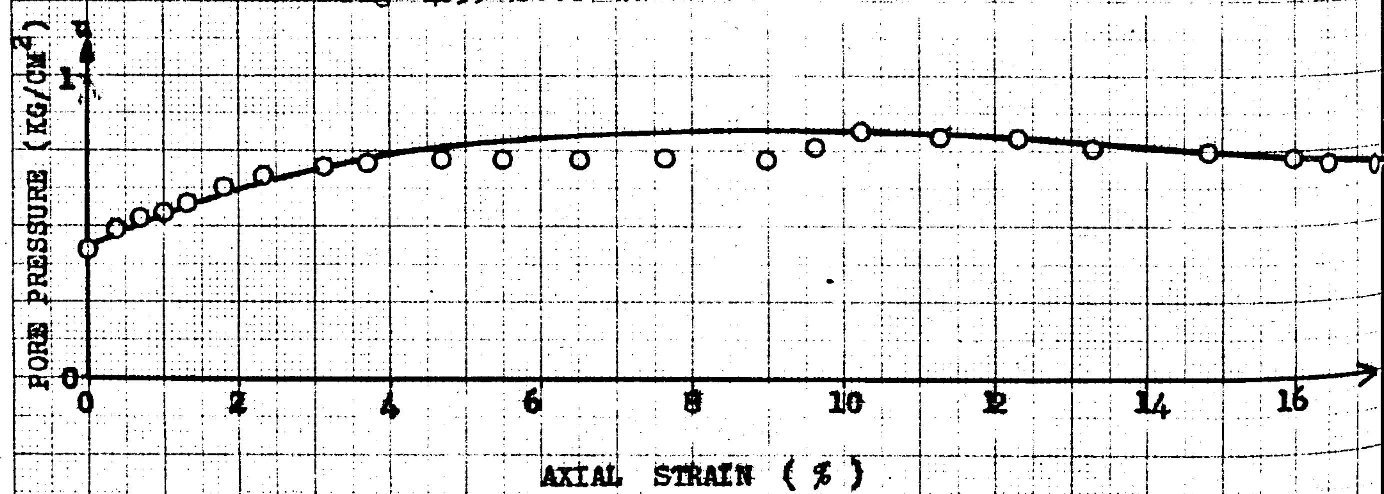

Fig 4.40 Deviator Stress versus Effective Mean Normal Stress

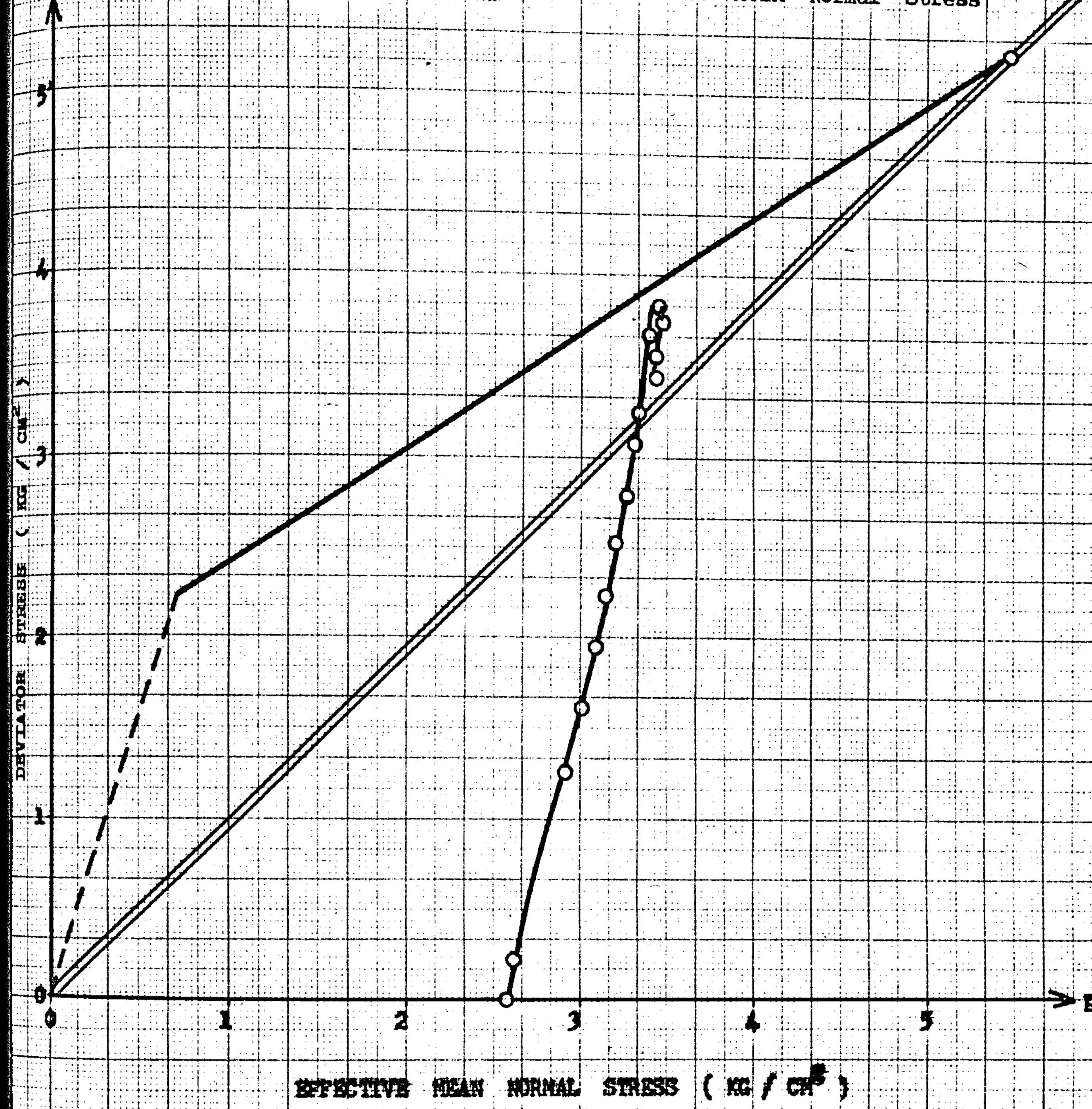

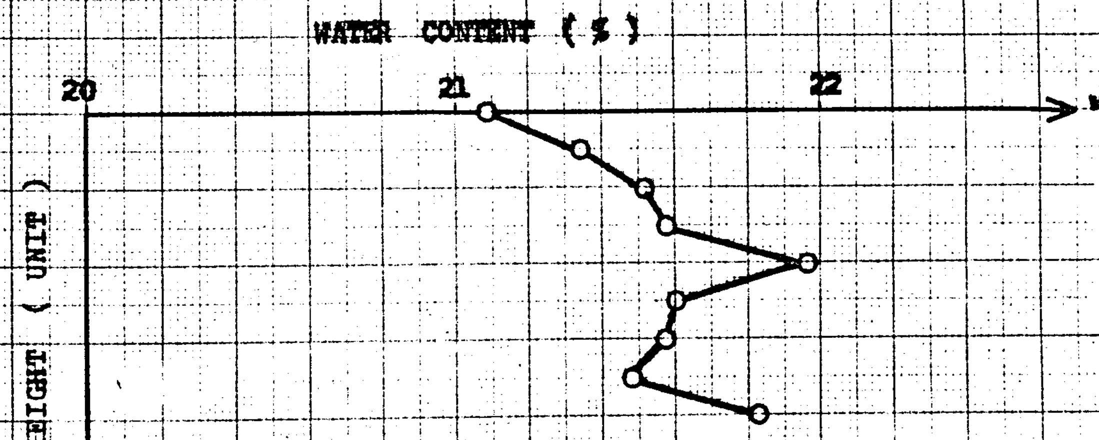

Fig 4.41 Height (Unit) versus Water Content

Consolidation Pressure : 7.5 $Kgcm^{-2}$

Equivalent Mean Normal Stress $(Pe)_i$:6.989 $Kgcm^{-2}$

Proving Ring Number and Constant : 12365/0.09639 O. C. R. : 5

Specimen Diameter Top :3.57cm. Bottom :3.59 cm. Average : 3.58 cm.

Specimen Weight : 167.89 gr. Specimen Height : 8.04 cm.

Av. Specimen Area :10.066 cm^2 Av.Loading Rate :0.0303 mm/min.

Loading dial In.$\times 10^{-4}$	Axial strain %	Pore pressure Kg. / cm^2	Deviator stress Kg. / cm^2	Ef. Mean normal stress Kg. / cm^2	Water Content %	
0.0	0.00	0.15	0.000	2.850	Slice	Water
37.5	0.17	0.16	0.351	2.956	No.	Content
110.0	0.42	0.19	1.030	3.098	1	21.145
189.0	0.80	0.24	1.745	3.220	2	21.455
200.0	1.23	0.29	1.825	3.298	3	21.493
239.0	1.85	0.33	2.160	3.383	4	21.619
279.0	2.72	0.38	2.501	3.456	5	21.805
290.0	3.16	0.40	2.588	3.475	6	21.645
320.0	3.91	0.42	2.839	3.521	7	21,865
340.0	4.40	0.44	3.004	3.533	8	22.693
366.5	5.77	0.47	3.193	3.585		
386.0	7.26	0.48	3.312	3.613	Average w :21.715	
397.0	9.13	0.49	3.371	3.642	Sketch of Failure	
409.0	12.36	0.492	3.452	3.668		
412.0	13.63	0.48	3.457	3.681		
419.0	15.97	0.46	3.472	3.701		
426.0	18.83	0.44	3.462	3.704		
424.5	22.09	0.41	3.280	3.675		
423.0	23.43	0.41	3.193	3.654		

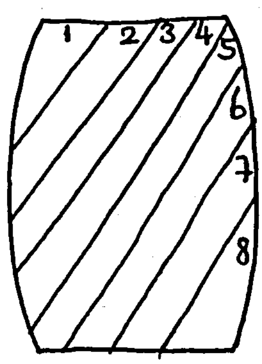

Max. Axial Stress:3.508 $kgcm^{-2}$ Water Con. at Failure Surface: 21.805 %

Fig 4.42 Deviator Stress versus Axial Strain

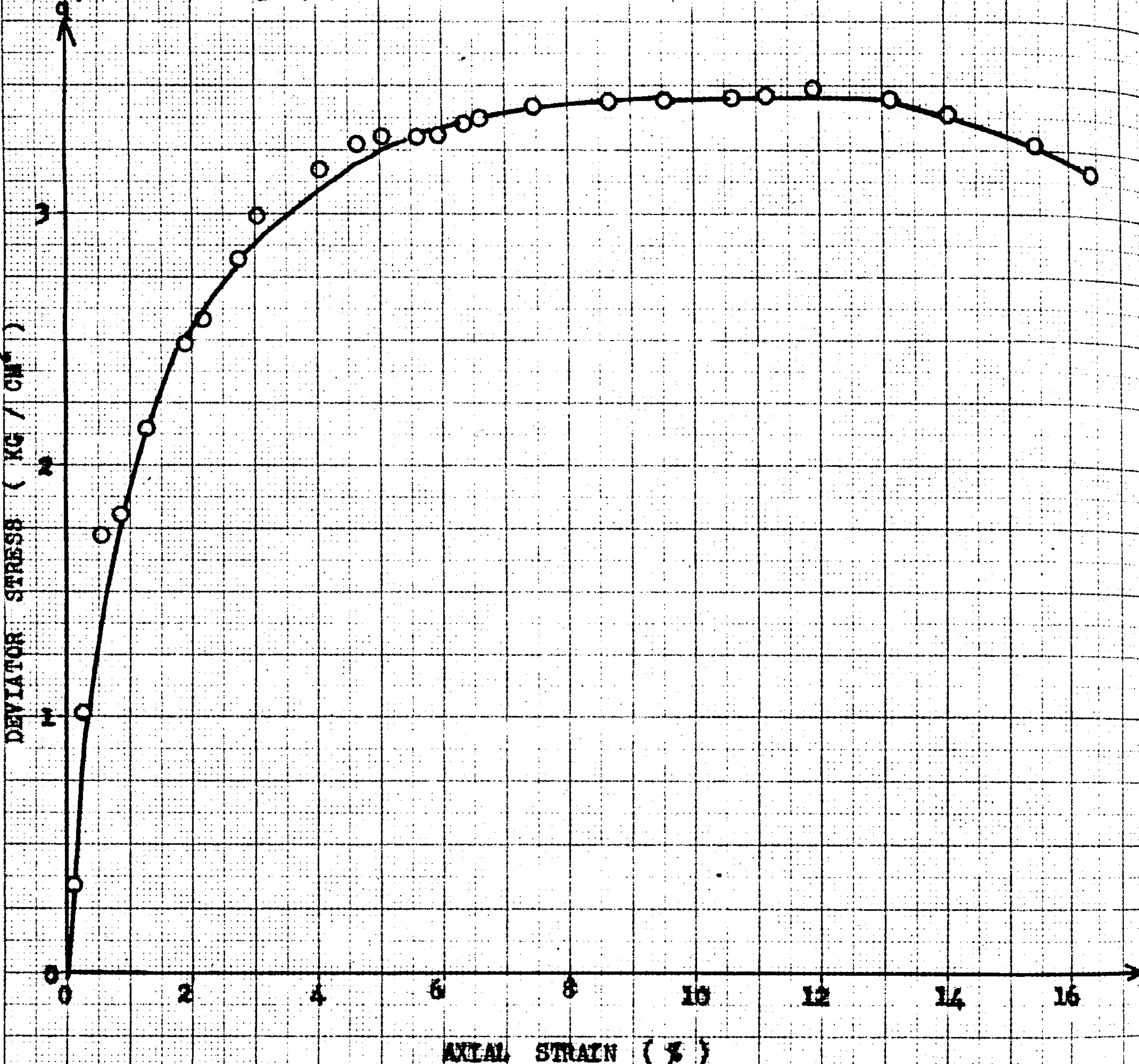

Fig 4.43 Pore Water Pressure versus Axial Strain

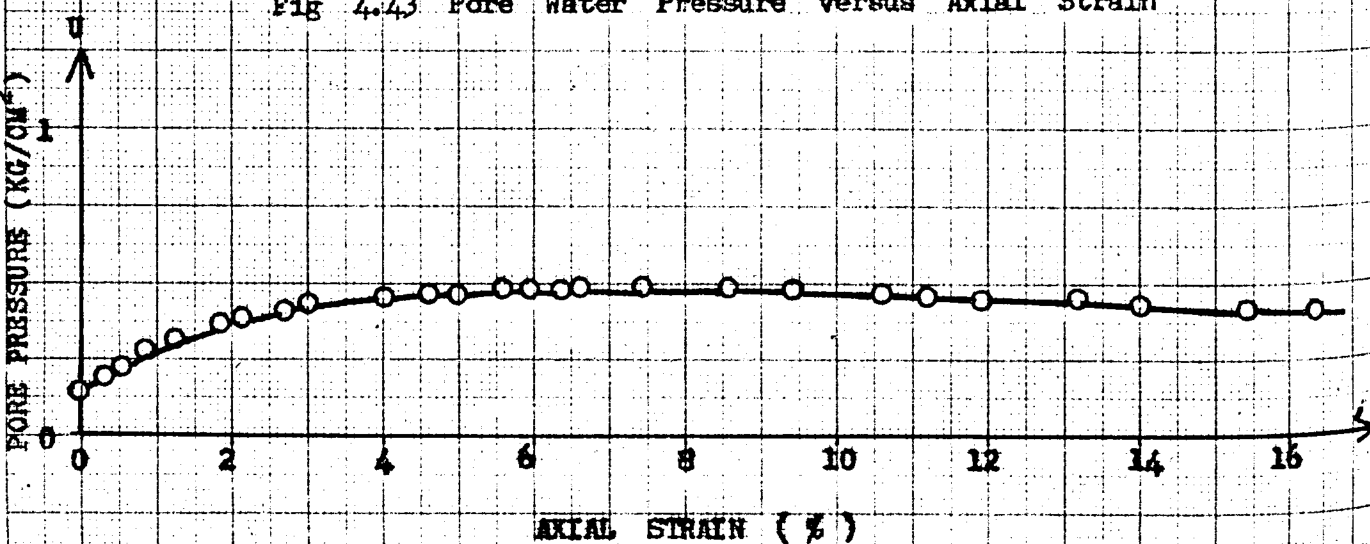

Fig 4.44 Deviator Stress versus Effective Mean Normal Stress

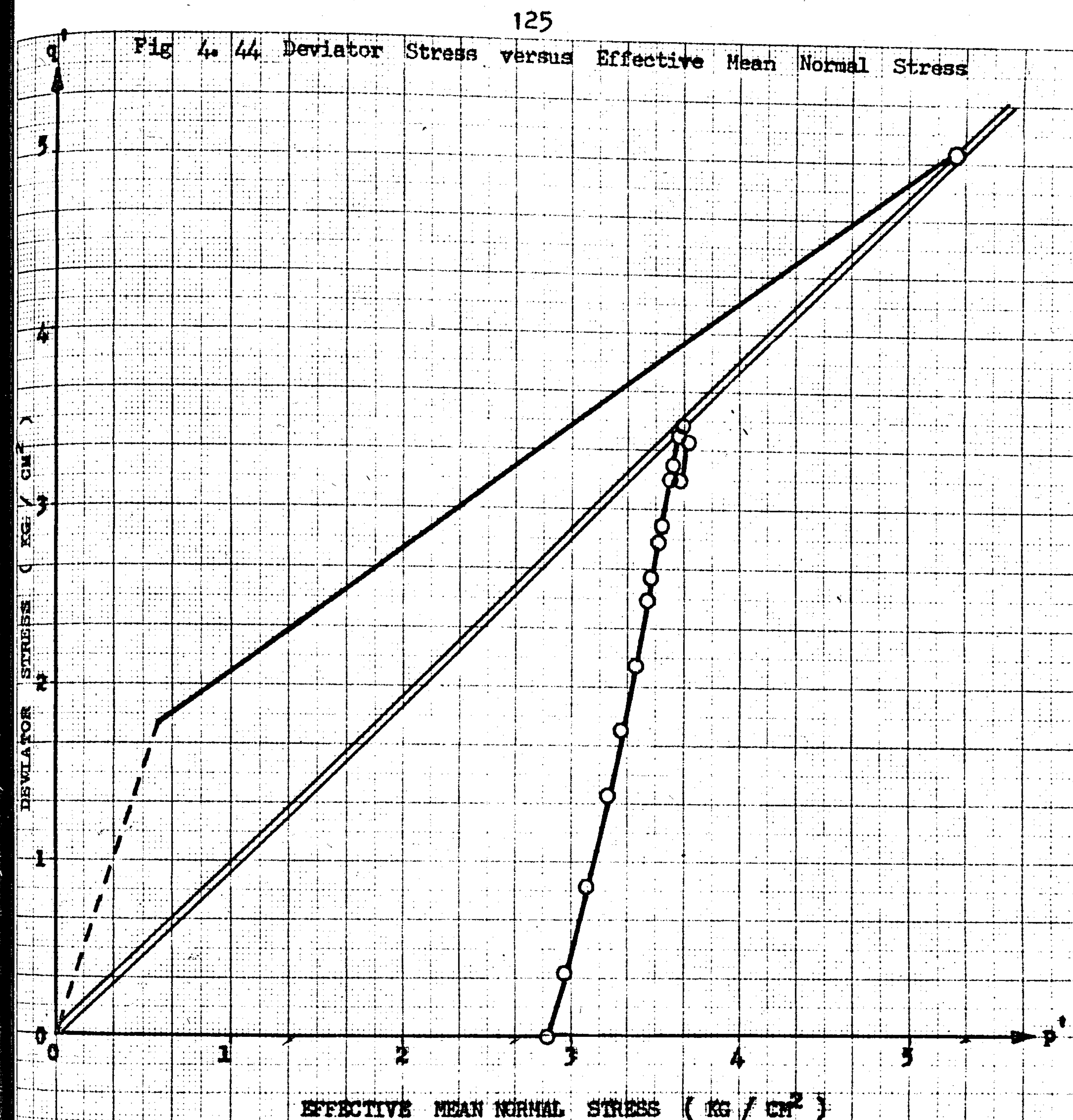

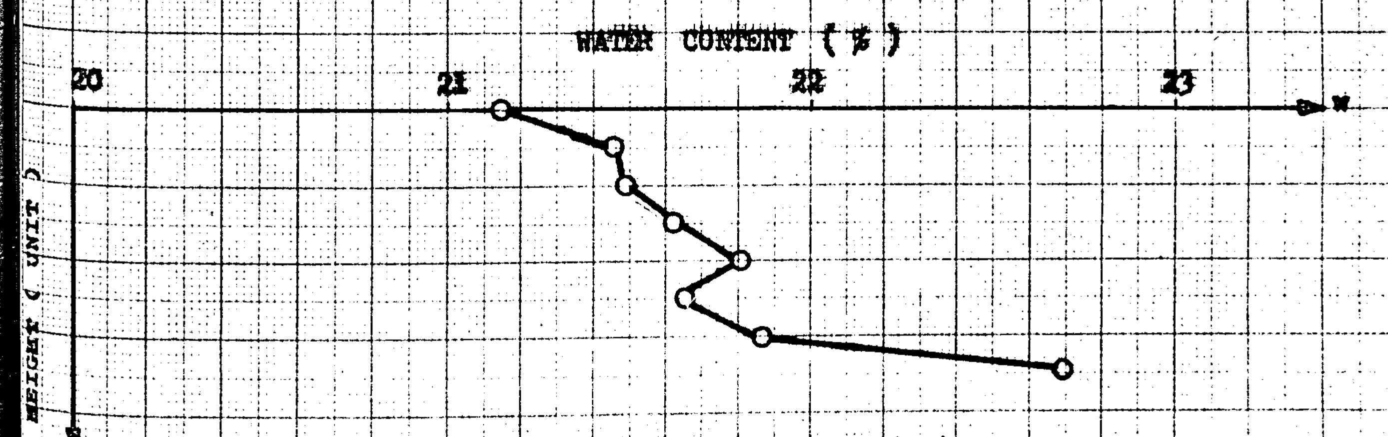

Fig 4.45 Height (Unit) versus Water Content

Consolidation Pressure : 7.5 $Kgcm^{-2}$

Equivalent Mean Normal Stress $(Pe)_i$: 4.351 $Kgcm^{-2}$

Proving Ring Number and Constant : 12365/0.09639   O. C. R. : 10

Specimen Diameter Top : 3.57 cm. Bottom : 3.57 cm. Average : 3.57 cm.

Specimen Weight : 166.39 gr.   Specimen Height : 7.97 cm.

Av. Specimen Area : 10.010 cm^2 Av. Loading Rate : 0.0303 mm/min.

Loading dial $In. \times 10^{-4}$	Axial strain %	Pore pressure Kg. / cm^2	Deviator stress Kg. / cm^2	Ef. Mean normal stress Kg. / cm^2	Water Content % Slice No.	Water Content
0.0	0.00	0.30	0.000	2.700		
21.0	0.10	0.39	0.200	2.710		
71.0	0.53	0.53	0.636	2.675	1	22.753
104.0	0.92	0.68	0.936	2.633	2	23.576
142.0	1.61	0.89	1.267	2.523	3	23.660
170.0	2.23	1.07	1.512	2.444	4	24.003
206.0	3.17	1.25	1.820	2.376	5	24.897
233.0	4.05	1.35	2.047	2.357	6	23.904
255.0	4.99	1.39	2.221	2.355	7	23.684
280.0	6.25	1.43	2.414	2.380	8	23.802
312.0	8.76	1.40	2.619	2.473		
323.0	10.10	1.37	2.672	2.521		
343.0	13.27	1.29	2.729	2.668		
354.0	15.53	1.22	2.738	2.691		
366.0	19.55	1.12	2.682	2.757		
367.0	20.80	1.10	2.641	2.762		
362.0	23.81	1.08	2.495	2.764		
359.0	24.82	1.05	2.427	2.756		
352.0	26.07	1.01	2.178	2.701		

Average w : 23.785

Sketch of Failure

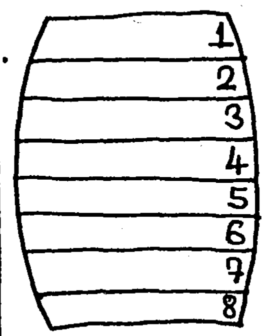

Max. Axial Stress: 2.749 $kgcm^{-2}$ Water Con. at Failure Surface: 24.897 %

Fig 4. 46 Deviator Stress versus Axial Strain

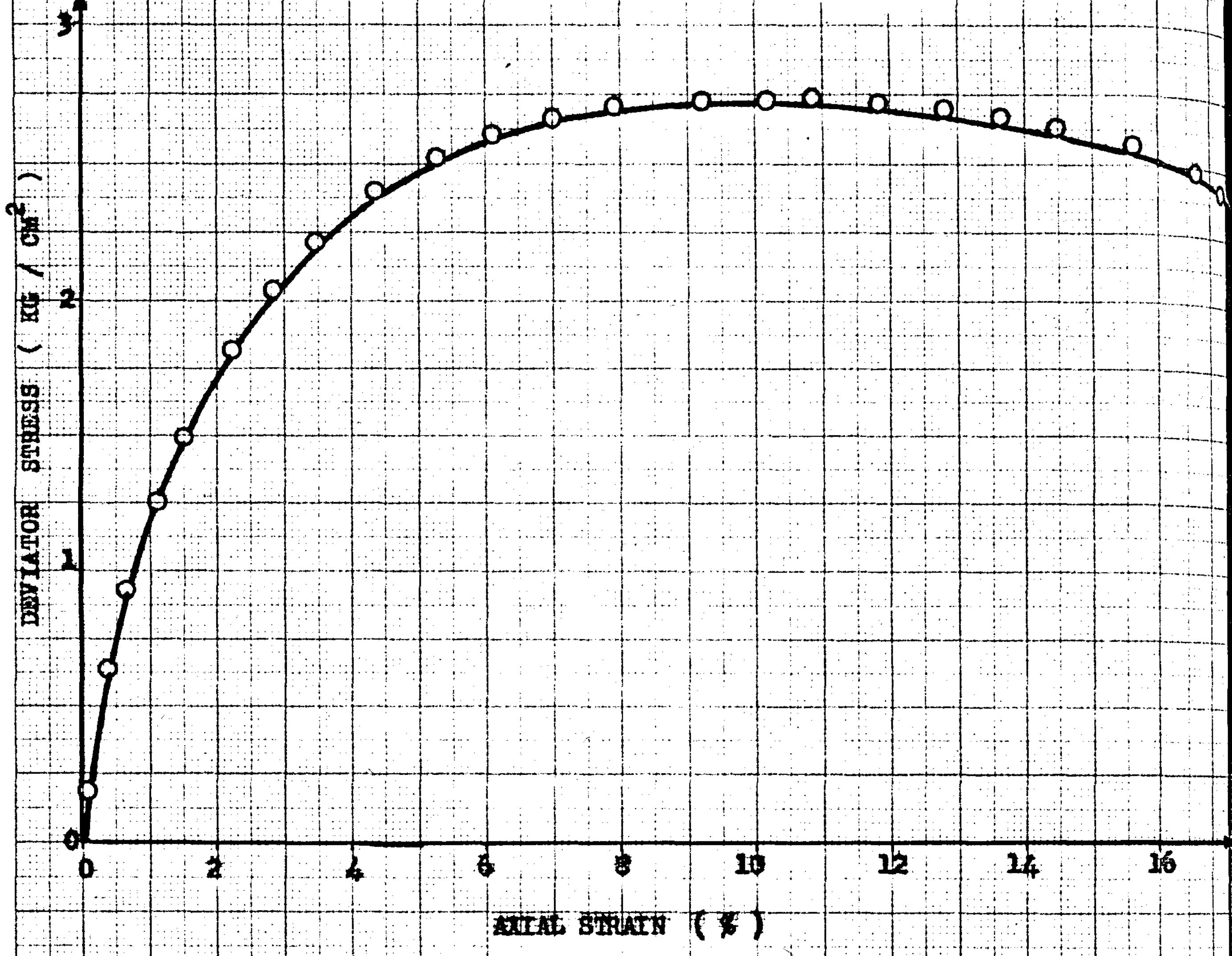

Fig 4. 47 Pore Water Pressure versus Axial Strain

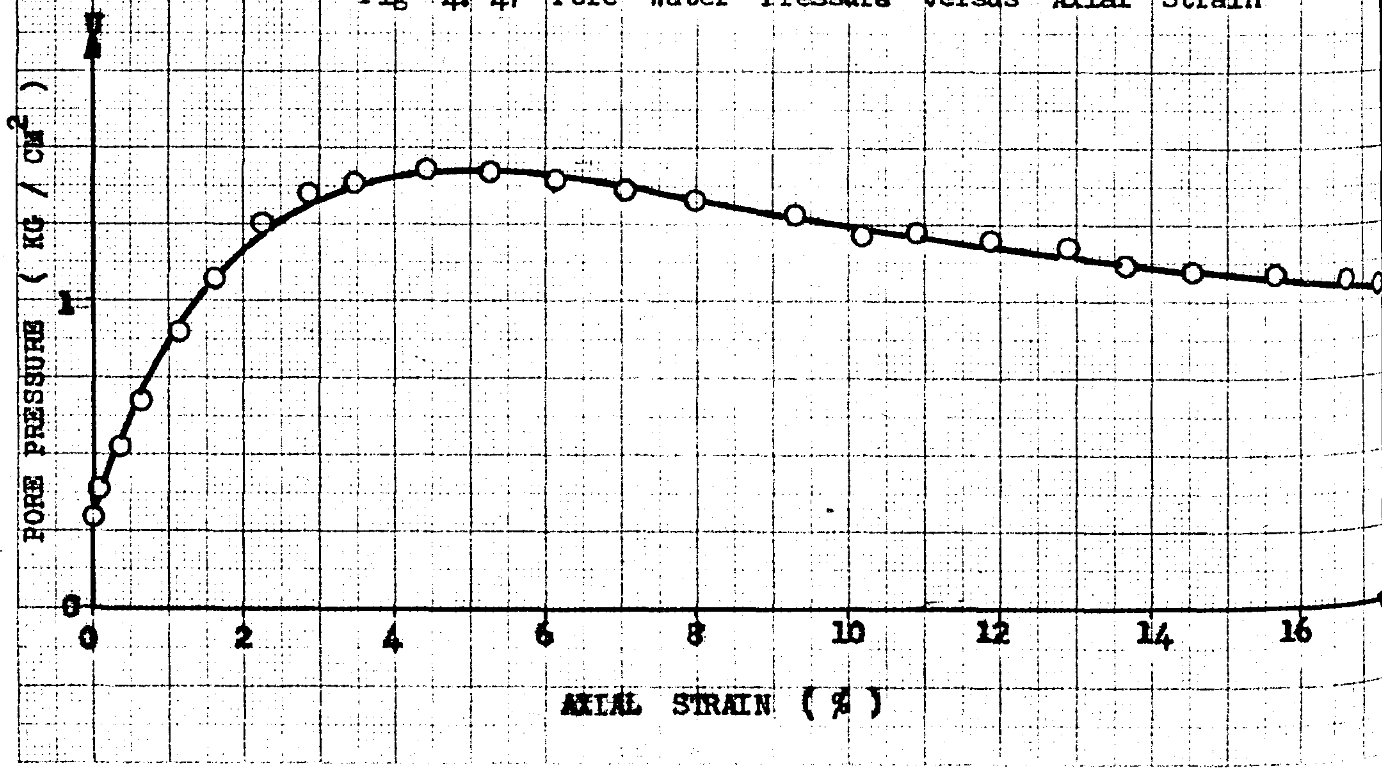

Fig 4. 48: Deviator Stress versus Effective Mean Normal Stress

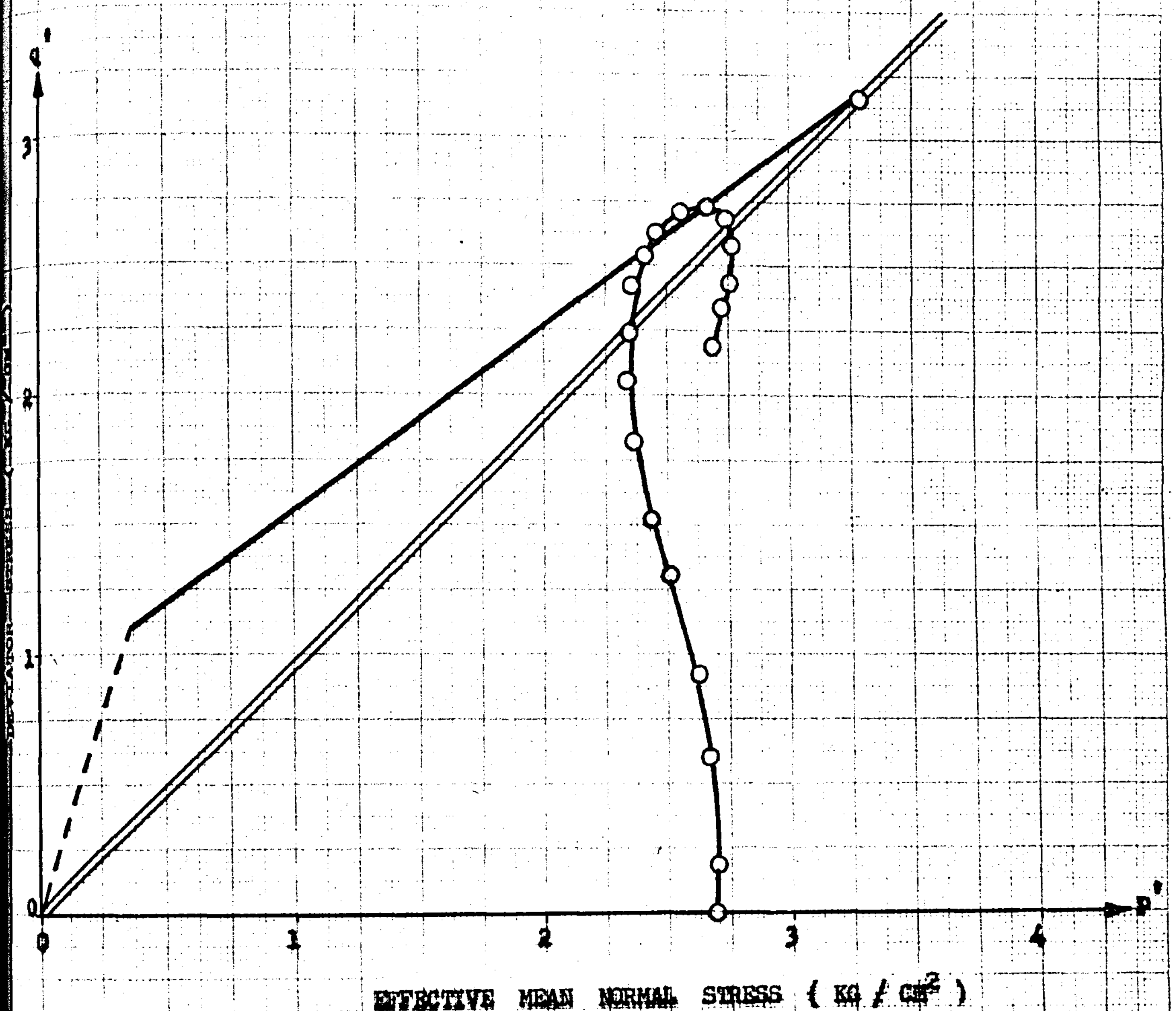

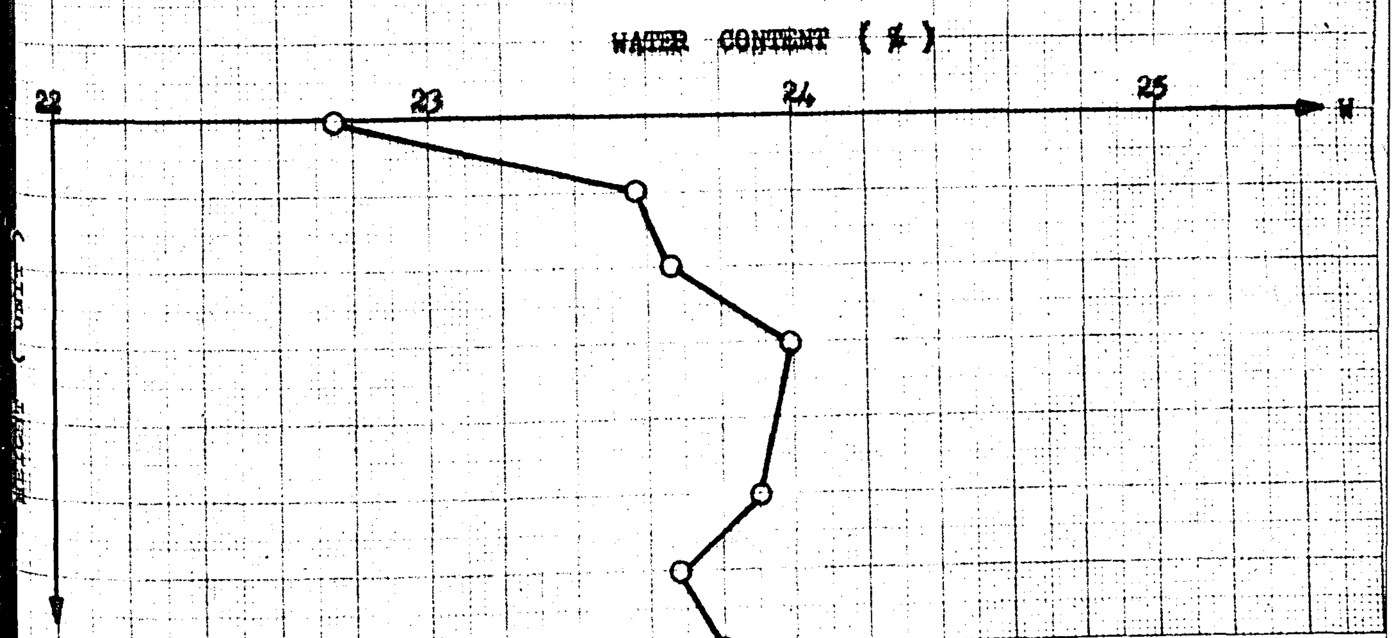

Fig 4.49 Height (Unit) versus Water Content

Consolidation Pressure : 7.5 $Kgcm^{-2}$

Equivalent Mean Normal Stress $(Pe)_i$: 6.379 $Kgcm^{-2}$

Proving Ring Number and Constant :12365/0.09639 0.20829 O. C. R. : 10

Specimen Diameter Top :3.56 cm. Bottom : 3.58 cm. Average : 3.57 cm.

Specimen Weight : 165.31 gr. Specimen Height : 8.01

Av. Specimen Area : 10.010 cm^2 Av.Loading Rate : 0.0303 mm/min.

Loading dial In.$\times 10^{-4}$	Axial strain %	Pore pressure Kg. / cm^2	Deviator stress Kg. / cm^2	Ef. Mean normal stress Kg. / cm^2	Water Content %	
0.0	0.00	0.40	0.000	2.600	Slice	Water
76.5	0.30	0.47	0.721	2.770	No.	Content
116.0	0.55	0.54	1.065	2.810	1	21.619
148.8	0.92	0.64	1.367	2.826	2	21.521
177.0	1.36	0.73	1.613	2.843	3	21.891
201.5	1.80	0.77	1.826	2.849	4	21.927
228.0	2.42	0.86	2.052	2.799	5	22.174
256.7	3.23	0.90	2.291	2.864	6	22.280
292.0	4.48	0.96	2.577	2.899	7	22.359
318.0	5.73	0.96	2.773	2.954	8	22.678
339.0	6.79	0.95	2.926	3.010	9	22.574
358.0	7.92	0.93	3.055	3.071	Average w :22.114	
371.8	9.04	0.90	3.134	3.125	Sketch of Failure	
382.5	10.60	0.85	3.166	3.200		
387.2	11.79	0.80	3.158	3.245		
395.0	14.16	0.75	3.147	3.322		
401.0	16.90	0.68	3.152	3.404		
407.0	19.15	0.61	3.144	3.442		
404.0	23.52	0.51	2.906	3.497		

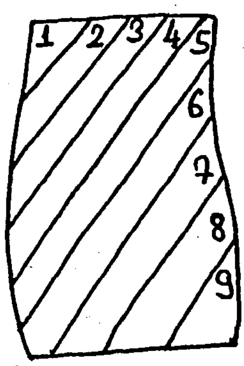

Max. Axial Stress: 3.166 $kgcm^{-2}$ Water Con. at Failure Surface: 22.678 %

Fig 4.50 Deviator Stress versus Axial Strain

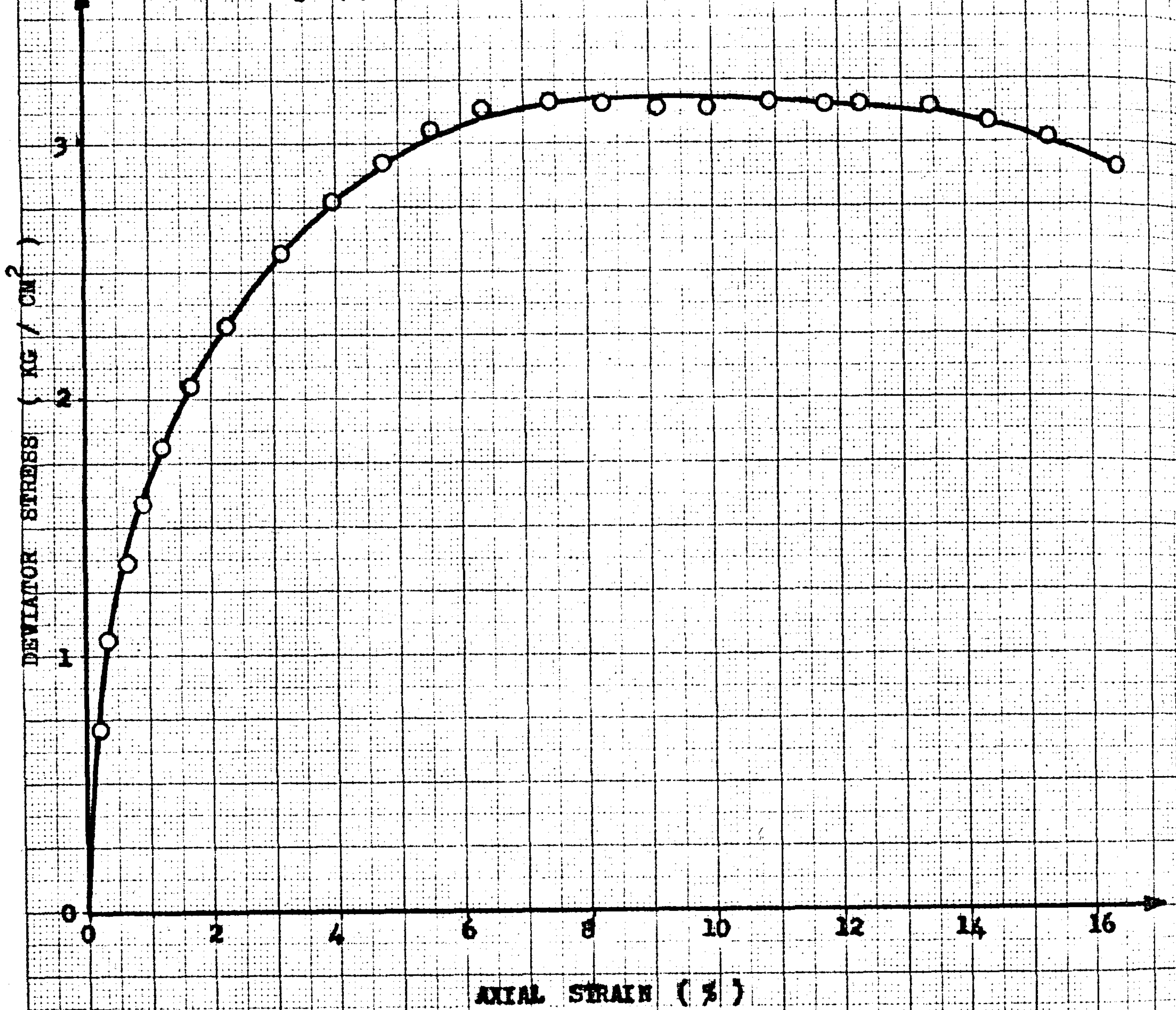

Fig 4.51 Pore Water Pressure versus Axial Strain

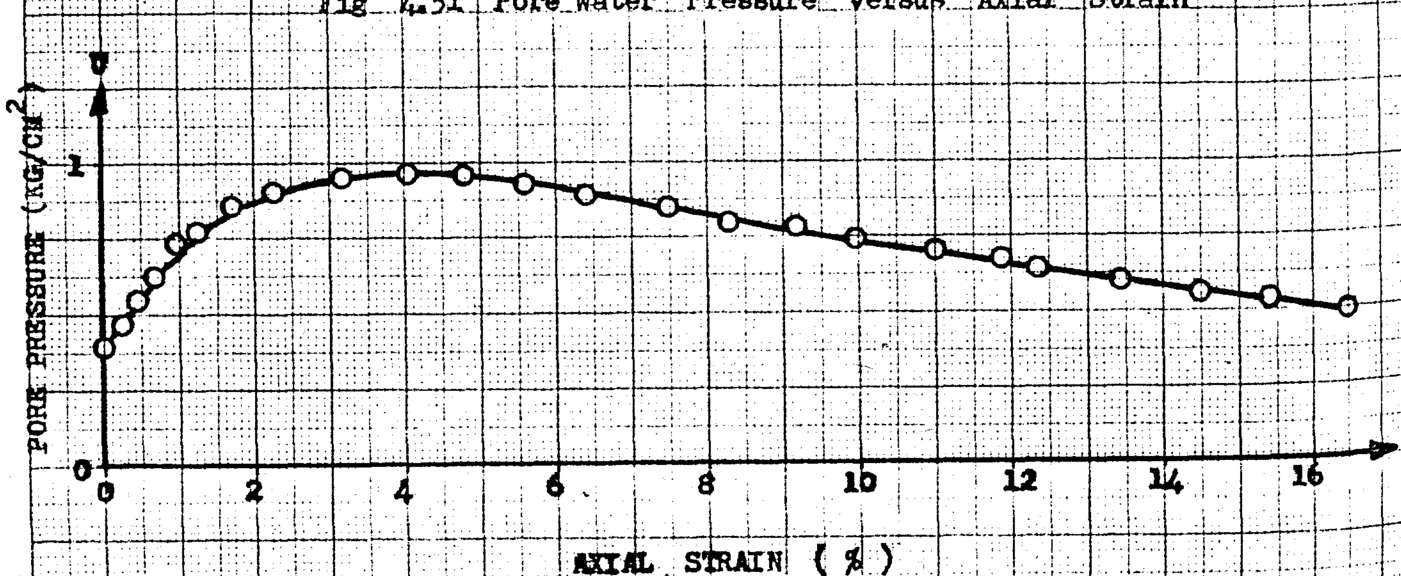

Fig 4.52 Deviator Stress versus Effective Mean Normal Stress

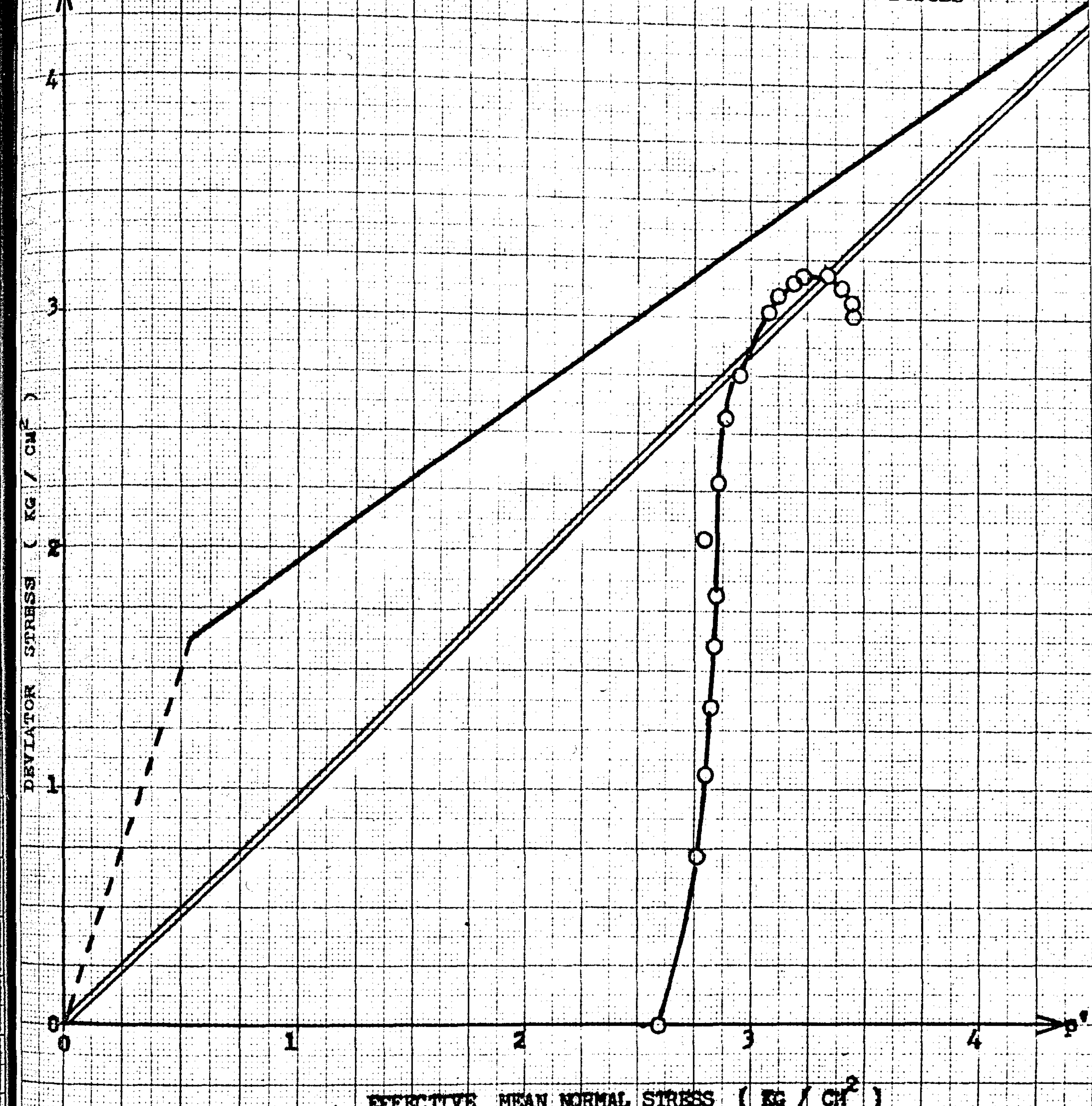

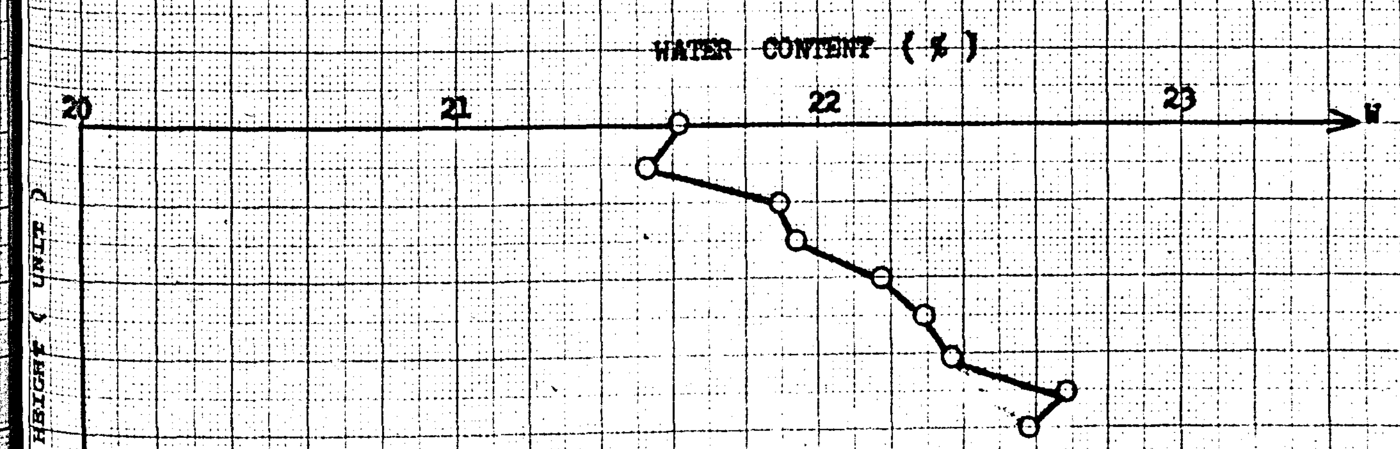

Fig 4.53 Height (Unit) versus Water Content

Consolidation Pressure : 7.5 $Kgcm^{-2}$

Equivalent Mean Normal Stress (Pe)i : 6.571 $Kgcm^{-2}$

Proving Ring Number and Constant :12365/0.09639 0.20829 O. C. R. : 15

Specimen Diameter Top :3.57 cm. Bottom :3.58 cm. Average : 3.575 cm.

Specimen Weight :165.11 gr. Specimen Height : 8.0 cm.

Av. Specimen Area : 10.039 Av.Loading Rate : 0.0303 mm/min.

Loading dial $In.x10^{-4}$	Axial strain %	Pore pressure Kg. / cm^2	Deviator stress Kg. / cm^2	Ef. Mean normal stress Kg. / cm^2	Water Content % Slice No.	Water Content
0.0	0.00	0.61	0.000	2.390		
80.0	0.27	0.76	0.754	2.491		
130.0	0.59	0.88	1.195	2.523	1	20.844
176.0	1.02	1.02	1.620	2.522	2	21.505
212.0	1.46	1.09	1.930	2.548	3	21.466
238.5	1.90	1.13	2.166	2.557	4	21.812
280.0	2.84	1.13	2.515	2.638	5	22.432
299.5	3.34	1.12	2.678	2.695	6	22.304
323.8	4.15	1.01	2.872	2.807	7	22.655
350.9	5.27	0.98	3.080	3.002	8	22.854
384.0	7.40	0.85	3.296	3.235		
396.2	9.78	0.71	3.339	3.402		
403.7	12.27	0.61	3.373	3.495		
407.5	13.84	0.56	3.374	3.538		
411.7	16.34	0.52	3.338	3.588		
413.1	18.52	0.48	3.177	3.663		
410.1	20.52	0.46	3.126	3.582		
407.0	21.65	0.45	3.026	3.554		
403.0	22.755	0.44	3.016	3.541		

Average w :21.984

Sketch of Failure

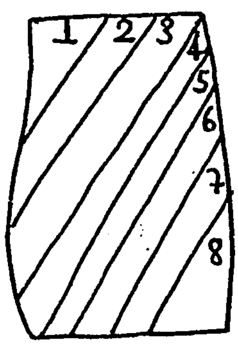

Max. Axial Stress:3.374 $kgcm^{-2}$ Water Con. at Failure Surface:22.655 %

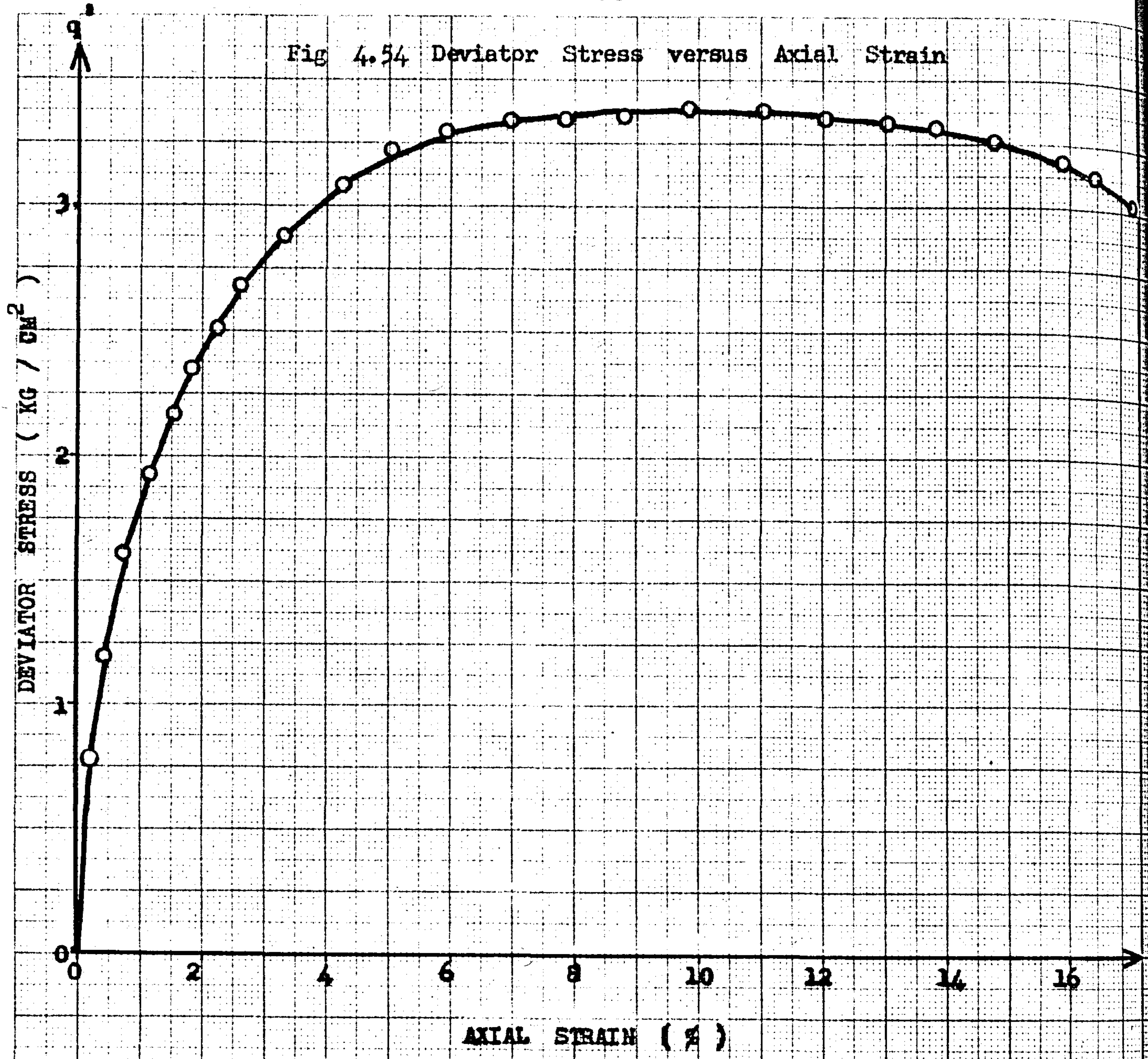

Fig 4.54 Deviator Stress versus Axial Strain

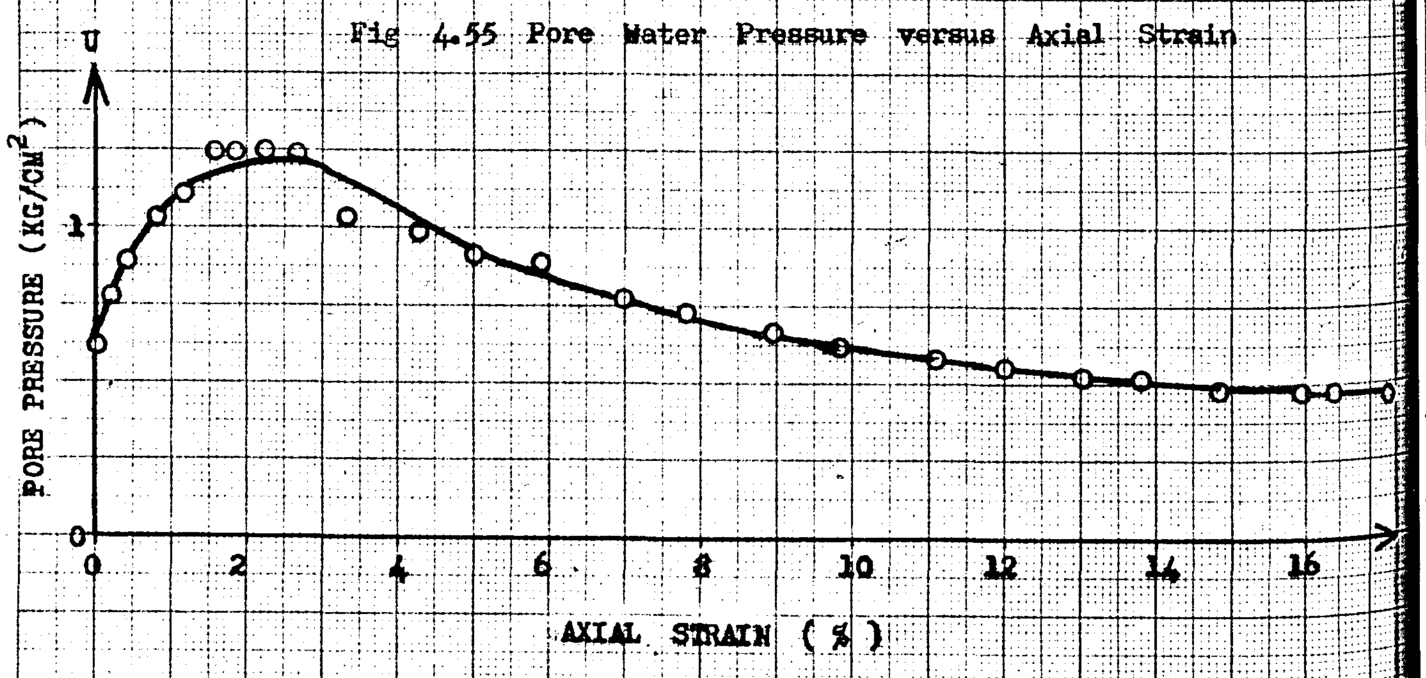

Fig 4.55 Pore Water Pressure versus Axial Strain

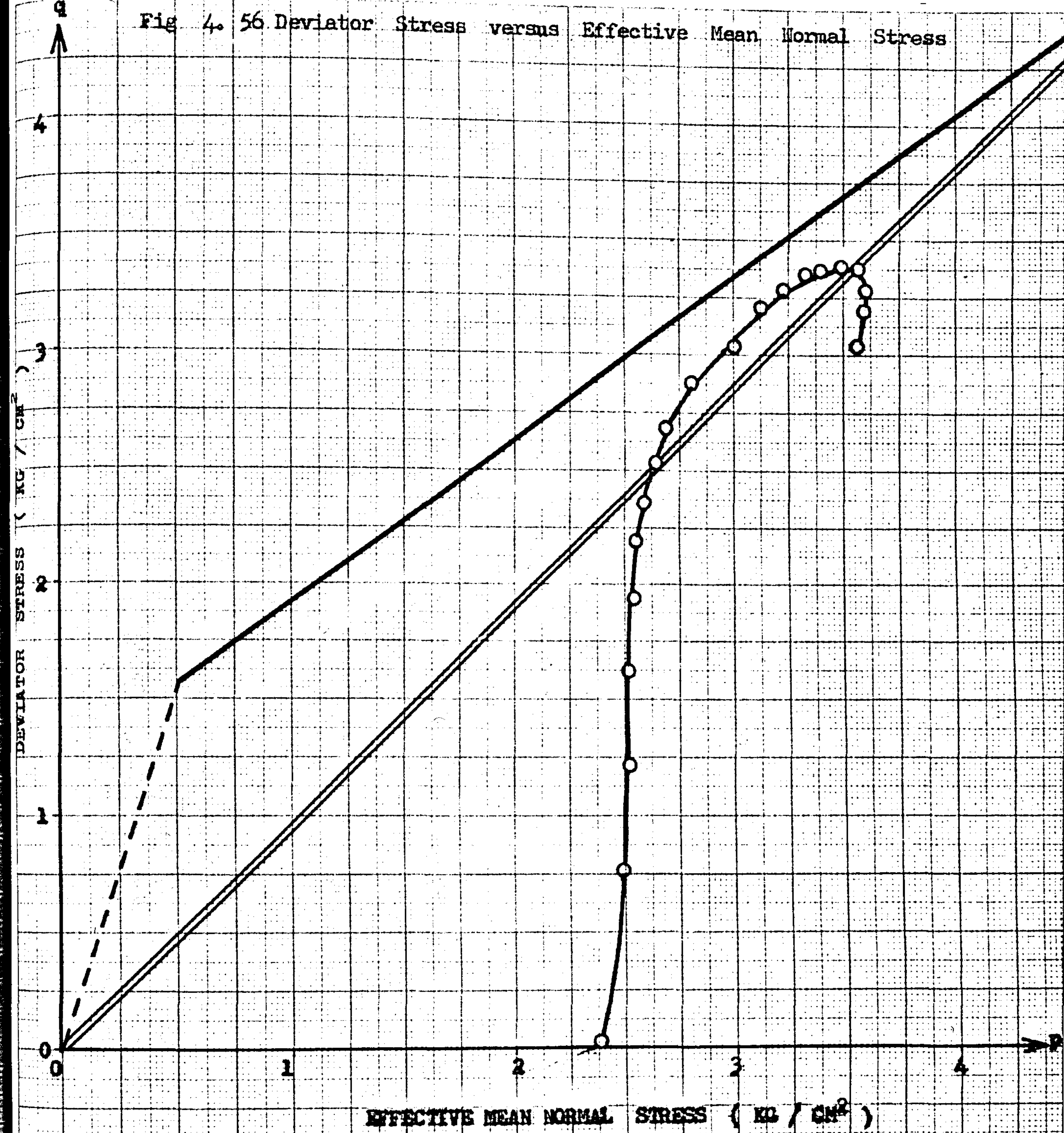

Fig 4.56 Deviator Stress versus Effective Mean Normal Stress

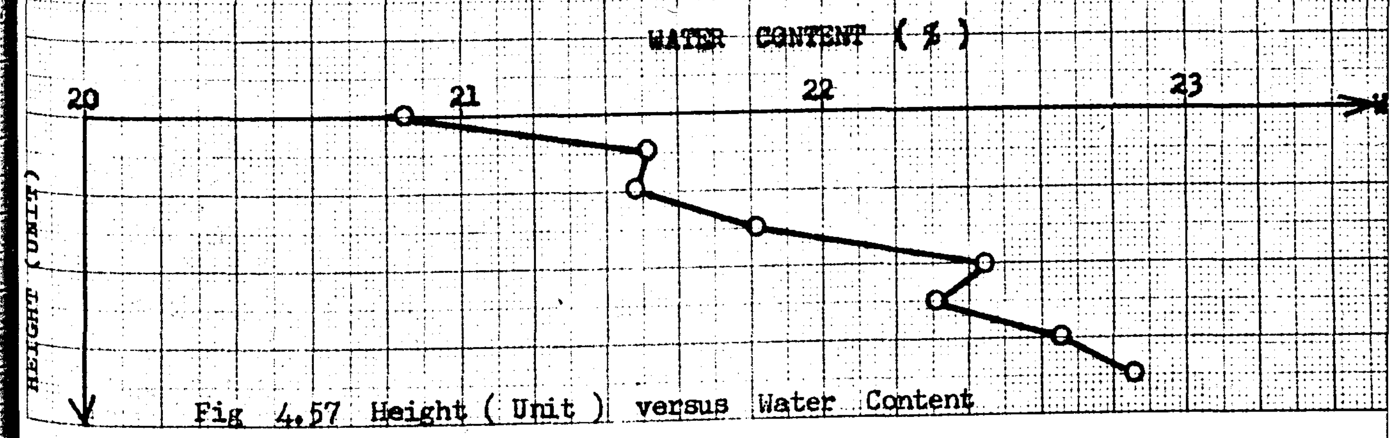

Fig 4.57 Height (Unit) versus Water Content

Consolidation Pressure : 7.5 $Kgcm^{-2}$

Equivalent Mean Normal Stress $(Pe)_i$: 4.600 $Kgcm^{-2}$

Proving Ring Number and Constant : 12365/0.09639 O. C. R. : 15

Specimen Diameter Top : 3.57 cm. Bottom : 3.57 cm. Average : 3.57 cm.

Specimen Weight : 164.24 gr. Specimen Height : 8.02 cm.

Av. Specimen Area : 10.010 cm^2. Av. Loading Rate : 0.0303 mm/min.

Loading dial $In.x10^{-4}$	Axial strain %	Pore pressure Kg. / cm^2	Deviator stress Kg. / cm^2	Ef. Mean normal stress Kg. / cm^2	Water Content %	
0.0	0.00	0.84	0.000	2.160	Slice	Water
72.0	0.35	1.05	0.675	2.017	No.	Content
120.4	0.79	1.28	1.100	2.048	1	22.735
158.0	1.28	1.45	1.435	2.012	2	23.039
176.0	1.73	1.50	1.586	2.066	3	23.457
216.1	2.34	1.53	1.943	2.115	4	23.889
233.0	2.78	1.52	2.085	2.158	5	23.639
262.0	3.78	1.51	2.323	2.263	6	24.334
281.2	4.59	1.48	2.476	2.438	7	24.230
311.0	6.77	1.39	2.675	2.542	8	23.015
323.0	8.45	1.30	2.726	2.588		
326.0	9.76	1.30	2.709	2.640	Average w :23.542	
324.0	12.26	1.15	2.606	2.637	Sketch of Failure	
319.5	13.13	1.21	2.538	2.616		
314.0	16.37	1.21	2.386	2.537		
298.6	17.49	1.21	2.226	2.497		
264.5	19.44	1.21	1.898	2.465		
258.0	20.74	1.21	1.737	2.432		
249.3	21.13	1.21	1.665	2.401		

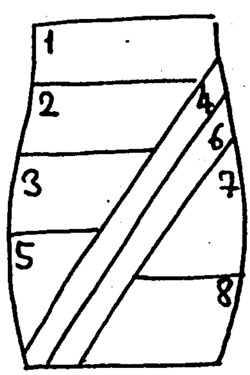

Max. Axial Stress: 2.726 $kgcm^{-2}$ Water Con. at Failure Surface: 24.334 %

Fig 4.58 Deviator Stress versus Axial Strain

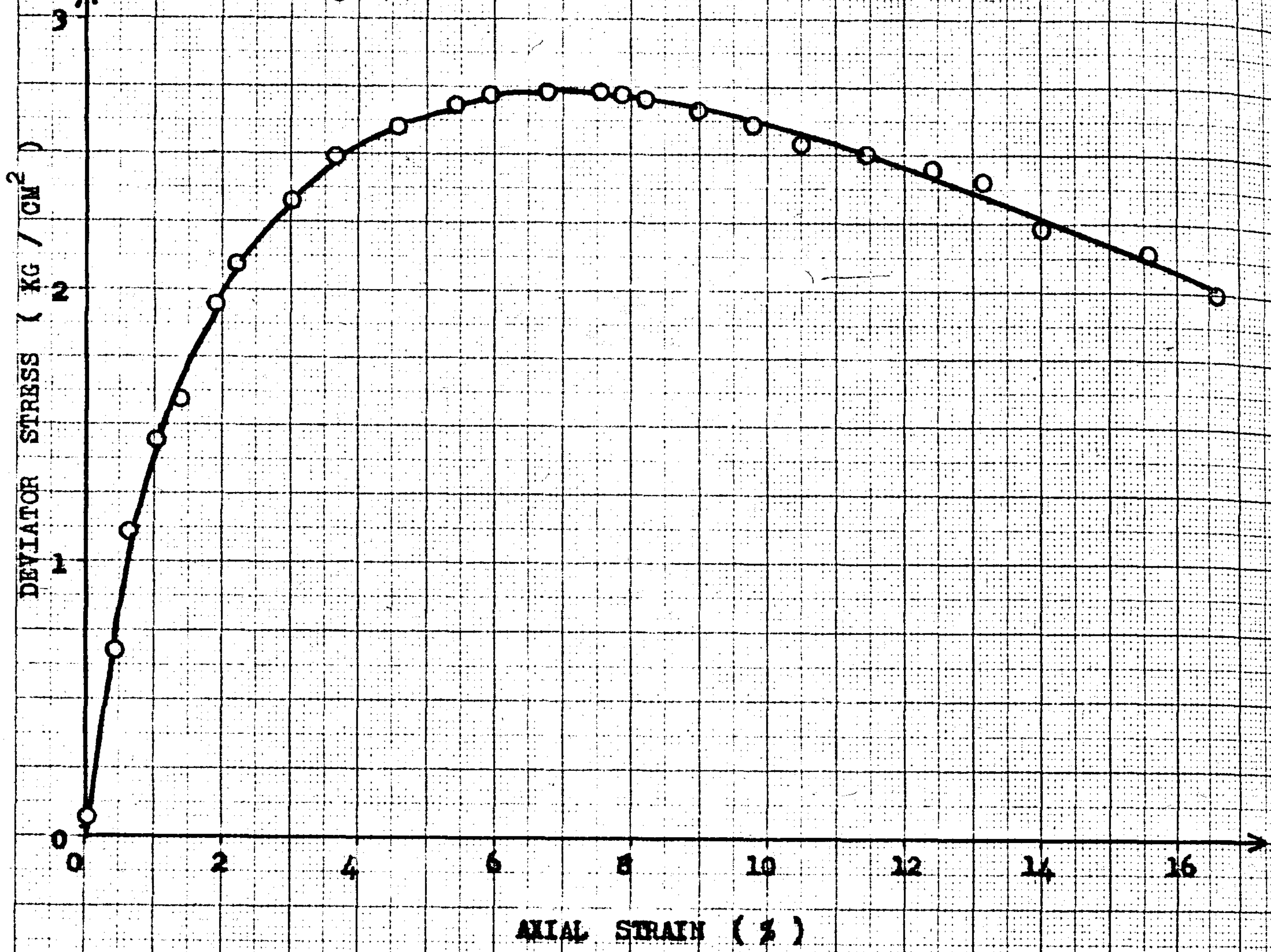

Fig 4.59 Pore Water Pressure versus Axial Strain

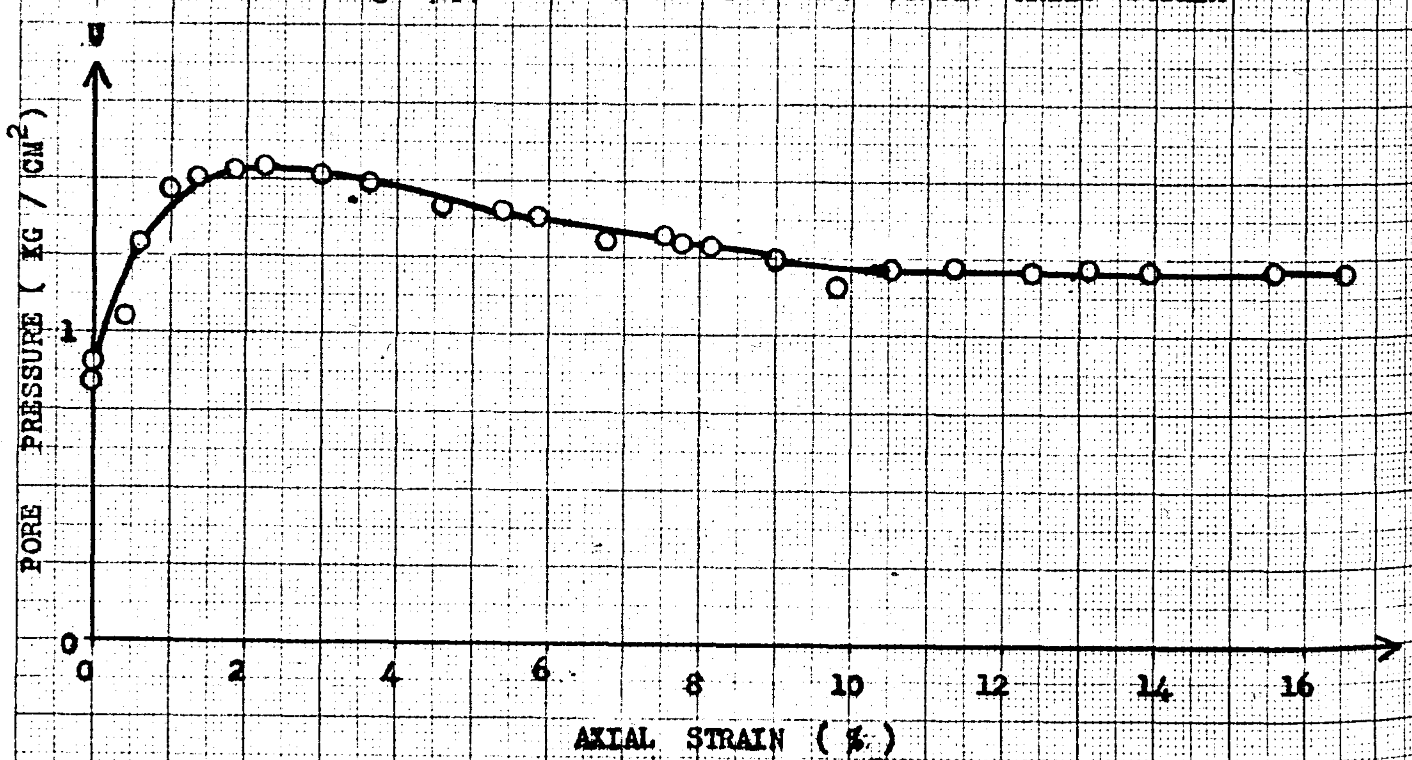

Fig 4.60 Deviator Stress versus Effective Mean Normal Stress

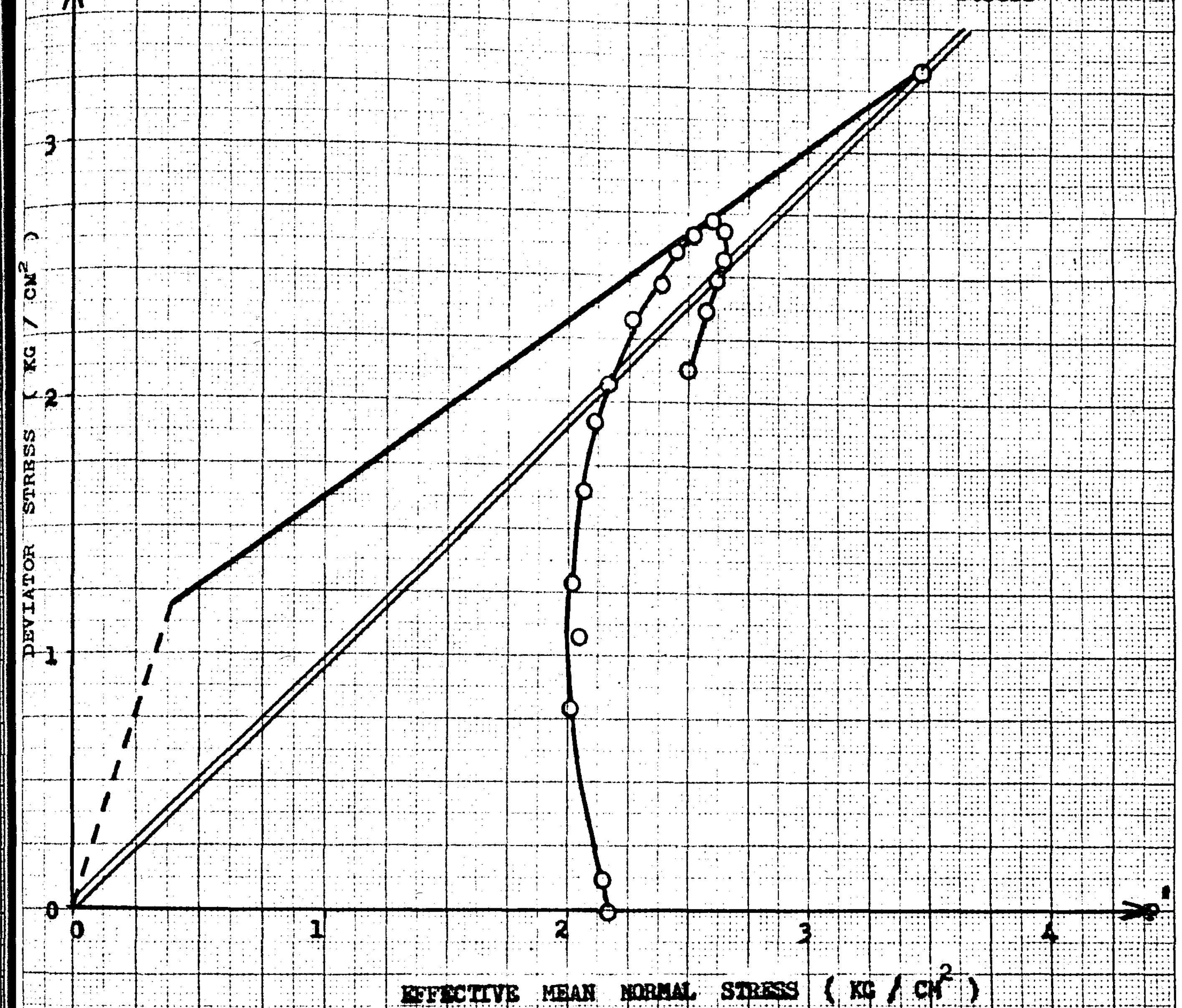

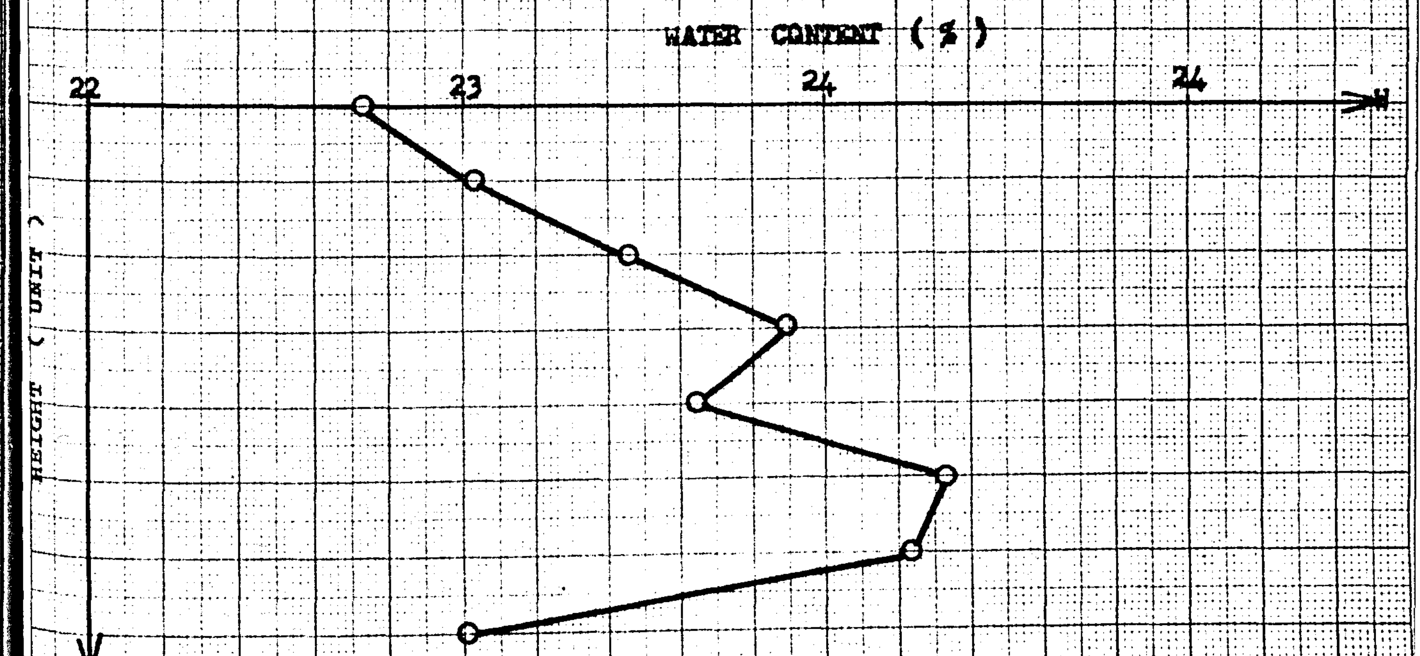

Fig 4.61 Height (Unit) versus Water Content

Consolidation Pressure : 2.5 $Kgcm^{-2}$

Equivalent Mean Normal Stress $(Pe)_i$: 3.253 $Kgcm^{-2}$

Proving Ring Number and Constant : 12365/0.09639 O. C. R. : 1

Specimen Diameter Top : 3.48 cm. Bottom : 3.48 cm. Average : 3.48 cm.

Specimen Weight : 150.90 gr. Specimen Height : 7.79 cm.

Av. Specimen Area : 9.511 cm^2 Av. Loading Rate : 0.0303 mm/min.

Loading dial $In. \times 10^{-4}$	Axial strain %	Pore pressure Kg. / cm^2	Deviator stress Kg. / cm^2	Ef. Mean normal stress Kg. / cm^2	Water Content %	
0.0	0.00	0.00	0.000	2.500	Slice	Water
10.0	0.06	0.03	0.098	2.515	No.	Content
85.5	0.45	0.08	0.843	2.700	1	25.243
114.0	0.83	0.12	1.095	2.730	2	24.861
129.0	1.19	0.16	1,226	2.730	3	24.917
146.0	1.73	0.24	1.375	2.722	4	24.716
159.0	2.25	0.30	1.486	2.687	5	25.044
171.7	2.69	0.39	1.597	2.662	6	24.864
193.0	3.98	0.54	1.772	2.578	7	25.083
213.0	5.01	0.69	1.939	2.473	8	24.958
227.4	5.97	0.80	2.054	2.410	9	25.817
236.0	6.80	0.85	2.112	2.405	Average w : 25.056	
245.4	7.89	0.86	2.172	2.346	Sketch of Failure	
258.0	9.50	0.89	2.242	2.368		
268.5	11.17	0.89	2.288	2.368		
278.0	13.29	0.89	2.308	2.370		
280.0	13.86	0.89	2.308	2.370		
284.2	15.34	0.87	2.298	2.375		
286.0	15.79	0.87	2.299	2.381		

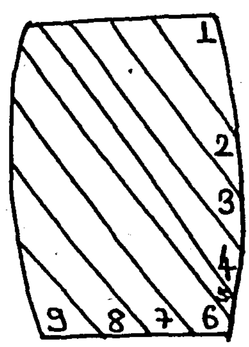

Max. Axial Stress: 2.308 $kgcm^{-2}$ Water Con. at Failure Surface: 25.083 %

Fig 4.62 Deviator Stress versus Axial Strain

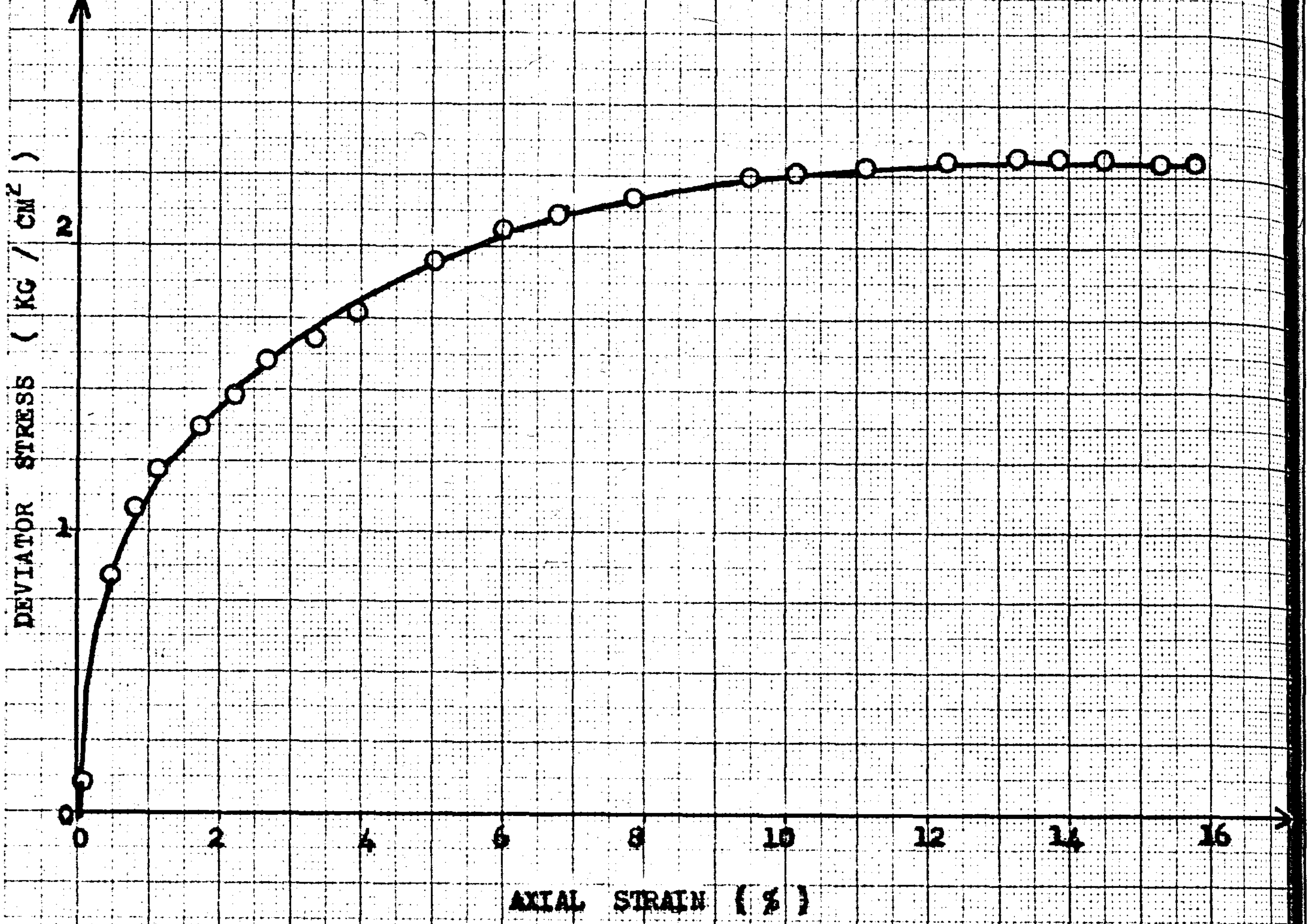

Fig 4.63 Pore Water Pressure versus Axial Strain

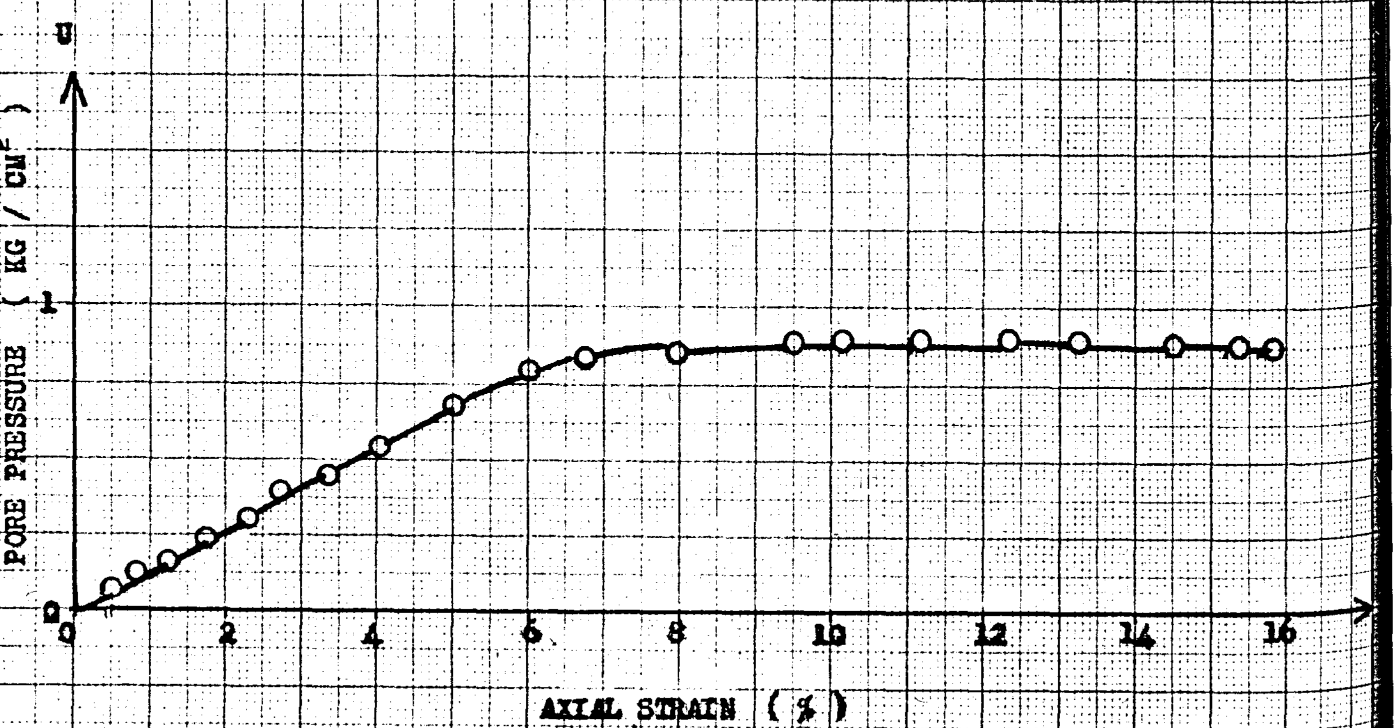

Fig 4.64 Deviator Stress versus Effective Mean Normal Stress

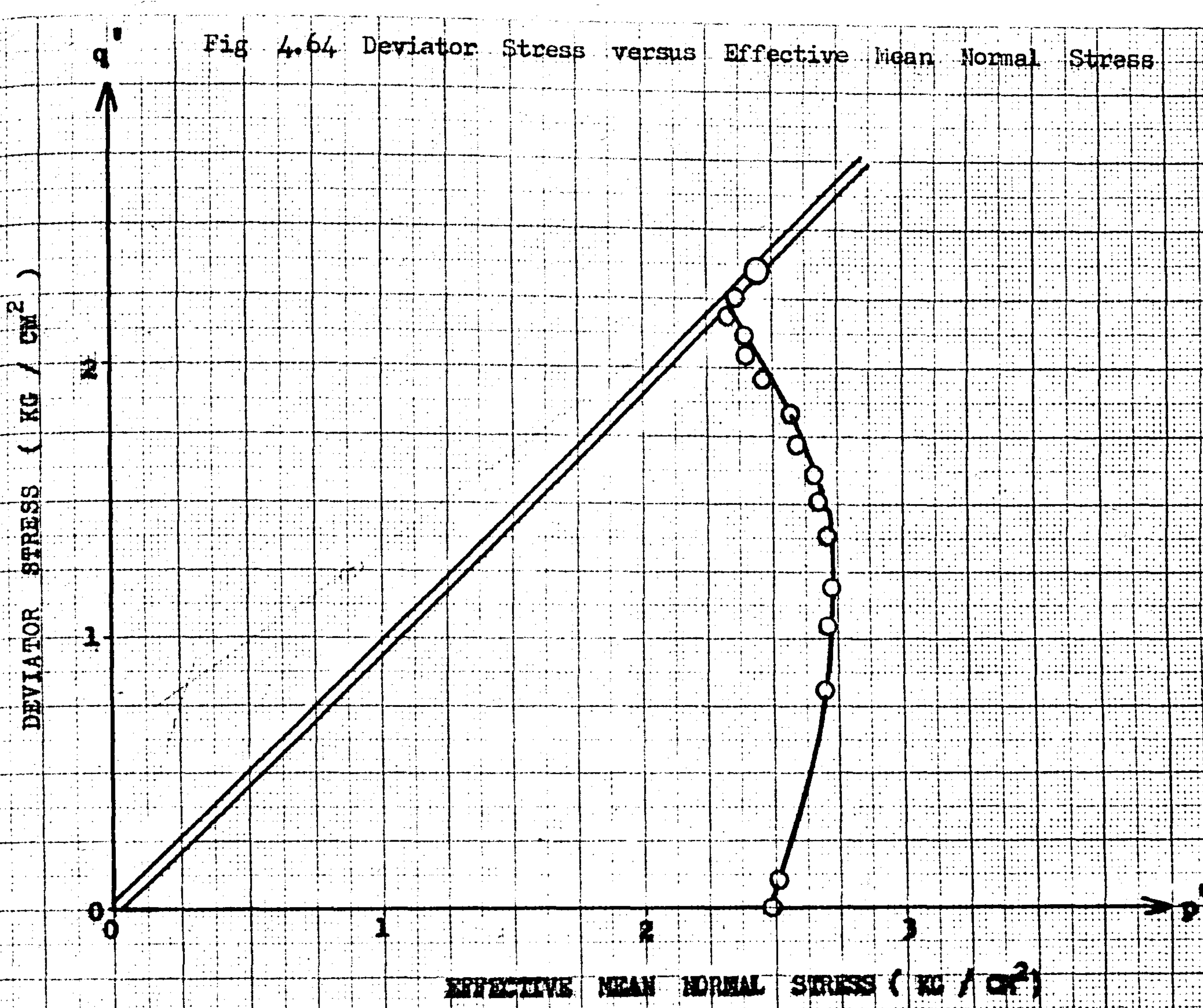

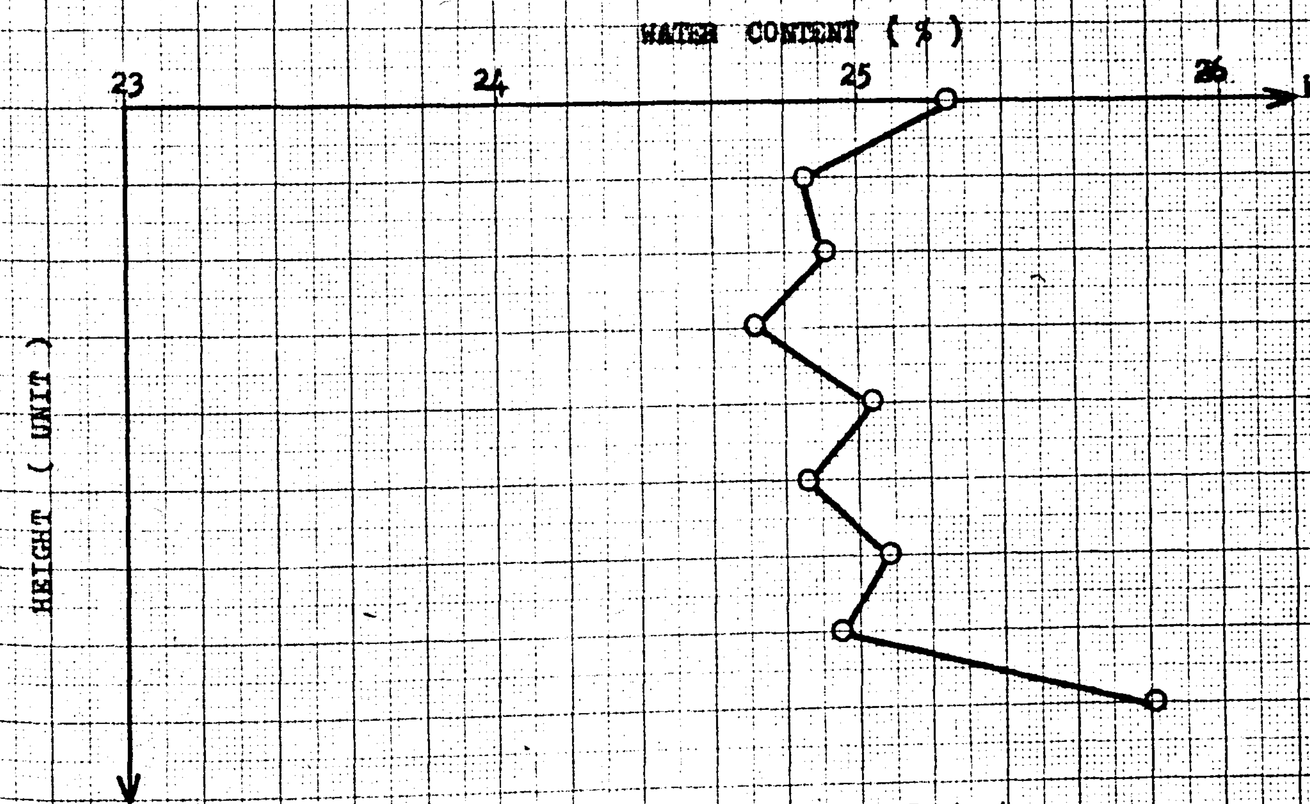

Fig 4.65 Height (Unit) versus Water Content

Consolidation Pressure : 2.5 Kgcm^{-2}

Equivalent Mean Normal Stress $(Pe)_i$: 2.462 Kgcm^{-2}

Proving Ring Number and Constant : 12365 / 0.09639 O. C. R. : 1

Specimen Diameter Top :3.45 cm. Bottom :3.47 cm. Average : 3.46 cm.

Specimen Weight :148.09 gr. Specimen Height : 7.84 cm.

Av. Specimen Area :9.402 cm^2 Av.Loading Rate : 0.0303 mm/min.

Loading dial In.x10^{-4}	Axial strain %	Pore pressure Kg. / cm^2	Deviator stress Kg. / cm^2	Ef. Mean normal stress Kg. / cm^2	Water Content %	
0.0	0.00	0.00	0.000	2.500	Slice No.	Water Content
59.0	0.43	0.12	0.560	2.548		
77.0	0.75	0.19	0.720	2.520	1	26.375
89.5	1.14	0.24	0.835	2.528	2	26.435
100.5	1.58	0.30	0.935	2.466	3	26.030
110.5	2.09	0.39	1.020	2.411	4	26.675
121.0	2.67	0.46	1.115	2.347	5	26.084
134.0	3.44	0.58	1.222	2.260	6	26.541
143.5	4.14	0.65	1.300	2.198	7	25.912
153.9	4.77	0.80	1.390	2.154	8	26.130
164.2	5.53	0.90	1.447	2.098		
175.7	6.49	0.98	1.550	2.041	Average w :26.273	
185.7	7.45	1.07	1.645	1.973	Sketch of Failure	
198.0	8.60	1.13	1.735	1.931		
205.0	9.63	1.20	1.765	1.896		
214.5	10.96	1.21	1.817	1.887		
223.1	12.55	1.25	1.860	1.880		
230.5	14.34	1.24	1.875	1.865		
231.0	15.42	1.24	1.880	1.862		

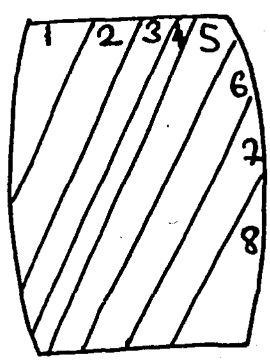

Max. Axial Stress: 1.880 kgcm^{-2} Water Con. at Failure Surface: 26.675 %

Fig 4.66 Deviator Stress versus Axial Strain

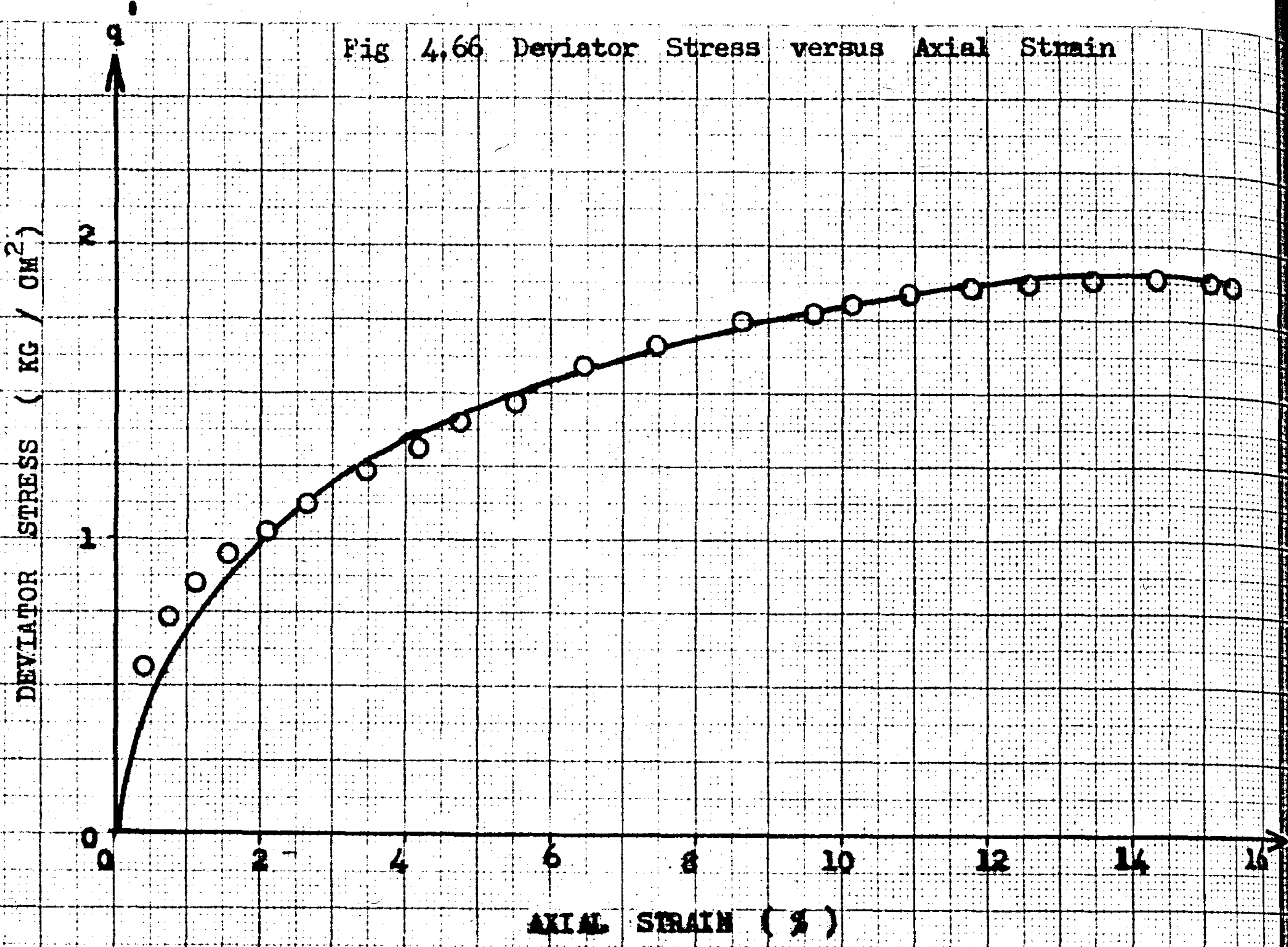

Fig 4.67 Pore Water Pressure versus Axial Strain

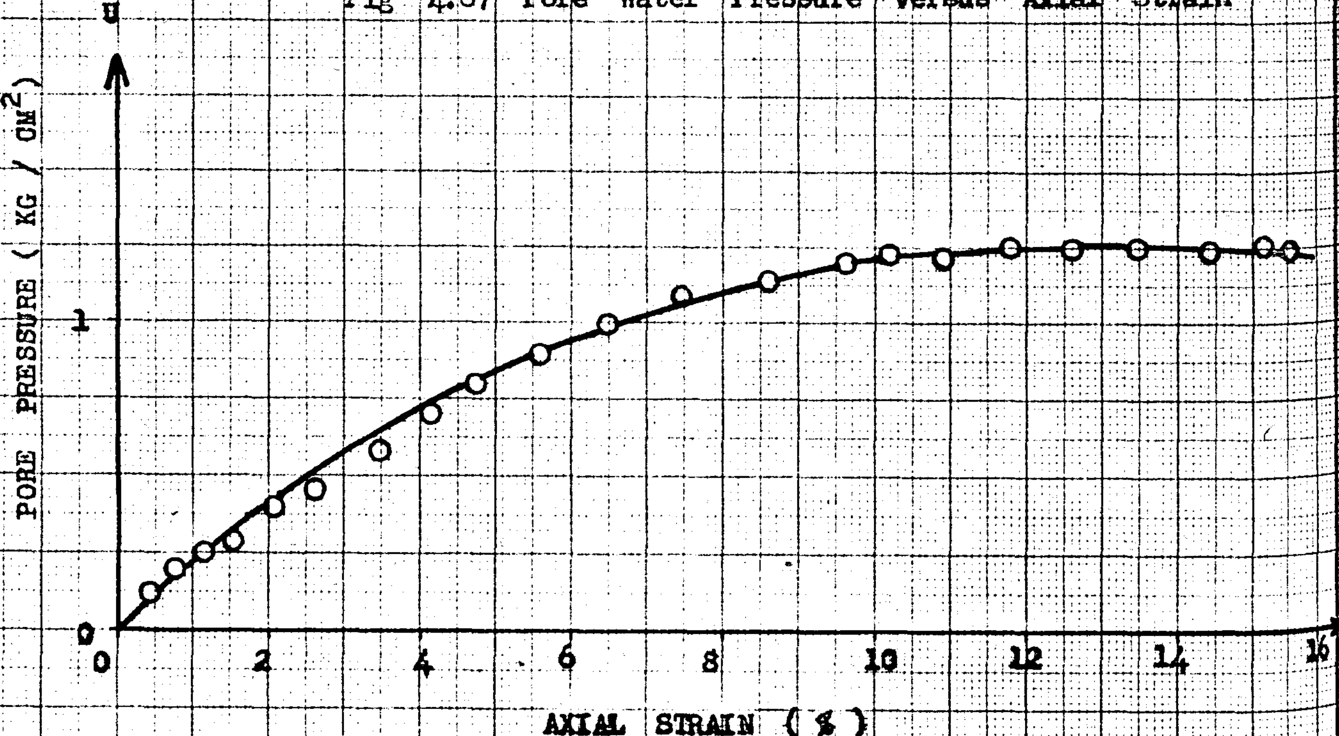

Fig 4.68 Deviator Stress versus Effective Mean Normal Stress

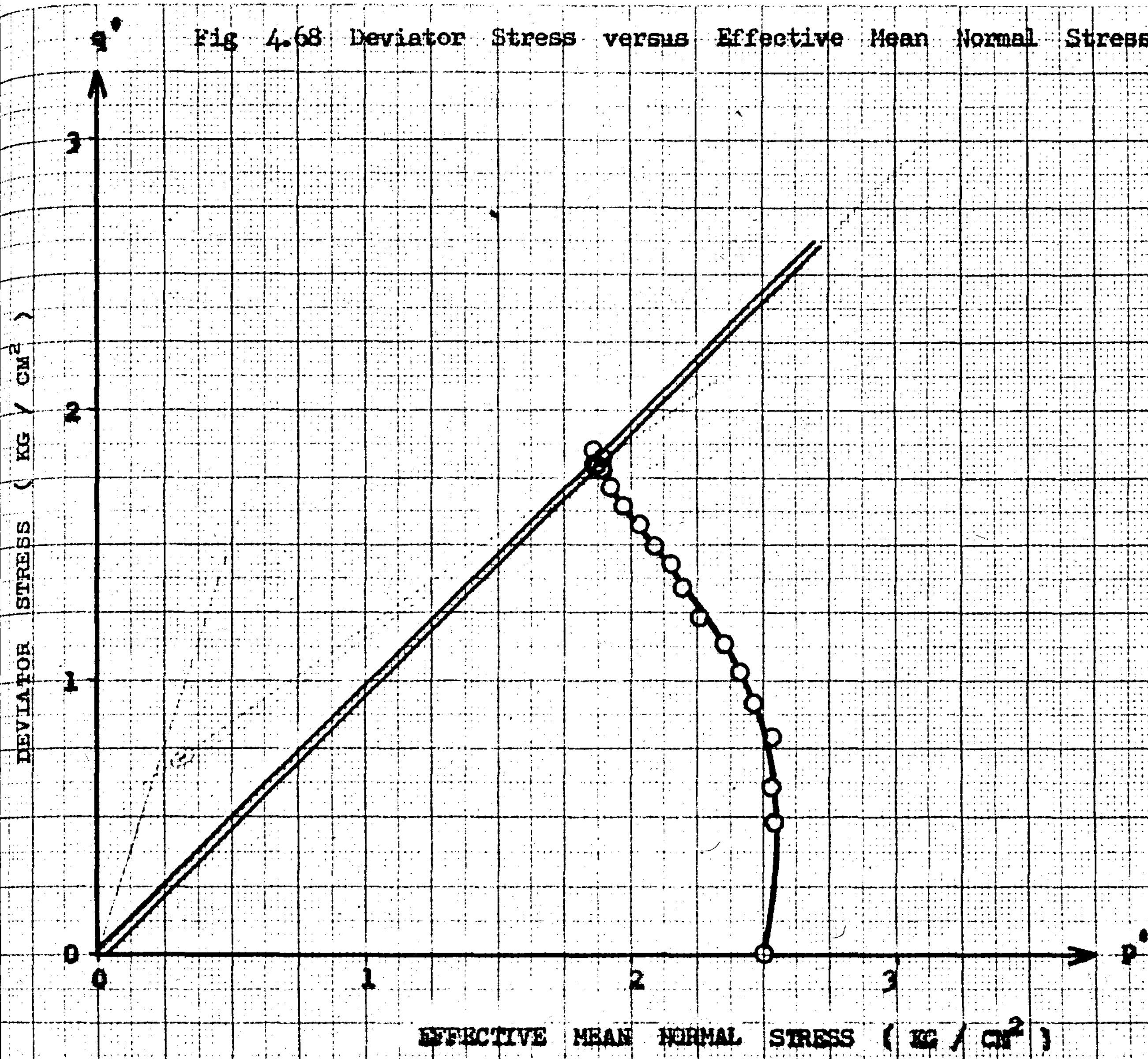

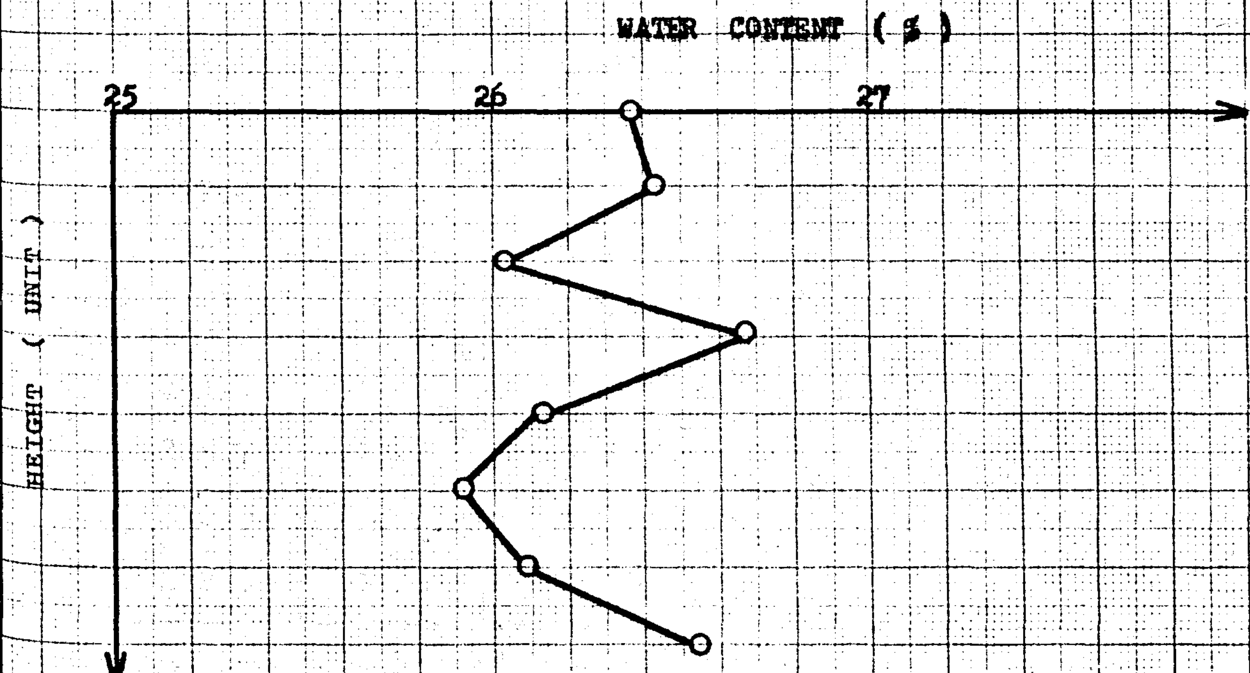

Fig 4.69 Height (Unit) versus Water Content

Consolidation Pressure : 2.5 $Kgcm^{-2}$

Equivalent Mean Normal Stress $(Pe)_i$: 2.483 $Kgcm^{-2}$

Proving Ring Number and Constant : 12365 / 0.09639 O. C. R. : 1

Specimen Diameter Top :3.44 cm. Bottom :3.44 cm. Average : 3.44 cm.

Specimen Weight : 149.02 gr. Specimen Height : 7.7 cm.

Av. Specimen Area :9.348 cm^2 Av.Loading Rate : 0.0303 mm/min.

Loading dial $In.x10^{-4}$	Axial strain %	Pore pressure $Kg./cm^2$	Deviator stress $Kg./cm^2$	Ef. Mean normal stress $Kg./cm^2$	Water Content %	
0.0	0.00	0.00	0.000	2.500	Slice No.	Water Content
53.5	0.26	0.09	0.525	2.597		
79.4	0.81	0.18	0.755	2.592	1	25.904
88.5	1.17	0.24	0.835	2.568	2	26.217
96.5	1.56	0.29	0.905	2.528	3	26.590
105.9	2.10	0.37	0.980	2.468	4	26.647
113.8	2.62	0.44	1.045	2.415	5	26.245
123.1	3.25	0.54	1.120	2.352	6	26.324
140.5	4.74	0.74	1.265	2.290	7	26.064
154.0	6.00	0.77	1.375	2.203	8	25.730
161.5	6.49	0.92	1.442	2.101	9	26.566
171.8	7.79	1.04	1.441	2.060	Average w :26.23	
177.0	8.44	1.08	1.513	1.964	Sketch of Failure	
185.8	9.74	1.13	1.549	1.936		
192.9	11.04	1.14	1.604	1.909		
201.1	12.47	1.16	1.640	1.882		
205.7	13.70	1.18	1.682	1.885		
210.5	14.95	1.19	1.694	1.875		
212.8	15.97	1.19	1.706	1.874		

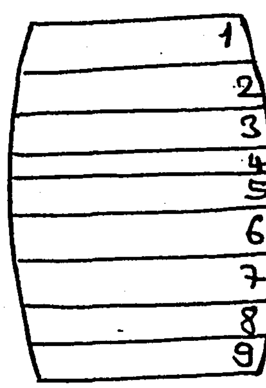

Max. Axial Stress: 1.706 $kgcm^{-2}$ Water Con. at Failure Surface:26.647 %

Fig 4.70 Deviator Stress versus Axial Strain

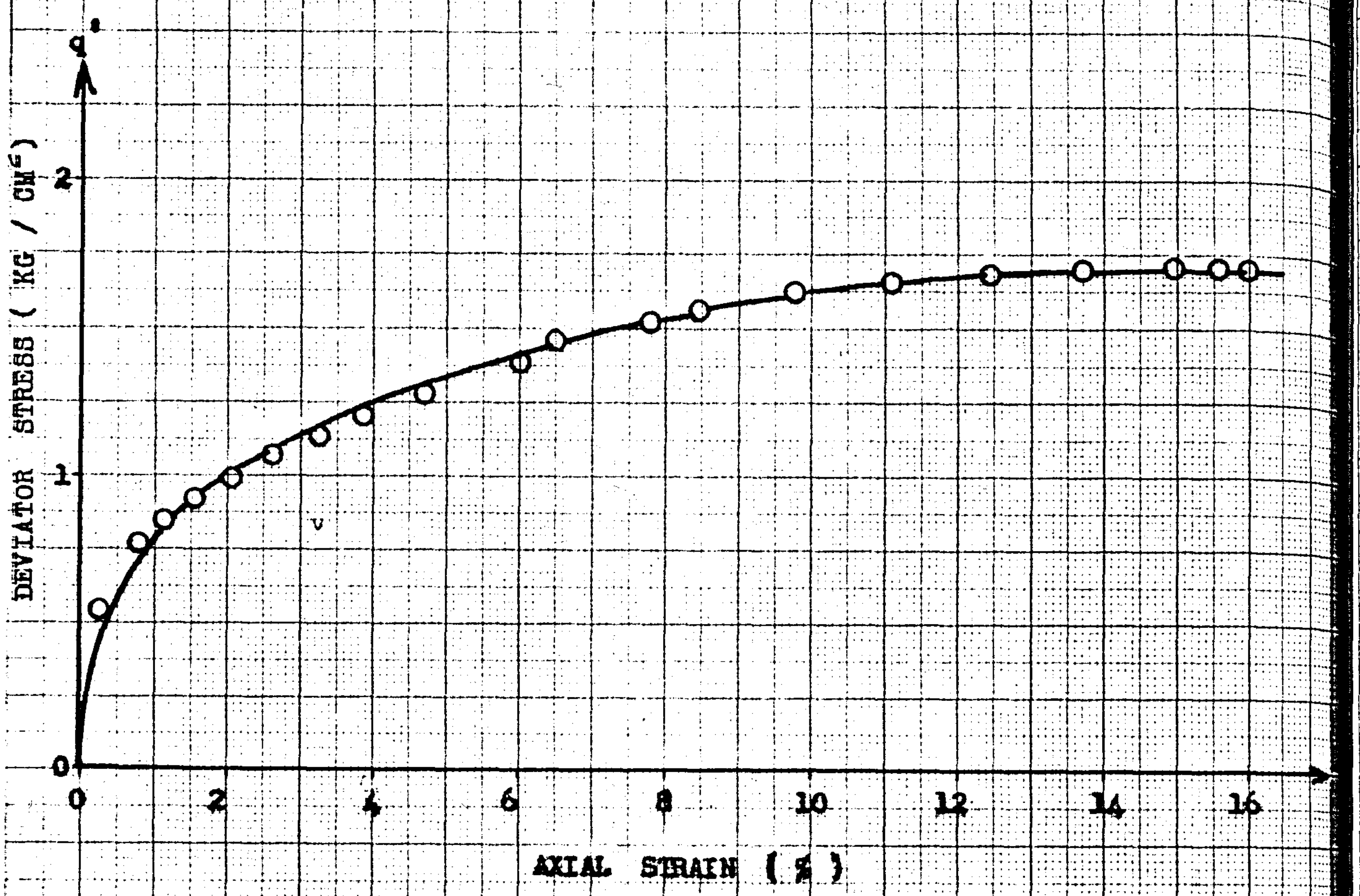

Fig 4.71 Pore Water Pressure versus Axial Strain

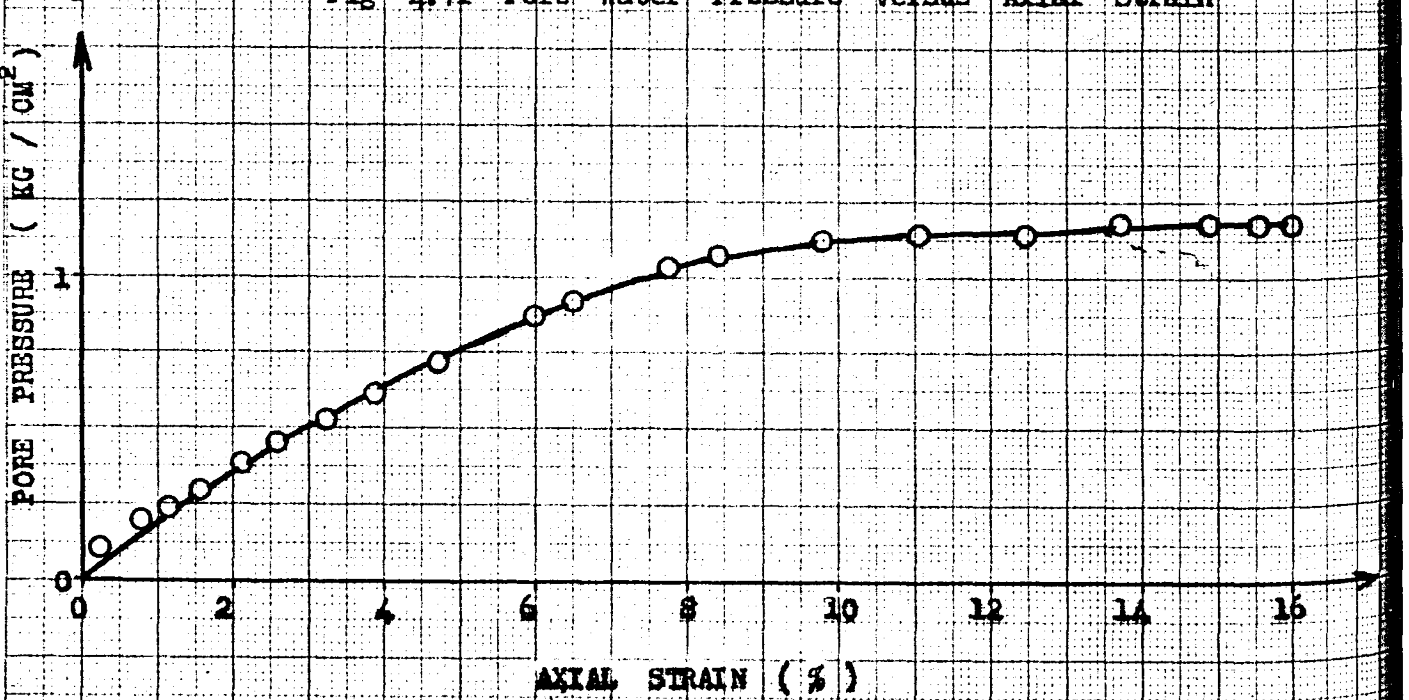

Fig 4.72 Deviator Stress versus Effective Mean Normal Stress

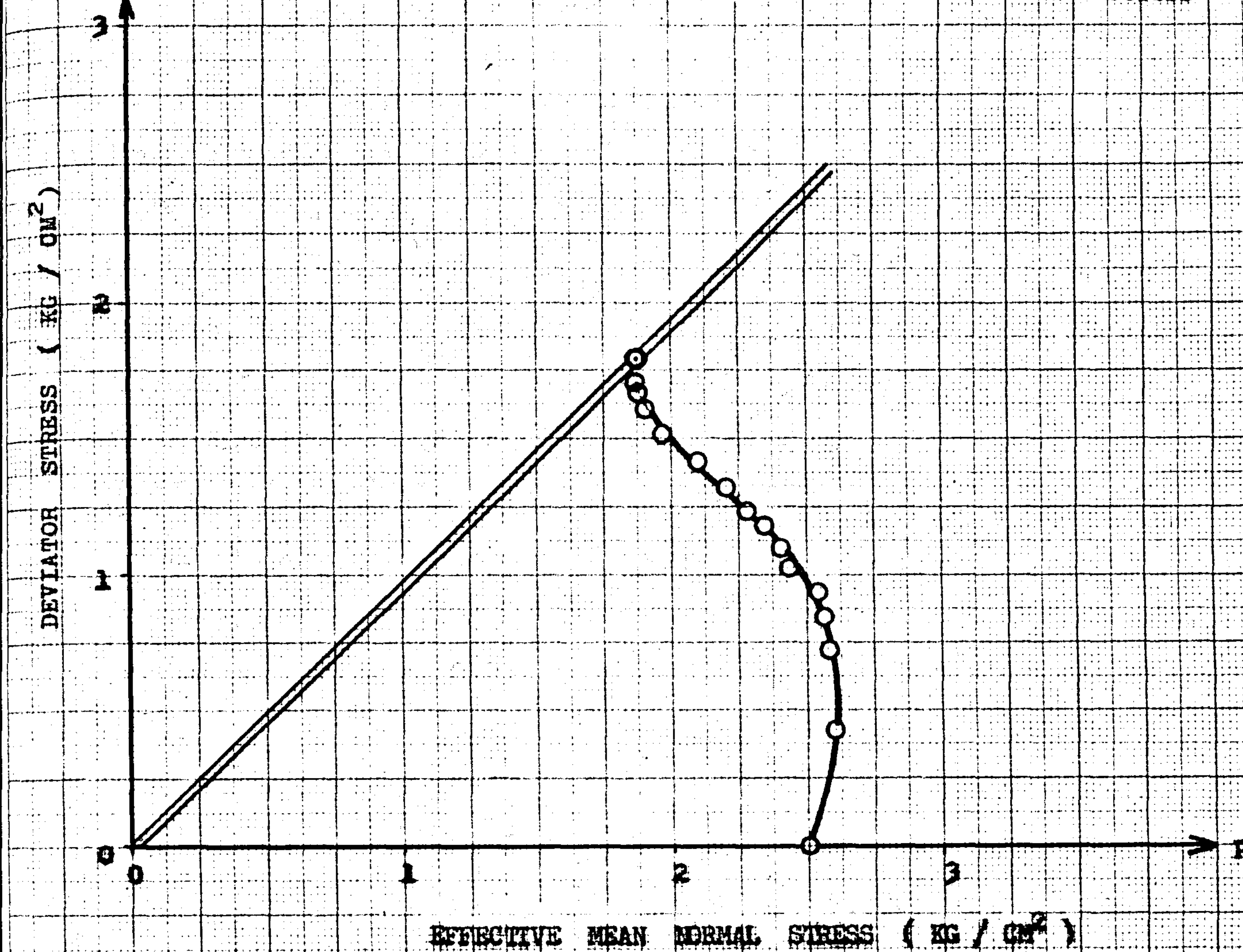

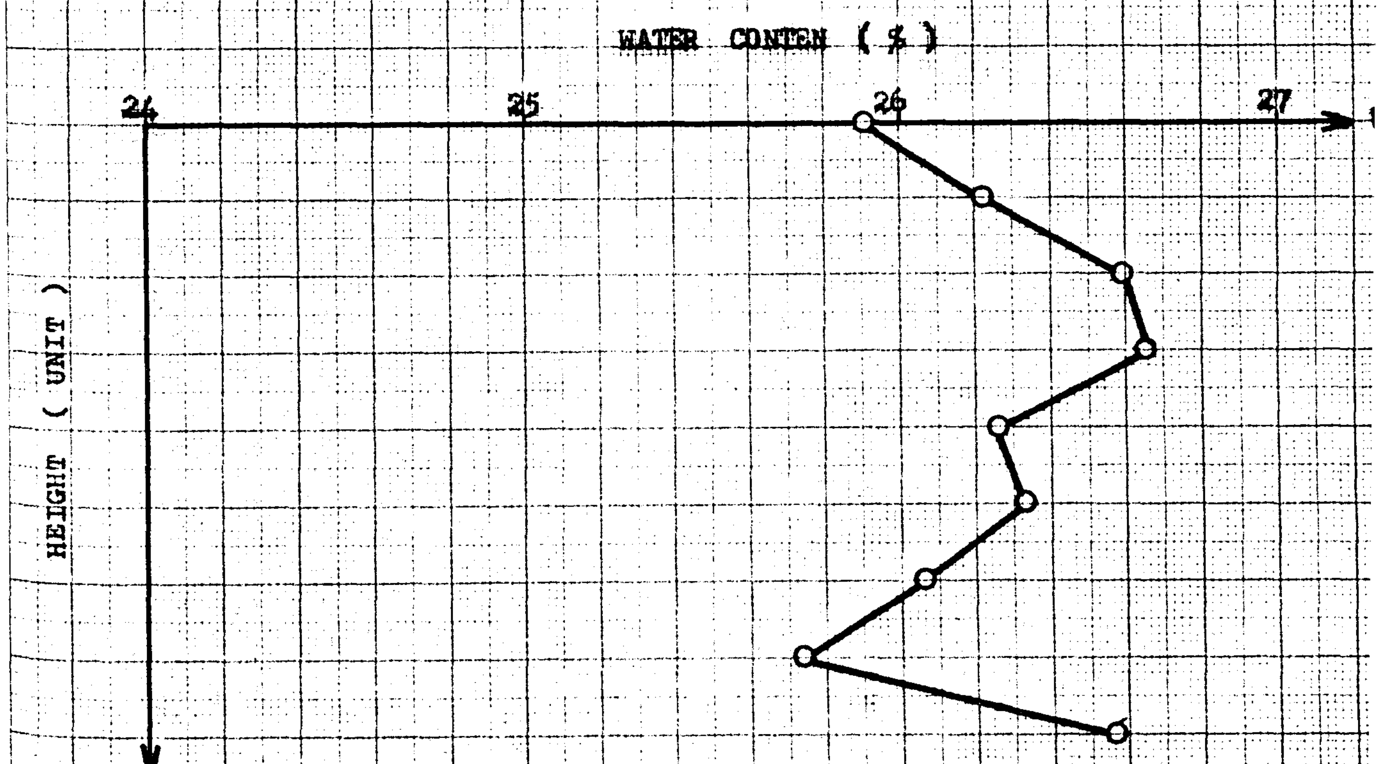

Fig 4.73 Height (Unit) versus Water Content

Consolidation Pressure : 5.0 $Kgcm^{-2}$

Equivalent Mean Normal Stress $(Pe)_i$: 5.013 $Kgcm^{-2}$

Proving Ring Number and Constant : 12365/0.09639 O. C. R. : 1

Specimen Diameter Top : 3.42 cm. Bottom : 3.42 cm. Average : 3.42 cm.

Specimen Weight : Specimen Height : 7.75 cm.

Av. Specimen Area : 9.186 cm^{-2} Av. Loading Rate : 0.0303 mm/min.

Loading dial In. $\times 10^{-4}$	Axial strain %	Pore pressure Kg. / cm^2	Deviator stress Kg. / cm^2	Ef. Mean normal stress Kg. / cm^2
0.0	0.00	0.00	0.000	5.000
21.5	0.12	0.22	0.220	4.923
109.5	0.31	0.47	1.131	5.077
149.0	0.59	0.55	1.508	4.953
163.2	0.76	0.66	1.649	4.800
201.5	1.28	0.94	2.020	4.548
226.0	1.79	1.39	2.253	4.371
255.5	2.54	1.70	2.518	4.159
286.5	3.60	2.05	2.793	3.961
303.0	4.27	2.10	2.936	3.868
329.0	5.53	2.30	3.148	3.757
350.0	6.82	2.40	3.305	3.702
365.0	7.92	2.50	3.406	3.700
381.0	9.28	2.48	3.508	3.729
388.8	10.05	2.45	3.543	3.747
394.5	12.05	2.32	3.525	3.775
395.0	12.44	2.30	3.518	3.787
396.5	13.23	2.30	3.511	3.846
397.5	13.82	2.30	3.505	3.868

Water Content %

Slice No.	Water Content
1	23.069
2	22.883
3	22.705
4	23.050
5	23.042
6	23.239
7	23.545
8	23.071
9	23.887

Average w : 23.166

Sketch of Failure

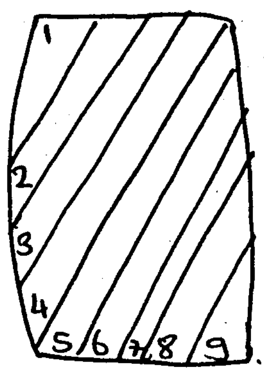

Max. Axial Stress: 3.543 $kgcm^{-2}$ Water Con. at Failure Surface: 23.545 %

Fig 4.74 Deviator Stress versus Axial Strain

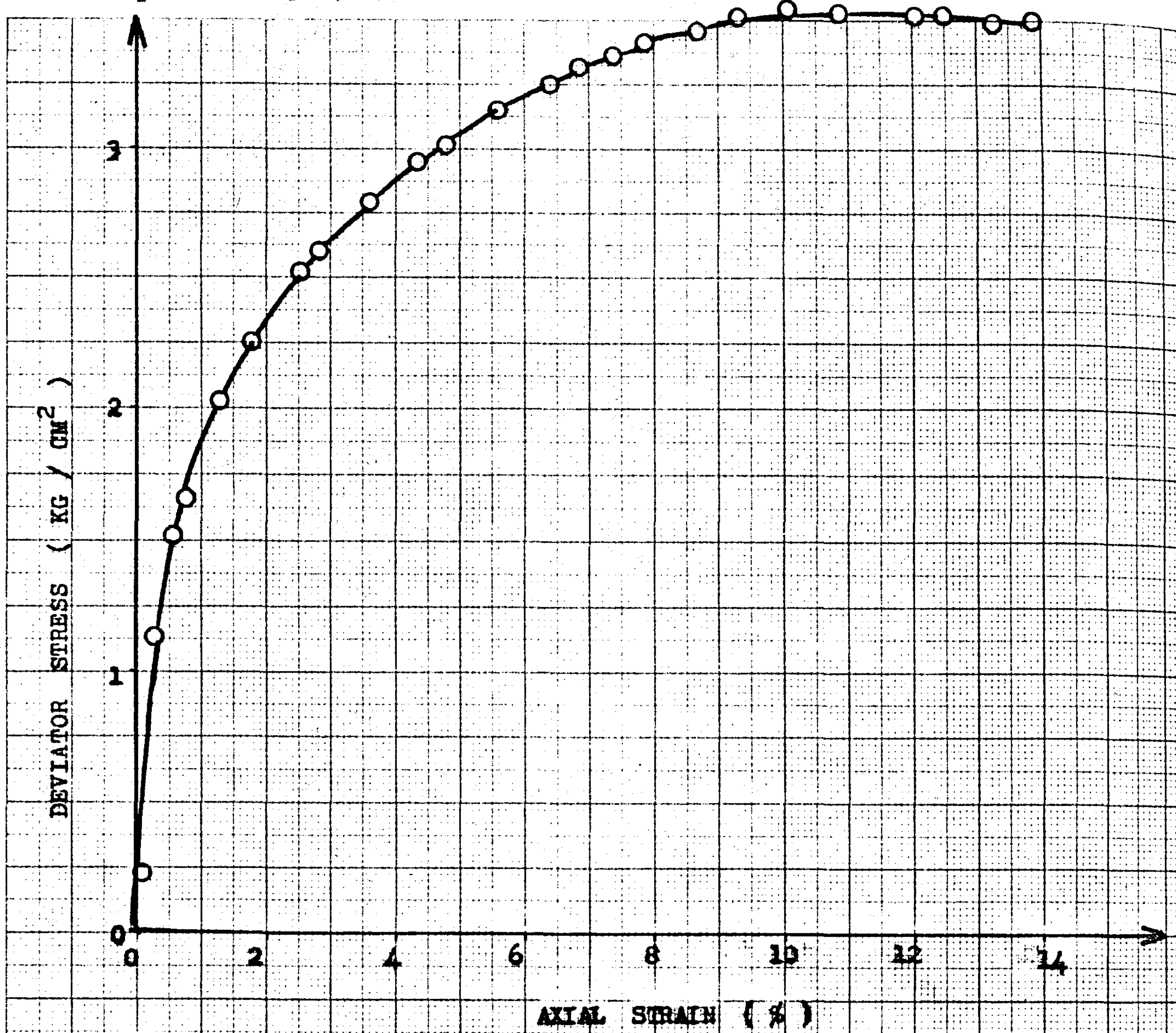

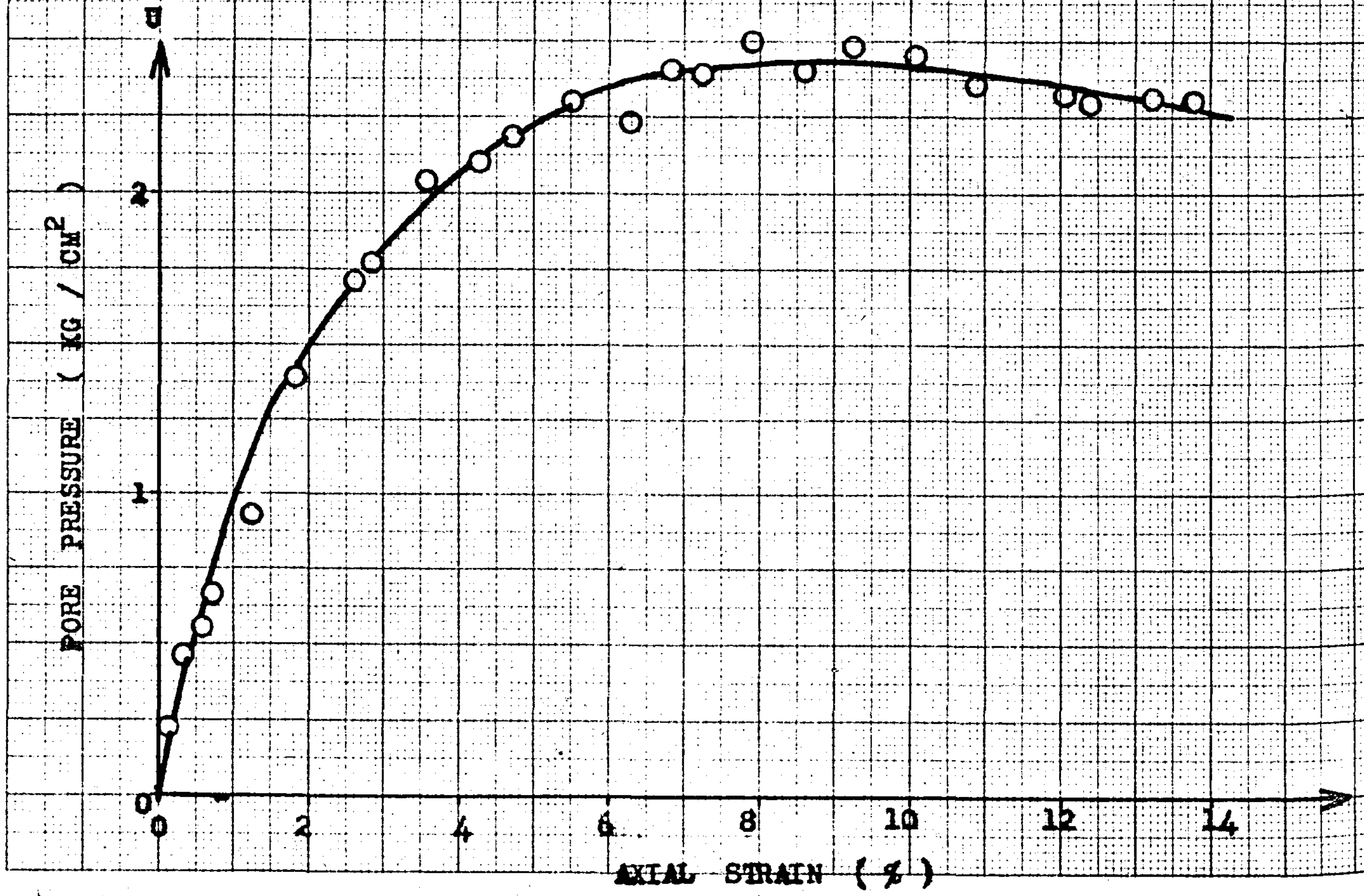

Fig 4.75 Pore Water Pressure versus Axial Strain

Fig 4.76 Deviator Stress versus Effective Mean Normal Stress

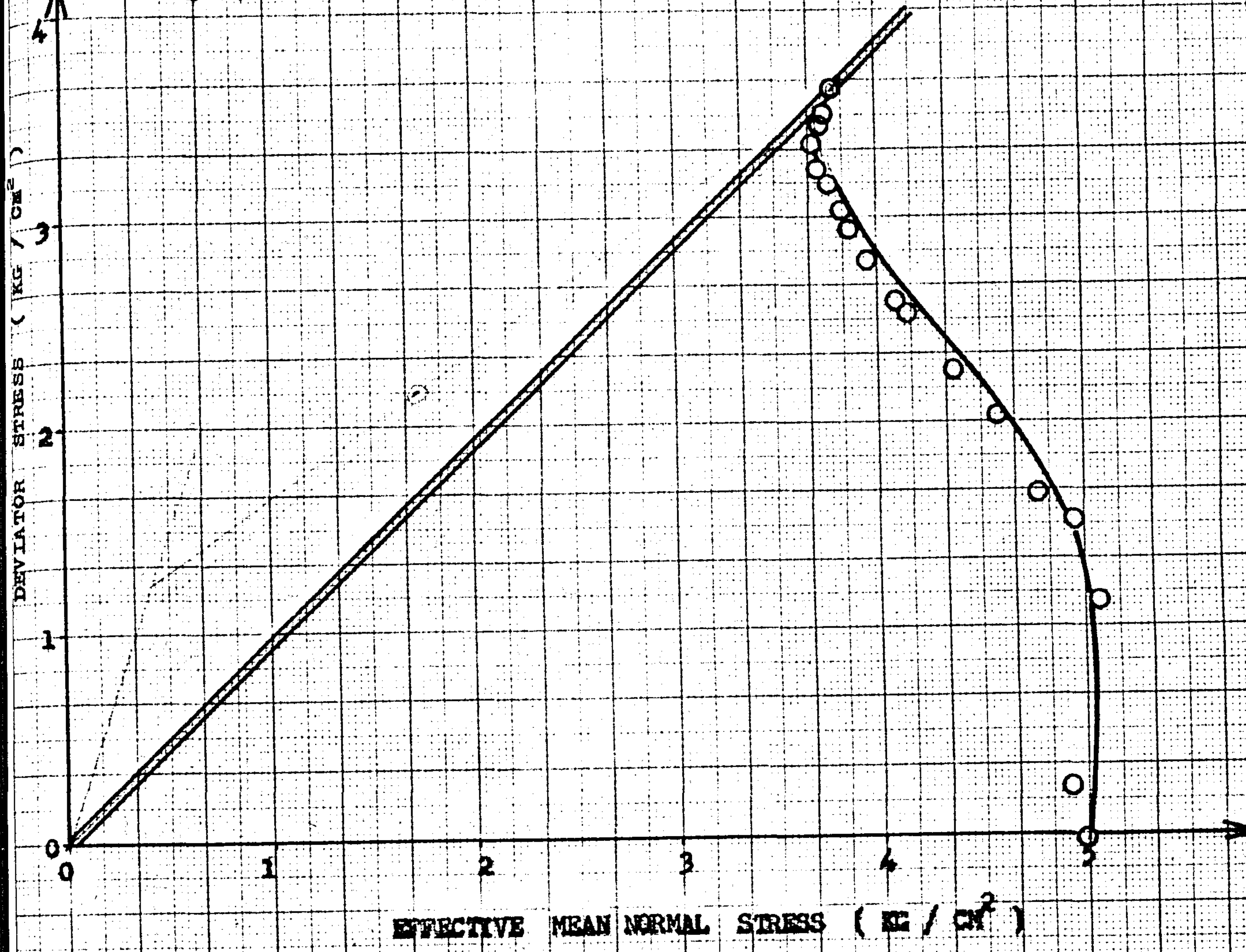

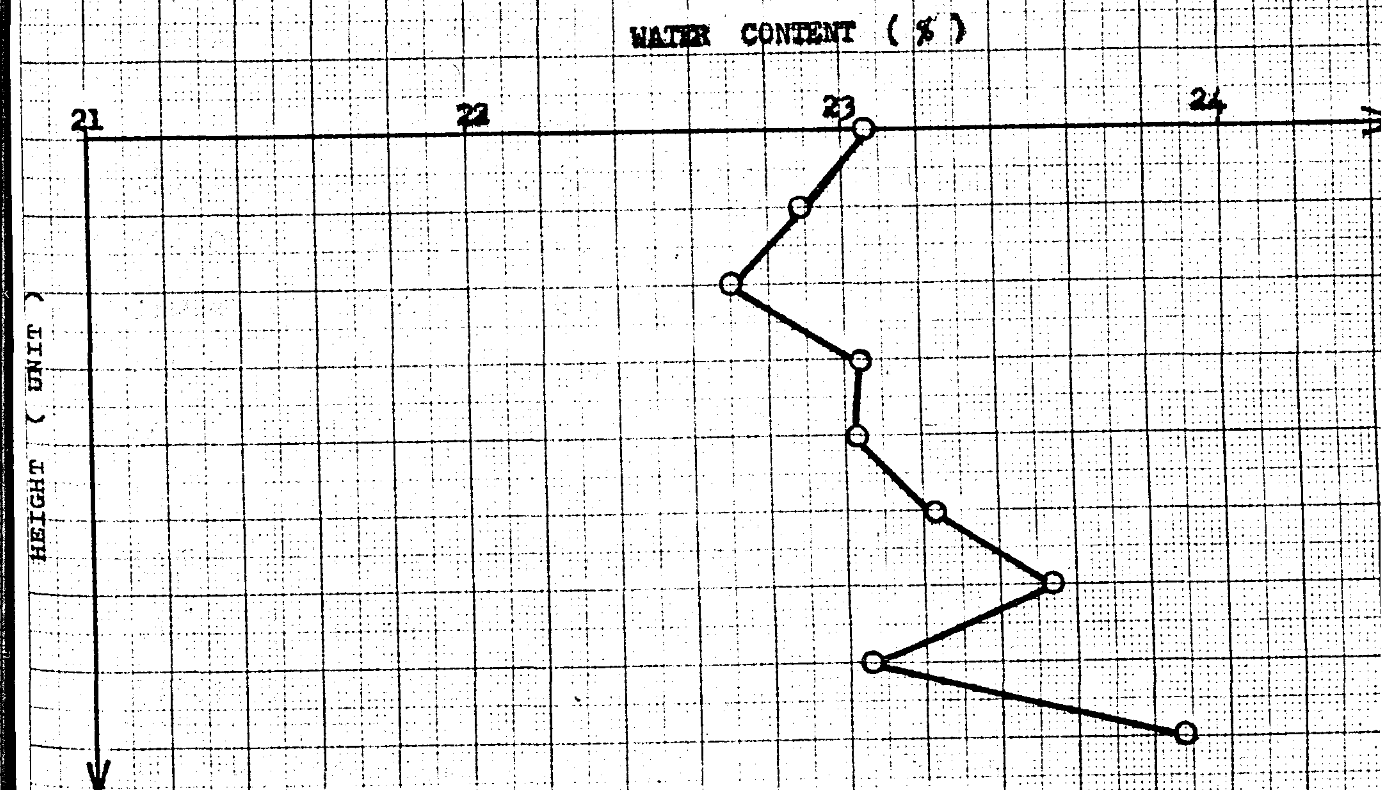

Fig 4.77 Height (Unit) versus Water Content

Consolidation Pressure : 5.0 $Kgcm^{-2}$

Equivalent Mean Normal Stress $(Pe)_i$: 5.935 $Kgcm^{-2}$

Proving Ring Number and Constant : 12365/0.09639 O. C. R. : 1

Specimen Diameter Top : 3.58 cm. Bottom : 0.20829 3.58 cm. Average : 3.58 cm.

Specimen Weight : 163.41 gr. Specimen Height : 8.0 cm.

Av. Specimen Area : 10.066 cm^2 Av. Loading Rate : 0.0303 mm/min.

Loading dial $In. \times 10^{-4}$	Axial strain %	Pore pressure Kg. / cm^2	Deviator stress Kg. / cm^2	Ef. Mean normal stress Kg. / cm^2	Water Content %	
					Slice No.	Water Content
0.0	0.00	0.00	0.000	5.000		
47.5	0.26	0.29	0.437	4.968		
121.0	0.51	0.55	1.108	4.909	1	22.265
159.0	0.79	0.80	1.461	4.762	2	22.041
204.0	1.25	1.23	1.863	4.326	3	22.504
244.1	1.88	1.82	2.214	3.872	4	22.847
269.0	2.37	2.17	2.425	3.662	5	22.482
285.0	2.75	2.33	2.558	3.563	6	22.523
305.5	3.31	2.50	2.726	3.469	7	22.683
322.6	3.89	2.63	2.863	3.414	8	22.094
351.2	5.00	2.60	3.083	3.375	9	22.425
376.0	6.25	2.65	3.261	3.419	Average w : 22.429	
390.4	7.54	2.61	3.338	3.504	Sketch of Failure	
400.0	9.19	2.61	3.425	3.592		
408.0	11.12	2.50	3.491	3.662		
411.5	12.37	2.48	3.501	3.698		
413.8	13.26	2.42	3.502	3.717		
417.2	14.64	2.42	3.501	3.742		
418.1	15.27	2.34	3.488	3.753		

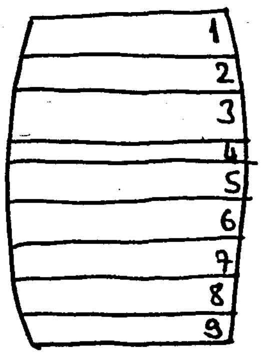

Max. Axial Stress: 3.502 $kgcm^{-2}$ Water Con. at Failure Surface: 22.847 %

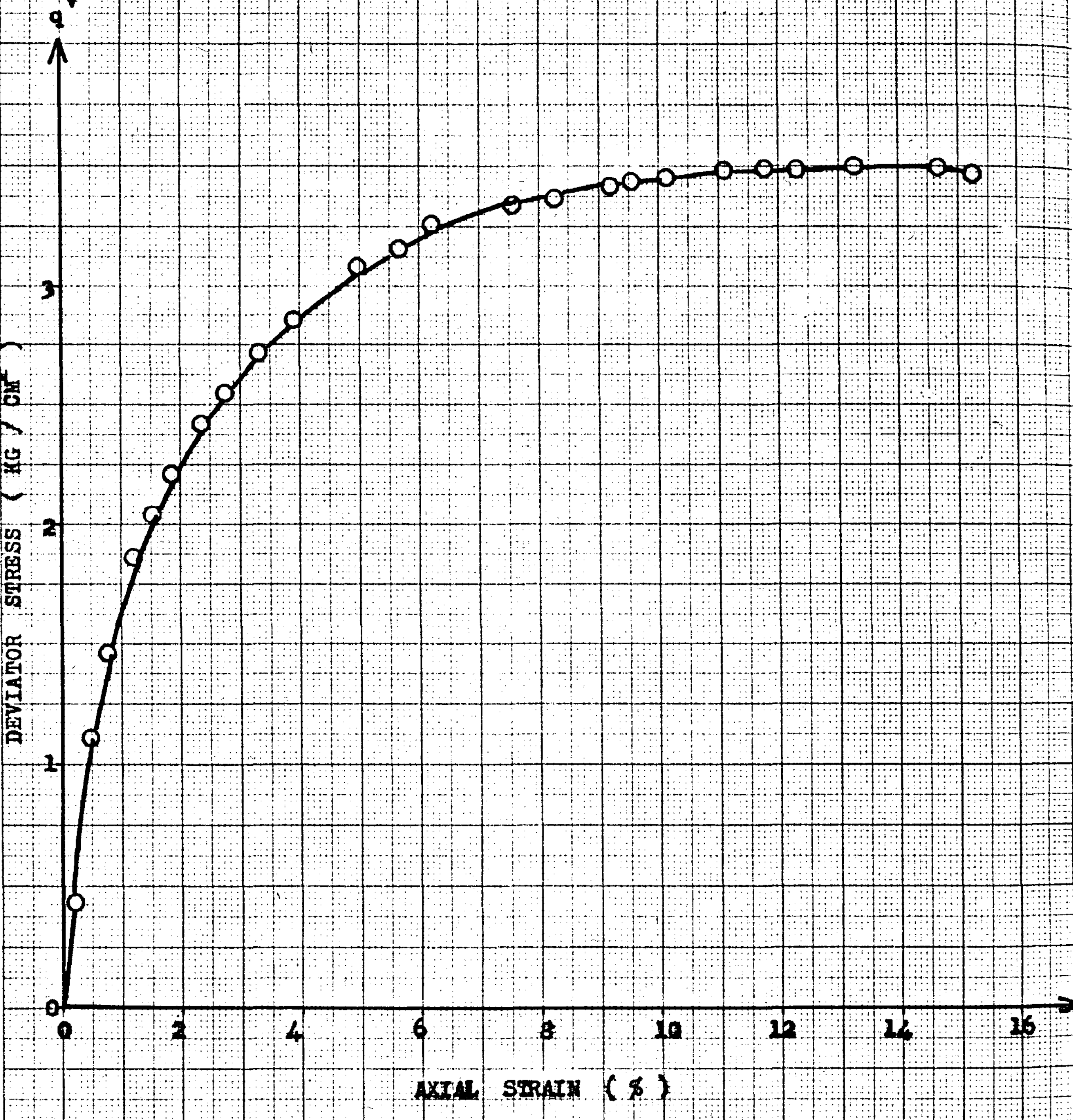

Fig 4.78 Deviator Stress versus Axial Strain

Fig 4.79 Pore Water Pressure versus Axial Strain

Fig 4.80 Devitor Stress versus Effective Mean Normal Stress

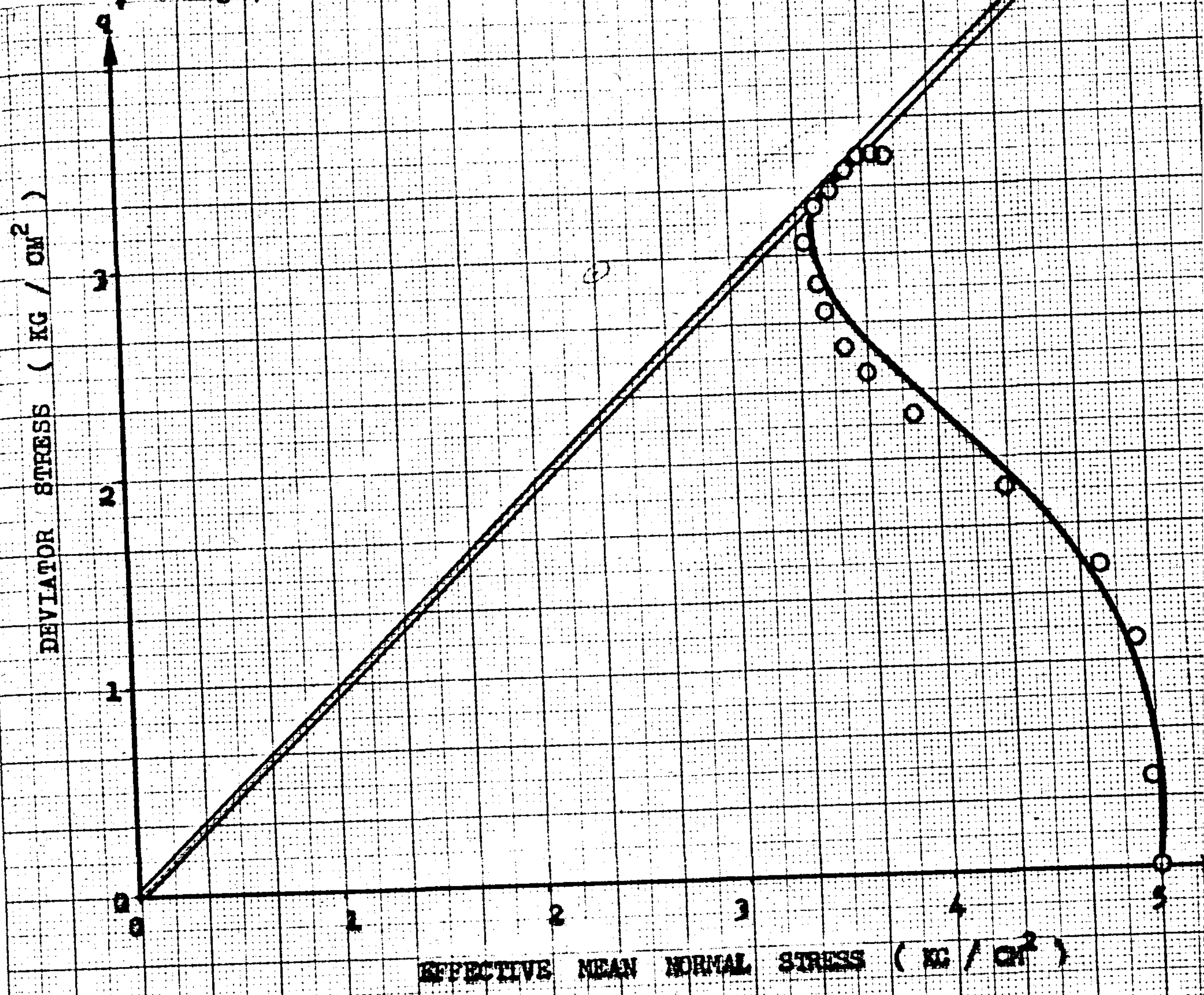

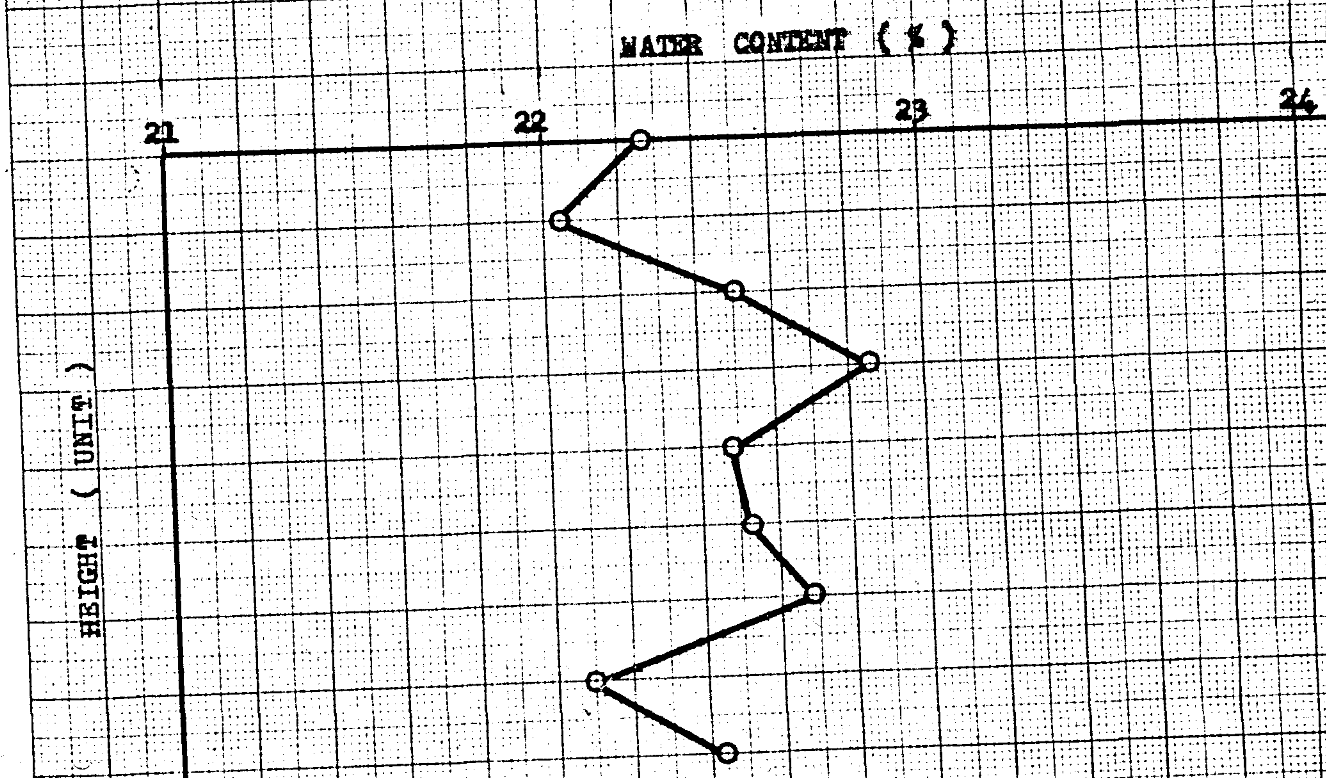

Fig 4.81 Height (Unit) versus Water Content

Consolidation Pressure : 5.0 $Kgcm^{-2}$

Equivalent Mean Normal Stress $(Pe)_i$: 4.535 $Kgcm^{-2}$

Proving Ring Number and Constant : 12365 / 0.09639 O. C. R. : 1

Specimen Diameter Top : 3.41 cm. Bottom : 3.41 cm. Average : 3.41 cm.

Specimen Weight : 148.65 gr. Specimen Height : 7.60 cm.

Av. Specimen Area : 9.133 cm^2 Av. Loading Rate : 0.0303 mm/min.

Loading dial $In. \times 10^{-4}$	Axial strain %	Pore pressure $Kg./cm^2$	Deviator stress $Kg./cm^2$	Ef. Mean normal stress $Kg./cm^2$	Water Content %	
0.0	0.00	0.00	0.000	5.000	Slice No.	Water Content
47.0	0.26	0.06	0.470	5.218		
104.0	0.46	0.12	1.051	5.230	1	23.487
140.5	0.79	0.22	1.415	5.252	2	23.619
173.2	1.32	0.38	1.733	5.203	3	24.197
190.0	1.71	0.50	1.900	5.133	4	23.979
220.0	2.50	0.73	2.180	4.995	5	23.665
240.0	3.22	0.93	2.370	4.863	6	23.097
254.0	3.75	1.08	2.490	4.757	7	23.143
280.0	4.93	1.36	2.700	4.540	8	23.775
294.0	5.66	1.52	2.810	4.423	9	23.471
308.0	6.45	1.65	2.924	4.325	Average w : 23.60	
318.0	7.17	1.75	2.995	4.248	Sketch of Failure	
328.0	8.03	1.83	3.070	4.184		
345.3	9.54	1.92	3.165	4.135		
354.7	10.79	1.95	3.211	4.120		
358.0	11.78	1.96	3.205	4.108		
363.5	13.55	1.97	3.195	4.100		
368.5	15.59	1.96	3.140	4.086		

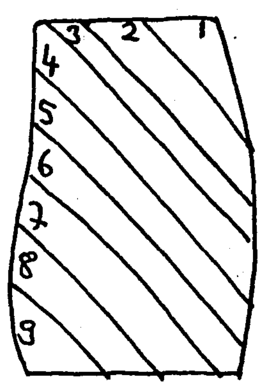

Max. Axial Stress: 3.205 $kgcm^{-2}$ Water Con. at Failure Surface: 24.197

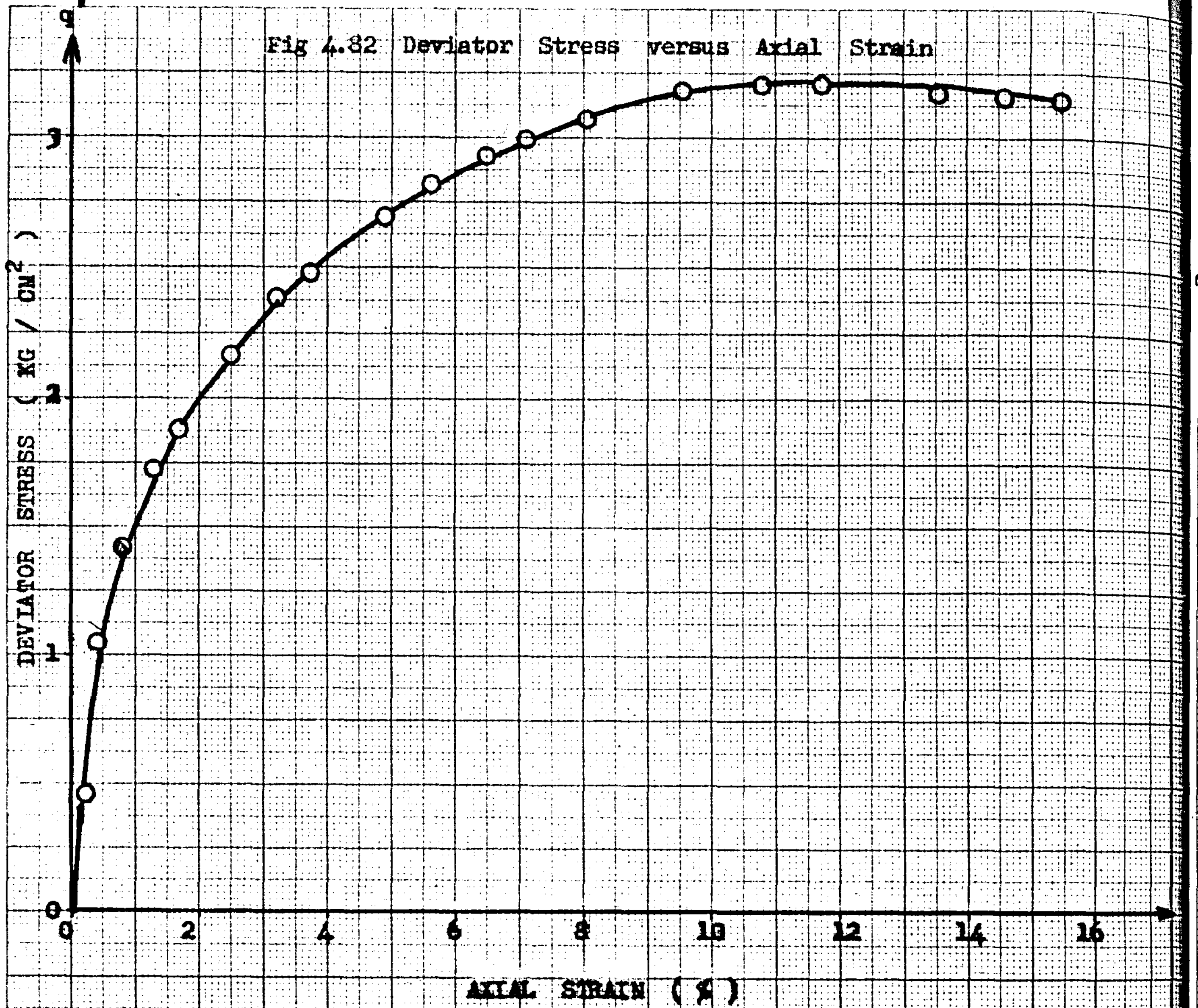

Fig 4.82 Deviator Stress versus Axial Strain

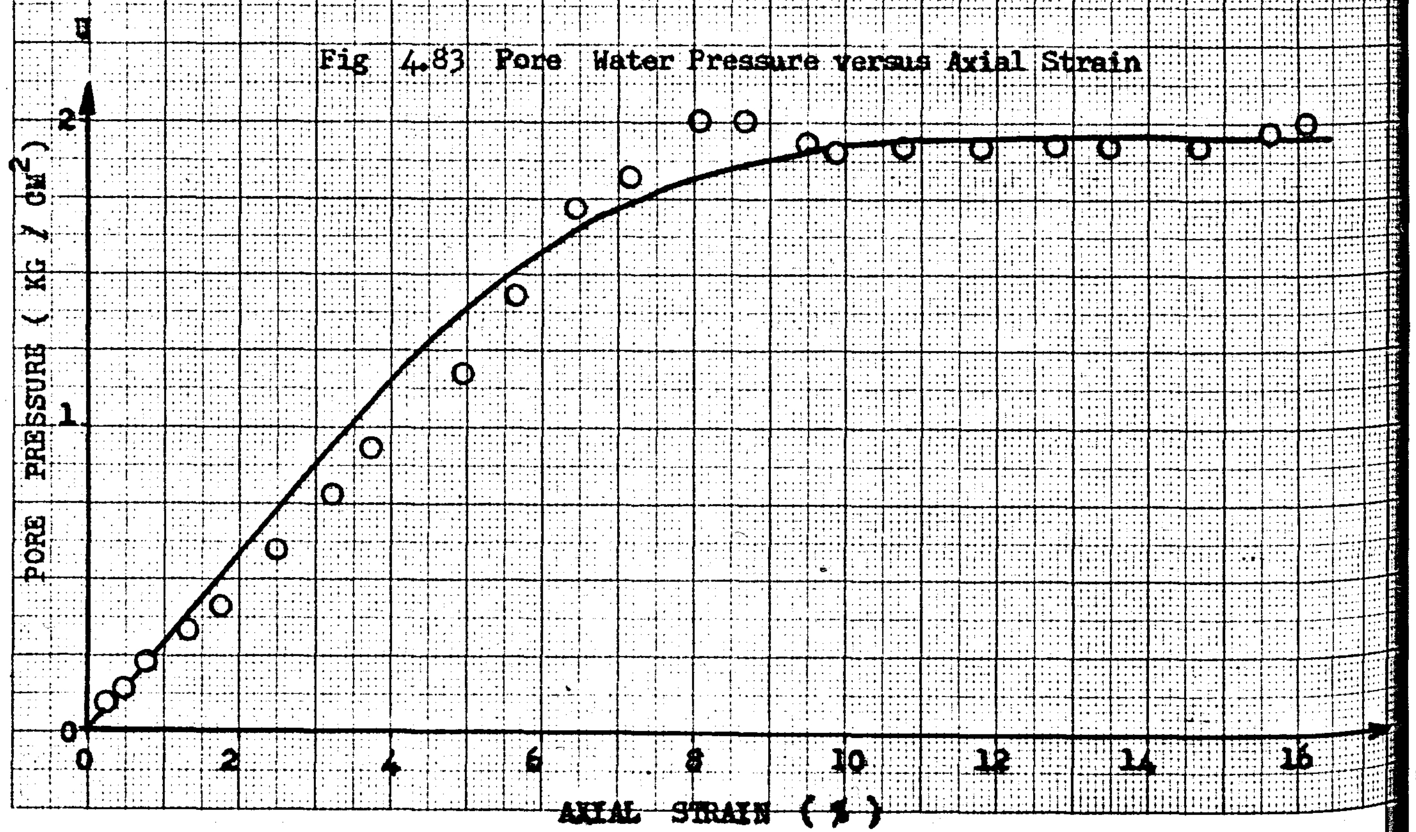

Fig 4.83 Pore Water Pressure versus Axial Strain

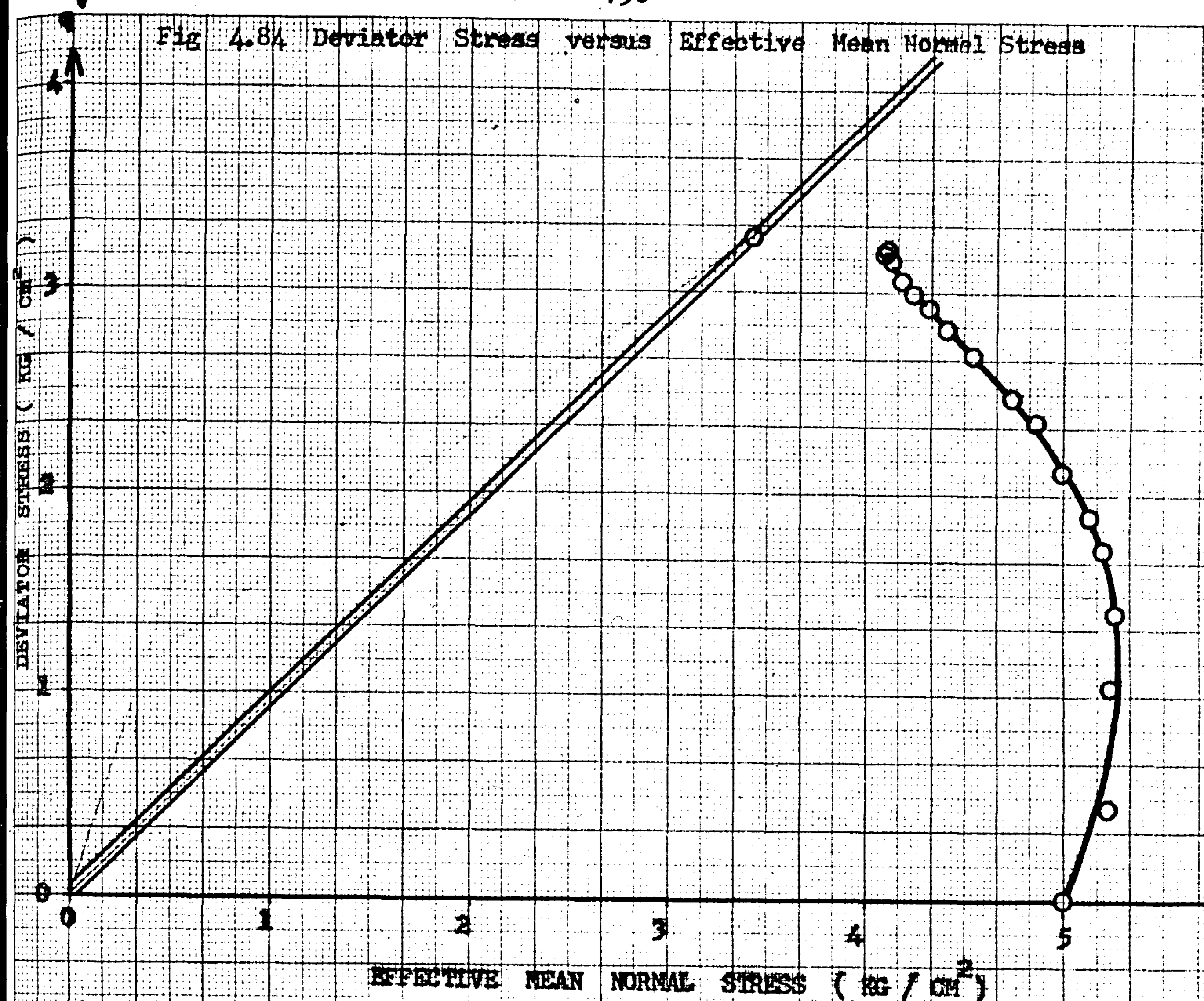

Fig 4.84 Deviator Stress versus Effective Mean Normal Stress

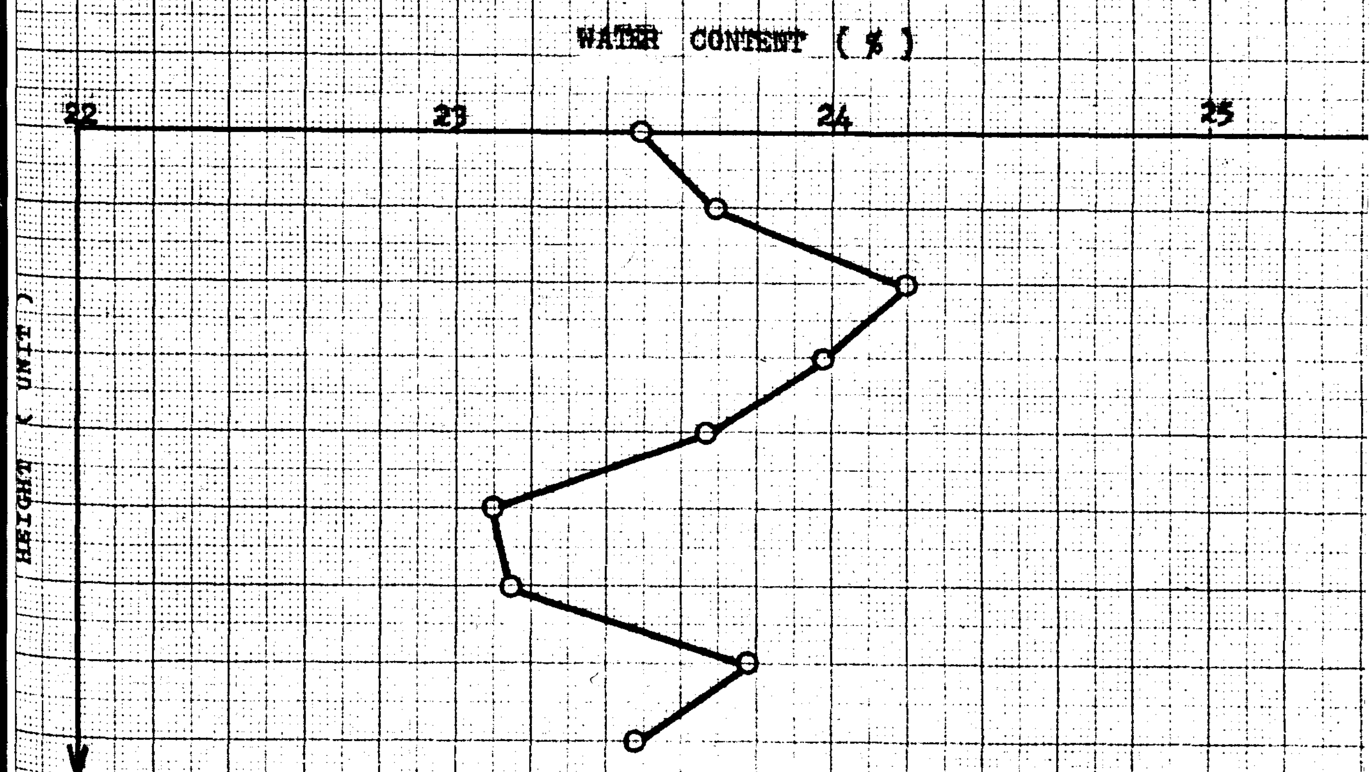

Fig 4.85 Height (Unit) versus Water Content

Consolidation Pressure : 7.5 $Kgcm^{-2}$

Equivalent Mean Normal Stress $(Pe)_i$: 7.393 $Kgcm^{-2}$

Proving Ring Number and Constant : 12256/0.13957 O. C. R. : 1

Specimen Diameter Top :3.41 cm. Bottom :3.42 cm. Average : 3.415 cm.

Specimen Weight : 154.29 gr. Specimen Height : 7.6 cm.

Av. Specimen Area :9.159 cm^{-2} Av.Loading Rate : 0.0303 mm/min.

Loading dial In. $x10^{-4}$	Axial strain %	Pore pressure Kg. / cm^2	Deviator stress Kg. / cm^2	Ef. Mean normal stress Kg. / cm^2	Water Content %	
					Slice No.	Water Content
0.0	0.00	0.00	0.000	7.500		
31.0	0.29	0.18	0.458	7.510		
59.0	0.55	0.22	0.848	7.523	1	21.059
84.0	0.88	0.29	1.217	7.500	2	21.327
102.8	1.21	0.36	1.311	7.467	3	21.164
143.5	2.12	5.45	2.051	7.284	4	22.180
154.0	2.39	0.64	2.200	7.223	5	21.245
170.0	2.92	0.85	2.418	7.081	6	21.197
196.5	3.84	1.24	2.773	6.824	7	21.610
208.5	4.30	1.47	2.932	6.705	8	21.757
219.0	4.76	1.77	3.068	6.580	9	21.680
238.8	5.68	2.20	3.318	6.331	Average w :21.469	
253.8	6.47	2.51	3.501	6.160	Sketch of Failure	
266.5	7.26	2.89	3.648	5.991		
280.0	8.26	2.95	3.793	5.847		
292.0	9.89	3.15	3.884	5.705		
303.8	11.08	3.16	3.988	5.662		
314.5	12.99	3.17	4.036	5.638		
317.8	15.68	3.16	3.942	5.664		

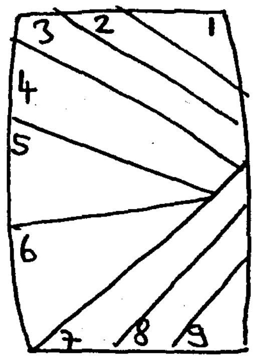

Max. Axial Stress:4.036 $kgcm^{-2}$ Water Con. at Failure Surface: 22.180 %

Fig 4.86 Deviator Stress versus Axial Strain

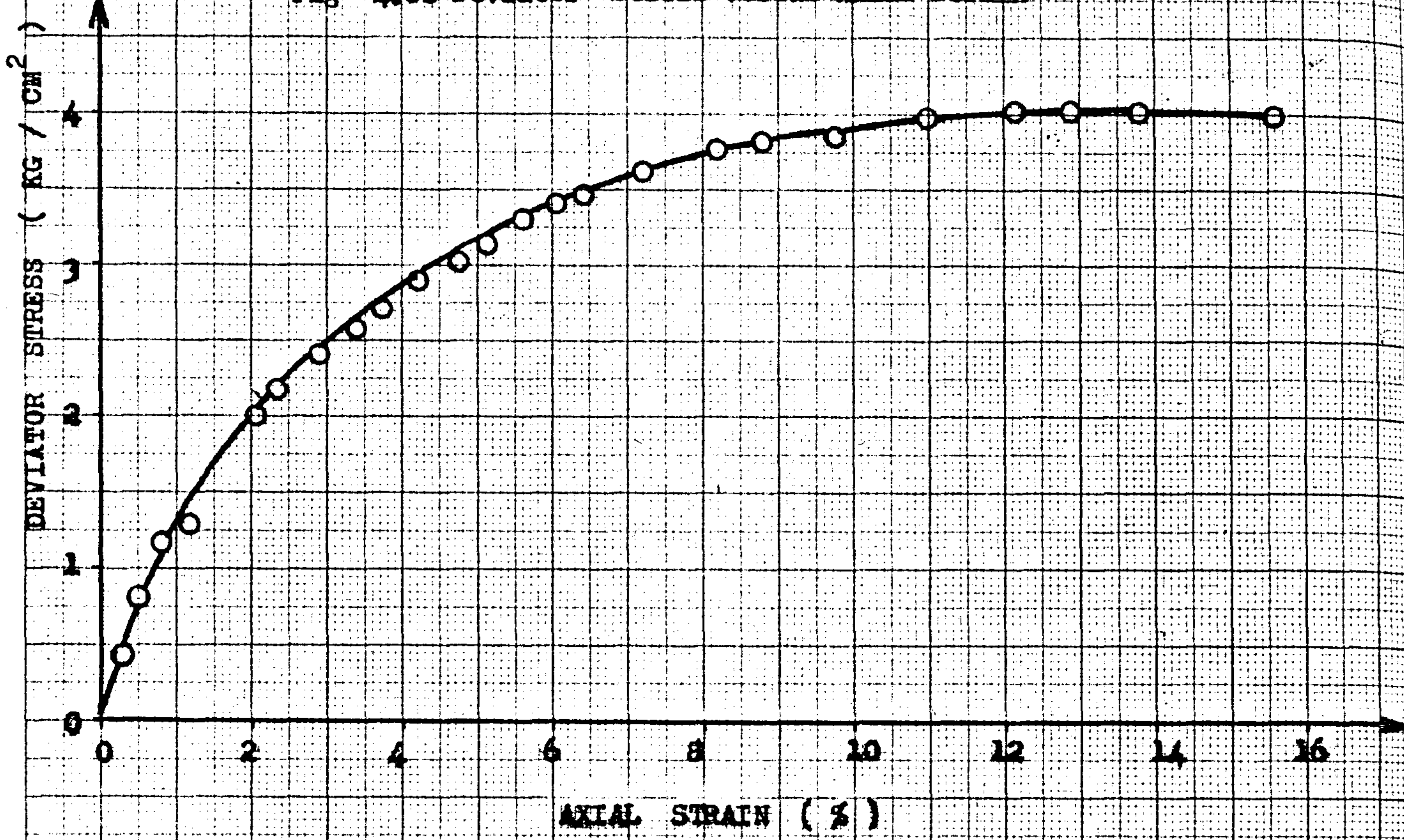

Fig 4.87 Pore Water Pressure versus Axial Strain

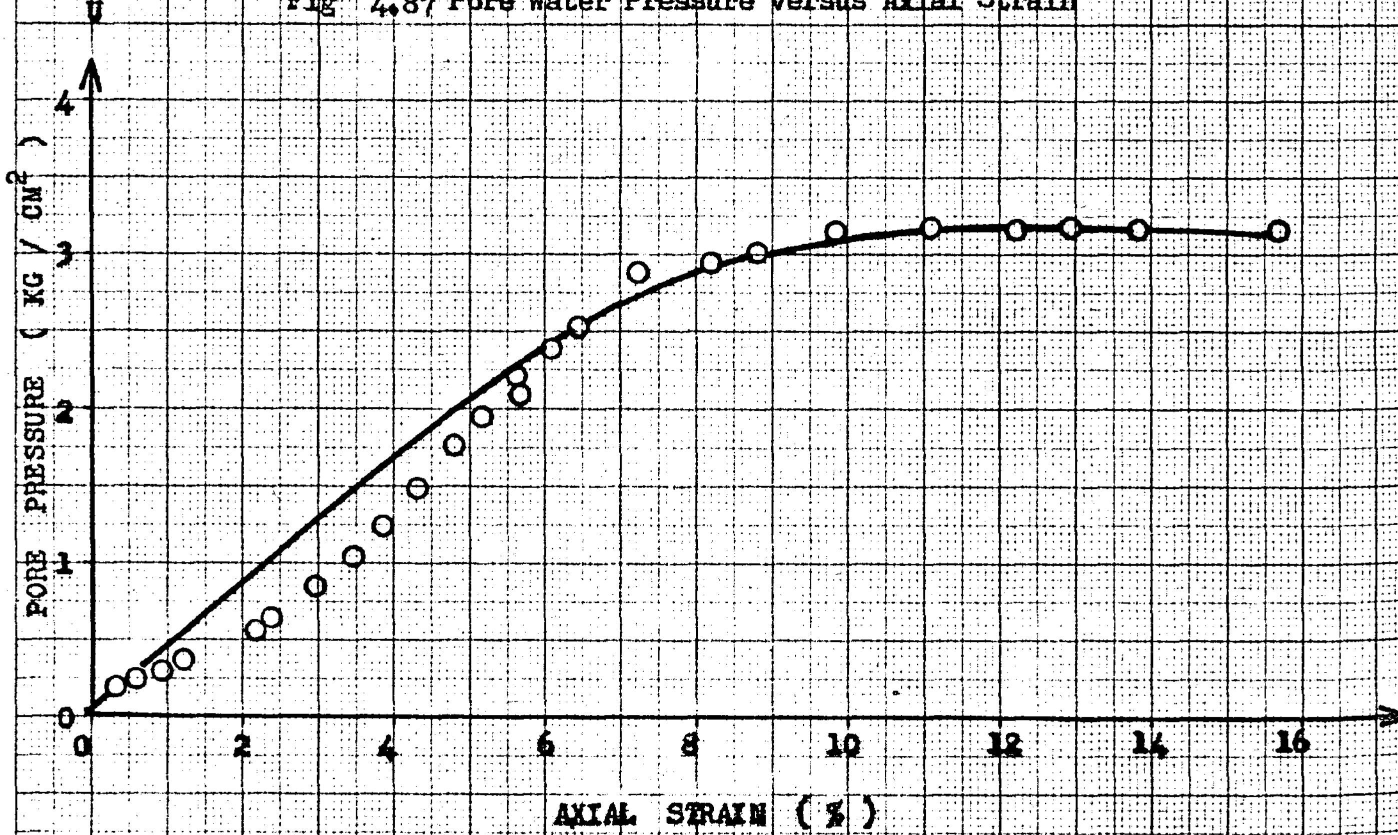

Fig 4.88 Deviator Stress versus Effective Mean Normal Stress

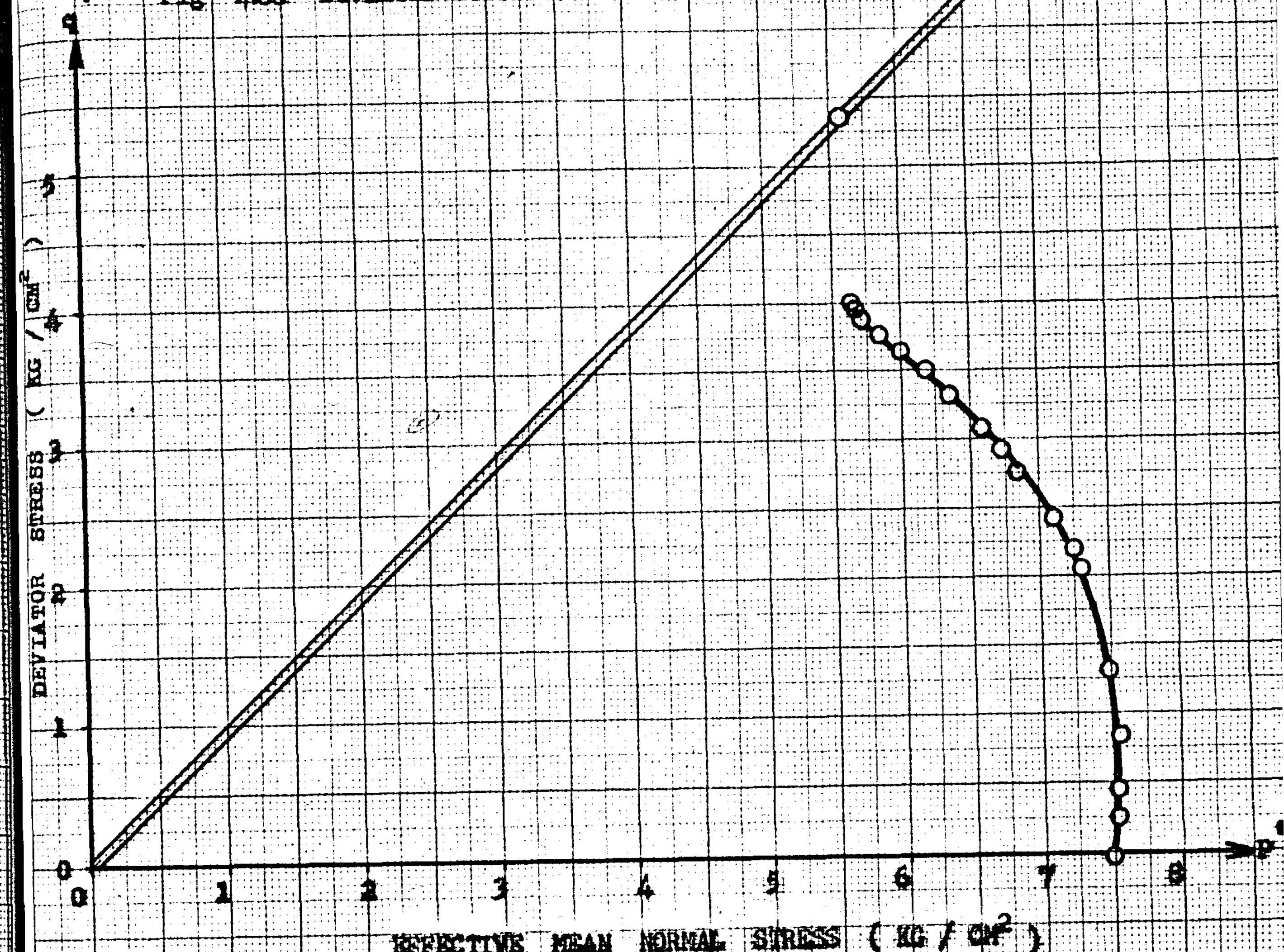

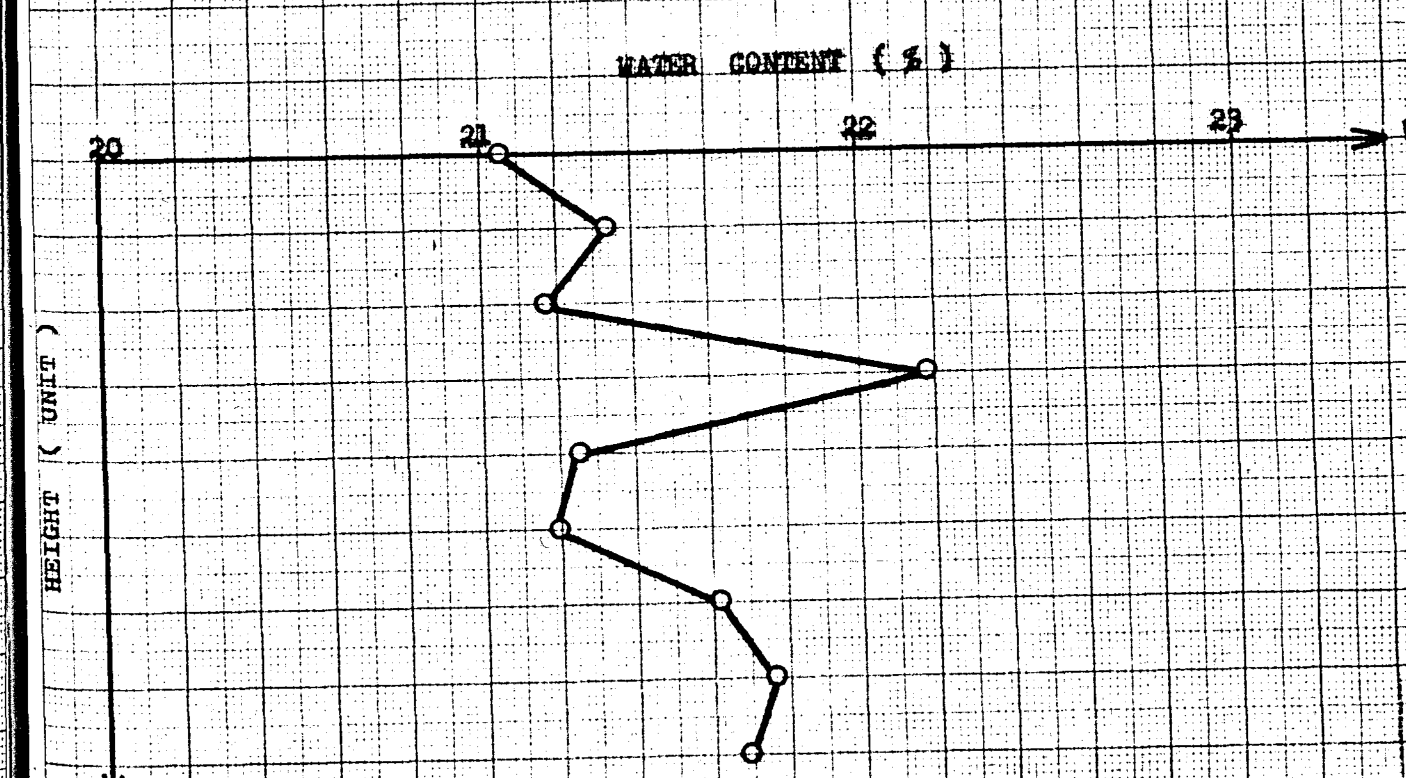

Fig 4.89 Height (Unit) versus Water Content

Consolidation Pressure : 7.5 $Kgcm^{-2}$

Equivalent Mean Normal Stress $(Pe)_i$: 8.875 $Kgcm^{-2}$

Proving Ring Number and Constant :12365 / 0.09639 O. C. R. : 1

Specimen Diameter Top : 3.42 cm. Bottom : 3.42 cm. Average : 3.42 cm.

Specimen Weight : Specimen Height :7.8 cm.

Av. Specimen Area : 9.186 cm^2 Av.Loading Rate : 0.0303 mm/min.

Loading dial In.x10^{-4}	Axial strain %	Pore pressure Kg. / cm^2	Deviator stress Kg. / cm^2	Ef. Mean normal stress Kg. / cm^2	Water Content %	
0.0	0.00	0.00	0.000	7.500	Slice No.	Water Content
87.0	0.17	0.05	0.903	7.768		
167.5	0.32	0.09	1.738	7.896	1	20.530
231.5	0.64	0.17	2.366	7.923	2	20.333
263.0	0.90	0.24	2.683	7.865	3	20.480
298.5	1.28	0.36	3.025	7.798	4	20.462
337.0	1.99	0.66	3.466	7.590	5	20.556
361.0	3.01	1.10	3.573	7.233	6	20.605
384.5	4.10	1.70	3.761	6.877	7	20.847
392.8	4.62	2.00	3.818	6.728	8	20.722
407.0	5.64	2.40	4.095	6.483	9	21.647
417.0	6.41	2.63	4.252	6.226	Average w : 20.67	
432.5	8.14	2.82	4.490	6.175	Sketch of Failure	
443.5	9.81	2.92	4,626	6.130		
446.8	10.38	2.92	4.661	6.130		
449.5	11.09	2.92	4.676	6.132		
455.1	12.31	2.89	4.718	6.162		
458.1	13.33	2.88	4.717	6.180		
461.3	14.81	2.88	4.591	6.188		

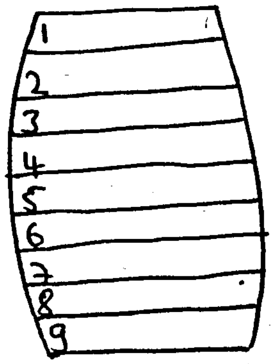

Max. Axial Stress: 4.718 $kgcm^{-2}$ Water Con. at Failure Surface: 20.847 %

Fig 4.90 Deviator Stress versus Axial Strain

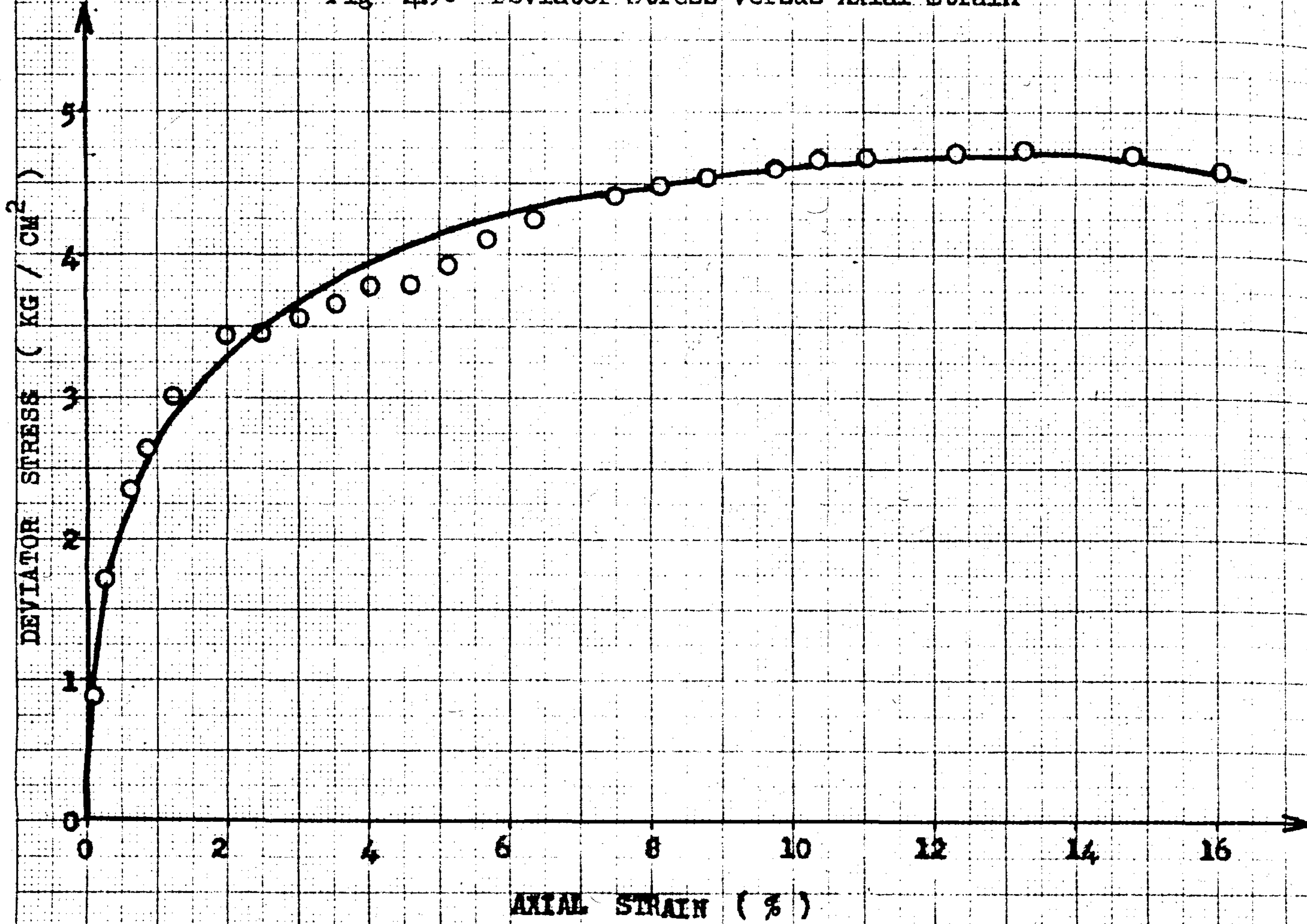

Fig 4.91 Pore Water Pressure versus Axial Strain

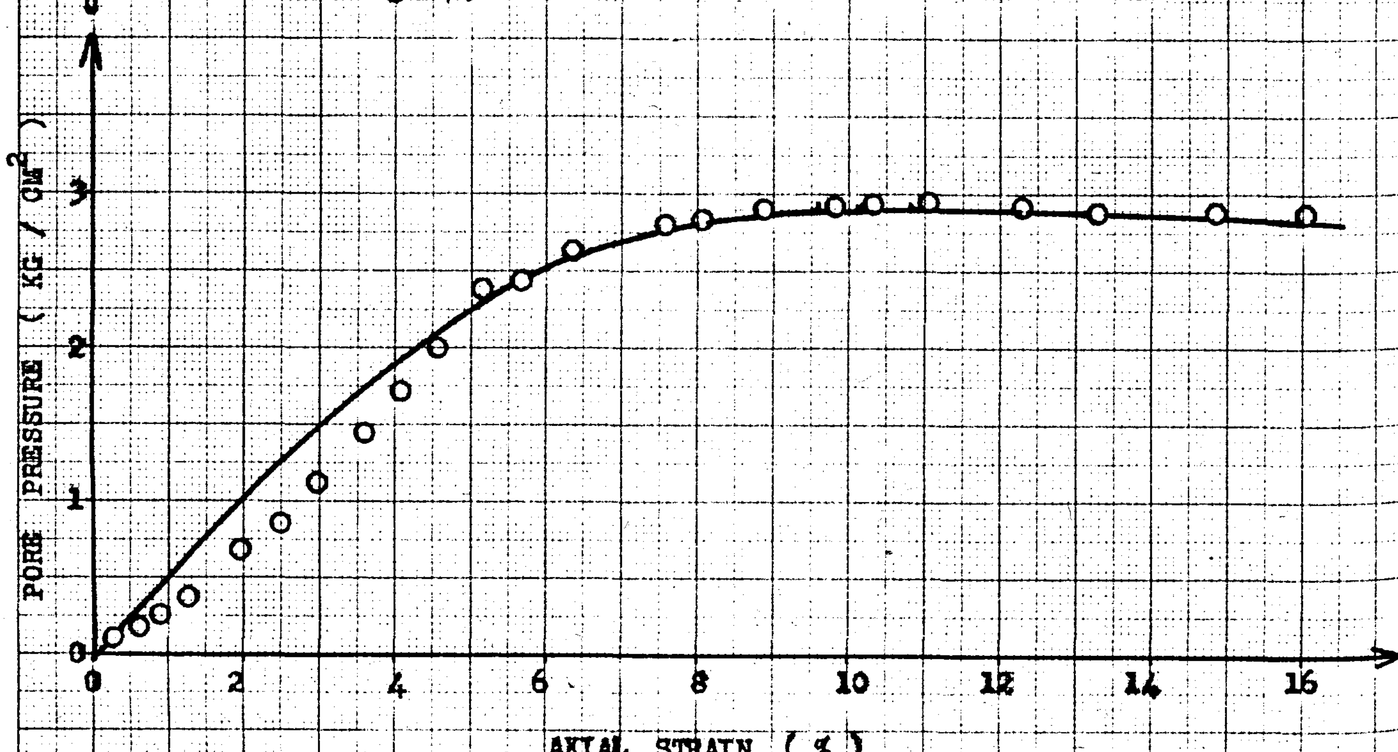

Fig 4.92 Deviator Stress versus Effective Mean Normal Stress

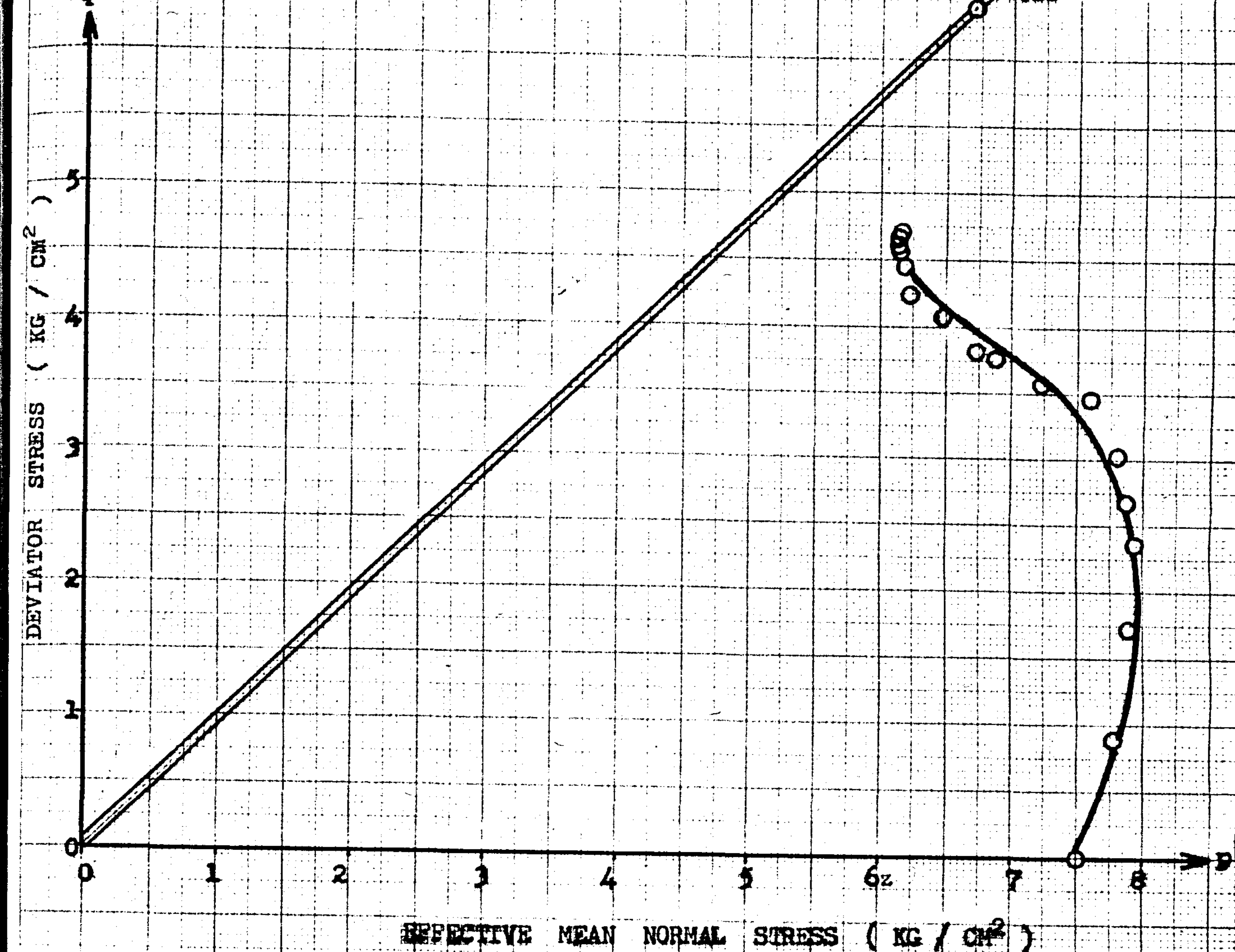

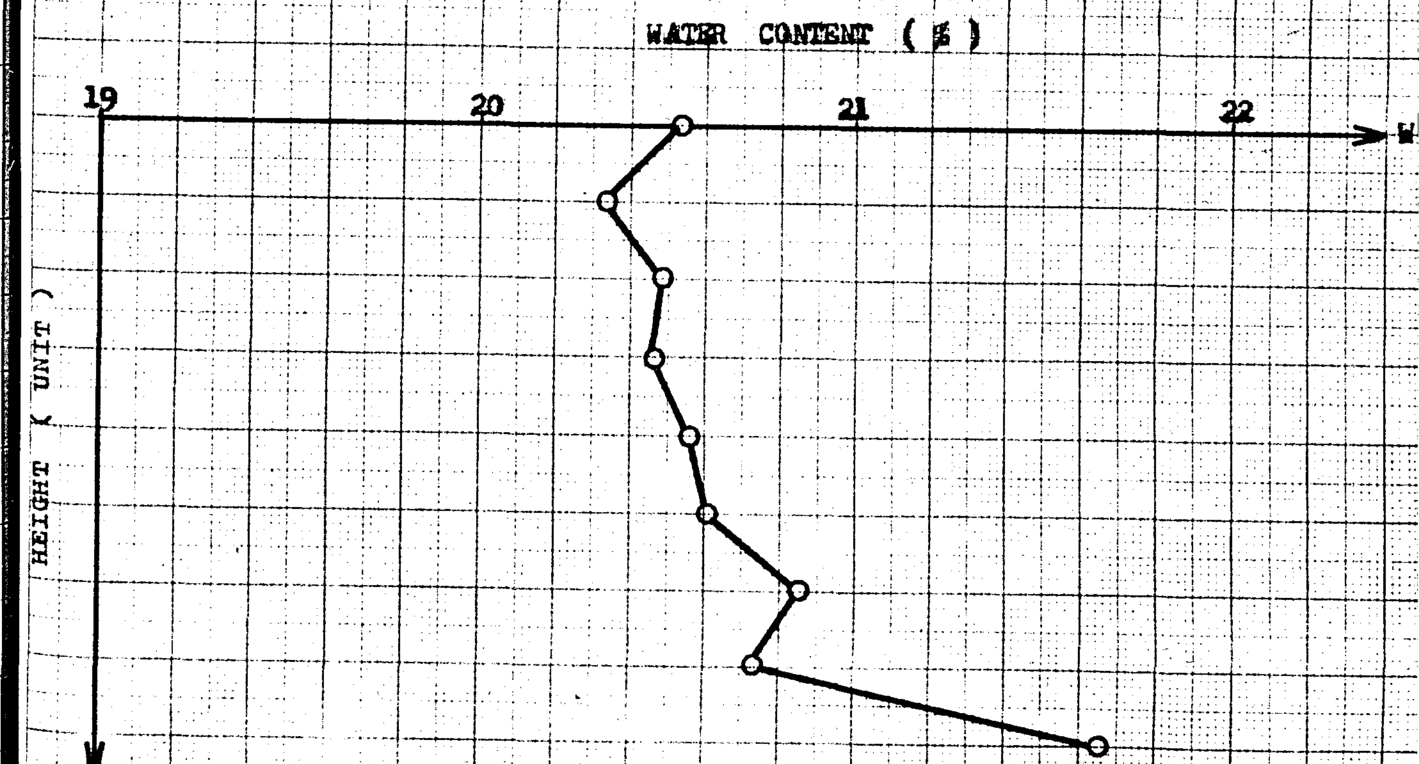

Fig 4.93 Height (Unit) versus Waetr Content

Consolidation Pressure : 7.5 $Kgcm^{-2}$

Equivalent Mean Normal Stress $(Pe)_i$: 6.072 $Kgcm^{-2}$

Proving Ring Number and Constant : 4766 / 0.20833 O. C. R. : 1

Specimen Diameter Top :3.40 cm. Bottom :3.40 cm. Average : 3.40 cm.

Specimen Weight : 141.76 gr. Specimen Height : 7.58 cm.

Av. Specimen Area :9.079 cm^2 Av.Loading Rate : 0.0303 mm/min.

Loading dial In.$\times 10^{-4}$	Axial strain %	Pore pressure Kg. / cm^2	Deviator stress Kg. / cm^2	Ef. Mean normal stress Kg. / cm^2	Water Content %	
0.0	0.00	0.00	0.000	7.500	Slice No.	Water Content
84.0	0.28	0.08	0.864	7.708		
140.0	0.47	0.12	1.500	7.880	1	21.976
173.0	0.66	0.22	1.770	7.931	2	22.211
217.0	1.12	0.25	2.212	7.987	3	22.475
256.0	1.72	0.34	2.590	7.897	4	22.786
278.5	2.11	0.58	2.811	7.862	5	22.442
314.0	2.97	0.95	3.125	7.592	6	22.488
336.0	4.09	1.66	3.350	6.962	7	22.139
352.5	5.28	2.59	3.430	6.171	8	22.308
360.5	6.07	3.00	3.480	5.694	9	22.327
371.5	7.26	3.38	3.533	5.430	Average w :22.32	
376.8	7.98	3.70	3.555	5.213	Sketch of Failure	
389.8	10.03	3.72	3.635	5.013		
395.9	11.21	3.85	3.636	4.976		
402.0	12.53	3.81	3.775	4.948		
406.0	13.85	3.79	3.791	4.948		
409.8	15.17	3.82	3.780	4.945		
411.8	16.62	3.82	3.768	4.941		

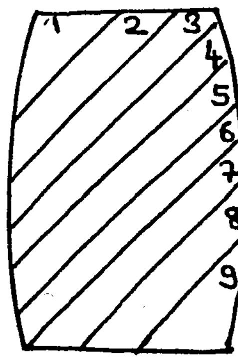

Max. Axial Stress:3.791 $kgcm^{-2}$ Water Con. at Failure Surface:22.786 %

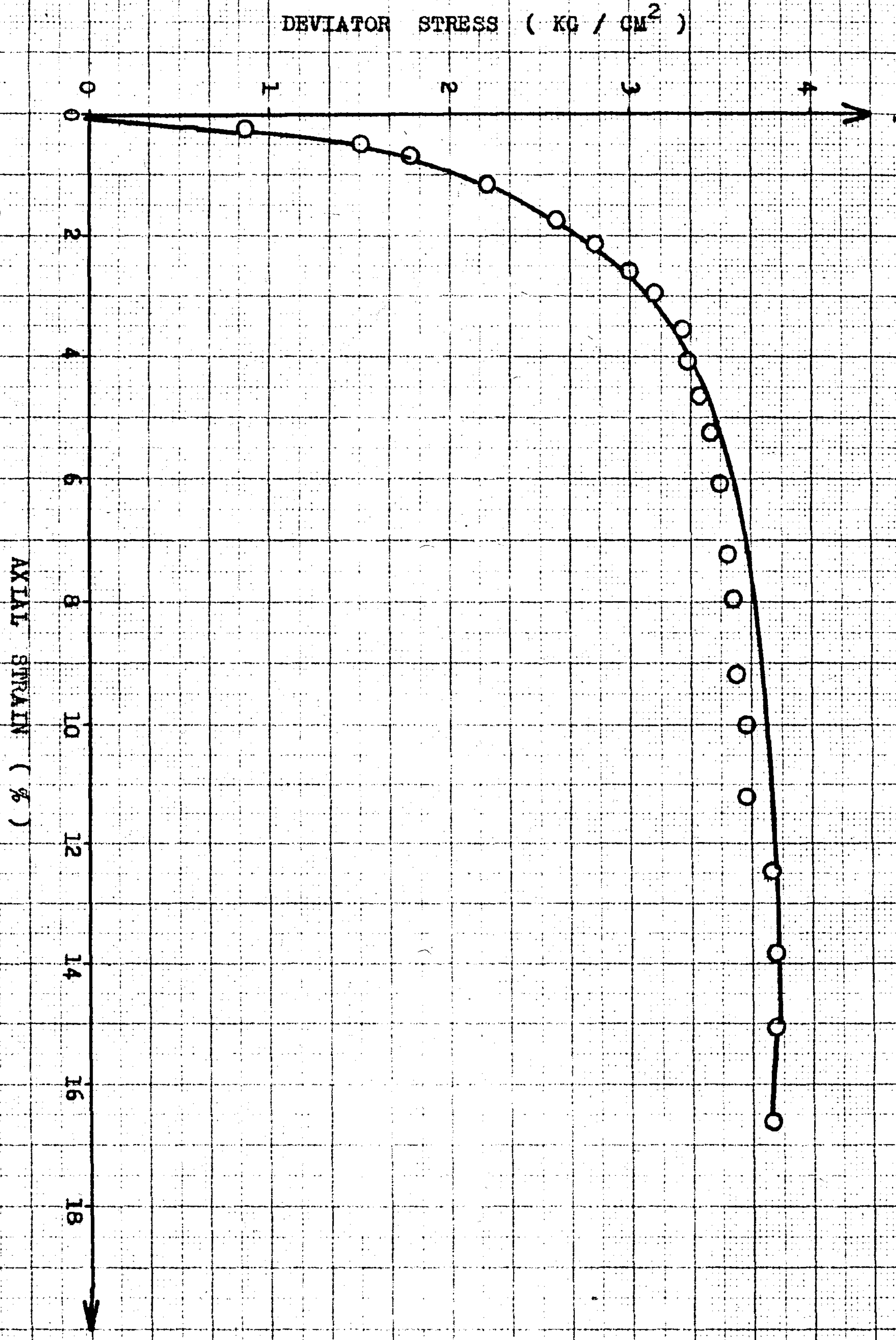

Fig 4.94 Deviator Stress versus Axial Strain

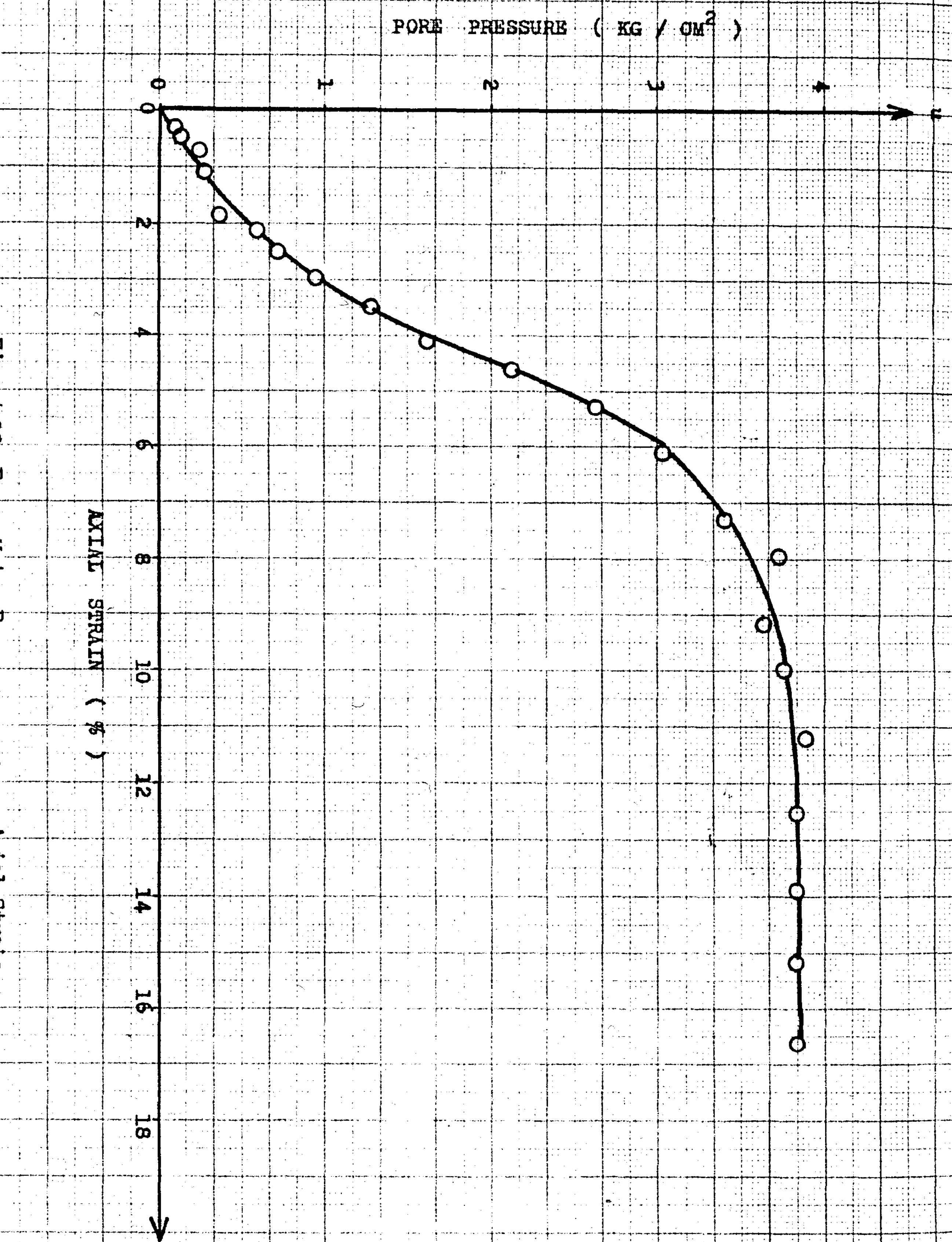

Fig 4.95 Pore Water Pressure versus Axial Strain

Fig 4.96 Deviator Stress versus Effective Mean Normal Stress

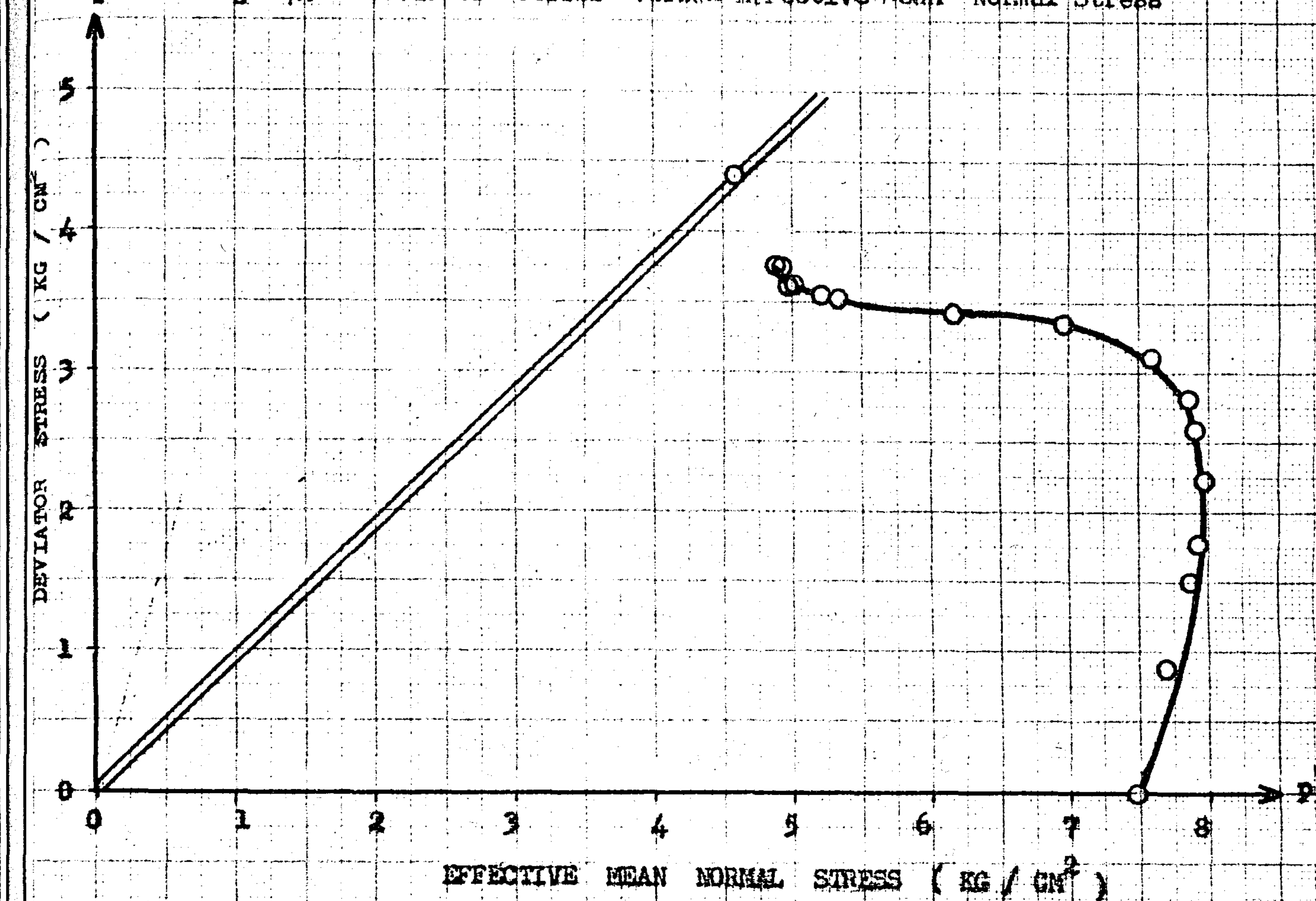

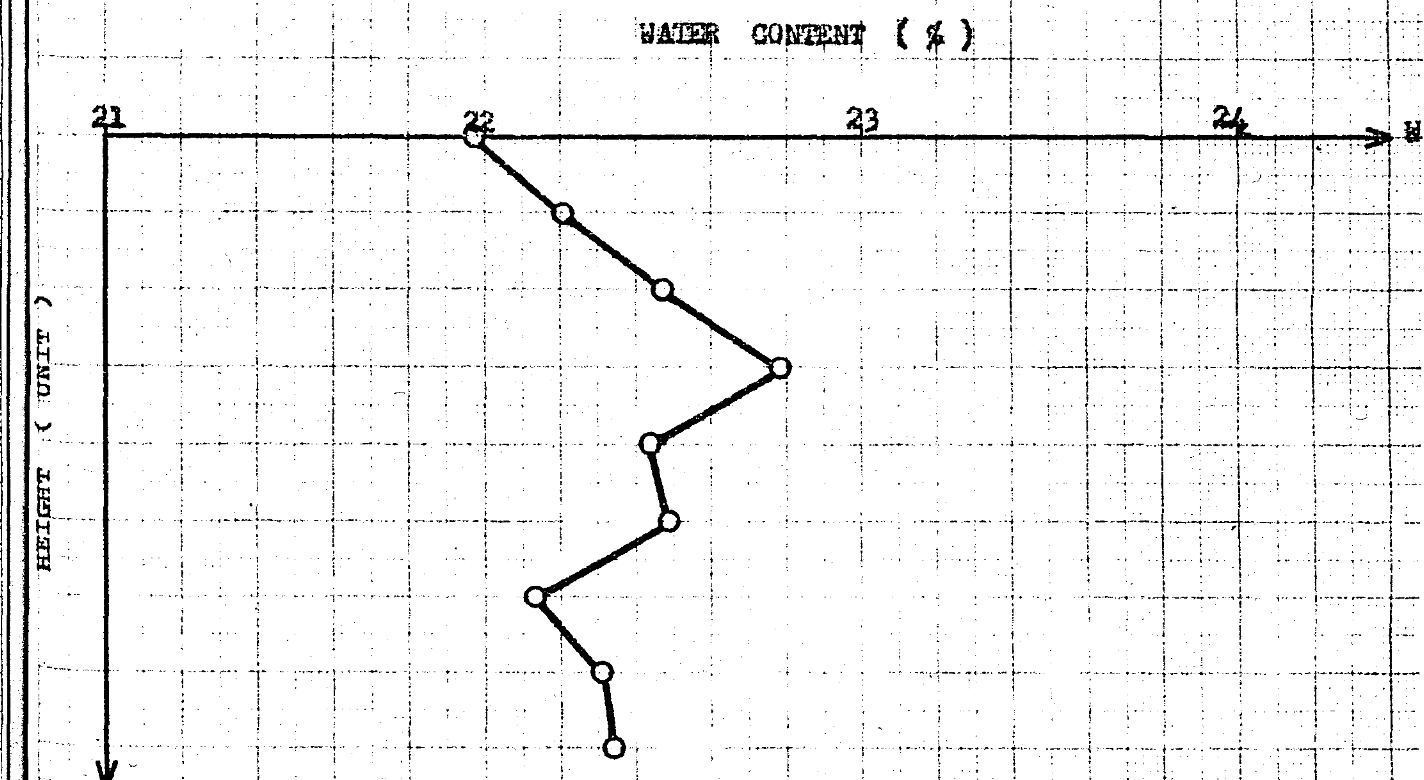

Fig 497 Height (Unit) versus Water Conten

CHAPTER 5 CONCLUSION

In this study, the behaviour of overconsolidated clay is investigated. When an overconsolidated clay is tested in an undrained condition, the deviator stress increases to a maximum value. From this point on the deviator stress decreases with increasing strain. This decrease may be explained as follows. When the stress path reaches the Hvorslev surface a shear zone develops in the specimen. This failure zone attracts water from the nearby surrounding. This is a contradiction to the undrained testing method. The stress path moves from its initial constant v plane to the new constant v plane (as seen in Fig 5.1 (a) and (b)). So the deviator stress decrease from its peak value and the specimen fails on the critical state line at a new v plane intersection point.

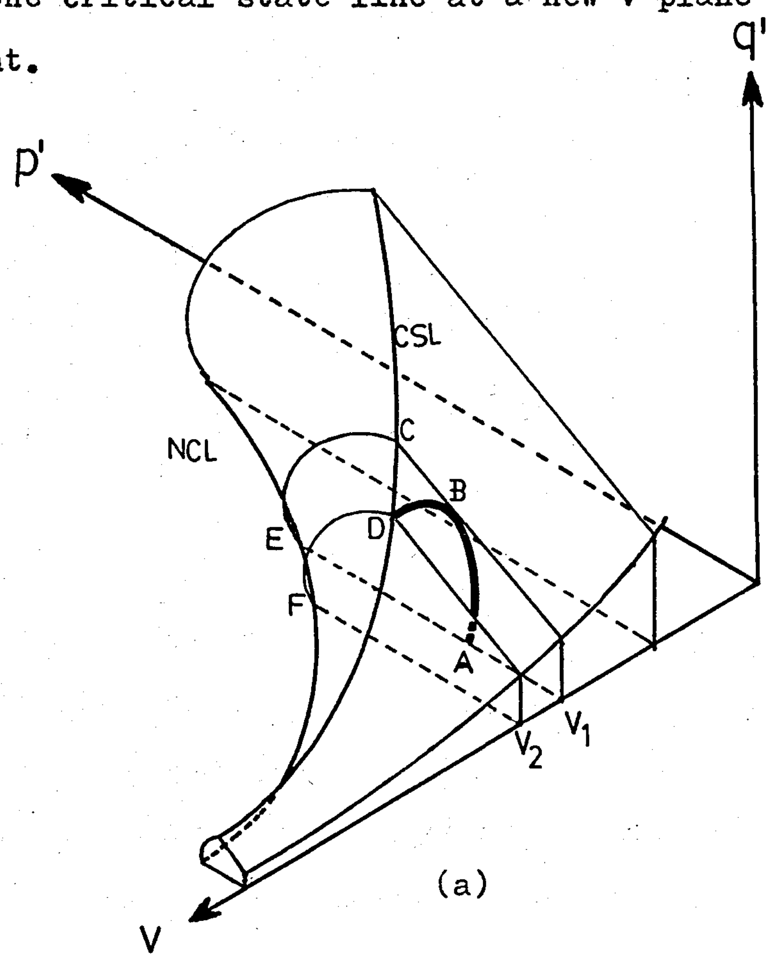

(a)

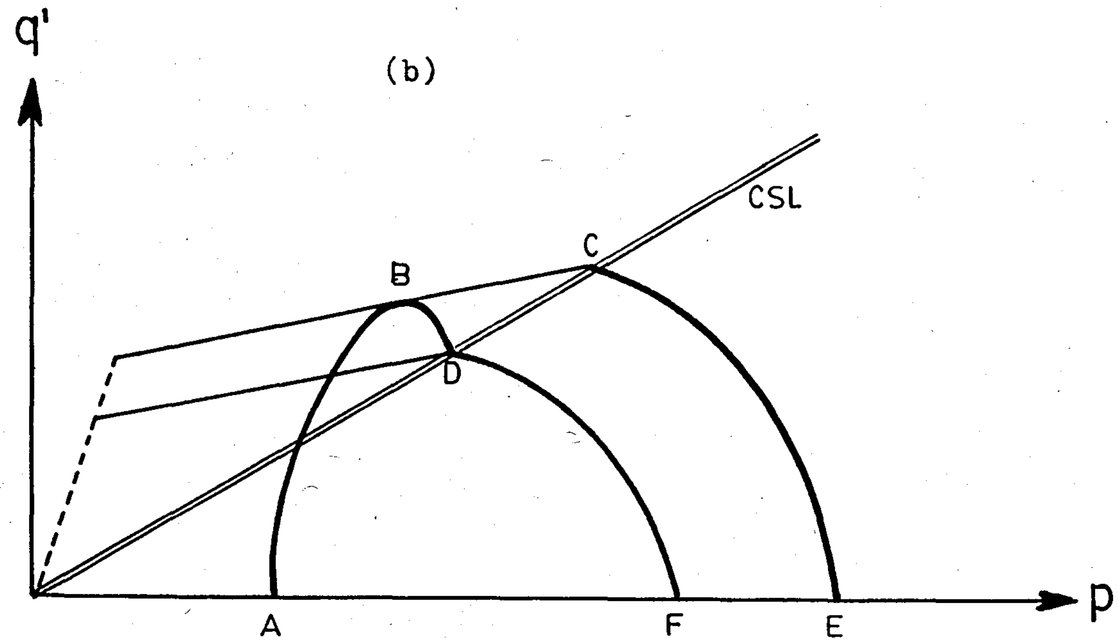

Fig 5.1 Failure Mechanism (a) in q':p': v space, (b) in q':p' space for an overconsolidated clay in undrained condition

Conclusions obtained from undrained triaxial tests on overconsolidated specimens can be summarized as follows.

(1) The soil parameters from normally consolidated specimens has been found as

$$M = 43.8^{\circ}$$

$$N = 1.8156$$

$$\Gamma = 1.7823$$

$$\lambda = -0.118$$

$$h = 34.5^{\circ}$$

(2) Water content distribution trough the specimen is initially uniform, but after reaching the Hvorslev surface a water content grater than the average water content at the failure surface of the specimen is created.

(3) The maximum deviator stress and the effective mean

normal stress at failure is a function of the water content

(4) The behaviour of a normally consolidated specimen is different from an overconsolidated specimen. Normally consolidated specimens fail when reaching directly the Critical State Line without make any peak value, and its stress paths follows the Roscoe Surface. But an overconsolidated specimen fails after reaching the Hvorslev Surface with making a peak value.

(5) The relationship between deviator stress (q), effective mean normal stress (p'), and specific volume (v) can be expressed with a curve. The projection of this curve on the lnp' vs. v space is a straight line. The projection on the q' vs. p' space is also a stright line passing through the origin.

(6) As seen from Fig 5.2, the use of the water content at the shear surface allows us to make a more reliable prediction of the shear strength.

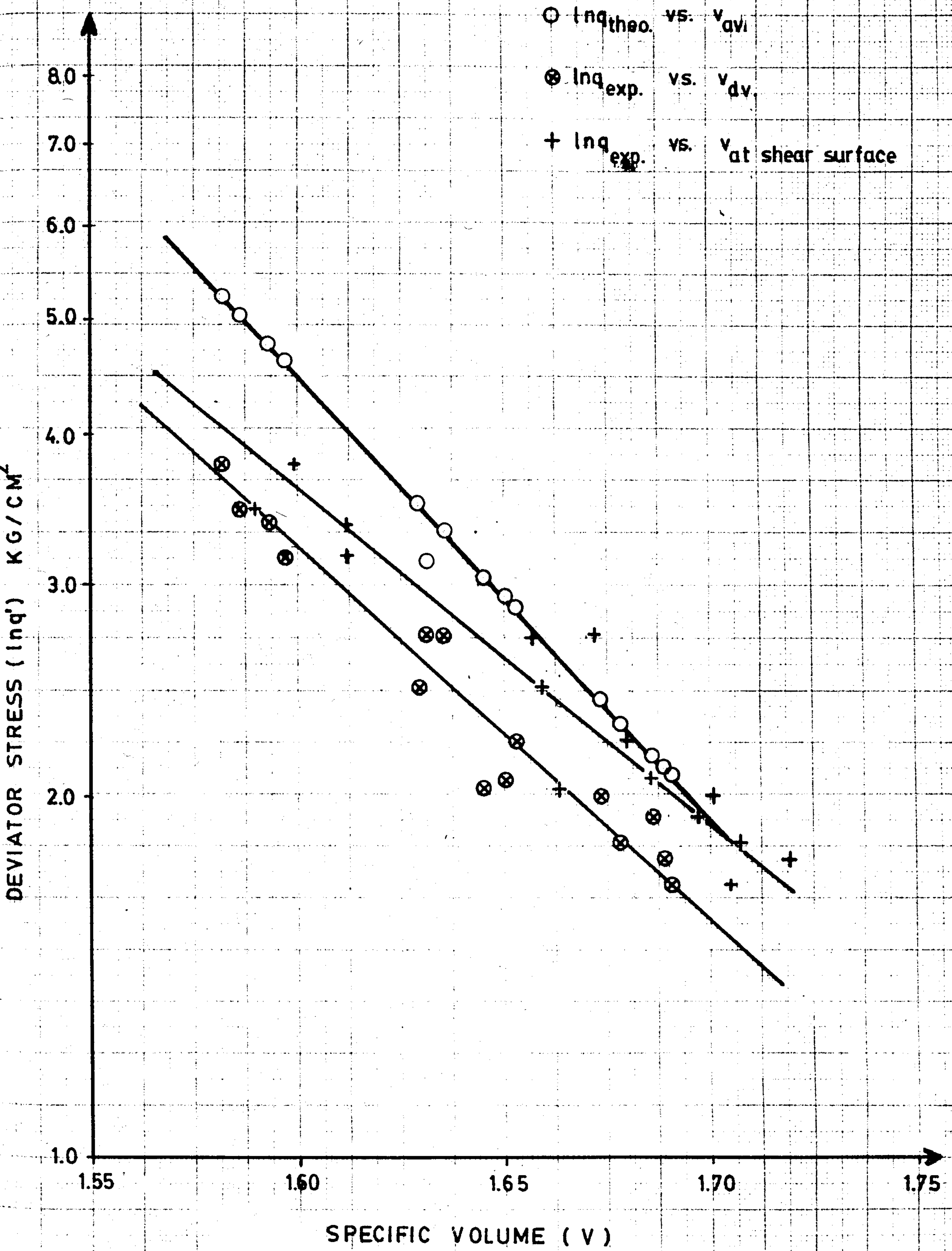

Fig 5.2 Deviator Stress (lnq') vs. Specific Volume

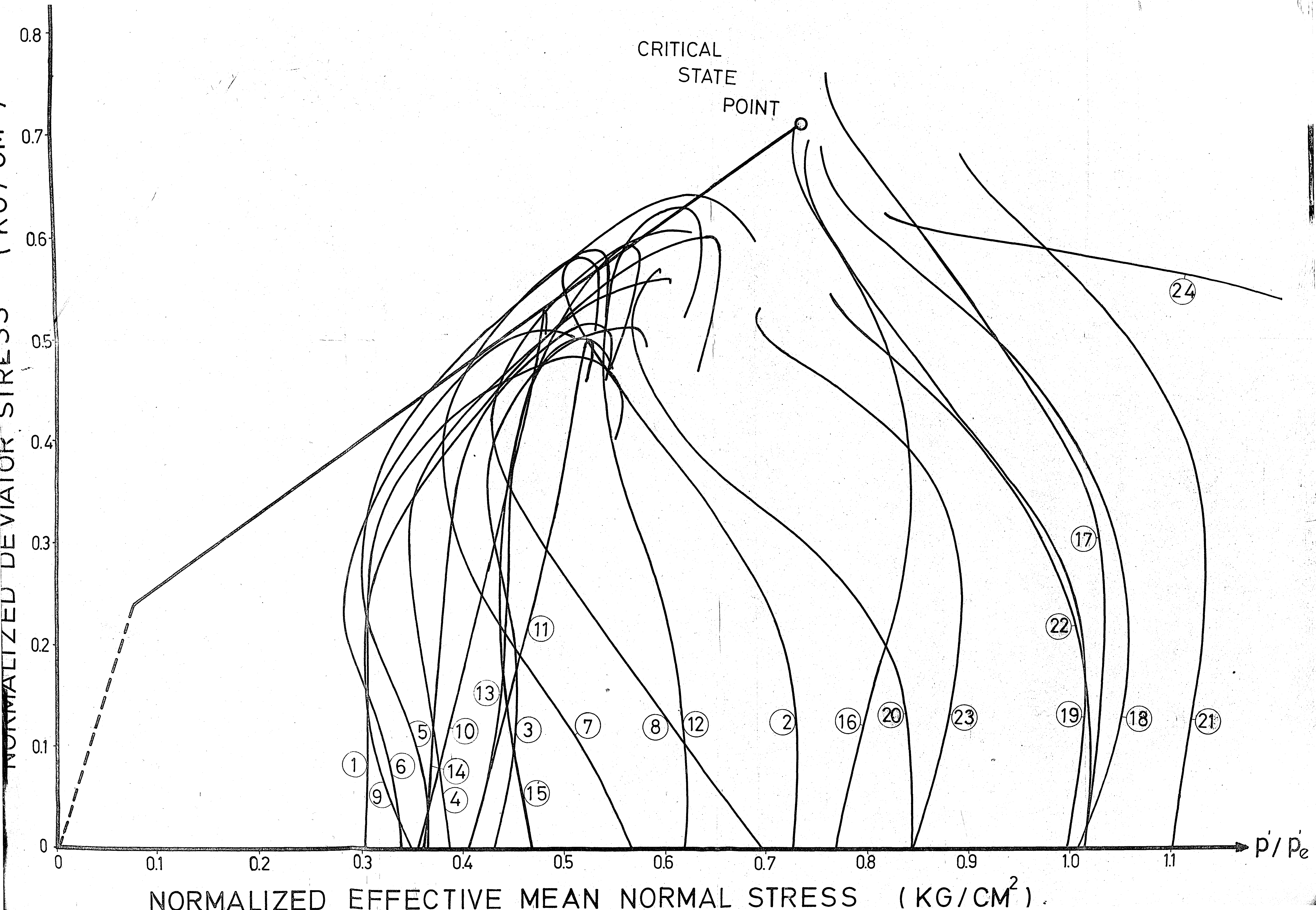

CRITICAL STATE POINT
NORMALIZED DEVIATOR STRESS (KG/CM²)
0.8
0.7
0.6
0.5
0.4
0.3
0.2
0.1
0
0.1
0.2
0.3
0.4
0.5
0.6
0.7
0.8
0.9
1.0
1.1
p'/p'e
NORMALIZED EFFECTIVE MEAN NORMAL STRESS (KG/CM²)
1
2
3
4
5
6
7
8
9
10
11
12
13
14
15
16
17
18
19
20
21
22
23
24

REFERENCES

ALAN, W., BISHOP, M. A.,and HENKEL, D. J.," The measurement of soil properties in the triaxial test", Edward Arnold, London, Second Edition 1962.

ATKINSON, J. H. and BRANSBY, P. L.," The mechanics of soil an introduction to critical state soil mechanics" McGraw-Hill Co., London, 1977.

BARDEN, L.," Examples of clay structure and its influence on engineering behaviour", Stress- Strain Behaviour of Soil Proceeding of the Roscoe Memorial Symposium, Cambridge University, 20-31 March 1971.

BLASUBRAMANIAM, A. S.," Some factor influencing the stress-strain behaviour of clay", PhD Thesis, University of Cambridge, 1969.

HENKEL, D. J.," The relationships between the effective stress and water content in saturated clays", Geotechnique, 10, 41-54, 1960.

HENKEL, D. J.," The effect of overconsolidation on the behaviour of clay during shear", Geotechnique 6, 139-156, 1956.

KEZDI, A.," Hendbook of soil mechanics ", Vol.1 Soil Physics, Elsevier, London, 1974.

LAMBE, T. W.," The structure of compacted clay", Journal of the Soil Mechanics and Foundation Division, ASCE, May, Vol. 84, 1958.

LOUDON, P. A.," Some deformation characteristics of Kaolin", Ph. D thesis, University of Cambridge, 1967.

PARRY, R. H. G.," Triaxial compression and extension test on remoulded saturated clay", Geotechnique, 10, 166-180 1960.

PARRY, R. H. G.," Discussion ", Geotechnique, 8, 183-186, 1958

ROSCOE, K. H., SCHOFIELD, A. N.,and WROTH, C. P.," On the yielding of soil ", Geotechnique, 8, 22-54, 1958.

PENDER, M. J.," A model for the behaviour of overconsolidated soil ", Geotechnique, 28, 1-26, 1978.

ROSCOE, K. H.," A theoretical and experimental study of strain in triaxial compression tests on normally consolidated clay", Geotechnique, 13, March, 1963.

ROSCOE, K. H., SCHOFIELD, A.N., and THURAIRAJAH, A.," Yielding of clays in state wetter than critical ", Geotechnique 13, September, 1963.

SCHOFIELD, A. N., and WROTH, C. P.," Critical state soil mechanics ", McGraw-Hill Book Co., London, 1958.

TOGROL, E.," Kohezyonlu zeminlerde kayma gerilmesi, effective basınç, ve su muhtevası arasında bağıntı ", Ph.D Thesis, University of Istanbul Technique, 1962.

TOGROL, E., " Zeminlerin mechanik davranışı ", Prof. Dr. Mustafa Inan Anısına, 1971.